DEVELOPMENT OF NON-VIRAL SYNTHETIC CARRIERS FOR GENE DELIVERY

A THESIS SUBMITTED TO
THE MAHARAJA SAYAJIRAO UNIVERSITY OF BARODA
FOR THE AWARD OF THE DEGREE OF

Doctor of Philosophy

in

Pharmacy

BY

MUKESH KUMAR

UNDER THE GUIDANCE OF

PROF. M. R. YADAV   **PROF. A. N. MISRA**

Pharmacy Department

Faculty of Technology and Engineering

The M. S. University of Baroda

Vadodara-390 001

NOVEMBER 2012

Date:

<u>CERTIFICATE</u>

This is to certify that the thesis entitled **"Development of Non-viral Synthetic Carriers for Gene Delivery"** submitted for the Ph. D. Degree in Pharmacy by Mr Mukesh Kumar incorporates the original research work carried out by him under our supervision.

Supervisor
(Prof. M. R. Yadav)

Co-Supervisor
(Prof. A. N. Misra)

HEAD
Pharmacy Department

DEAN
Faculty of Technology & Engineering,
The M.S. University of Baroda,
Vadodara – 390 001

DECLARATION

I hereby declare that the topic entitled **"Development of Non-viral Synthetic Carriers for Gene Delivery"** submitted herewith to The Maharaja Sayajirao University of Baroda, Vadodara for the fulfillment of the award of the degree of DOCTOR OF PHILOSOPHY IN PHARMACY is the result of the work carried out by me in Pharmacy Department, Faculty of Technology and Engineering, The M. S. University of Baroda, Vadodara.

The result of this work has not been previously submitted for any degree/fellowship.

Date:

Place: Vadodara   Mukesh Kumar

Dedicated to My

Family

And

Teachers

<u>Acknowledgement</u>

List of Figures

List of Tables

Abbreviations

*p*DNA	Plasmid deoxyribonucleic acid
kDa	Kilodalton
RNA	Ribonucleic acid
RES	Reticuloendothelial system
PLL	Poly[*l*-lysine]
PEI	Polyethylenimine
DEAE	Diethylaminoethyl
pDMAEMA	Poly[2-(dimethyalamino)ethyl methacrylate]
PHP	Poly(4-hydroxylproline ester)
PAGA	Poly[*γ*-(4-aminobutyl)-*L*-glycolic acid]
PLGA	Poly(lactide-co-glycolic acid)
DOTMA	*N*-[1-(2,3-dioleyloxy)propyl]-*N,N,N*-trimethylammonium chloride
DOTAP	1,2-dioleoyloxy-3-(trimethylammonio)propane chloride
DMRIE	1,2-dimyristyloxypropyl-3-dimethyl-hydroxyethyl ammonium bromide
DLRIE	*N*-(3-aminopropyl)-*N,N*-dimethyl-2,3-bis(dodecyloxy)-1-propanaminium bromide
DOTAP	1,2-dioleoyloxy-3-(trimethylammonio)propane chloride
DOGS	dioctadecylamidoglycylspermine
DOSPA	2,3-dioleyloxy-*N*-(2-sperminecarboxamido)ethyl-*N,N* dimethyl-1-propanaminium trifluroacetate
TMTPS	*N,N',N'',N'''*-tetraethylpalmitylspermine
GAs	Gemini amphiphiles
CTAB	Cetyl trimethylammonium bromide
DORIE	1,2-dioleoyl-3-dimethylhydroxyethyl ammonium bromide
DORI	1,2-dioleoyloxypropyl-3-dimethylhydroxyethyl ammonium chloride
DHMHAC	*N,N*-di-*n*-hexadecyl-*N*-methyl,*N*-(2-hydroxyethyl)ammonium chloride
DHDEAB	*N,N*-di-*n*-hexadecyl-*N,N*-dihydroxyethylammonium bromide
DDAB	Dioctadecyldimethylammonium bromide
DMHMAC	*N,N*–myristyl-*N*-(1-hydroxyprop-2-yl)-*N*-methylammonium chloride
DC-Chol	3-β-[*N*-(*N',N'*-dimethylaminoethane)carbamoyl]cholesterol hydrochloride
EDOPC	*o*-Ethyl dioleoylphosphatidylcholine
DMPC	1,2-dimyristoyl-sn-glycero-3-phosphocholine
ONPG	*o*-Nitrophenyl-*β-D*-galactopyranoside
MTT	3-(4,5-dimethylthiazol-2yl)-2,5-diphenyltetrazolium bromide
MFI	Mean fluorescence intensity
PEG-ML	Polyethylene glycol monolaurate
GFP	Green fluorescent protein
TEM	Tranmission electron microscopy

AFM	Atomic force microscopy
SAXS	X-ray scattering
β-gal	*pCMV-SPORT-β-gal*
PMR	Proton magnetic resonance
SLS	sodium lauryl sulphate
Kb	Kilobase pairs
ONP	*o*-Nitrophenol
cmc	Critical miceller concentration
CD	Circular dichroism
FBS	Fetal bovine serum
FACS	Florescence-assisted cells sorting
^{99m}Tc	Radioactive pertechnetate
TLC	Thin layer chromatography
ppm	Parts per million
LB	Luria broth
DMEM	Dulbacco modified eagle's medium
PDI	Poly-dispersibilty index
PBS	Phosphate buffer saline
DTPA	Diethylenetriaminepentaacetic acid
mCi	Milli curie
M	Mole
ML	Milli litre

INDEX

1. INTRODUCTION

A number of common human diseases have underlying genetic causes, and pharmacological approaches often fall short of curing many of these diseases. Gene therapy provides a unique approach that can be used in the treatment of both inherited and acquired diseases. Gene therapy has drawn a lot of attention in the field of medicine, pharmaceutical sciences and biotechnology due to its potentials for treating chronic diseases and genetic disorders. At onset, the primary goal of gene therapy was to swap a deficient gene in a genetically inherited disease with a normal copy to restore production of functional protein. Later this goal was broadened to include genetic defects beyond inherited disorders, as numerous acquired diseases also involved alteration in the regulation of gene expression. Therefore, gene therapy apart from replacing a defective gene could also modulate gene expression and integrate functions into cells not originally present but which could serve certain therapeutic purposes. Researchers in gene therapy have used ways for correcting defective genes such as replacement of a non-functional gene with a normal gene, or an abnormal gene with a normal gene, through homologous recombination; or for repairing an abnormal gene through selective reverse mutation or selectively controlling expression of a defective gene[1]. In another type of application, the genes may also be delivered as genetic vaccines to induce both cell-mediated and humoral immune responses.

The fundamental principle underlining gene therapy is theoretically straightforward, but difficult to achieve satisfactorily in practice. The two essential components in current gene therapy are: (i) an effective therapeutic gene that can be expressed at a target site[2] and (ii) an efficient and safe delivery system that delivers the therapeutic genes to a specific target tissue or organ[3]. Many genes capable of correcting diseased phenotypes have been identified, and it is now possible to produce engineered DNA that carries a therapeutic gene in sufficient quantities for clinical trials. A method that delivers a therapeutic gene (trans-gene) to selected cells after intravenous administration where proper gene expression can be achieved is always desirable. The bottleneck of gene therapy is the development of a method by which a therapeutic gene can be delivered to a cell site where gene expression can be

accomplished. The desirable qualities of an ideal gene delivery carrier could be summarized as follow[4]:

- It should be able to condense or encapsulate DNA into a size small enough to enter into the cell.
- It should be capable of protecting DNA from the external environment.
- It should maintain integrity and stability of DNA after its *in vivo* administration.
- It should possess some functional moieties to facilitate escape of DNA from the endosomes into the cytoplasm.
- It should release DNA from the carrier into the cell in its active form.
- It should possess a targeting moiety to direct the delivery of DNA to a particular type of cell for gene transfection and nuclear localization.

Since the first clinical trial in human gene therapy in 1989, approximately 1714 clinical trials have been either completed, ongoing or approved up to June 2011, but the issue of delivering the gene efficiently at target site has not yet been resolved completely[5]. The development of vectors capable of addressing issues related to gene delivery could render gene therapy for many diseases as a general treatment. Since gene delivery is a multi-step process, in which an appropriate property of carriers would be needed to carry forward each step, rationally designed multifunctional vectors could overcome a series of extra- and intra-cellular barriers at molecular level[6].

1.1 Barriers and challenges to gene delivery

Gene delivery can be regarded as a special problem in drug delivery. It is special in a way that the "drug" to be delivered is a specific piece of DNA, with success rate depending upon the effectiveness of delivery carrier in overcoming the barriers. The main barriers to gene transfer are described in **Table 1** along with suggested opportunities that can be employed to circumvent them[7]. Barriers in gene delivery may broadly be classified into extra- and intra-cellular barriers.

Table 1. List of barriers and challenges in gene delivery

Location	Nature of barrier	Challenges	Opportunities
Blood circulation	Blood nucleases; Particle instability; Particle opsonization, Clearance by macrophages in liver and spleen; Unwanted capillary blockade.	Protection of DNA from nucleases; Steric stabilization of particles; Prevention of unwanted opsonization.	Systemic delivery after i.v. injection; Selectivity mediated by tissue-specific promoters.
Capillary endothelium	Tissue specific characteristic, continuous in muscle, skin and lung etc, fenestrated in kidney, endocrine glands etc and discontinuous in liver and spleen.	Extra-vasation particularly in organs with endothelia.	Delivery to hepatocytes via discontinuous endothelium; Delivery to tumors; Delivery to sites of angiogenesis; Selective receptor-mediated extra-vasation.
Tissue interstitium	Extra-cellular nucleases; Poor distribution within tissues; High hydrostatic pressure in tumors.	Protection of DNA from nucleases; Prevention of unwanted binding which prevents convective flow.	Direct intramuscular injection extended expression of genes for systemic effect; expression of DNA vaccines;
Cell surface	Poor cellular internalization	Optimize physical properties for uptake; Understand uptake of naked DNA; Maximize rate of uptake by receptor mediated uptake.	Direct injection into tumors. Selective uptake by receptor mediated endocytosis; Direct uptake into cytoplasm using membrane active peptides.
Endosome	Trafficking to lysosome and consequent degradation	Incorporate endosomolytic agent.	Utilize viral peptides for escape of endosome or proton sponge properties of vector.
Cytoplasm	Inefficient cytoplasmic transport; Poor uncoupling of DNA and carrier.	Optimize size of escape from the vesicular system.	Make use of microtubule transport system to deliver DNA to perinuclear region.

1.1.1 Extra-cellular barriers

Main extracellular barriers to gene delivery could be summarized as:

1) Opsonins,

2) Phagocytic cells,

3) Degradative enzymes, and

4) Extra-cellular matrix

Opsonins are proteins that attach themselves to a gene or a delivery system thereby making it visible to phagocytic cells. Phogocytes are cells that seek out, engulf and actively digest the delivery systems. After opsonization, phagocytosis occurs, which is the engulfing and eventual destruction or removal of foreign materials from the bloodstream. Together these two processes form the main clearance mechanism for the removal of undesirable components larger than the renal threshold limit from the blood. Without the presence of surface bound or adsorbed opsonin proteins, the phagocytes will typically not be able to bind or recognize the foreign particles. The bound opsonin proteins undergo conformational changes from an inactive protein present in the blood serum to an activated protein structure that can be recognized by phagocytes. Phagocytic cell surfaces contain specialized receptors that interact with the modified conformation of these various opsonins thus alerting them to the presence of a foreign material. Alternatively, the non-specific adherence of phagocytes to surface adsorbed blood serum proteins can result in the stimulation of phagocytosis as well[8]. Complement activation also results in the binding and phagocytosis of the foreign particle by the mononuclear phagocytes. The other barrier faced by the delivery vehicles is the DNases present in the serum and extracellular fluid, which can rapidly digest unprotected DNA. Finally, before entering the cell, the delivery vehicle has to traverse through the extracellular matrix, which is a zone of polymerized proteins and carbohydrates present between cells protecting the plasma membrane of the target cell, and it can be difficult for a relatively large DNA carrier system to pass through this barrier[9].

1.1.2 Intra-cellular barriers

The intra-cellular barriers for gene delivery include:

1) Plasma membrane,

2) Endosomal membrane, and

3) Nuclear membrane

Once the gene delivery system reaches the target cell, it encounters the plasma membrane, which must be traversed before the gene can be expressed. The uptake of most of the macromolecules or particles into the cells by passive diffusion across the plasma membrane is limited due to their low solubility in lipid bilayers therefore leading to pinocytosis, adsorptive endocytosis, receptor mediated endocytosis or phagocytosis[10, 11]. After crossing the membrane, it is to be endocytosed but then the delivery system must have a mechanism to escape from the endosome lest it will be degraded in the lysosomal compartment. The implication is that a specific or generic means of escape is required; otherwise most of the internalized DNA will be lost by degradation. Finally, the gene should be able to cross these barriers and enter the cell cytoplasm; it must still have a means of getting across the nuclear membrane. The nuclear membrane is a barrier preventing uptake of most macromolecules greater than 70 kDa into the nucleus, unless they are able to interact with the nuclear pore active transport system[12]. Any gene delivery system that is intended to be viable for *in vivo* applications or gene therapy must at the very least be equipped with the capacity for rapid endosomal uptake followed by efficient endosmolysis, cytosolic trafficking and nuclear entry. Obviously, efficient nuclear entry is required only for DNA but not if RNA is involved. However, this may well depend upon both vector characteristics and the nature of cells in the organs of choice that have been selected for nucleic acid delivery.

In order to overcome these barriers various gene delivery systems have been developed that involve various aspects of molecular biology, DNA condensation technology and ligand conjugation chemistry. Therefore, for successful gene therapy, an efficient, safe and selective vector, an appropriate technique and an appropriate gene are the pre-requisites.

1.2 Problems in naked DNA delivery

A naked DNA injection, without any carrier into local tissues or into the systemic circulation is probably the simplest and safest physical/mechanical approach of gene delivery. Naked plasmid DNA is an attractive non-viral gene vector because of its inherent simplicity and because it is easily produced in bacteria and manipulated using standard recombinant DNA techniques. It shows very little dissemination and transfection at distant sites following delivery and can be re-administered multiple times into mammals (including primates) without eliciting an immune response. However, since DNA is a long, slender, hydrophilic and poly-anionic molecule having micrometer dimensions its systemic applications are limited when delivered alone[13]. Naked DNA delivery after systemic administration is significantly inhibited by the barriers of size, shape, and poly-anionic charge of DNA, thus inhibiting the cell permeability of DNA. Naked DNA has susceptibility against serum nuclease when administered intravenously. This degradation can be partially resolved by mixing the DNA with a cationic lipid, polymer, or inorganic material capable of complexing with or entrapping the DNA by ionic interaction. Moreover, colloidal stability due to its negative charge, RES uptake, organ and cellular targeting are the major barriers rendering the application of naked DNA delivery a big challenge[14]. A number of carriers/vectors have been developed to address the afore-mentioned problems associated with naked DNA delivery.

1.3 Vectors for gene delivery

The size and hydrophilicity of poly-anionic DNA restrict its application by direct gene transfer methods. Therefore, gene delivey systems/vectors are required to fulfill the delivery requirement of DNA. Traditionally, gene delivery systems are broadly classified as either viral-mediated or non-viral mediated (**Figure 1**). Every gene delivery system has its own advantages and disadvantages as summarized in **Table 2**[15].
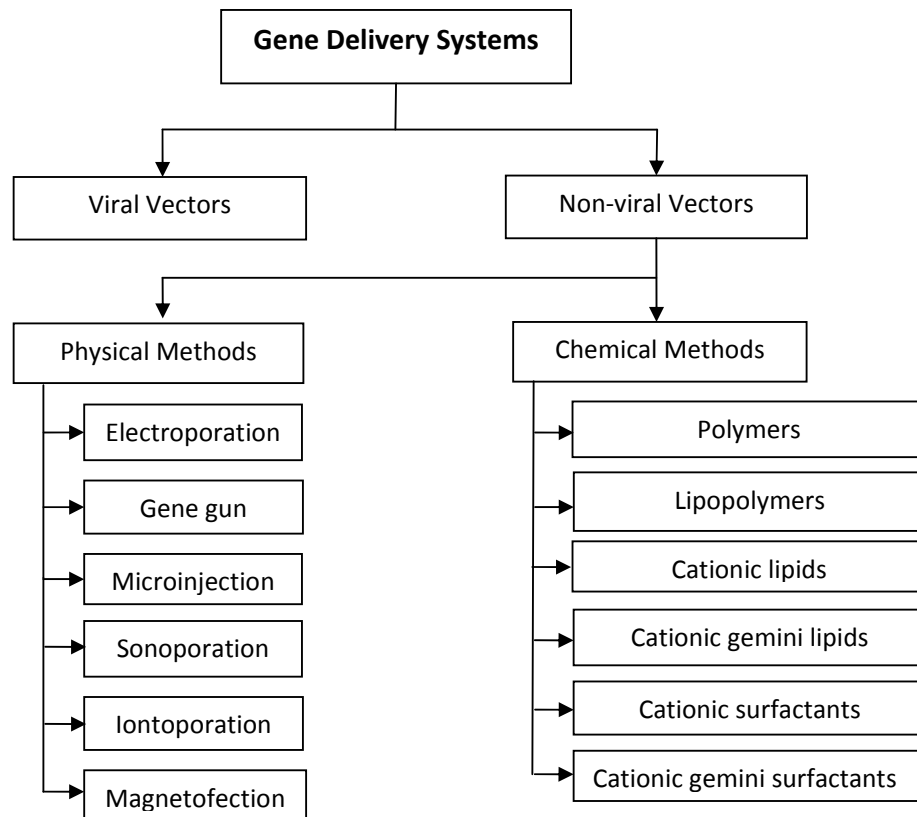
Figure 1. Classification of gene delivery vectors

1.3.1 Viral vectors for gene delivery

Due to their natural ability to infect cells efficiently, viral vectors such as retrovirus, adenovirus, adeno-associated virus and herpes virus, with part of their coding sequences replaced by that of a therapeutic gene have been investigated for *in vivo* viral-mediated gene delivery[16]. These vectors can be extremely efficient at producing expression, with essentially only a single viral particle necessary to induce a measurable effect. However, clinical applications of these vectors are hampered by the barriers of viral immunogenicity, mutagenicity, host rejection, inability to transfect non-dividing cells, possible oncogenicity and limited DNA cargo carrying capacity[17-20].

Table 2. Comparison among viral and non-viral methods of gene delivery

S. No.	Gene delivery method	Advantages	Disadvantages
1	Viral Vectors	High transfection efficiency in dividing and non-dividing cells; Possible targeted delivery; Systemic delivery is possible; Stable expression	Not easy to manufacture and require cold storage; Cumbersome quality control requirement; High cost, immunogenicity and oncogenicity risks; Size of gene to be inserted is limited
2	Non-viral vectors (a) Physical methods	Higher local tissue transfection efficiency; Transfection in all cell types, even in difficult to transfect cells is achievable; Easy process standardization; Less limit on gene size; Mostly *ex vivo* applicable.	Need for a specific instrument; Need of parameter optimization for different types of cells; Higher tissue damage observed.
	(b) Chemical methods	High *in vitro* transfection achieved; Possible *in vivo* organ targeting; Simple to manufacture in small batches and storage conditions are more flexible; Less costly; Less limit on gene size; Higher reproducibility compared to biological vectors; High commercial interest.	Low *in vivo* transfection efficiency; Low efficiency in primary and non-dividing cells; Limited clinical success; Consistent reproducible large scale manufacturing is not easy to achieve.

1.3.2 Non-viral vectors for gene delivery

Due to problems associated with viral vectors for gene delivery, a number of non-viral vectors including physical and chemical methods both, were developed. The physical methods involved the utilization of physical forces for gene delivery; while, chemical methods involved the use of polymeric, lipidic and other amphiphilic carrier systems.

1.3.2.1 Physical methods of gene delivery

(A) Electroporation

Naked gene delivery without any physical force and vector has been a disappointment, with therapeutically low gene transfection, and the use of vectors and methods employing physical force has been employed to enhance gene expression. Electroporosis has proved to be a successful method for drug delivery across the skin *in vitro* and *in vivo* and has also been used as an effective *in vitro* gene delivery system in prokaryotic and eukaryotic cells[21]. It employs physical force to import therapeutic drugs and macromolecules, such as DNA and proteins, from extracellular compartments into cells having transiently increased cell membrane permeability caused by short, pulsed electric field application, temporarily disrupting the structural integrity of cell membranes. This electric pulse is applied to the cells between the electrodes to form small membrane pores across the cell membrane within 3 milliseconds (ms), which may increase up to 120 nm within 20 ms [22, 23]. These formed pores are transient in nature, and get resealed within a few seconds to minutes, without causing any significant damage to the cell membrane of the exposed cells. During this period of time, a wide variety of macromolecules such as proteins, DNA and drugs can be introduced into the exposed cells by local electrophoretic effect.

(B) Gene gun method

Efficient gene gun delivery of macromolecules, like DNA, RNA, proteins, or peptides, to the target cells involves coating the macromolecules onto micro-carrier particles such as gold and tungsten, which are then introduced into the target cells with a high-velocity stream, using an electric discharge or a pressurized helium pulse[24]. The coated micro-carrier particles can be transported into numerous cells in a single delivery, as they easily pierce the cell cytoplasm of the target cells. A gene gun carries multiple genes by coating them onto the micro-carriers, inert, non-toxic, and sub-cellular sized (0.5–5 µm) spheres with enough density to enter the target tissues[25].

(C) Microinjection

Microinjection is a direct method to introduce DNA into either cytoplasm or nucleus. It is a microsurgical procedure conducted on a single cell, using a glass

needle (i.e., a fine, glass micro-capillary pipette), a precision positioning device (a micromanipulator) to control the movement of the micropipette, and a micro-injector. Extrusion of fluid containing the genetic material through the micropipette uses hydrostatic pressure. Injections are typically carried out under direct visual control, using a microscope[26]. Conceptually, microinjection is the simplest gene delivery method. However, it is difficult to apply. Although pronuclear injection of DNA is very efficient, it is a laborious procedure; only one cell at a time can be injected, typically allowing for only a few hundred cells to be transfected per experiment. The cytoplasmic injection of DNA has been observed to be less effective probably because of cytoplasmic degradation of DNA by cytoplasmic nuclease enzymes[27].

(D) Hydrodynamic method

Systemic administration of naked plasmid DNA by conventional needle injection is prone to degradation by nucleases and clearance by the mononuclear phagocyte system. However, hydrodynamic gene delivery combines naked DNA and hydrodynamic pressure generated using rapid injection of a large volume of fluid into a blood vessel, to deliver genetic materials into parenchyma cells[28].

This delivery system finds parenchyma cells as the main target because parenchyma cells are directly associated with capillary endothelial cells, allowing immediate access of DNA to parenchyma cells once the endothelial barrier is disrupted. In addition, the capillary wall is thin, stretchable, and relatively easy to break. The high pressure produced during the injection of a high volume of DNA solution into the blood vessels is the driving force for hydrodynamic gene delivery, by increasing the capillary endothelial permeability through enlargement of fenestrations and creating pores in the adjacent parenchymal cell plasma membrane, which provides the path for DNA to enter into the cell[29]. Shortly after injection, the membrane pore locks, and the injected DNA molecules are entrapped inside the cell.

(E) Sonoporation

In vivo electroporation and hydrodynamic and gene gun–mediated DNA delivery all have been shown to be very efficient techniques of DNA transfection. However, these techniques have been less preferred because of their invasiveness.

Hence, other non-invasive techniques such as sonoporation have also been studied for the delivery of plasmid DNA inside cells by employing external physical force.

Sonoporation works by transient permeabilization of the cell membrane and by transferring therapeutic DNA effectively across tissue and into cells by application of ultrasound energy. The ultrasound technique has shown the advantages of simplicity, non-invasiveness, and high safety profile, along with enhanced gene transfection *in vitro* and *in vivo* by 10 to 15 folds when compared with naked DNA injection[30]. The ultrasound technique is based on the principle of cavitation and micro-bubble formation. After applying ultrasound energy to a liquid during *in vitro* and *in vivo* conditions, formation of vapor-filled bubbles or cavities in the solution takes place. The diameter of these bubbles enlarges on applying energy, but on acquiring pressure, the bubbles later collapse. The collapse of these micro-bubbles releases a large amount of energy, which significantly permeabilizes the cell wall, alters the cell structure transiently, and enhances the entry of the macromolecules, including DNA, into the cytoplasm from extracellular milieu. This formation and collapsing of the ultrasound induced micro-bubbles is called cavitation[31].

(F) Iontophoresis

Iontophoresis involves the application of a low-density electric current for enhancing the penetration of preferably charged molecules through pre-existing cellular pathways in cells and tissues[32]. This method is used to enhance the penetration of nucleic acids non-invasively. The ease of application, minimization of systemic side effects and increased drug penetration directly into the target region has resulted in an extensive clinical use of iontophoresis mainly in the transdermal field[33].

The mechanisms of iontophoretic transport across a membrane include direct interactions of the electric field with the charge of an ionic compound (electrophoresis or electro-migration), convective solvent flow affecting the transport of both neutral and ionic compounds (electro-osmosis), and electric field-induced pore formation in the membrane (electro-permeabilization)[34].

(G) Magnetofection

The technique of magnetofection is used to deliver DNA to the target organ, using the magnetic field. Magnetofection basically involves attaching DNA onto a magnetic nanoparticle coated with a cationic polymer like polyethylenimine[35]. The magnetic nanoparticles are generally made up of a bio-degradable substance like iron oxide, and its coating onto the polymeric particle is done by salt-induced colloidal aggregation. These prepared nanoparticles are then localized in the target organ by the application of an external magnetic field, which allows the delivery of attached DNA to the target organ. This method also increases the uptake of DNA into target cells as the contact time between the target organ and magnetic nanoparticles increases. In addition, the magnetic field pulls the magnetic nanoparticles into the target cells, which also helps to increase the uptake of DNA[36].

1.3.2.2 Chemical methods for gene delivery

One of the widely used non-viral gene delivery systems comprises of an expression repository, inserted into a plasmid which is ionically complexed to cationic lipid (lipoplex), cationic polymer (polyplex), or a mixture of cationic polymer and lipid (lipopolyplex). These complexes carry an overall positive charge which is responsible for interaction with the cellular membrane. The complexes are subsequently endocytosed and the DNA complex or DNA alone is transferred to the nucleus.

1.3.2.2.1 Polymer based gene delivery vectors

The polymers play a vital role in the delivery of DNA to the cell. In contrast to conventional polymeric formulation, where the drug either simply diffuses or is released by hydrolysis or esterification of polymer, the DNA cannot diffuse easily because of its high molecular weight. Thus, polymeric vectors continue to play a key role in interaction with cell membranes, intra-cellular trafficking, and transcription of the trans-gene in the nucleus. An efficient vector polymer delivers the trans-gene to the nucleus after bypassing several barriers and their classification is shown in **Figure 2**. The basic mechanisms of DNA polymer complex formation involve either condensation of DNA with polymers (e.g., poly(*l*-lysine), polyethylenimine) or

encapsulation of DNA into the polymers (e.g., poly(β-aminoesters), polylactide, poly(lactide-*co*-glycolide)). Cationic polymeric gene vectors, owing to their positive charge, usually form complexes as a result of electrostatic interaction between cationic amino groups of polymeric gene vectors and anionic phosphate groups of DNA. The so-formed complexes are called polyplexes[37].

(A) Condensing polymers

Condensing cationic polymeric gene vectors, owing to their condensing property and positive charge, usually condense DNA to 1/1000 to 1/10,000 of its original volume, by forming complexes. Various polymers of this class used for gene delivery are briefly discussed below:

```
                    Polymeric carriers for gene delivery

        Condensing                              Non-condensing
        polymers                                polymers

  Non-biodegradable    Biodegradable      Non-biodegradable    Biodegradable
  polymers             polymers           polymers             polymers

  Poly (l-lysine)      Poly( ß-amino      Poloxamers           Poly(d,l-lactide-co-
  Polyethylenimine     esters)            Poly(N-vinyl         glycolide)
  Poly(2-(dimethylamino)  Polyesters      pyrrolidine          Poly
  ethyl methacrylate)                                          (alkylcyanoacrylate
```

Figure 2. Classification of polymeric vectors used for gene delivery

(a) Poly[*l*-lysine] (PLL) and copolymers

PLL and its copolymer **(Figure 3)** were the first cationic polymers widely explored for *in vivo* gene delivery. PLL is a bio-degradable linear polypeptide of varying length consisting of 20–1000 amino acids[38]. Due to its positive charge (ε-

amine groups), PLL is able to condense DNA in nano-range of 50-100 nm and protects DNA from cellular degradation by nucleases and has shown better transfection efficiency compared to naked DNA. However, it is unstable in physiological saline, exhibits toxicity to cells, and its complex with DNA is precipitated in physiological saline[39]. Better results are obtained with molecular weight above 3000 Da, as smaller chains lose their ability to bind in physiological saline. Very high molecular weight PLL is desirable for higher transfection efficiency; however, it increases associated toxicity and the tendency of aggregation, depending upon its ionic strength[40, 41]. Although, intra-cellular uptake of PLL polyplexes is quite efficient, their successive escape from intra-cellular vesicles into the cytoplasm presents a major bottleneck. The transfection efficiency of polyplexes of PLL increases more than 1000-fold by addition of a lysosomotropic agent (e.g., chloroquine), which is believed to act by reducing lysosomal degradation and enhancing the release of DNA into the cytoplasm[42]. Modifications in the PLL have been done to reduce cytotoxicity [(PLL-polyethylene glycol) copolymer[43]] and specific interactions [(antibody conjugated PLL, folate conjuagated PLL)[44]].

(b) Polyethylenimine (PEI) and copolymers

PEI is a cationic polymer composed of several 43 Da ethyleneimines (CH_2-CH_2-NH) as a basic moiety **(Figure 3)** and synthesized by acid-catalyzed aziridine (ethyleneimine) ring opening or by hydrolysis of poly(2-ethyl-2-oxazolium)oxazoline, leading to branched or linear polymeric backbones. Unlike PLL, PEI shows efficient gene transfer without the need of any agent facilitating receptor-mediated uptake as it promotes endosomal escape from intracellular vesicles. This attribute is based on the "proton sponge" effect[45]. PEI has a very high charge density because every third atom in the backbone is amino nitrogen capable of being protonated over almost the entire *p*H range, thus offering a considerable buffering capacity[46]. PEI is able to change its protonation with respect to surrounding *p*H. Electrostatic interaction between these positively charged amino groups in PEI and the negatively charged phosphate groups in DNA molecules permits condensation of DNA, thereby causing the formation of polyplexes. The buffering provided by PEI due to acidic *p*H in the endosome causes proton accumulation and subsequent influx of chloride ions into the vesicle. Further

osmotic swelling by the influx of water ruptures some of the endosomes, which allows the escape of PEI–DNA complexes into the cytosol.

The condensation process and the diameter of polyplexes formed depend on the N/P ratio (PEI nitrogen/DNA phosphate), PEI molecular weights and the salt concentration. Generally, the N/P charge ratio of 6 or higher generate polyplexes of size 50 nm that possess considerable buffering capacity at lower endosomal *p*H[45]. As molecular weight of PEI is increased from 600 to 70,000 Da, transfection efficiency also increased due to easy entry into cells and better protection of the DNA[47]. However, high-molecular-weight polymers also exhibit higher cytotoxicity[48]. PEI revealed superb transfection efficiency *in vitro*; but *in vivo* transfection efficiency was modest. Also the toxicity is a major constraint for its clinical use. Linear PEI is reported to be less toxic than branched PEI. PEI exhibits non-specific interactions via positively-charged complexes interacting with negatively charged components of the blood, thereby removing particles out of circulation. The common mechanisms of particle removal are nonspecific binding to erythrocytes, RES uptake of the particles and complex segregation by albumin[49]. The major concerns in delivery of PEI are cytotoxicity and aggregation. In an attempt to reduce cytotoxicity and aggregation, PEI-grafted PEGs (PEI-*g*-PEG) with different PEG grafting ratios were synthesized[50]. Targeting moieties have also been attached to PEI such as folic acid and antibodies for targeted gene delivery[51, 52].

(c) Chitosan

Chitosan is a biodegradable amino-polysaccharide composed of two subunits, *D*-glucosamine and *N*-acetyl-*D*-glucosamine linked together by *β*-(1,4)-glycosidic bonds (**Figure 3**). The amino groups of chitosan confer positive charge to chitosan. These amino groups exhibit intrinsic *p*Ka values of 6.5 and thus chitosan behave as a polycation at acidic and neutral *p*H[53]. The cationic charge of chitosan enables it to interact with negatively charged polymers, macromolecules and certain polyanions in an aqueous environment. From a biopharmaceutical point of view, chitosan has a special feature of adhering to mucosal surfaces, a fact that makes it a useful polymer for mucosal drug delivery[54]. The low toxicity, bio-compatibility and bio-degradability of chitosan make it attractive for gene delivery purposes[55]. Several chitosan

derivatives have been synthesized in the last few years in order to obtain modified carriers with altered physicochemical characteristics[56].

(d) Dextran

Diethylaminoethyl (DEAE)-dextran was the very first chemical vector used for DNA delivery **(Figure 3)**. Initially in 1965, Vaheri and Pagano reported use of DEAE-dextran to enhance the viral infectivity of cells[57]. DEAE-dextran-mediated transfection method has gained much attention in the early to mid-1980s because of the simplicity, efficiency, and reproducibility of the procedure[58, 59]. Similar to cationic polymers, DEAE-dextran forms complexes with DNA through electrostatic interaction. Owing to their net positive charge, these complexes are assumed to bind negatively charged plasma membrane and then are internalized through endocytosis. DEAE-dextran exhibited higher transfection efficiency than calcium phosphate; however, it varies with the type of cells and other experimental conditions. Several dextran derivatives are synthesized for improved transfection efficiency. Dextran-spermine polycations exhibited comparable transfection efficiency to Transfect and DOTAP[60].

(e) Poly(β-aminoesters)

To overcome cytotoxicity and poor transfection efficiency of polymeric carriers such as PLL and PEI; modifications of the chemical structures of the polymers have been done to achieve the desirable attributes, such as bio-degradability, minimal cytotoxicity, and improved transfection efficiency. Poly(β-aminoesters) **(Figure 3)** are synthetic hydrolytically biodegradable cationic polymers with tertiary amines in their backbones that are synthesized by addition of either primary or bis(secondary) aliphatic amines to diacrylate esters[61-62]. Moreover, pH-dependent solubility of several poly(β-aminoesters) favors its formulation in nanoparticle or nanosphere formulations that can prompt the polymer degradation and release of encapsulated DNA in the acidic pH of endosomal vesicles[63]. Owing to its cationic nature, they are capable of condensing DNA into complexes of the order of 50–200 nm.

(f) Poly[2-(dimethyalamino)ethyl methacrylate](pDMAEMA)

pDMAEMA (**Figure 3**) is a water soluble cationic polymer, capable of forming compact complexes by electrostatic interaction with DNA[64]. The size of the complex depends on molecular weight. High molecular weight pDMAEMA (>300 kDa) was capable of condensing DNA effectively into particles of 150–200 nm, whereas low molecular weight pDMAEMA forms larger particles of size 0.5–1.0 µm[65].

(g) Polyesters

Polyesters are water-soluble, readily degradable cationic polymers. Poly(4-hydroxylproline ester) (PHP) was the first polymer of this class used as a gene vector[66]. PHP formed complex with DNA and demonstrated stability for a minimum period up to 4 hrs in presence of nucleases. The transfection efficiency of PHP polyplexes was comparable to that of PLL. In addition, serum proteins did not affect the transfection efficiency of PHP-based polyplexes. Importantly, PHP possesses significantly reduced cytotoxicity as compared to PEI or PLL[67].

Poly[*γ*-(4-aminobutyl)-*L*-glycolic acid] (PAGA) (**Figure 3**) is an amine-substituted polyester that showed rapid initial degradation followed by slow hydrolysis for several months. PAGA could efficiently condense a *p*DNA to form nanoparticles with an average size of 326 nm[68]. The PAGA–DNA complexes revealed stability similar to PHP. PAGA–DNA complexes were stable for 8 hrs and dissociated completely in 1 day, showing their suitability for gene expression. PAGA polyplexes demonstrated three fold higher transfection activity compared to PLL polyamide analogue of PAGA *in vitro* without any cytotoxicity in the concentration range tested[69].

(B) Non-condensing polymers

(a) Poloxamers (Pluronic® Block Copolymers)

Pluronic® block copolymers are composed of hydrophilic ethylene oxide (EO) and hydrophobic propylene oxide (PO) blocks arranged in a basic A–B–A structure EOx-POy-EOx (**Figure 3**). BASF Corp. (Parsippany, NJ, USA) manufactures over 30 Pluronic® molecules with different lengths of EO (NEO) and PO (NPO) blocks.

These molecules are characterized by different hydrophilic–lipophilic balance (HLB) and critical miceller concentration (cmc). Pluronic® block copolymers are synthesized by sequential addition of PO and EO monomers in the presence of an alkaline catalyst[70]. Initially the reaction proceeds with polymerization of the PO block followed by the growth of EO chains at both ends of the PO block. Highly purified block copolymers are obtained by chromatographic fractionation to remove the presence of admixtures, mainly of the PPO homopolymer and block copolymers containing shorter PEO chains. Unimer above cmc and individual block copolymer molecules have the tendency to self-assemble into micelles in aqueous solutions, through a process called micellization. The driving force for micellization is the hydrophobic interactions of the PO blocks. The micelles have a hydrophobic PO core and a hydrophilic EO shell, and their shape can be spherical, lamellar, or rod like, depending on the lengths of the PO and EO chains[71]. Polycation-conjugated Pluronics® were used as the vector in gene delivery. The conjugates retained their inherent ability to self-assemble into micelle-like aggregates. In presence of DNA, conjugates form mixed micelle-like aggregates exhibiting two types of interaction; hydrophobic interactions of the PO chain segments and electrostatic interactions of the polycation and DNA. The hydrophilic EO blocks of Pluronic® impart stability to the complex in aqueous dispersion. Initially, Pluronics® demonstrated increased expression of genes delivered into cells using non-viral vectors[72-73].

(b) Poly(*D,L*-lactide-co-glycolide)

Poly(lactide-co-glycolic acid) (PLGA) and polylactic acid (PLA) are the most widely studied bio-degradable and biocompatible polymers used for formulating DNA matrix particles **(Figure 3)**[74]. PLGA is approved for human use by the FDA. The long history of safe use in drug delivery of protein and peptides in medical applications such as resorbable sutures, screws, and implants makes PLGA a promising candidate for use in DNA delivery. PLGA polymeric matrix protects DNA from nucleases and allows modulated DNA release from micro- or nanoparticles. Thereby, slow release of DNA from the micro- or nanoparticles facilitates sustained levels of gene expression. PLGA degrades through a process of hydrolysis by breakage of the chemical bond between glycolide and lactide monomers to yield

individual monomers of lactic acid and glycolic acid, which are removed from the body by the citric acid cycle. Because the rate of degradation is slow, degraded produ-
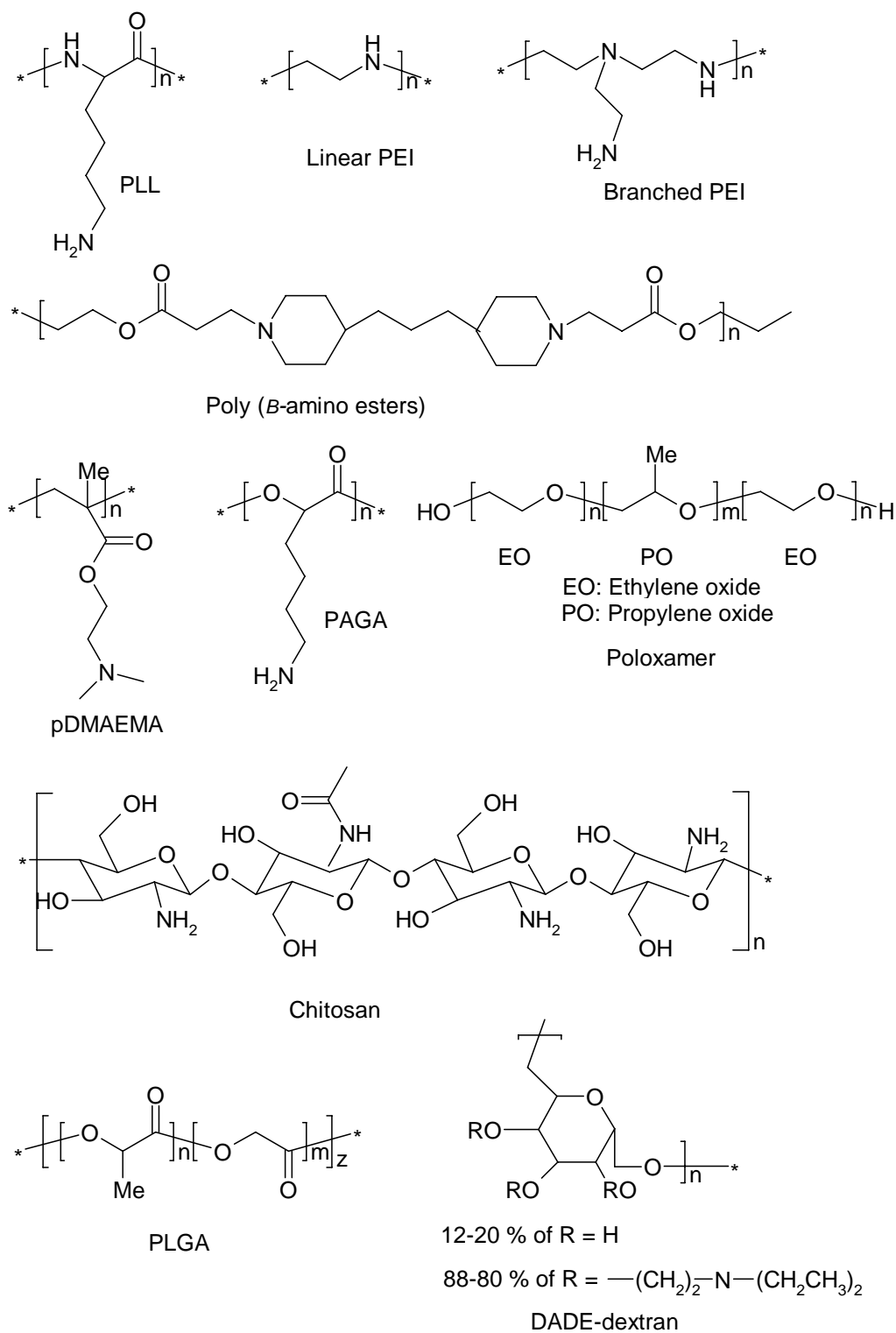
Figure 3. Chemical structures of polymer based gene delivery vectors

ct do not affect the normal functioning of the cell. DNA-loaded PLGA is generally formulated using the water–oil–water double-emulsion solvent-evaporation technique[75]. However, the spray-drying technique was also reported in some studies[76].

1.3.2.2.2 Lipid based gene delivery vectors

Lipids are amphiphilic organic molecules that contain a hydrophobic part and a hydrophilic head group. Various types of aggregates that are formed in water have numerous applications, which include gene delivery, drug encapsulation, developing supra-molecular assemblies and gels etc[77].

Molecular design of lipids is currently an active area of research in chemical biology. Depending upon the charge on the head group, lipids can be cationic, anionic or neutral, but cationic lipids are currently receiving an intense attention among researchers, because of their promise in gene delivery. Due to their opposite surface charge, cationic liposomes can form an overall positively charged complex with negatively charged DNA. Lipid-DNA complexes (popularly known as lipoplexes) do not face any electrostatic barrier in penetrating the negatively charged biological cell surfaces and are therefore endocytosed by the cell plasma membrane. In addition, cationic liposomes also protect DNA from attack by the *en-route* deoxyribonucleases (DNases). Thus, broadly speaking, cationic transfection lipids are designed to compact DNA so that favorable cellular uptake of the lipoplexes results. The transfection efficiency is not determined solely by one part of the cationic lipid but by combination of them. The optimal characteristics of the hydrophobic, head group and linker depend upon the general structure of the lipid. Different types of lipids can have opposite structural requirements in terms of the optimal length of hydrocarbon chains, types of linkages and headgroups. Therefore, modular approach is useful for planning and designing new vectors. Trends in aggregation properties of the liposomes can be obtained by studying the effect of variations in the chemical structures of different parts of cationic lipids. On the basis of structure of polar heads, cationic lipids have been classified into four different categories:

   a)   Quaternary ammonium salt lipids,
   b)   Lipoamines,
   c)   Cationic lipids containing quaternary ammonium salt and lipoamines, and

      d)   Amidinium salt lipids and miscellaneous cationic entities.

(A) Quaternary ammonium salt lipids

      Cationic lipid, *N*-[1-(2,3-dioleyloxy)propyl]-*N,N,N*-trimethylammonium chloride (DOTMA) the first cationic lipid used for gene delivery by Felgner et al. in 1987,[78] belongs to this class of quaternary ammonium salt lipids. These positively charged groups were basically quaternary ammonium salts linked to a lipid moiety that played the role of maintaining a self-assembling system with DNA and promoted fusion with the cell membrane. By virtue of its excess positive charges at the surface of the complex, cationic lipid DOTMA facilitates adhesion to the cell membrane. The combination of cationic lipid DOTMA with neutral lipid DOPE termed as Lipofectin[TM] was described as a liposomal vector by Syntex Inc.[79].
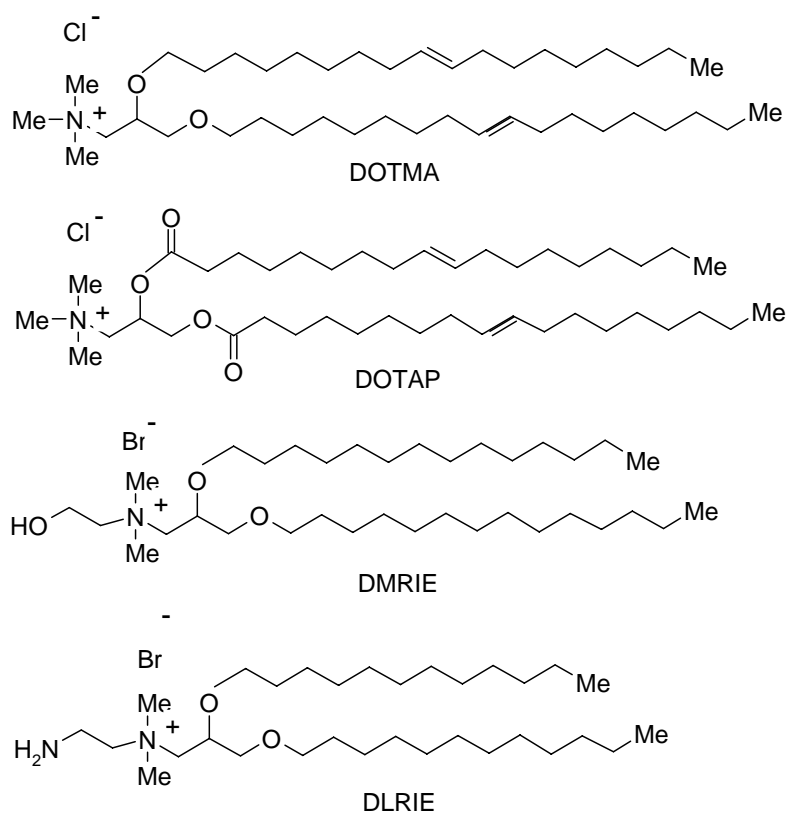
Figure 4. Chemical structures of quaternary ammonium salt lipids

When diether bonds of DOTMA were replaced by diester bonds, they formed a bio-degradable agent, 1,2-dioleoyloxy-3-(trimethylammonio)propane chloride (DOTAP) **(Figure 4)**, which has been shown to accumulate less in tissues than DOTMA. The quaternary ammonium salts of DOTMA can be substituted with alkylene alcohol or alkylene amines and differing lipid chains, to give 1,2-dimyristyloxypropyl-3-dimethyl-hydroxyethyl ammonium bromide (DMRIE) and *N*-(3-aminopropyl)-*N*,*N*-dimethyl-2,3-bis(dodecyloxy)-1-propanaminium bromide (DLRIE) **(Figure 4)**. Few compounds of this class have demonstrated a substantial increase in transfection efficiency and moved successfully to the clinical stage[80, 81]. To discover the structural characteristics responsible for high transfection efficiency in DOTMA, a series of DOTMA analogues have been synthesized[82, 83] that concluded that paired oleoyl chains, such as a lipid anchor attached to the cationic head group by ether linkage to the 1,2 position of the glycerol backbone, were responsible for high transfection efficiency. Polyquaternary ammonium salt has also gained much attention for gene delivery. Life Technologies has described a family of polyquaternary ammonium salts such as (*N,N',N'',N'''*-hexamethyl, *N,N',N'',N'''*-tetrapalmyl)spermine and (*N,N',N'',N'''*-tetramethyl, *N,N',N'',N'''*-tetrapalmyl)spermine, which are co-formulated with DOPE **(Figure 5)**[84]. These compounds demonstrated comparable transfection efficiency with reduced cytotoxicity. University of California described a family related to DOTAP/DOTMA, possessing two quaternary ammonium salts, for example, Poly Gum/DOPE **(Figure 5)**[85]. These compounds demonstrated enhanced *in vitro* gene transfer on NIH3T3 cells as compared to DOTAP/DOPE.

(*N,N',N'',N'''*-Hexamethyl,*N,N',N'',N'''*-tetrapalmyl)spermine

(*N,N',N'',N'''*-Tetramethyl,*N,N',N'',N'''*-tetrapalmyl)spermine

PolyGum
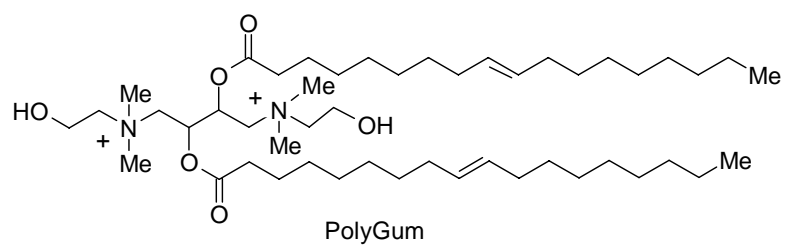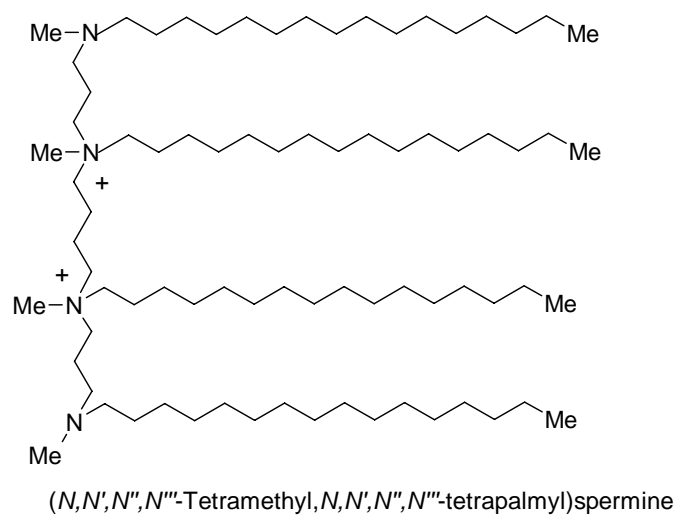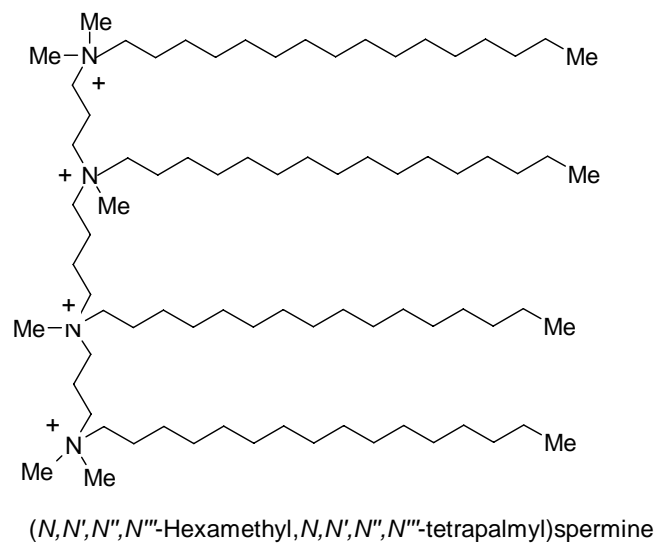
Figure 5. Chemical structures of polyquaternary ammonium salt lipids

(B) Lipoamines

Behr proposed another rational approach for DNA vectorization, which differs from Felgner's quaternary ammonium salt lipids. The approach utilizes the property of naturally nucleus-occurring polyamine spermine, which is supposed to condense DNA during cell division. By attaching a lipophilic anchor to spermine, dioctadecylamidoglycylspermine (DOGS or Transfectam[TM]) was prepared as the first cationic lipid of this class of transfection vectors **(Figure 6)**[86, 87].
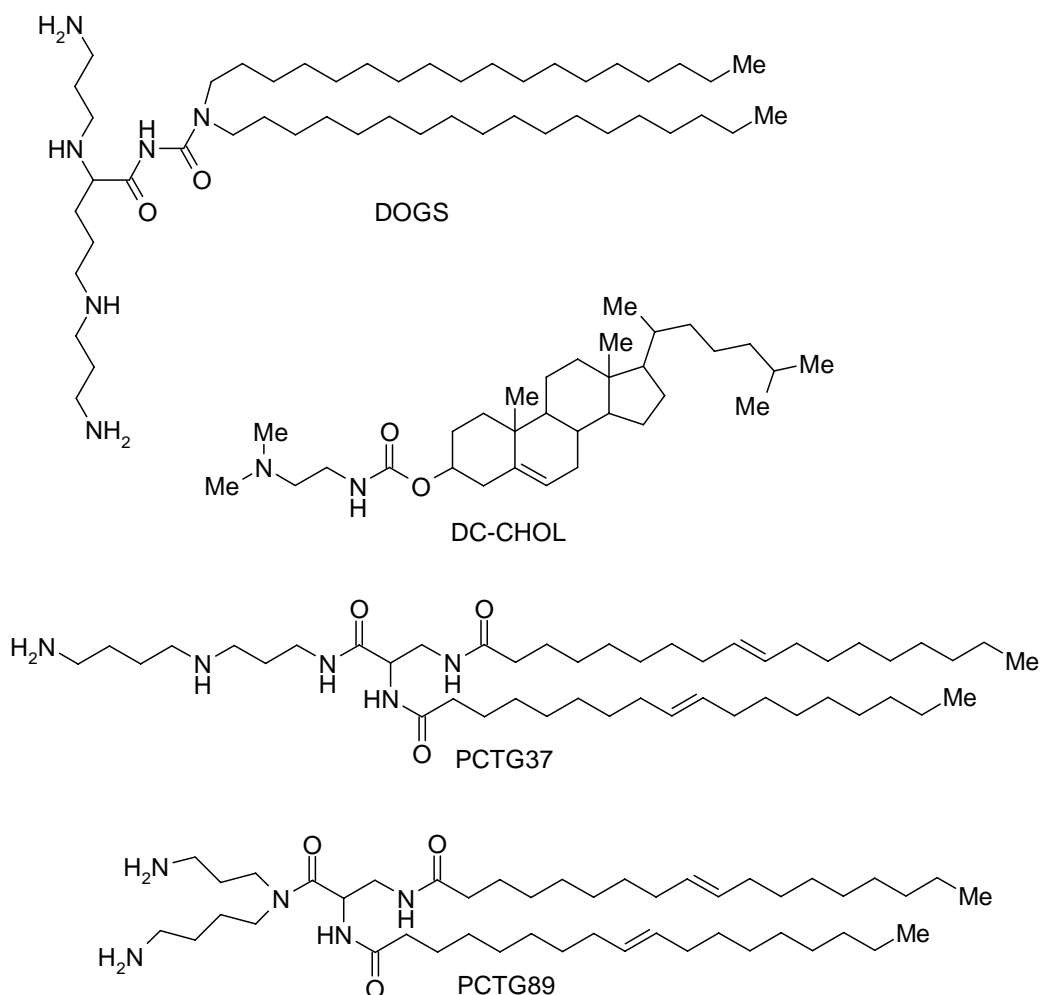
Figure 6. Chemical structures of lipoamines used for gene delivery

It was observed that DOGS confer increased transfection efficacy as compared to quaternary ammonium salts. Unlike quaternary ammonium salts, lipoamines

condense DNA efficiently without the aid of any helper lipid for attaining significant levels of transgene expression *in vitro* and *in vivo*[88]. With the objective of reducing side effects associated with protein kinase C inhibition, tertiary amines are introduced instead of quarternary amines. The lipoamine DC–Chol was introduced with the tertiary amine linked through a spacer to a cholesteryloxy-carbonyl lipid **(Figure 6)**[89]. In addition, another aspect of this strategy was the introduction of different hydrophobic group cholesteryl carbamates, which do not form bilayers but rather intercalate into bilayers formed by DOPE. Because this DC–Chol does not confer enough compactness to DNA, it could be co-formulated with an additive lipid to obtain significant transfection level. DC–Chol complexes of DNA were the first to be used in clinical trials[90, 91]. Insufficient physicochemical characterization of DC–Chol complexes prior to those trials does not justify the modest result obtained in terms of formulation.

Moreover, spermidine derivatives, pcTG 37 and T-shaped pcTG89 derived from diaminopropionic acid were proposed as effective transfection vectors either alone or in combination with DOPE **(Figure 6)**[92]. These compounds demonstrated efficient transfection against dog myoblast and human pulmonary epithelial carcinoma A549 cells *in vitro* and C57BL/6 mice *in vivo*.

(C) Cationic lipids containing both quaternary ammonium salt and lipoamines

The first cationic lipid of this class containing both quaternary ammonium salt and polyamines in one lipid was 2,3-dioleyloxy-*N*-(2-sperminecarboxamido)ethyl-*N,N* dimethyl-1-propanaminium trifluroacetate (DOSPA) **(Figure 7)** which was co-formulated with DOPE to give Lipofectamine[TM 93, 94]. Although Lipofectamine[TM] is a highly efficient transfecting agent, relatively high cytotoxicity *in vitro* and *in vivo* has prevented its further clinical development. Later, GAP-DLRIE containing one amine and one quaternary ammonium salt **(Figure 7)** was introduced, which displayed a high level of transfection with low cytotoxicity[80]. Life Technologies has proposed DOSPA and GAP-DLRIE and compounds A and B containing carbamate linker bonds, with the objective of improving bioavailability and reducing toxicity **(Figure 7)**[95]. These compounds displayed low toxicity when tested *in vitro* and *in vivo*.
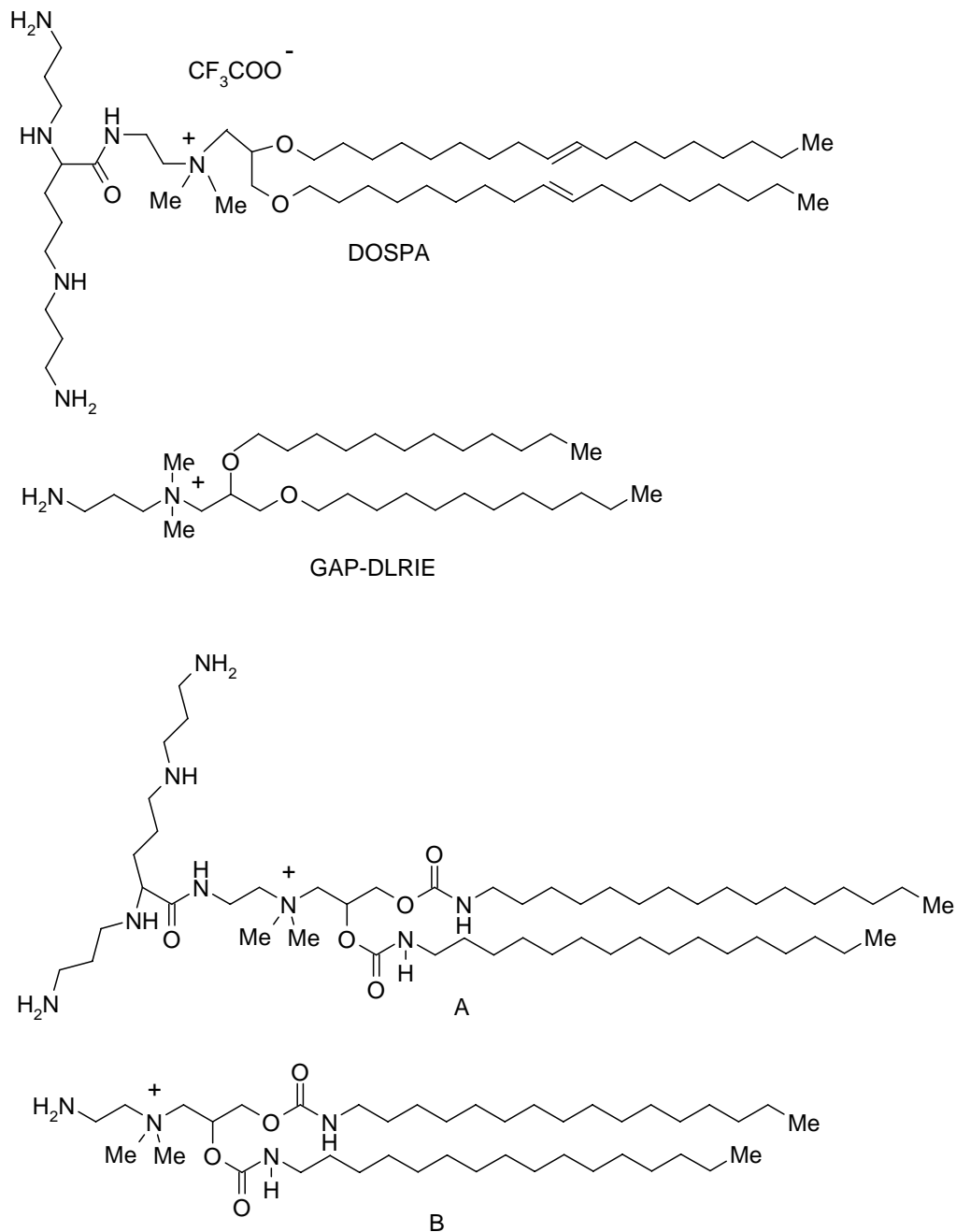
Figure 7. Cationic lipids containing both quaternary ammonium salt and lipoamines-I

The use of piperazine backbone to synthesize mixed polar head cytofections C, D, and E was proposed by Vical Inc. (**Figure 8**)[96, 97]. These compounds, when co-formulated with DOPE, demonstrated comparable or higher transfection efficiency against C2C12 and COS-7 cells as compared to the DMRIE-DOPE system. Following

in-vivo administration, compound C displayed higher transfection activity than GAP-DLRIE in mouse tumor assay and intra-lung transfection assay. Also, transfection assay after IP administration in C57/B16 mice displayed a modest result in some
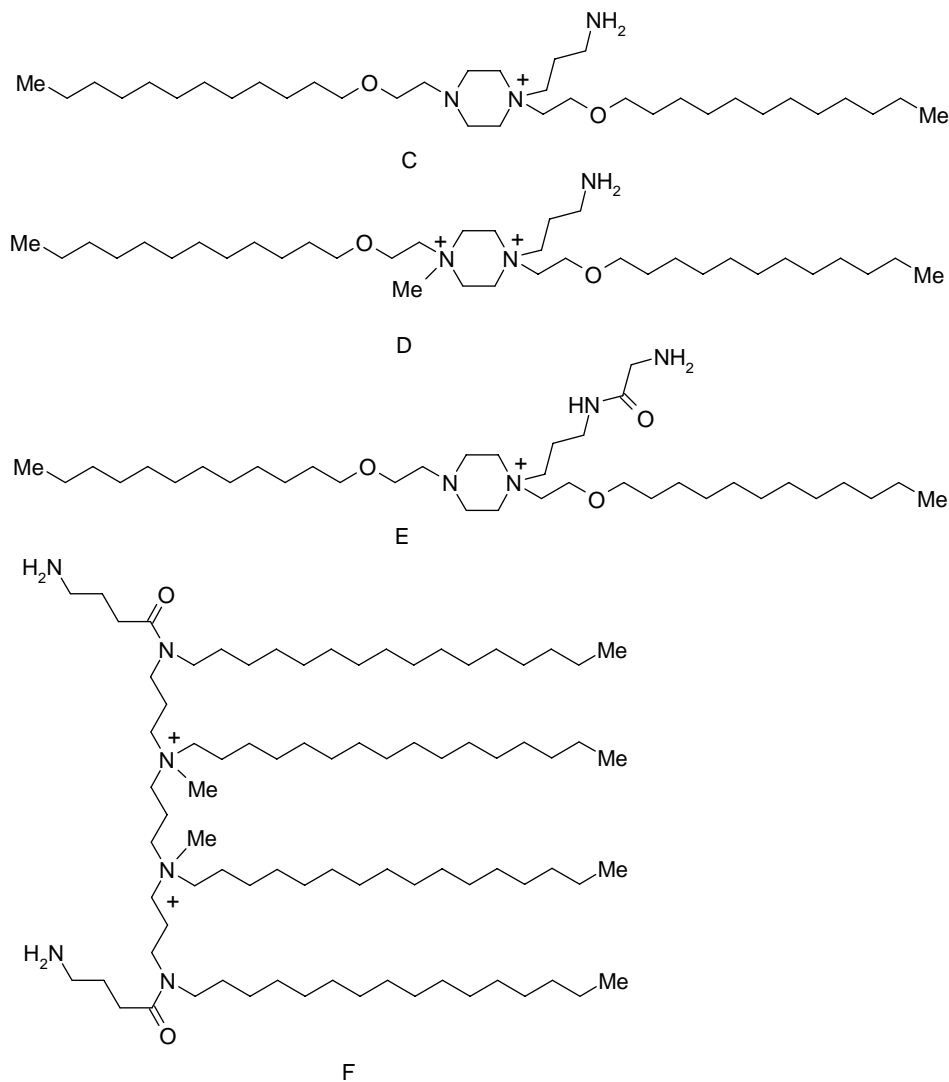
Figure 8. Cationic lipids containing both quaternary ammonium salt and lipoamines

II

cases but was lower than those obtained for GAP-DLRIE. Haes introduced spermine scaffold–based diamino-bis-quarternary ammonium salt lipid, F **(Figure 8)**[98]. These compounds, when co-formulated with DOPE, demonstrated 2 to 2.4 folds transfection

efficiency against HepG2 and Hela cells as compared to *N,N',N'',N'''*-tetraethylpalmitylspermine (TMTPS). In addition, its transfection efficiency was more than five folds higher than Lipofectin[TM] when tested in primary human trachea-bronchial cells.

(D) Amidinium salt lipids and miscellaneous cationic entities

Ruysschaert et al. demonstrated the use of amidine-based moieties as efficient transfection vectors[99]. Megabios Corp. revealed the first gene delivery system based
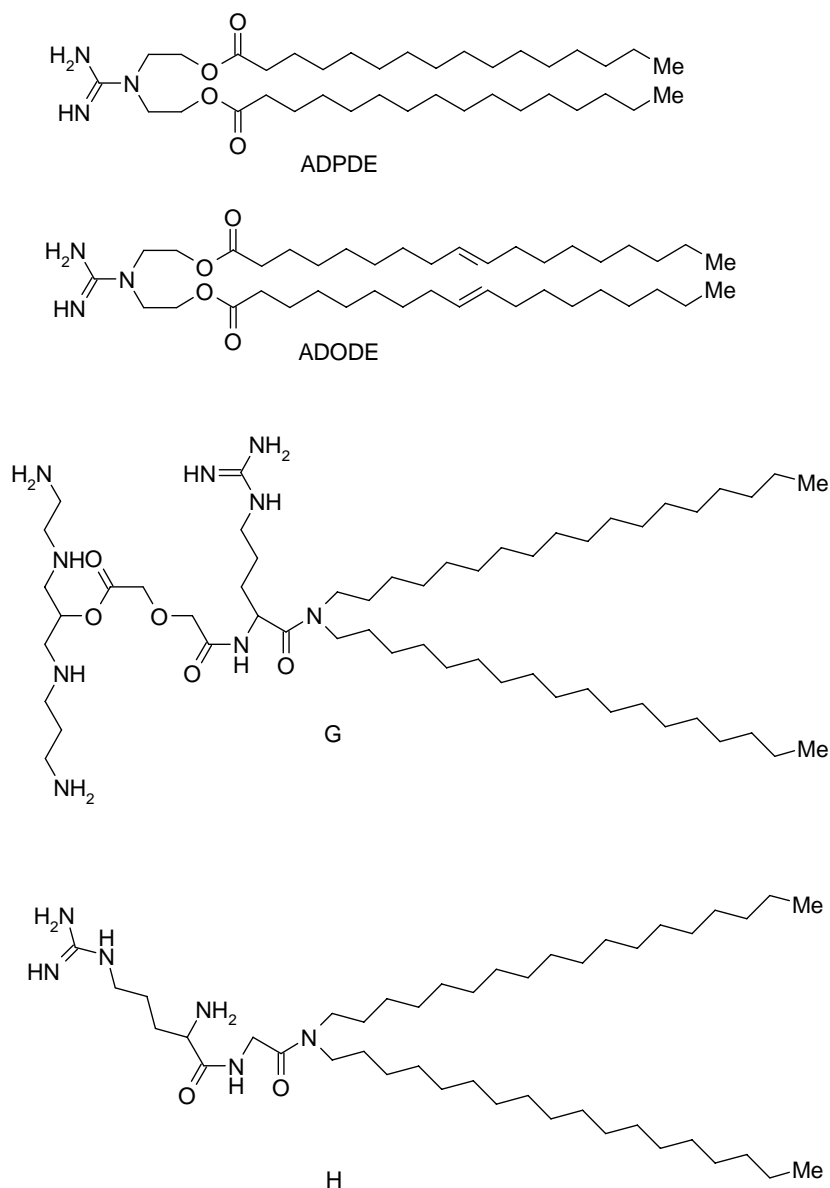
Figure 9. Amidinium salt lipids and miscellaneous cationic entities

on amidinium lipids[100]. Following i.v. administration of compounds ADPDE and ADODE co-formulated with cholesterol demonstrated comparable transfection efficiency, specifically, chloramphenicol acetyl transfer (CAT) gene activity of DDAB–Chol complexes when tested in several organs of mice.

Byk et al. introduced guanidinium group in the position of linker between lipids and polyamine compounds that gave compound G **(Figure 9)**, which demonstrated enhanced transfection efficiency as compared to Lipofectamine[TM] on NIH3T3, Rabbit SMC, 3LL Lewis lung, and CaCO-2 colon carcinoma cell lines[101]. In another study, the same group has introduced cyclic guanidine–based moieties in lipopolyamine to obtain compounds of either linear or globular polar head groups[102]. In another strategy, amidinium moiety was introduced in the form of arginine amino acid[103]. This compound H **(Figure 9)** co-formulated with DOPE, demonstrated transfection efficiency similar to Lipofectin[TM] and DC–Chol using *β*-galactosidase plasmid when injected intra-dermally into Swiss Webster mice.

1.3.2.2.3 Gemini amphiphiles-based gene delivery vectors

Gemini amphiphiles (GA) represent a class of synthetic amphiphiles that have been designed to improve the transfection properties of conventional amphiphiles. The polar 'head-groups' of cationic lipidic non-viral vectors generally consisted of monovalent quaternary ammonium salts (as in cetyl trimethylammonium bromide, CTAB and DOTAP). It appeared that introduction of a second quaternary ammonium group could increase the strength of its interaction with DNA and perhaps generate an improved transfection agent. Thus, synthetic route to generate a molecule with two dimethylammonium groups, and two long-chain alkyl groups diquaternary ammonium salts, constitute a new class of reagents (GA) for mediating transfection of DNA. Many of the GAs reported in the literature form vesicle system or liposomes when co-formulated with helper lipids above their transition temperature. These formulated GAs when mixed with plasmid DNA, condensed it into small particles known as lipoplexes providing protection to DNA. The transfection efficiency of these lipoplexes *in vitro* depend upon a number of factors like chemical structure of the GA, the structure and proportion of helper lipid, N/P ratio between the cationic part and DNA, size and zeta potential of prepared lipoplexes, and the type of cell line

used. GAs can be broadly classified into two classes on the basis of their structures as follows:

1) Gemini analogues of lipids (multiple head groups and at least four or more hydrophobic chains), and

2) Gemini analogues of surfactants (multiple head groups and at least two or more hydrophobic chains).

Many of the GAs have been reported for gene delivery applications, their structure–activity correlations and physicochemical properties in relation to transfection efficiency are of current interest in the area of gene delivery.

1.3.2.2.3.1 Gemini analogues of lipids in gene delivery

The concept of using gemini lipids for gene delivery arose from cardiolipins (glycerol-bridged dimeric phosphatidic acids), a class of complex dimeric phospholipids that occur mainly in the heart and skeletal muscles[104]. Dimeric structure of cardiolipins provides them capabilities to form micellar, lamellar and hexagonal phases in aqueous dispersions. In biological systems cardiolipin exists mainly in the lamellar phase, with a strong tendency to form transient non-lamellar structures, which deeply affect the membrane functions[105]. Cardiolipin **(Figure 10)** has two negatively charged phosphate groups, which can be replaced with quaternary ammonium groups to give cationic cardiolipin analogues so that they can effectively bind to the negatively charged DNA through electrostatic interactions. The gemini lipids reported so far in the literature for gene delivery applications can be categorized, depending upon their structures, as discussed below.

(A) Cationic cardiolipin analogue gemini lipids

A number of cationic cardiolipin analogue gemini lipids have been synthesized and manipulated suitably taking inspiration from cardiolipins to meet certain key requirements of gene delivery. For example, the negative phosphate groups of cardiolipins were replaced by the quaternary ammonium groups to facilitate the electrostatic interaction with negatively charged DNA; the hydrophobic chains were connected to the hydrophilic core by an ether linkage, rather than an ester linkage, because cationic lipids with ether linkage, such as DOTMA had been shown

to display higher transfection efficiency in comparison to the corresponding ester analogues, such as DOTAP[106]. And finally, the hydrophilic spacer has been varied by introducing oxyethylene unit(s) as shown in the **Figure 10**.

Ahmad *et al* synthesized different stereoisomeric cardiolipin analogues as shown in **Figure 10** (i.e. CGL(1) in the S/S form and stereoisomeric mixture; CGL(2) in pure S/S, R/R forms and as mixture of stereoisomers; CGL(3) and CGL(4) only in the R/R form). When these gemini lipids were evaluated as liposomal formulations with DOPE on Chinese hamester ovary (CHO) cells, the order of transfection efficiency followed the trend, CGL(2)> CGL(3)> CGL(4). The formulations with CGL(4) showed minor efficiency, which was because of the bulky hydrophilic region hindering the formation of a fusogenic hexagonal H_{II} phase, that promoted the escape of DNA. Additionally, these formulations exhibited low toxicities to the cells[107].

The cardiolipin analog CGL(2), was studied *in-vitro* on many human cell lines like lung cancer A549; ovarian cancer SK-OV-3; prostate cancer PC-3; breast cancer MX-1 and MDAMB-231; hepatocellular carcinoma HepG2 and CHO cells etc. using luciferase or β-galactosidase reporter plasmids with DOPE and cholesterol as helper lipids. The results showed that 1:2 formulation of CGL(2):DOPE had high transfection efficiency in all the cell lines used[108]. In the *in vivo* experiments, the CGL(2) gemini lipid based formulation showed a better transfection capability and a lower toxicity compared to DOTAP-based commercial kit and Lipofectin. Further, CGL(2) based formulations were shown to transfect efficiently SiRNA.

Bhattacharya *et al* have designed and synthesized another type of gemini lipids **(Figure 11)** based on pseudoglyceryl backbone mimicking cardiolipins to investigate structure activity relationship[109]. The series CGL (5) contains two types of gemini lipids having polymethylene $((-CH_2)_m-)$ spacers (m = 3, 5, 8 and 12) and hydrophobic tails of n-$C_{14}H_{29}$ and n-$C_{16}H_{33}$ respectively. Series based on CGL(6) contains two types of gemini lipids having oxyethylene $(-CH_2-(CH_2-O-CH_2)_m-CH_2-)$ spacers (m = 1, 2 and 3) and hydrophobic tails of n-$C_{14}H_{29}$ and n-$C_{16}H_{33}$. Liposomes could be conveniently prepared from each gemini lipid either alone or with DOPE as helper lipid. The parameters like mean fluorescence intensity (MFI) and number of transfected cells were considered to evaluate the optimized transfection efficiency into HeLa cells for *p*EGFP expression as both, the number of transfected cells and the

amount of gene expression mattered for successful gene therapy[110]. The results indicate that incorporation of DOPE enhances the transfection efficacy of gemini lipids dramatically, especially in terms of MFI.
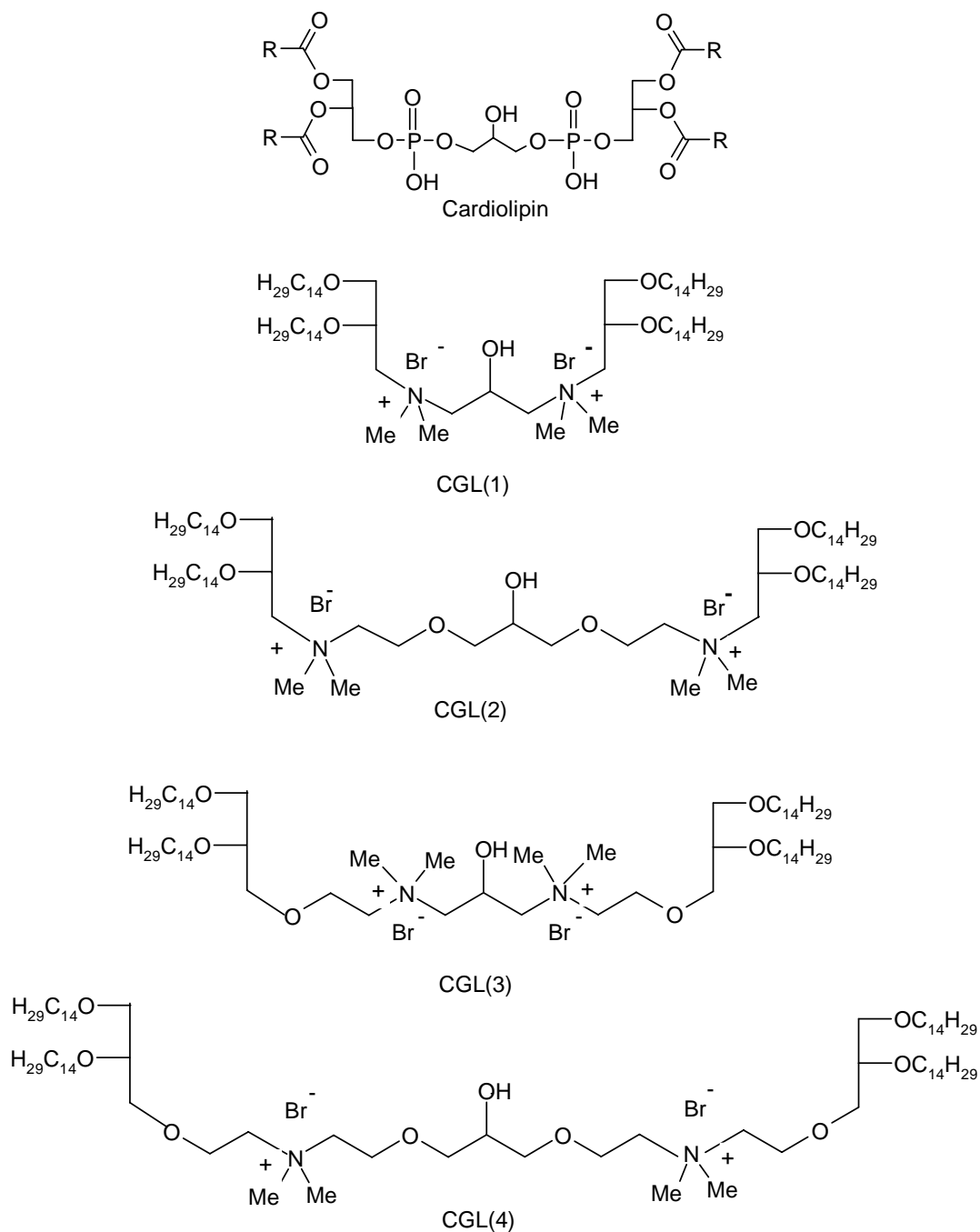
Figure 10. Cardiolipin analogue gemini lipids

Among gemini lipids series CGL(5) containing n-$C_{14}H_{29}$ chains, the lipid possessing a pentamethylene (-$(CH_2)_5$-) spacer was found to be the best transfecting agent, and with further increase in the length of the spacer, the transfection efficiency decreased. However, in the presence of serum, the gemini lipid possessing a longer spacer (-$(CH_2)_{12}$-) showed enhanced transfection efficiency. Among gemini lipids of series CGL(5) with n-$C_{16}H_{33}$ chains, lipids with (-$(CH_2)_3$-) and (-$(CH_2)_5$-) spacers were found to be better transfecting agents than other analogues. Comparative transfection profiles showed that the gemini lipids bearing n-$C_{14}H_{29}$ chains were better transfecting agents as compared to the lipids bearing n-$C_{16}H_{33}$ chains.

CGL(5)
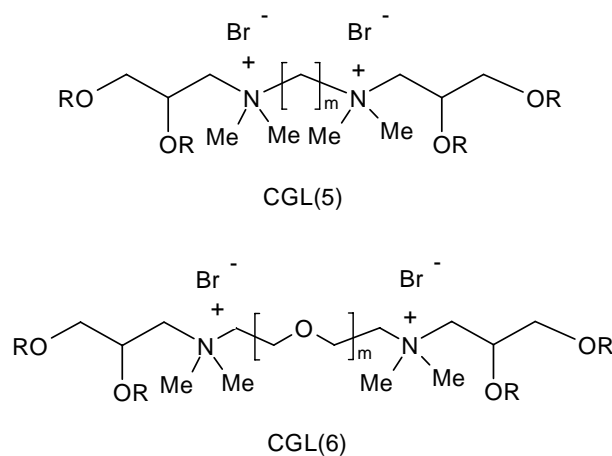
CGL(6)

Figure 11. Pseudoglyceryl backbone based gemini lipids

In CGL(6) oxyethylene series having n-$C_{14}H_{29}$ spacers, all lipids with DOPE exhibited transfection efficiencies comparable to Lipofectin in terms of the number of transfected cells, whereas, in the presence of 10% serum (serum is known to be major barrier in cationic lipofection)[111], their transfection efficacies increased dramatically. While the DOPE containing CGL(6) gemini lipids with n-$C_{16}H_{33}$ were found to be as effective as Lipofectin with or without serum in terms of MFI. Overall, pseudoglyceryl gemini lipids bearing an oxyethylene (-CH_2-$(CH_2$-O-$CH_2)_m$-CH_2-) spacer were found to be superior gene transfecting agents as compared to those bearing polymethylene (-$CH_2)_m$-) spacers.

The results obtained in the tranfection studies were correlated to the surface hydrations and transition temperatures (Tm) of the gemini lipids. In case of CGL(5) gemini lipids containing n-$C_{14}H_{29}$ chains, transfection activities were found to

increase with decrease in hydration, similar to CGL(5) gemini lipids containing n-$C_{16}H_{33}$ chains with a few exceptions. While in case of CGL(6) gemini lipids containing n-$C_{14}H_{29}$ chains the transfection activities increased with an increase in hydration around the liposomes. Similarly, in CGL(6) gemini lipids containing n-$C_{16}H_{33}$ chains the transfection activity decreased with a decrease in lipid surface hydration**.** The gemini lipids possessing n-$C_{16}H_{33}$ chains showed higher Tm compared to the gemini lipids bearing n-$C_{14}H_{29}$ chains. Among CGL(5) gemini lipids, lipids bearing a -$(CH_2)_3$- spacer possessed the highest Tm among the analogues having the same hydrocarbon chain lengths. The high Tm values of the lipid aggregates could be responsible for their low transfection activity, as at 37 °C, the corresponding membranes may be too rigid to affect good transfection. Similar, results were obtained for CGL(6) series also.

(B) Aromatic backbone-based gemini lipids

      Bhattacharya *et al* have designed and synthesized a new family of gemini lipids based on aromatic backbone, AGL(1) to explore structure–activity correlations. Three series of gemini lipids differing in the length of the hydrocarbon chains (**Figure 12**) and polymethylene spacers of varying length (m = 3, 4, 5, 6, 12) between the head groups were synthesized and evaluated for transfection efficiencies and toxicity using *p*EGFP in HeLa and HT1080 cells[112]. All the cationic gemini lipids were dispersed in water at ∼70 ^{0}C. The results of tranfection experiments showed that geminilipids based on n-$C_{12}H_{25}$ and n-$C_{14}H_{29}$ hydrocarbon chains were better transfecting agents than those possesing n-$C_{16}H_{33}$ chains in HeLa cells at an optimum ratio with DOPE. Formulations based on gemini lipids possessing the n-$C_{14}H_{29}$ chain and pentamethylene -$(CH_2)_5$- spacer were found to be the best in transfection efficiency (nearly three times more than the commercially available Lipofectin in terms of the number of cells and four times more efficient in terms of the MFI), good cell viability and serum compatibility. In HT1080 cells, formulations based on monomeric lipids with n-$C_{12}H_{25}$ tails, gemini lipids with n-$C_{12}H_{25}$ tails and -$(CH_2)_3$-, -$(CH_2)_5$-, -$(CH_2)_6$- spacers and gemini lipid with n-$C_{14}H_{29}$ chain and -$(CH_2)_5$- spacer were found to be the best transfecting agents. MFI observed in HT1080 cell lines was lower when

compared to that in HeLa cells, which indicated that the release of the DNA from lipoplexes in HT1080 was more difficult than in HeLa cells.
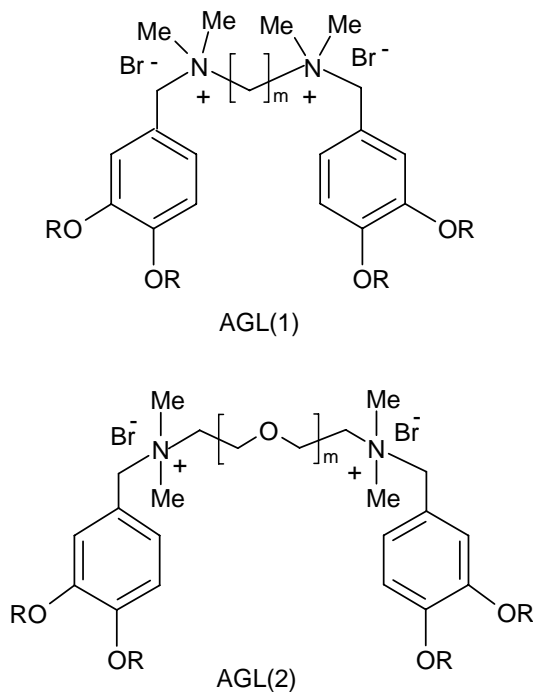
Figure 12. Aromatic backbone based gemini lipids

Furthermore, six new cationic gemini lipids based on AGL(2) possessing oxyethylene spacer (m = 1, 2 and 3) between headgroups and aromatic backbone containing hydrophobic chains **(Figure 12)** were synthesized[113]. The liposomal formulations of these gemini lipids were prepared alone or with DOPE for gene transfer activities using *p*EGFP-c3 and tested on HeLa cells. Gene transfer activities of these gemini lipids were found to depend on the hydrocarbon chain lengths and the length of the oxyethylene spacers. Among the AGL(2) gemini lipids bearing n-$C_{14}H_{29}$ hydrocarbon chains, the transfection efficacy decreased with the increase in length of the spacer. The maximum transfection was observed for gemini lipid formulation with (-CH_2-CH_2-O-CH_2-CH_2-) spacer. But, in case of AGL(2) having n-$C_{16}H_{33}$ hydrocarbon chains, transfection efficacy increased with increase in the length of the spacer and the lipid with a (-(CH_2-CH_2-O-CH_2-CH_2-O-CH_2-CH_2-O-CH_2-CH_2)-) spacer showed the maximum transfection activity which was even greater than that

showed by Lipofectin and monomeric lipid analogue in presence of serum. However, the actual mechanism for transfection mediated by these lipid formulations is still not known.

Lipophilic pyrylium salts provide a procedure that generates simultaneously the heterocyclic ring and the positively charged nitrogen atom on reaction with primary amines, yielding pyridinium salts. The choice of the appropriately substituted primary amine, diamine or polyamine, allows the design of the shape of the final lipids, gemini surfactants, or lipophilic polycations. The structure-activity relationship study of three series of pyridinium cationic lipids revealed that the most efficient representative was the *N*-(1,3-dimyristoyloxypropan-2-yl)collidinium derivative[114-118]. This amphiphilic compound, because of its truncated cone shape, induces a higher radius of curvature of the lipid bilayer, thus generating smaller, more transfection-efficient liposomes. To assess how the chain length influences the transfection activity, a library of lipids were synthesized, which involved the reaction of pyrylium salts with primary amines to generate cationic headed lipophilic pyridinium salts with 10-17 carbon atoms and hexafluorophosphate as counterion. The transfection experiments of liposomal formulations of these synthesized pyridinium salts with cholesterol as helper lipid at 1:1 molar ratio showed that maximum transfection was obtained when two myristyl chains (C_{14}) were attached to pyridinium ring.

Since gemini amphiphiles provided a higher (positive) charge per mass ratio than the cationic lipids and have the ability to help the endosomal release of the DNA complexes by destabilizing the endosomal membrane via associations with the gemini anionic lipids,[119] gemini lipids with pyridinium polar heads (**Figure 13)** were designed and investigated for their gene delivery efficacy. The gemini lipids based on AGL(3) had varying spacer length from two to eight carbons while gemini lipids based on AGL(4) and AGL(5) contained hydrophilic spacers having secondary amino groups[120]. The critical temperatures of these gemini lipids depended markedly on the structure of the spacer. As a general trend, gemini cationic lipids with alkyl linkers display higher transition temperatures than their congeners bearing polar secondary amino moieties in the spacer.

Figure 13. Pyridinium based cationic gemini lipids

When the transfection efficiency of these compounds were evaluated as 1:1 molar mixture with cholesterol using *p*GL3 plasmid in lung cancer cell line (NCI-H23), compounds with structures AGL(4) and AGL(5) displayed much lower transfection efficiencies compared to their hydrophobic congeners AGL(3). Among the AGL(3) series, the compound with the shortest spacer of two carbon atoms displayed the highest transfection efficacy, which was comparable to that of standard DOTAP:Cholesterol (1:1) system. Gemini compounds based on AGL(5) were substituted with myristoyl or palmitoyl chlorides and palmityl chloride to obtain gemini lipids having structures AGL(6) and AGL(7), respectively. When the transfection efficacies were compared, compound (AGL(7)) displayed the highest activity when co-formulated with DOPE in 1:1 molar ratio, which was even superior to that of Lipofectamine.

1.3.2.2.3.2 Gemini analogue of surfactants in gene delivery

A number of gemini surfactants have been designed and synthesized to be utilized as gene delivery carriers. These can be categorized depending upon their structures as discussed below.

(A) Diquaternary ammonium salt-based gemini surfactants

Developing diquaternary compounds for gene delivery applications was conceptulized by the fact that dimethyldioctadecylammonium bromide, when formulated with an equimolar amount of DOPE, was shown to be quite an effective DNA transfecting agent[121]. It appeared possible that introduction of a second quaternary ammonium group could increase the strength of interaction with DNA and perhaps generate an improved transfecting agent. The diquaternary ammonium gemini surfactants have been extensively studied to explore structure activity relationships for their gene delivery applications. They are used in liposomal formulations either alone or with some helper lipid (DOPE, DMPC etc.). The general structure of various diquaternary ammonium gemini surfactants used for gene delivery are shown in **Figure 14**.

The DGS(1)-based gemini surfactants with long hydrophobic tails (oleyl and hexadecyl) and different spacer chain lengths (n = 2, 3, 6) were synthesized. All the gemini surfactants rapidly form complexes with negatively charged DNA (*p*CMV-*β*-gal). These gemini surfactants showed different morphologies in aqueous dispersions i.e all saturated chain gemini surfactants showed lamellar phase while unsaturated gemini surfactants with shortest and longest spacers exhibited lamellar and micellar phases, respectively. In transfection studies on BHK-21 hamster kidney cells, all of the diquaternary ammonium salts exhibited good to excellent transfection activity, but the transfection activity decreased when formulated with equimolar DOPE. In saturated derivatives, n = 6 exhibited highest transfection, while in oleyl unsaturated series, n = 3 and 6, both were highly efficient. These diquaternary ammonium salts, at optimal lipid:DNA ratio and dose were at least as effective transfection agents as *O*-ethyl-dioleoylphosphatidylcholine (EDOPC). In all of the cases, the presence of 10 % serum significantly reduced transfection efficacy[122].

In another study, series of DGS(1)-based gemini surfactants, having hydrocarbon tails (dodecyl, hexadecyl and oleyl) were synthesized. Dodecyl series, (n = 3, 4, 6, 8, 10, 12, 16), hexadecyl series (n = 3) and oleyl series (n = 2, 3, 6) were synthesized and tested for *in vitro* transfection efficiency using the *p*GTmVMV.IFN-
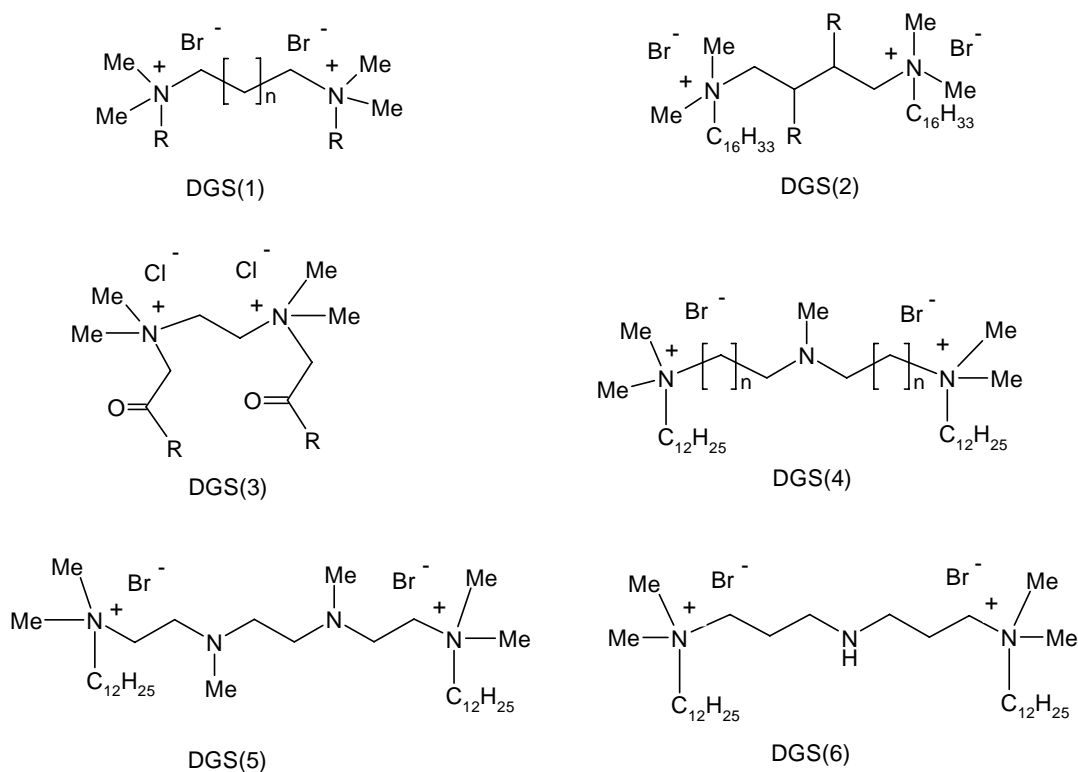
Figure 14. Diquaternary ammonium salt based gemini surfactants

GFP plasmid coding for IFN-γ and GFP on PAM212 murine keratinocyte cells with DOPE as helper lipid. The transfection efficiency was found to be dependent on the length of the spacer between the two positively charged head groups, with the n = 3 spacer showing the highest activity among all the series. No IFN-γ was detected when the cells were transfected without DOPE in the dodecyl series. The effect of the tail length influenced the transfection efficiency, with longer tails being associated with higher protein expression. In compaction study all of the studied gemini surfactants bind to DNA and induce changes of the B-DNA into a highly compacted ψ-DNA, and

the degree of this change was dependent on the spacer length and nature of the tails. Further, in the *in vivo* studies, the DGS(1)-based gemini surfactant formulations exhibited higher IFN-γ expression and less skin irritation compared to DC-chol/DNA complexes[123, 124].

Influence of the spacer length (n = 2, 3, 4) of DGS(1)-based gemini surfactants with hexadecyl chains on the hydration of lipoplexes was investigated. The results demonstrated that shorter spacers exhibited a lower hydration level of liposomes, a higher hydration of lipid double layer upon addition of DNA and a higher extent of DNA conformational changes toward a C-form, while gemini compounds with longer spacers exhibited more level of hydration and a higher extent of dehydration promoted by the addition of DNA, and a minor extent of DNA conformational change[125].

The gemini surfactants based on DGS(2) with hexadecyl chain and spacer (R = OCH_3) in three different stereochemistry (i.e, 2*S*,3*S*; 2*R*,3*R* and 2*R*,3*S*) were synthesized to investigate the role of the stereochemistry of the spacer in transfection efficiency of the lipoplexes. The transfection efficiencies of their liposomal formulations (with DMPC as helper lipid) were evaluated on COS-7, LA7 and human fibroblast cell lines, using CMVGFP plasmid[126]. The formulation of gemini with spacer stereochemistry (2*R*,3*S*) exhibited best transfection, even better than the commercially available transfection agent and the gemini surfactant without –OCH_3 groups in spacer, on all cell lines used. Further, circular dichroism investigations for DNA complexation show that the liposomes containing gemini amphiphiles induce a structural transition from a B-form of the plasmid to a typical *ψ*-phase. Among the three diastereoisomers, the meso form showed the highest efficiency, both in the DNA condensation and in transfection. The presence of methoxy groups on C_2 and C_3 positions of the spacer improves the condensation and transfection capability especially in 2*R*,3*S* configuration[127].

Furthermore, in order to reduce the uptake of liposoms by the reticuloendothelial system (RES), polyethylene glycol monolaurate (PEG-ML) was incorporated in prepared liposomal formulations. The transfection studies using CMVGFP in COS-7 cells showed that all PEGylated lipoplexes formulated with gemini surfactants transfected cells more efficiently than those in the absence of PEG-

ML. PEGylated lipoplexes formulated with gemini (2*R*,3*S*) and gemini without – OCH$_3$ were more efficient than commercially available kits[128].

DGS(2)-based gemini surfactants with hexadecyl tails were used as liposomal formulations with DMPC (1,2-dimyristoyl-sn-glycero-3-phosphocholine) to investigate the effect of surface charge density on the transfection efficiency using enhanced green fluorescent protein coding plasmid and COS-1 cells. The transfection efficiency of liposomes was dependend upon the lipid stoichiometry. Using the techniques like static light scattering, ethidium bromide intercalation assay, differential scanning calorimetry and fluorescence anisotropy of diphenylhexatriene, it was concluded that surface charge density and the organization of positive charges appear to determine the mode of interaction of DNA with (2*S*,3*R*)-2,3-dimethoxy-1,4-bis(N-hexadecyl-N,N-dimethylammonium)butane dibromide and DMPC liposomes, resulting in DNA condensation only when DGS(3) > 0.05. Conclusively, the condensation of DNA by gemini surfactant has been required for efficient transfection[129]. DGS(3)-based gemini surfactants are different from those based on DGS(1) in having ester linkage between the quaternary nitrogens and the hydrophobic tails. Moreover, the counter ions are chloride rather than bromide in DGS(3). These gemini surfactants were evaluated using EGFP plasmid on RD-4 cells and the results indicated that all the gemini surfactants (R = C$_{10}$, C$_{12}$, C$_{14}$) exhibited transfection capabilities comparable to a standard transfecting agent when formulated with DOPE as helper lipid, the most efficient being R = C$_{12}$ [130].

DGS(4) and DGS(5) based gemini surfactants with aza (N-CH$_3$) groups in spacer, and DGS(6) gemini surfactants with imino group spacer, all having dodecyl chains were synthesized taking inspiration from polyamines [131,132]. The transfection capabilities of these gemini surfactants were investigated on COS7 cells using plasmid encoded for luciferase production and compared with DGS(1)-based gemini having trimethylene spacer and dodecyl chain, DC-Chol and Lipofectamine. The results show that addition of DOPE to gemini-DNA complexes significantly improve the transfection efficacies except for DGS(6), that contains imino group in spacer which may be responsible for structural changes occuring on transition from neutral to acidic *p*H, leading to the release of DNA, once the complex has been incorporated within the cell. For the aza-substituted compounds, DGS(4) with n = 2 show the

highest while DGS(5) the lowest transfection efficiencies. Further, DGS(6)-based gemini surfactants exhibited significant increase in transfection compared to unsubstituted gemini surfactants, aza group-containing gemini surfactants and DC-Chol, while it was comparable to Lipofectamine Plus. Finally, the aza and imino gemini surfactants had similar toxicity profiles to Lipofectamine in COS7 cells[133].

(B) Cholesterol-based gemini surfactants

Cholesterol-based gemini surfactants represent that class of gemini surfactants, which contains cholesterol moiety as a part of their hydrophobic chain. In literature, they are often referred as "Cholesterol based gemini lipids" may be due to bulky cholesterol moiety as a hydrophobic chain. Here, cholesterol-based gemini compounds are referred as gemini surfactants because they contain two cholesterol moieties as hydrophobic chains. The rational for using cholesterol as the hydrophobic moiety is that in many lipids such as DC-Chol, a cationic cholesterol derivative has been successfully used as a co-aggregate with DOPE to prepare liposomes that transfect mammalian cell efficiently[134].

A series based on ChGS(1) **(Figure 15)** containing polymethylene spacers (n = 3, 4, 5, 6 and 12) and two cholesterol chains were synthesized by Bhattacharya *et al*.[135]. The hydrophilic portion of these gemini surfactants were joined to the hydrophobic cholesterol moieties through ether linkage as the inclusion of the ether linkage leads to a dramatic increase in transfection efficiencies of cholesterol-based cationic lipids as compared to the ester or urethane-based cholesterol lipid analogues[136, 137]. The presence of the ether linkage makes these compounds hydrolytically stable, and their aqueous suspensions are also found to have long shelf-life. These gemini surfactants form stable suspensions in water and exhibited closed membranous aggregates as revealed by electron microscopy. The transfection activities of liposomal formulations of these gemini surfactants with DOPE were evaluated using *p*EGFP-c3 in HeLa cells.

The transfection efficacies of these gemini surfactants got enhanced by incorporation of DOPE when compared to the monomeric lipids, as revealed from flow cytometric analysis. With the increase in length of the spacer from trimethylene to pentamethylene, the transfection efficiency increased, whereas further increase in

the spacer length to dodecamethylene led to a decrease in the transfection activity. Gemini surfactant with pentamethylene spacer was the most effective one, showing two times higher transfection activity compared to the commercially available transfecting reagents. All of the gemini formulations did not show any toxicity at the concentrations at which transfections were performed.
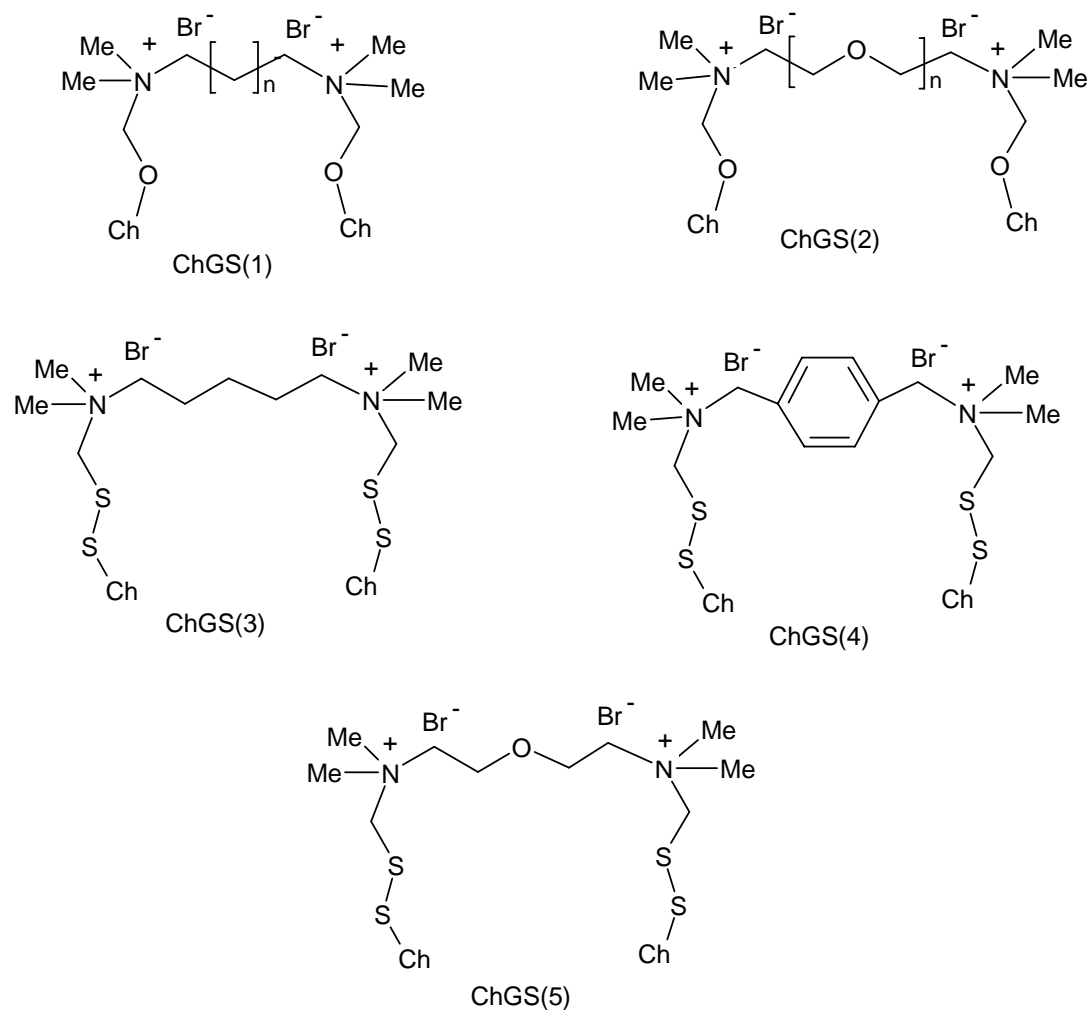
Figure 15. Cholesterol based gemini surfactants

In order to derive a structure-activity correlation of cholesterol-based gemini surfactants four new compounds based on ChGS(2) bearing oxyethylene spacers (n = 1, 2, 3 and 5) in between the head groups were synthesized (**Figure 15**). These gemini

surfactants form vesicle-like aggregates in aqueous suspensions[138]. In the transfection experiments using *p*EGFP on Hela cells with DOPE as co-lipid, incorporation of an oxyethylene spacer between the cationic ammonium headgroups dramatically increased the transfection activities of these gemini surfactants as compared to their monomeric lipids, even in presence of serum. Each gemini required different amount of DOPE to elicit maximum transfection efficiency. The formulation containing gemini spacer, ($-CH_2-CH_2-O-CH_2-CH_2-$) showed highest transfection efficiency at optimum DOPE and N/P ratio. Further, its transfection properties improved in presence of serum.

The difference between the extra-cellular and intra-cellular glutathione levels can be utilized for intracellular delivery. The disulphide linkers in cationic lipids had been reported in literature to ensure the effective release of lipid-DNA complex inside the cell cytoplasm after reduction of disulfide bond by the intracellular glutathione pool[139, 140]. In order to improve the biodegradability (due to the presence of non-scissile ether linkage) Bhattacharya *et al* incorporated the disulfide linkage between the head group and the hydrophobic chain of cholesterol-based gemini surfactants differing in the nature of the spacers between cationic headgroups i.e. hydrophobic flexible $-(CH_2)_5-$ (ChGS3) to hydrophobic rigid ($-C_6H_4-$) (ChGS4) to hydrophilic flexible ($-CH_2-CH_2-O-CH_2-CH_2-$) (ChGS5) chains[141].

Liposomal formulations of these gemini surfactants with DOPE were studied for transfection activities on HeLa, HT1080, PC3AR and HaCaT cell lines using *p*EGFPc-3. The results showed that transfection efficacies of these formulations depended on the type of cell lines used. The formulations of ChGS(3) and ChGS(5) were effective on HeLa cell lines; formulation of ChGS(5) was found to be more effective than ChGS(3) on HT1080 cell lines and formulation of ChGS(4) was found to be the best in PC3AR cells. When these formulations were compared to commercially available agents Lipofectin and Lipofectamine on PC3AR cells, the gemini lipid formulations were much superior to Lipofectin while, formulation of ChGS(3) showed comparable transfection efficacy to Lipofectamine. On HaCaT cells, formulations of ChGS(3) and ChGS(4) showed higher transfection efficiencies that were comparable to Lipofectamine.

(C) Peptide based gemini surfactants

The peptide based gemini surfactants are characterized by peptide head groups, a spacer (thioether, bisulphide or spermine) and hydrophobic tails. These are relatively simple to synthesize using standard peptide chemistry; bio-compatible and their chemical structures can readily be tailored for effective interaction with DNA. They can be incorporated into liposome formulations, providing further dimension in the optimization of these molecules for *in vivo* studies.

A large library of peptide gemini surfactants **(Figure 16)** based on structure PGS (1) were synthesized to develop structure activity relationship by varying nature of both the "head" peptide (AA)*n* and the "tail" group (R, unbranched) systematically. The thioether linkage was incorporated using two cysteine residues, which were connected to heads groups through cysteine amino groups while the hydrophobic chain was connected to central parts via serine residues.

The transfection activities of PGS(1) based 14 compounds were evaluated on Chinese hamster ovary (CHO-DG44) cells using luciferase reporter gene either alone or with DOPE and compared to that of Lipofectamine 2000[142]. The optimum transfection activity requires both, the optimum head group and chain length. Increase in the length of the hydrocarbon tail leads to a substantial increase in transfection activity. The nature of the amide linkage between the three lysine residues in the head group also influences the transfection capability. Thus, three lysines linked through their ε-amino groups rather than through partial or total α-linkage appear to provide optimal interaction of these gemini surfactants with DNA. The most effective compound, among all of them, had (AA)n = Lys-ε-Lys-ε-Lys- and R = C18:1$^{\Delta 9}$. Further, the inclusion of basic peptide i.e. plus reagent and polylysine very much improves the transfection efficiency of the compound to even better than Lipofectamine 2000. Gemini surfactants based on PSG(1) having dodecyl chains were studied using TEM and AFM to correlate the aggregation properties with their transfection efficiencies.

A correlation was established between surfactant morphology and transfection efficiency. Gemini surfactants that formed arrays or fibril structures were ineffective as transfection agents, whereas those lacking these features were highly effective in CHO-K1 cells[143, 144].

A series of PGS(2) based gemini surfactants were synthesized to take the advantage of *in situ* dimer formation reaction to direct the DNA condensation process toward the smallest possible particles using a versatile polymer-supported synthetic strategy. The oxidative conversion of the thiol containing detergent gives rise to gemini surfactants having disulfide bond[145]. Since cysteine based detergents with deca hydrocarbon chains were ineffective at transfecting cells (as the dimeric molecules were still exchanging between the DNA complexes and the medium or the cell mem-
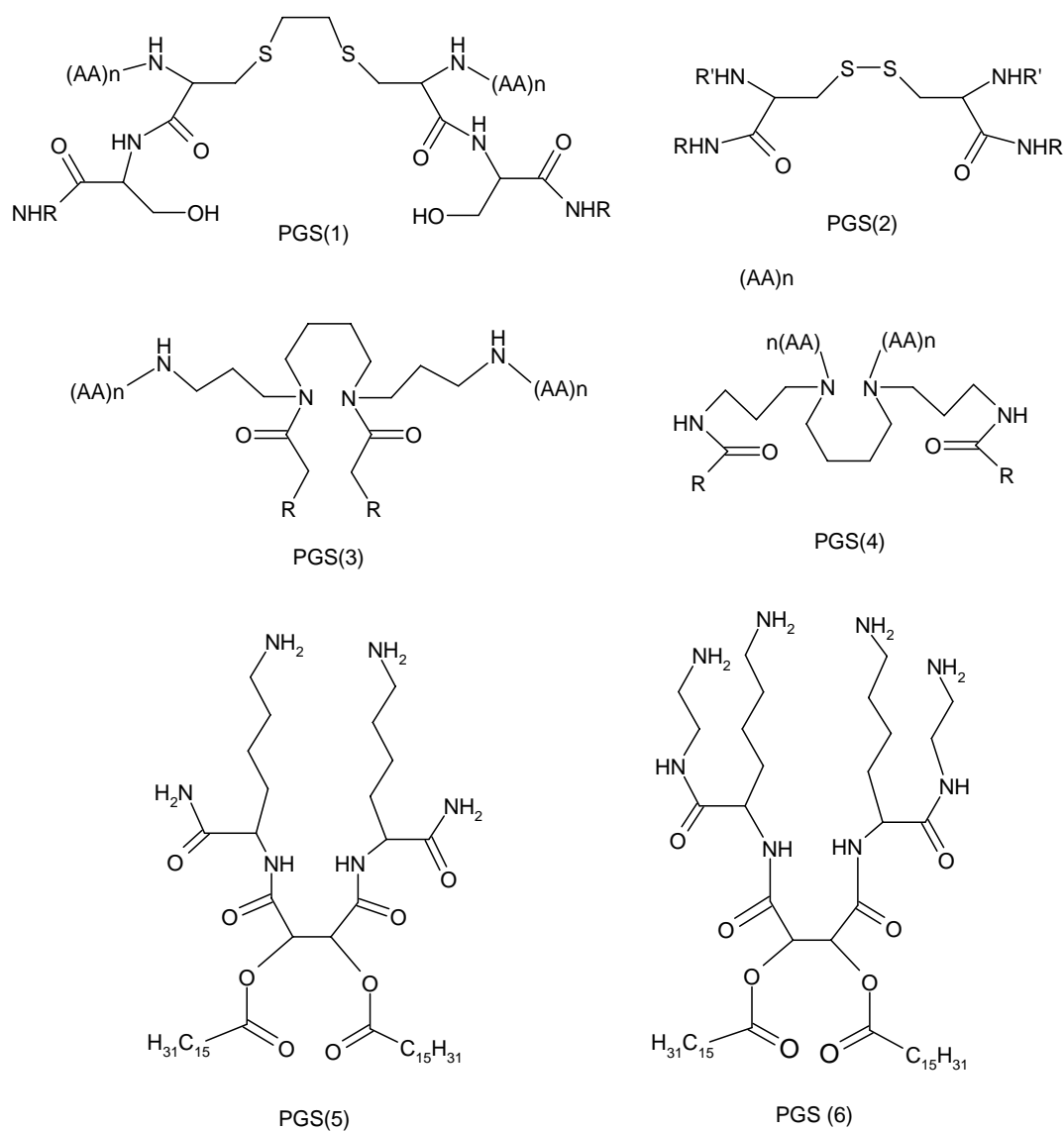
Figure 16. Peptide based gemini surfactants

brane), [146] hydrocarbon chains (C_{12}, C_{14} and C_{16}) linked to carboxylic group of cysteine residue through peptide bond have been synthesized. Because the α-amino group of cysteine was not sufficiently protonated at neutral *p*H, it was derivatized with ornithine and carboxyspermine headgroups which widened the range of cmc's and DNA binding affinities[147]. The transfection capabilities of these gemini surfactants were evaluated in 3T3 cells using *p*CMV-Luc plasmid. The relative transfection efficiencies of ornithine head

group containing gemini surfactants increased with increase in hydrocarbon chain. The gemini containing carboxyspermine head group and tetradecyl chain exhibited lower transfection and higher toxicity compared to gemini containing ornithine head group and tetradecyl chain, which was correlated to the higher cmc value of former.

A library of two isomeric series [PGS(3) and PGS(4)] of gemini surfactants were synthesized to utilize spermine skeleton in the head group as spermine-based cationic surfactants, such as dioctadecylamidoglycylspermine-4 trifluoroacetic acid (DOGS) and 2,3-dioleoyloxy-*N*-[2-(sperminecarboxamido)ethyl]*N,N*-dimethylpropan -1-aminium trifluoroacetate (DOSPA) are commercially available and are widely used for *in vitro* gene transfection studies. These spermine-based detergents were sufficiently soluble in water making them highly suitable for gene delivery applications. In transfection studies using CHO-DG44, C2C12 (mouse muscle cell line), non-adherent MOPC315 (mouse tumour cell line) and 1321N1 (neuronal cell line) cell lines, similar peptide head-group gemini surfactants of type PGS(4) possessed better transfection efficiencies than type PGS(3), and the oleoyl chain generally gave the most efficient transfection comparable to Lipofectamine 2000[148].

Feiters *et al* reported cationic gemini surfactants based on tartaric acid, biocompatible palmitoyl tails, lysine head group (PGS(5)) and combined lysine-ethylenediamine head group (PGS (6)). PGS(5)-based gemini showed plate like structures while no definite structure for PGS(6) was evidenced from electron microscopy. Ethidium bromide assay and agarose gel electrophoresis experiments showed the capabilities of these gemini compounds to complex with DNA. In transfection experiments using luciferase gene and CHO-K1 cells, both the gemini compounds were found to be active but exhibited toxicity[149].

(D) Sugar-based gemini surfactants

Sugar based gemini surfactants are characterized by reduced carbohydrate head groups linked by spacer and having the hydrocarbon tails **(Figure 17)**. When it was reported that sugar based gemini surfactants with reduced glucose as head groups connected via a $(-CH_2-)_6$ spacer and hexadecyl chains showed *p*H dependent vesicle to micelle transition,[150] a library of sugar based gemini surfactants were designed and synthesized because of their biocompatibility, biodegradability, and improved solubility as compared to other surfactants, especially for gene delivery applications, because a transfection carrier with *p*H dependent phase behavior is desirable for the release of DNA from endosomal compartment- a most crucial step in gene delivery. Johnsson *et al* reported that sugar based gemini surfactants with reduced glucose as head group connected via a short ethylene oxide spacer and two oleyl chains, formed vesicles in dilute aqueous solution near neutral *p*H and underwent vesicle to micelle transition (i.e. *p*H dependent aggregation behavior)[151].
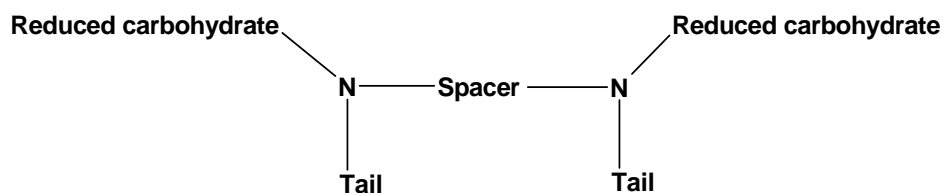
Figure 17. General structure of sugar-based gemini surfactant

When the transfection efficiency of glucose-headed gemini surfactants were evaluated, compound SGS(1) in cis/trans ratio of 80%/20% showed excellent transfection efficiency (approximately 3 times than that of the commercial transfection agent Lipofectamine 2000 Plus), which peaked at a surfactant to base pair ratio of 2:1 and did not require helper lipids like DOPE. However, its saturated analogue with $(-CH_2-)_6$ spacer was less active and required a much higher surfactant to base pair ratio. To determine the mechanism of transfection, the structure of the lipoplex formed from DNA and the sugar-based cationic gemini surfactant SGS(1) has been investigated in the *p*H range 8.8-3.0 utilizing small angle X-ray scattering (SAXS) and cryo-electron microscopy (cryo-TEM). The study showed that lipoplexes

exhibited three well-defined unique morphologies i.e. a lamellar phase, a condensed lamellar phase, and an inverted hexagonal (H_{II}) columnar phase, upon gradual acidification. Finally, the efficacy of gemini surfactant SGS(1) as a gene delivery vehicle was explained on the basis of *p*H-induced formation of the inverted hexagonal phase of the lipoplex in the endosomal *p*H range. This change in morphology leads to destabilization of endosome through fusion of the lipoplex with the endosomal wall, resulting in release of DNA into the cytoplasm[152].

The presence of two tertiary nitrogens provide special characters to sugar based gemini surfactants as they can be protonated at physiological *p*H range. The curvature of aggregates that are formed by sugar based gemini surfactant is sensitive to the solution *p*H. Furthermore, the aggregation behavior of sugar based gemini surfactants shown in **Figure 18** were studied and compared by means of light scattering, cryo-transmission electron microscopy, electrophoretic mobility and fluorescence measurements. Variations in the structures were incorporated by introducing a different sugar head group (reduced mannose), by varying the spacer between the two main surfactant parts, and by introducing, in one of the surfactants, an amide linkage (instead of an amine linkage) between the head group and the unsaturated ($C_{18:1}$) hydrocarbon tails[153].

The results show that all gemini surfactants form vesicles near neutral or high *p*H. However, the vesicles made from the amine-containing geminis [SGS(1), SGS(2), SGS(3)] were transformed into cylindrical or wormlike micelles at lower *p*H values (*p*H < ~5.5). The nature of the sugar or spacer had little influence on this process and the gemini surfactant with the amide instead of the amine functional group (SGS(4)) in the head group did not undergo the vesicle-to-micelle transition but displayed only vesicle formation within the investigated *p*H range. The micelle formation at acidic *p*H is explained by the protonation of amines in the gemini head group, leading to an increased electrostatic repulsion between the head groups[154, 155].

Wasungu *et al* had investigated the *in vitro* and *in vivo* transfection capacity of novel *p*H-sensitive sugar-based gemini surfactants shown in **Figure 18** which formed bilayer vesicles at physiological *p*H but underwent a lamellar-to-micellar phase transition in the endosomal *p*H range as a consequence of an increased protonation state. Similarly, lipoplexes made with these amphiphiles exhibited a lamellar

morphology at physiological pH and a non-lamellar phase at acidic pH. The study showed that the sugar-based gemini surfactants SGS(1), SGS(2), SGS(3) and SGS(5) which were mono-protonated at pH 7.4, could efficiently form complexes with
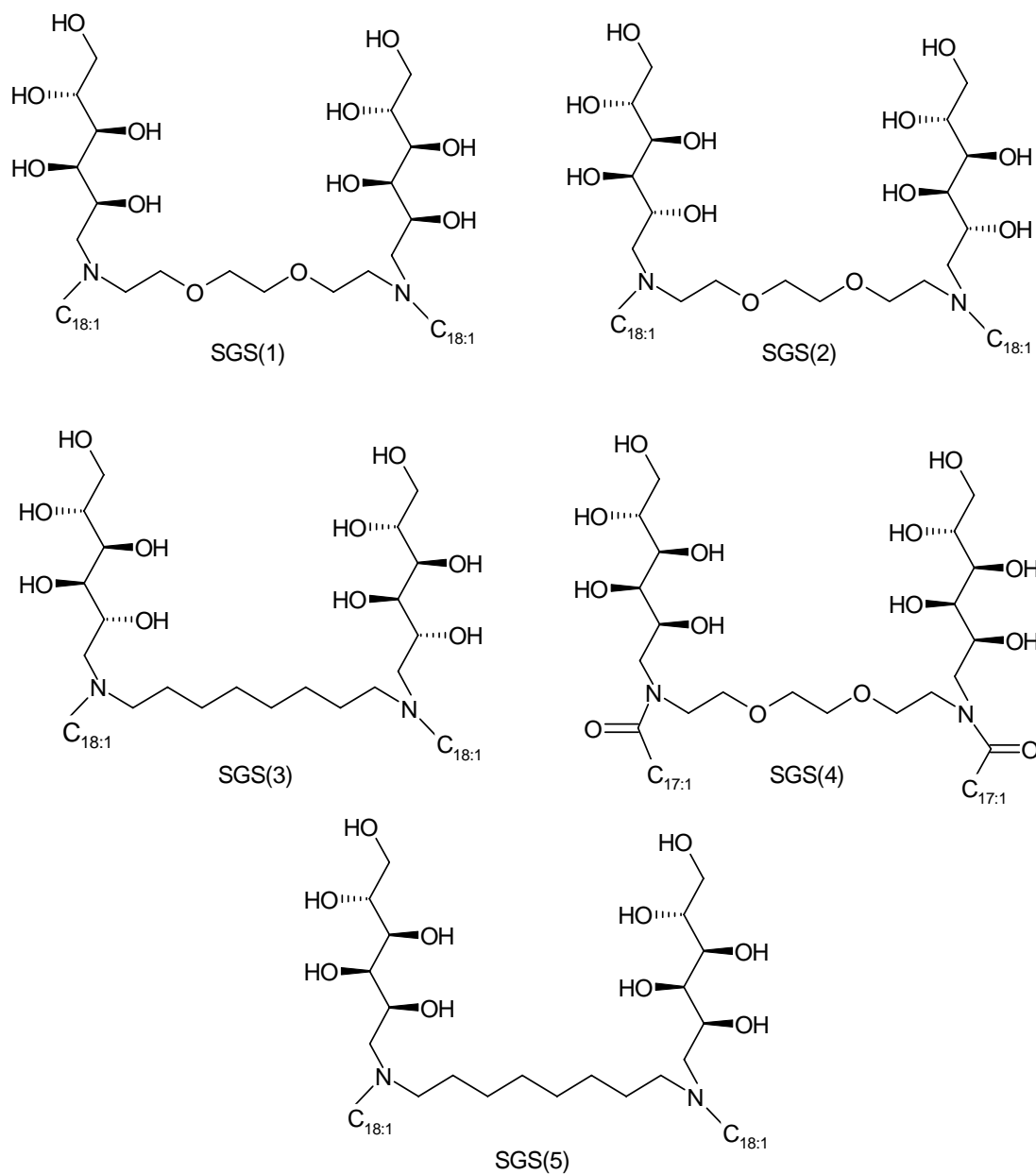
Figure 18. Sugar based gemini surfactants

plasmid DNA (*p*EGFP-N1). However, SGS(4), which was neutral at pH 7.4 failed to form lipoplexes. In the *in vitro* transfection studies on CHO cells, SGS(1), SGS(2), SGS(3) and SGS(5) exhibited comparable transfection efficiencies to Lipofetamine 2000, while SGS(4) showed poor transfection efficacy. When the toxicity of GSs were compared, SGS(5) showed relatively high toxicity, followed by SGS(3). As both of these GSs had aliphatic spacer, GSs with ethylene oxide spacer appeared to be safe and effective as well[156].

The two GSs i.e. SGS(1) and SGS(2) were selected for *in vivo* tranfection studies based on the *in vitro* performance for luciferase expression in nude mice using luminescence imaging. The lipoplexes of SGS(1) and SGS(2) exhibited good colloidal stability in salt and in serum at physiological *p*H, which might be due to their lamellar organization. These lipoplexes exhibited no transfection in lungs when injected in nude mice *in vivo*. An explanation was given that upon acidification, SGS(1) and SGS(2) lipoplexes undergo a lamellar to a H_I non-inverted micellar transition and that this transition was impeded when the H_{II} (i.e., inverted) phase preferring DOPE was included[157]. This explained why the inclusion of DOPE inhibited rather than promoted transfection of gemini complexes. Finally, the potential of avoiding preliminary capture in the lungs by these gemini surfactants may be further exploited in developing devices for specific targeting of gemini lipoplex.

Other acid sensitive bis-detergents or gemini surfactants were synthesized to overcome the problems associated with single-tailed, *p*H-sensitive detergents for the cytosolic delivery of macromolecules like their low limit of incorporation in stable liposomal formulations. Two bis-detergents [BD(1) and BD(2)] as shown in **Figure 19** were synthesized with oxyethylene [BD(1)] or acid-labile acetal [BD(2)] moieties. Liposomes composed of BD(1) or BD(2) and egg phosphatidylcholine (PC) collapsed into micelles at mildly acidic *p*H similar to that found in endosomes/lysosomes. The collapse of BD(2):PC liposomes was more efficient than that of BD(1):PC liposomes presumably due to acid catalyzed hydrolysis of the acetal spacer that led to accumulation of single-tailed, micelle favoring detergent species within the liposomal bilayer. These liposomes when utilized to encapsulate antisense oligonucleotides, promoted delivery of entrapped contents into the cytosol of HeLa cells. The efficiency
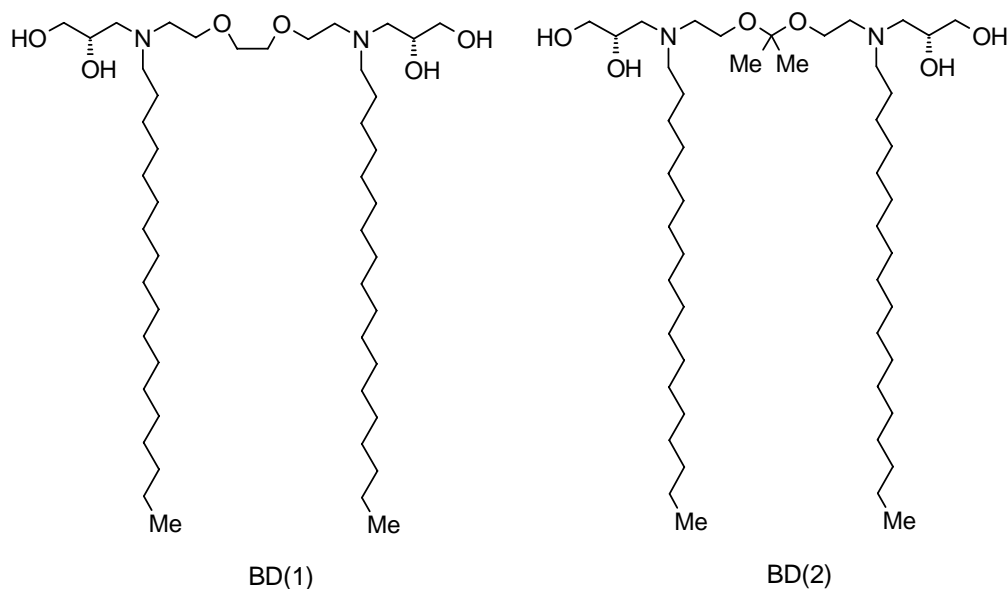
Figure 19. Acid sensitive gemini surfactants

Table 3. List of Patent Applications filed for gene delivery applications of GAs.

S.No.	Category of GA	Patent application Number	Inventor(s)	Reference
1	Peptide based gemini compounds composed of basic amino acids	US 20030119188A1	Camilleri et al	159
2	Diaminodicarboxylic acid-peptide based gemini compounds	US 20040138139A1	Camilleri et al	160
3	Spermine-peptide based gemini compounds	US 20050089493A1	Camilleri et al	161
4	Ester linked peptide based gemini compounds	US 7425645 B2 US 7569720 B2	Castro et al	162, 163
5	Substituted diquaternary and asymmetric gemini compounds	US 20090054368A1	Wettig et al	164
6	Amide and peptide derivatives of tetraalkylenepentamines	US 20090149401A1	Castro et al	165
7	Diquaternery gemini lipids	US 6696424B1	Wheeler	166
8	Polyhydroxy diamine surfactants	US 7005300B1	Camilleri et al	167

of cytosolic delivery was comparable to Lipofectamine which further improved substantially in the presence of serum[158].

Finally due to excellent transfection results of GAs based gene delivery carriers in various cell lines, number of patent applications have been filed as listed in **Table 3**.

1.4 Gene transfection and cationic amphiphiles: Role of head group modification

Molecular design of cationic amphiphiles is currently an active area of research in gene delivery. Due to their opposite surface charge, cationic amphiphiles can form an overall positively charged complex with negatively charged DNA. The transfection efficiency is not determined solely by one part of the cationic lipid but by combination of them. The optimal characteristics of the hydrophobic, headgroup and linker depend upon the general structure of the amphiphiles. Different types of amphiphiles can have opposite structural requirements in terms of optimal length of hydrocarbon chains, types of linkages and head groups. Therefore the modular approach is useful for planning and designing new vectors for gene delivery.

Head group modifications in the structure of cationic amphiphiles have shown significant improvement in the transfection efficiency. For instance, hydroxyethylation has been proven to drastically improve the transfection efficiency. Accordingly, gene transfection by the lipids, *N*-[1-(2,3-dioleyloxy)propyl]-*N,N,N*-trimethylammonium chloride (DOTMA) and 1,2-dioleoyloxy-3-(trimethylammonio)propane chloride (DOTAP), were improved by incorporation of a hydroxyethyl group to yield vectors 1,2-dioleoyl-3-dimethylhydroxyethyl ammonium bromide (DORIE) and 1,2-dioleoyloxypropyl-3-dimethylhydroxyethyl ammonium chloride (DORI) respectively **(Figure 20)**[168, 169]. Studies in literature showed that both monohydroxylation and dihydroxylation resulted in higher transfection compared to corresponding non-hydroxyethylated amphiphiles. Monohydroxylated lipid DHMHAC (*N,N*-di-*n*-hexadecyl-*N*-methyl,*N*-(2-hydroxyethyl)ammonium chloride)[170] and dihydroxylated lipid DHDEAB (*N,N*-di-*n*-hexadecyl-*N,N*-dihydroxyethylammonium bromide)[171] (**Figure 20)** were found to mediate high levels of gene delivery compared to structurally similar dioctadecyldimethylammonium bromide (DDAB).

The hydroxyethyl group can be derived from lactic acid and saccharides. In case of lipid, *N,N*–myristyl-*N*-(1-hydroxyprop-2-yl)-*N*-methylammonium chloride

DOTMA, R = CH$_3$
DORIE, R = C$_2$H$_4$OH
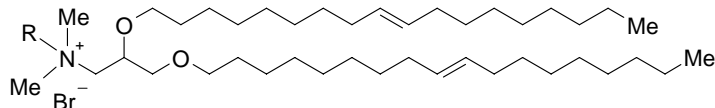
DOTAP, R = CH$_3$
DORI, R = C$_2$H$_4$OH
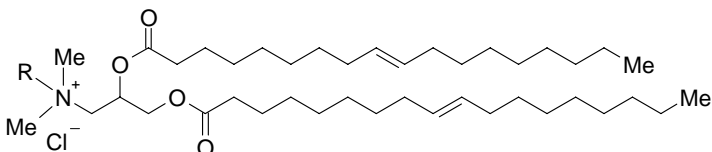
DDAB, R1 = R2 = CH$_3$
DHMHAC, R1 = CH$_3$
        R2 = C$_2$H$_4$OH
DHDEAB, R1 = CH$_3$
        R2 = C$_2$H$_4$OH
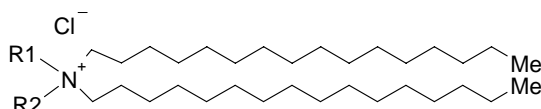
DMHMAC
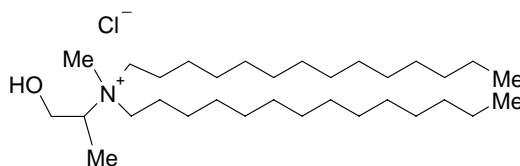
Lipid 1
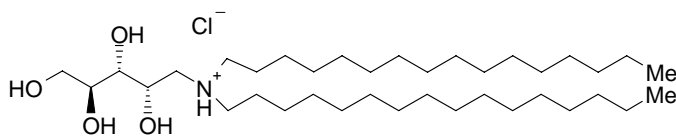
Lipid 2
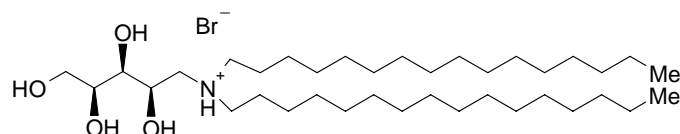
Figure 20. Structures of cationic amphiphilic carriers showing incorporation of hydroxyethyl group in their head group region

(DMHMAC), wherein hydroxyethyl portion has been derived from lactic acid, it was found to be twice as efficient as DDAB/DOPE in the *in vitro* studies[172]. Moreover, in lipid I, 1-deoxy-1-[methyl(ditetradecyl)ammonio]-*D*-arabinitol and lipid II, 1-deoxy-1-[dihexadecyl(methyl)ammonio]-*D*-xylitol, which are respectively derivatives of

arabinose and xylose, incorporation of more than two hydroxyethyl moieties in the headgroup appears to convey increased transfection levels and decreased toxicity[173]. Hydroxyethylation in the head group region has also shown promising results in case of 3-β-[*N*-(*N'*,*N'*-dimethylaminoethane)carbamoyl]cholesterol hydrochloride) (DC-Chol) derivatives. Lipid IV, 3-cholesteryl carboxyamidoethylene-*N*-hydroxyethylamine **(Figure 21)** was more efficient than its non-hydroxyethylated dimethyl tertiary amino homologue. The transfection ability of Lipid IV may be relat-
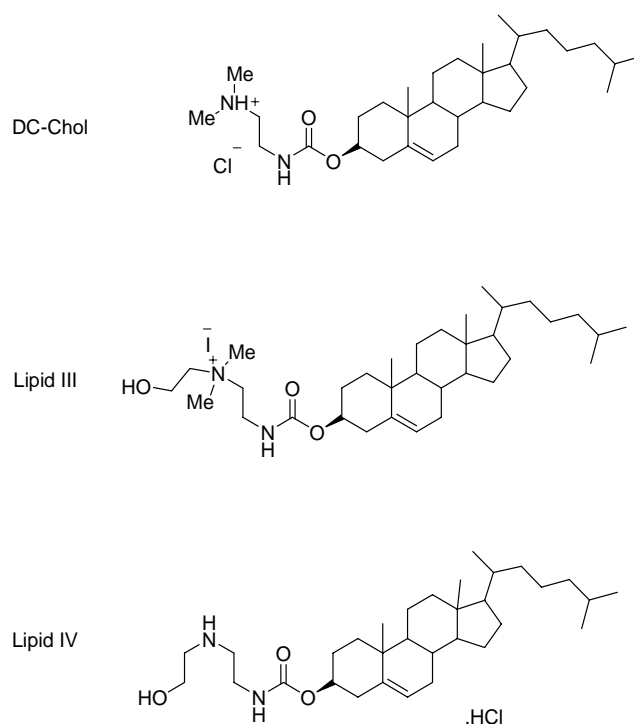
Figure 21. Structures of hydroxyethyl derivatives of DC-Chol

ed to lipoplex instability in the endosomes resulting in facilitated DNA release into the cytoplasm. However, the transfection efficiency was dramatically reduced by addition of a second hydroxyethyl group to the amino group of the lipid. Moreover, the transfection activity of the ester analogue Lipid III, 3-cholesteryl carboxyamido-*N*,*N*-dimethyl-*N*-2-hydroxyethylammonium iodide, was found to be related to the lipoplex charge ratio i.e., efficiency was higher than methylated homologues at ratios

above 7, at which the dimethyl and trimethyl homologues were actually inefficient[174, 175].

1.5 Mechanism of lipofection

The first essential step in lipofection is the complexation and consequent compaction of nucleic acid polyanion by the cationic carriers. Due to charge interaction, cationic lipids spontaneously associate with nucleic acids, resulting in the formation of lipoplex **(Figure 22)**. Lipoplexes are membranous structures that are capable of transducing into cells, eventually leading to expression of genes. Following complexation, DNA has to sufficiently compact in nano-size range for efficient cellular entry. Gene delivery appears to be most effective when the complexes are formed where the ratio of positive charges of cationic carrier to the nucleic acid negative charge lies around 1.0 and above[176, 177].

The mechanism involved in the cellular uptake of the lipoplex is most likely endocytosis which occurs after non-specific charge mediated binding to cellular receptors as demonstrated using electron microscopy[178, 179]. Endocytosis involves a controlled invagination of the cell membrane, allowing the lipoplex to be enveloped by the cell membrane. The membrane then "buds off" to form a new vesicle inside the cell. Such vesicles can combine to form endosomes which develop increasingly powerful hydrolytic capabilities, with the internal pH falling sharply, until they eventually merge with lysosomes. Only a fraction of the complexed DNA escapes from the endosome and the rest is eventually digested either in the late endosome or after fusion with a lysosome (lysosomes deploy powerful acid hydrolases such as nucleases, peptidases, glycohydrolases etc. to provide an efficient recycling capability). DNA within the lipoplex/polyplex is protected from nuclease action, but will inevitably be degraded unless it is released from the endosome, perhaps still complexed to the vector.

Endosomal escape is the most crucial step in gene delivery to avoid lysosomal degradation of lipoplex. The release of DNA into cytoplasm is generally attributed to the ability of the cationic carrier to destabilize the endosome membrane. DOPE is most frequently added to the cationic formulations to aid in early endosomal escape of lipoplex. DOPE has the tendency to promote significant polymorphic changes in the lipid phase under physiological conditions. In particular, DOPE readily promotes the

formation of an inverted hexagonal phase (at room temperature and physiological *p*H) from lamellar liquid crystalline characteristics of most biological membranes[180, 181]. This hexagonal phase is frequently observed when membranes fuse. Therefore DOPE could provide a means for endosome disruption by promoting membrane fusion.
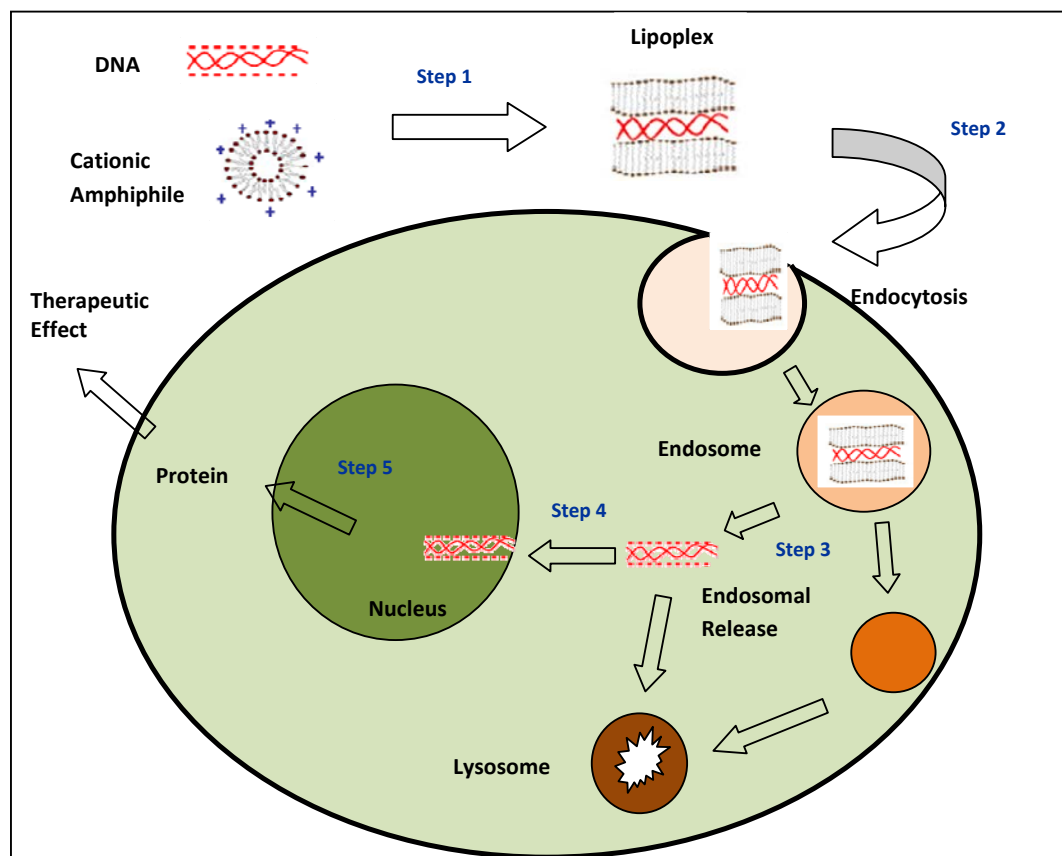
Figure 22. Schematic representation of key steps involved in amphiphilic carrier mediated gene delivery leading to expression of a new protein

Electrostatic interaction between cationic liposome and endosome membrane induces the flip-flop of anionic lipids from the monolayer of the endosome membrane that faces the cytoplasm. These membranes laterally diffuse into the complex where they form neutral ion pairs with cationic lipids. Ionic interactions between the DNA and cationic lipids are thereby disrupted allowing the DNA to diffuse freely into the cytoplasm[182].

Release of the DNA from the lipoplex presumably occurs at or before this stage because passage through the nuclear membrane appears to involve uncomplexed DNA. The rate of the passage through nuclear membrane has to compete with the rapid degradation of uncomplexed DNA by cytoplasmic nucleases. After entry into nucleus, the DNA expresses itself to produce the encoded protein[183]. Thus, the strategic points at which vector design can be expected to have significant effects on the efficiency of lipofection are the formation of the lipoplex, its passage through the cell, the release of the lipoplex from the endosome and its subsequent dissociation.

1.6 Plasmid DNA Profile (*p*CMV.SPORT-*β*-gal) and its estimation

Plasmid *p*CMV·SPORT-*β*-gal is used as a positive control for monitoring expression in eukaryotic cells **(Figure 23)**. The plasmid contains the reporter gene *β*-galactosidase (*β*-gal) from *E. coli* cloned as a *Not* I fragment into plasmid
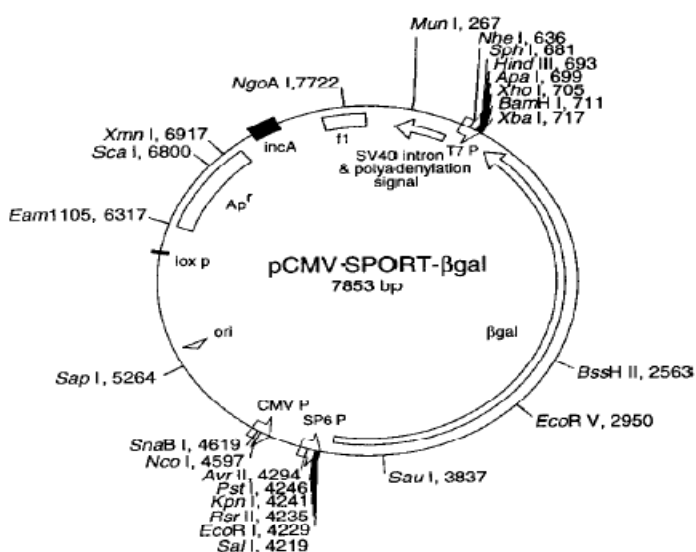
Figure 23. Plasmid DNA (*p*CMV-SPORT-*β*-gal) Map

*p*CMV·SPORT1. The plasmid also contains a CMV promoter upstream of the *β*-gal gene, followed by the SV40 t-intron and polyadenylation signal. The *β*-lactamase gene allows selection for ampicillin resistance in *E. coli.*

Spectrophotometric analysis serves to be quickest, promising and reliable method for routine analytical needs. The estimation of *p*DNA by UV-visible

spectrophotometry is based upon the fact that plasmid DNA absorbs strongly at 260 nm in aqueous buffer such as Tris buffer. Although the preparations of DNA absorb at 260 nm, the RNA absorbs more strongly in the same region. Proteins absorb maximally at 280 nm but significantly at 260 nm also. The other contaminants like phenol and chloroform may also interfere with DNA preparations and estimation. Therefore a method for an accurate determination for purity of double stranded plasmid DNA devoid of RNA and proteins is required. The ratio of absorbance at 260 nm and 280 nm provides an estimate of the plasmid purity. For pure *p*DNA, the ratio should be in between 1.8 to 2.0. Higher and lower ratio indicates contamination with RNA and proteins respectively[184].

1.7 Estimation of *β*-galactosidase

β-Galactosidase estimation method represents a classical colorimetric assay for estimation of *β*-galactosidase gene expression. It provides a simple, reliable and economical quantitative estimation of *β*-gal expression by measuring enzyme activity directly.
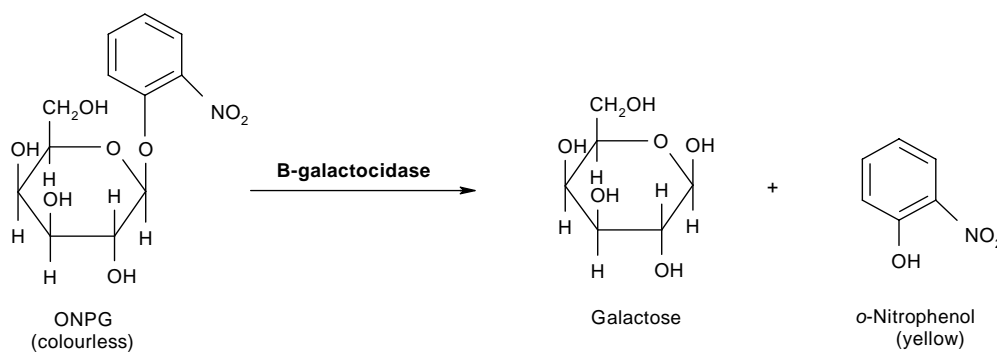
Figure 24. Hydrolysis of ONPG (colourless) to *o*-nitrophenol (yellow) and galactose

The expressed *β*-galactosidase protein is able to hydrolyze the galactose sugar bond. In the described assay, the artificial chromogenic substrate ortho-nitrophenyl-*β*-*D*-galactopyranoside (ONPG) is used, which is cleaved at *β*-1,4-glycosidic bond between 2-nitrophenol and galactose leading to release of ortho-nitrophenol (**Figure 24**). ONPG is colorless, while its hydrolyzed product *o*-nitrophenol has a yellow color and absorbs light at 405 nm. The intensity of the developed color directly correlates with the quantity of *β*-galactosidase expressed in the cell[185].

2. RESEARCH ENVISAGED

Gene therapy has enormous potential for the treatment of diseases of mankind. The lack of safe and efficient gene-delivery methods is a limiting obstacle to human gene therapy. Both viral and non-viral delivery systems have been tried to satisfy the needs of gene therapy. But so far no ideal vector system has been discovered for gene delivery. Synthetic gene delivery agents, although safer than viruses, generally do not possess the required efficacy. In recent years, a variety of effective polymers and amphiphiles have been specifically designed for gene delivery, and much has been learnt about their structure–function relationships. With the growing understanding of gene delivery mechanisms and continued creative efforts of scientists in this direction, it is likely that non-viral gene delivery systems will become important tools for human gene therapy in very near future.

Major problems associated with the gene delivery are the size and negative charge of DNA. Therefore cationic carriers are of great interest in gene delivery to reduce the micron sized DNA into suitable nano-carriers utilizing the electrostatic charge interaction[1]. The first report published in 1989 stating that the double chain monovalent quaternary ammonium lipid, *N*-[1-(2,3-dioleyloxy)propyl]-*N*,*N*,*N*-trimethylammonium chloride, effectively binds and delivers DNA to cultured cells paved the pathway to design and synthesize hundreds of synthetic amphiphilic gene delivery carriers[78]. These amphiphiles differ by the number of charges in their hydrophilic head and structure of their hydrophobic moiety. The polar 'head-groups' of cationic lipidic non-viral vectors generally consists of monovalent quaternary ammonium salts such as CTAB and DOTAP. It appeared that introduction of a second quaternary ammonium group could increase the strength of its interaction with DNA and perhaps generate an improved transfection agent. So, diquaternary GAs are one of the most widely studied category used as cationic component in gene delivery carriers.

The superior amphiphilic properties of cationic GAs are applied to the complex problem of introducing genes into cells. GAs typically show enhanced surfactant properties relative to the corresponding monovalent (single chain, single head group) compounds. This makes them special for biological and especially biomedical applications, where it is essential to optimize the safety profile of any

foreign compound; the first and the simplest step is to minimize its concentration *in vivo*. Using less amount of the compound to achieve the same effect also has clear economic advantages. Moreover, diquaternary GAs, have the advantage of being easily prepared and offer a wide range of possibilities for structure modulations as they are composed of three basic parts namely, head, spacer and hydrocarbon chains allowing the design of GAs showing low toxicity, very low immunogenicity, high stability in biological fluids and biodegradability, which are essential requirements for a gene delivery system[186, 187]. The multivalent positive charge in the head group of GAs allowed efficient complexation and compactation of polyanionic DNA into particles (lipoplex) of small sizes that can be easily endocytosed by the cells[188]. The double hydrocarbon chains provide a propensity of forming vesicular structure depending upon the packing parameter of the gemini molecule. Moreover, the nature, length and stereochemistry of spacer also have significant effects on the transfection efficacy of GAs[122-126].

It is evident from literature survey that modifications in the head group region of lipidic carriers cause significant improvement in the transfection efficacy. For instance, examples are there in literature where improved transfetion efficacy was obtained following hydroxyethylation of the quaternary nitrogen[168-171, 189].

Apart from modular design for the required structural features for efficient gene delivery carriers, formulation factors are equally important. DOPE and cholesterol have shown promising results when formulated with cationic carriers including gemini amphiphiles[190]. These helper components favor the endosomal escape of lipoplexes by using different mechanisms which is one of the crucial steps in gene delivery[191, 192].

Keeping the above discussed points in mind, it was planned to synthesize hydroxyethylated diquaternary gemini amphiphiles **(Figure 25)** and determine their potential as non-viral gene delivery carriers. To verify the importance of hydroxylethyl group on the quaternary nitrogen atoms, it was planned to attach the hydroxyethyl group to nitrogen atom in a systematic way i.e. synthesis of GAs without hydroxylethyl group, synthesis of GAs with one hydroxylethyl group on each quaternary nitrogen and synthesis of GAs with two hydroxylethyl groups on each quaternary nitrogens. The idea of doing so was to evaluate the impact of

hydroxylethyl group attached to the quaternary nitrogens of GAs on their transfection efficacy and cytotoxicity. While making such a change, other variables like length of hydrocarbon chain and nature of polymethylene spacer were kept constant.

It was also thought of making changes like varying the hydrophobic flexible (polymethylene) linkers to rigid (*p*-xylene) and to hydrophilic flexible (oxyethylene) linkers in the synthesized GAs. Length of hydrophobic tail was also planned to be varied to optimize structural features in the synthesized GAs for effective gene delivery.

Wherein,

$Z =$ $-CH_2-C_6H_4-CH_2-$

        $-CH_2-CH_2OCH_2-CH_2-$

        $-(CH_2)n-$, $n = 4, 6$

$Y =$ $-CH_3$, $-C_2H_4OH$

$R1 =$ $-CH_3$, $-C_2H_4OH$

$R =$ C_nH_{2n+1} , $n = 12\text{-}18$
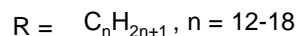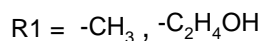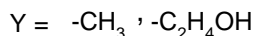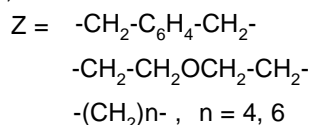
Figure 25. General structure of the proposed Gemini Amphiphiles (GAs)

It was also planned to develop formulations containing synthesized GAs along with DOPE and cholesterol as helper lipids. It was envisaged to evaluate the formulations so developed for DNA complexation and to see the stability of the complexed DNA against DNase; and try to develop a relationship between the GA structures with transfection efficiency and cytotoxicity.

3. RESULTS AND DISCUSSION

The research carried out to achieve the aims and objectives of this thesis has been discussed under the following heads:

- Synthesis and characterization of gemini amphiphiles
- Formulation development and characterization
- *In vitro* cell line studies
- *In vivo* studies

3.1 Synthesis and characterization of gemini amphiphiles

Syntheses of gemini amphiphiles required for the purpose of gene delivery were performed by using a simple strategy. Secondary amines were first converted into tertiary amines and the resulting tertiary amines were reacted with dibromo derivatives of the requisite spacer to obtain the desired bisquaternary GAs.

3.1.1 Synthesis of DMA series of compounds

Scheme 1 was adopted for the synthesis of GAs belonging to DMA series. The tertiary amine (**1**) on reaction with the dibromo derivatives of the required spacers (**2I-2IV**) yielded the desired products (**3I-3IV**).

DMA Series

Z: I = -CH$_2$-C$_6$H$_4$-CH$_2$-; II = -CH$_2$-CH$_2$-O-CH$_2$-CH$_2$-; III = -(CH$_2$)$_4$-; IV = -(CH$_2$)$_6$-
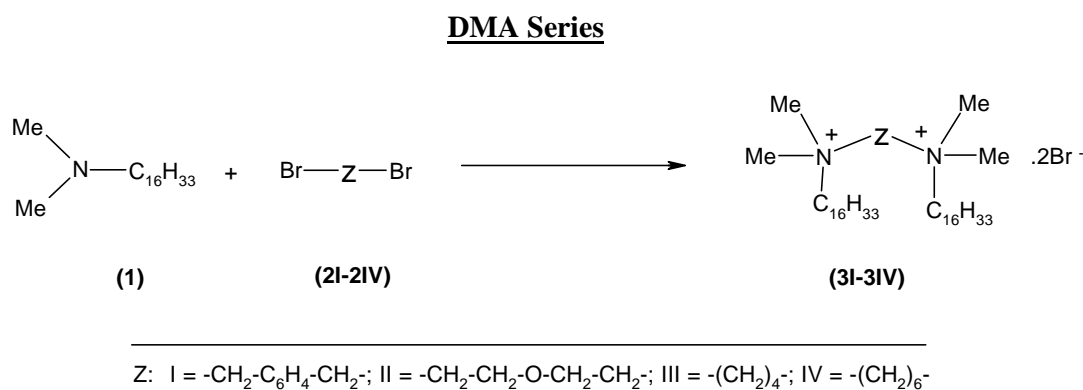
Scheme 1

1,4-Di[(*n*-hexadecyldimethylammonium)methyl]benzene   dibromide   **(3I)** showed PMR peaks at δ 0.87 (t, 6H, 2 × CH_{3a}), 1.25-1.36 (b m, 52H, 13 × CH_{2b}), 1.67- 1.85 (b m, 4H, 2 × CH_{2c}), 3.22 (s, 12H, 4 × N^+-CH_{3ef}), 3.55 (t, 4H, N^+-CH_{2d}), 5.36 (s, 4H, 2 × CH_{2h}) and 7.80 (s, 4H, Ar-H_i).
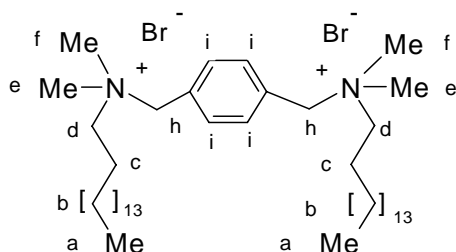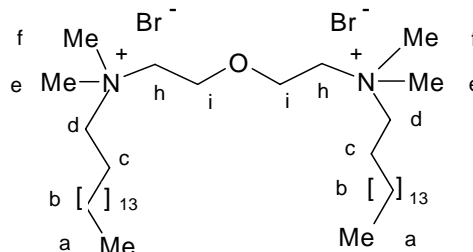
(3I)   **(3II)**

2,2'-Di(*n*-hexadecyldimethylammonium)ethyl]ether dibromide **(3II)** showed PMR peaks at δ 0.88 (t, 6H, 2 × CH_{3a}), 1.25-1.35 (b m, 52H, 13 × CH_{2b}), 1.72 (b m, 4H, 2 × CH_{2c}), 3.44 (s, 12H, 4 × N^+-CH_{3ef}), 3.58-3.63 (t, 4H, 2 × N^+-CH_{2d}), 4.07 (bs, 4H, 2 × N^+-CH_{2h}) and 4.33 (t, 4H, 2 × OCH_{2i}).

1,4-Di(*n*-hexadecyldimethylammonium)butane dibromide **(3III)** showed PMR peaks at δ 0.88 (t, 6H, 2 × CH_{3a}), 1.25-1.36 (b m, 52H, 13 × CH_{2b}), 1.77-1.77 (b m, 4H, 2 × CH_{2c}), 2.18 (t, 4H, 2 × N^+-CH_{2d}), 3.26 (s, 12H, 4 × N^+-CH_{3ef}), 3.37-3.42 (t, 4H, 2 × CH_{2i}) and 4.00 (t, 4H, 2 × N^+-CH_{2h}).
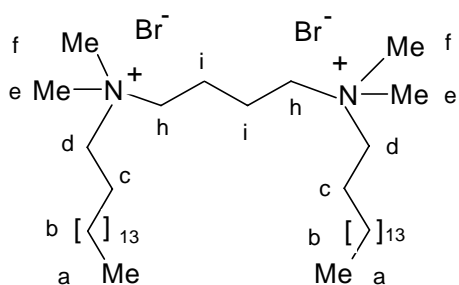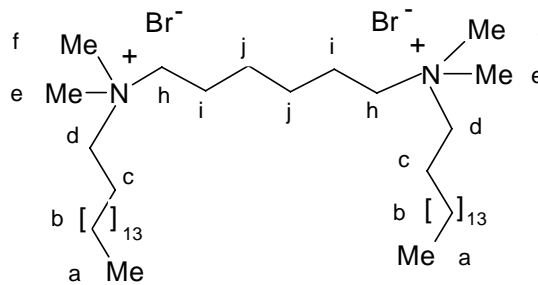
(3III)   **(3IV)**

1,6-Di(*n*-hexadecyldimethylammonium)hexane   dibromide   **(3IV)**   showed PMR peaks at δ 0.88 (t, 6H, 2 × CH_{3a}), 1.25-1.35 (b m, 52H, 13 × CH_{2b}), 1.61-1.72 (b m,12H, 6 × CH_{2cij}), 2.06 (t, 4H, 2 × N^+-CH_{2d}), 3.46 (s, 12H, 4 × N^+-CH_{3ef}) and 3.76 (t, 4H, 2 × N^+-CH_{2h}).

3.1.2 Synthesis of MEA series

Scheme 2 was adopted for the synthesis of GAs belonging to MEA series. Secondary amine (4) on reaction with the desired alkyl bromides (5a-5d) yielded the tertiary amines (6a-6d) as yellow colored viscous liquids. The tertiary amines on further

MEA Series

[7a (I-IV) - 7d (I-IV)]

R = a-d ; Z = I-IV

R : a = $C_{12}H_{25}$; b = $C_{14}H_{29}$; c = $C_{16}H_{33}$; d = $C_{18}H_{37}$

Z: I = $-CH_2-C_6H_4-CH_2-$; II = $-CH_2-CH_2-O-CH_2-CH_2-$
III = $-(CH_2)_4-$;   IV = $-(CH_2)_6-$
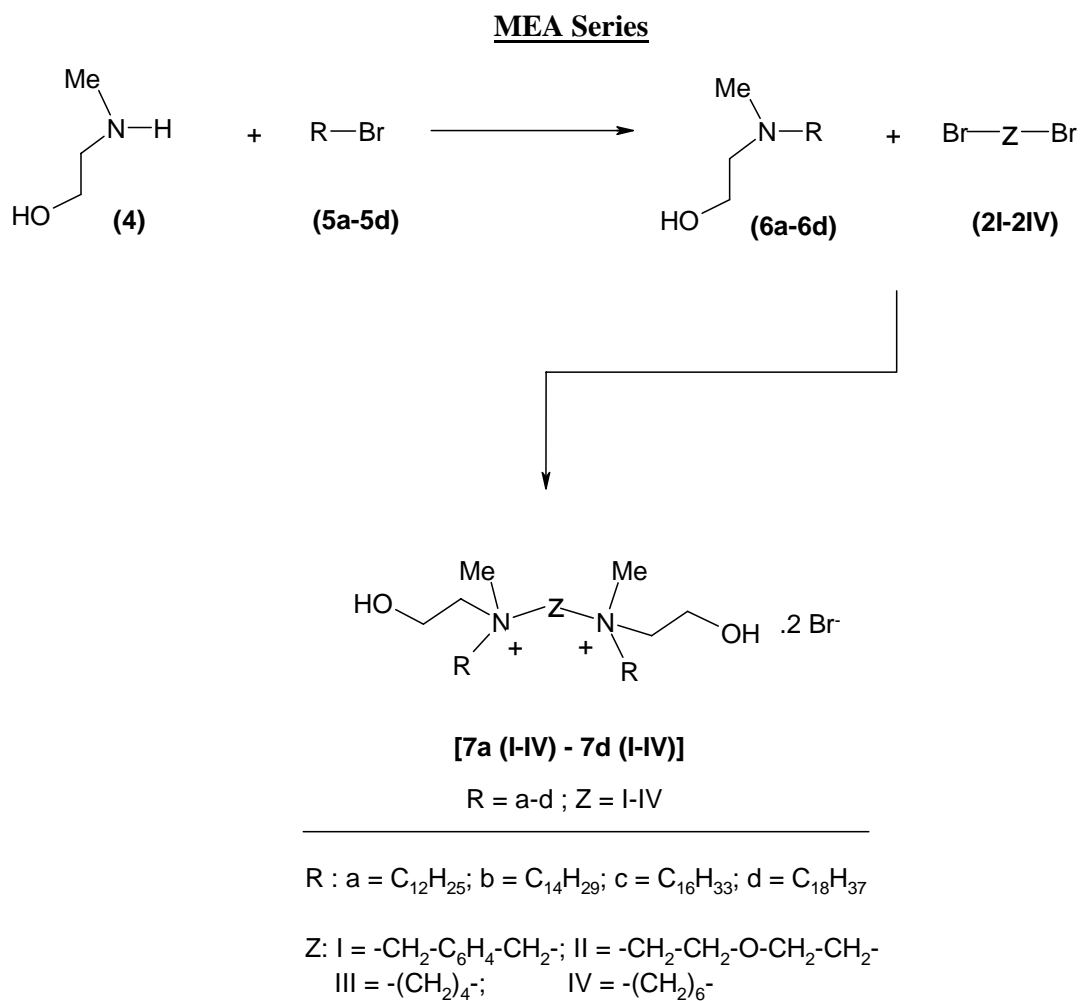
Scheme 2

reaction with the dibromo derivative (2I-2IV) of the required spacers yielded the desired products [7a (I-IV) - 7d (I-IV)].

1,4-Di{[*n*-dodecyl(2-hydroxyethyl)methylammonium]methyl}benzene dibromide (**7aI**) showed peaks at δ 0.59 (t, 6H, 2 × C*H*$_{3a}$), 0.99 (b m, 36H, 18 × C*H*$_{2b}$), 1.53 (m, 4H, 2 × C*H*$_{2c}$), 2.72 (s, 6H, 2 × N$^+$-C*H*$_{3e}$), 3.07 (t, 4H, 2 × N$^+$-C*H*$_{2d}$), 3.17-3.21 (t, 4H, 2 × N$^+$-C*H*$_{2f}$), 3.64 (t, 4H, 2 × N$^+$-C*H*$_{2h}$), 4.40 (t, 4H, 2 × OC*H*$_{2g}$), 5.12 (b s, 2H, 2 × O*H*) and 7.43 (s, 4H, 4 × Ar-*H*i) in its PMR spectrum.
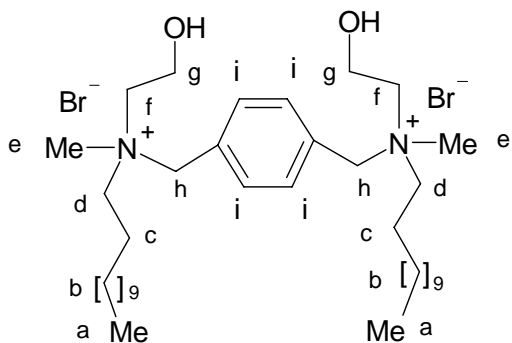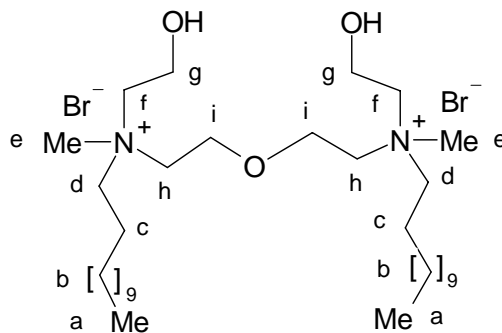
(**7aI**)   (**7aII**)

2,2'-Di{[*n*-dodecyl(2-hydroxyethyl)methylammonium]ethyl}ether dibromide (**7aII**) showed peaks at δ 0.85 (t, 6H, 2 × C*H*$_3$a), 1.25-1.34 (b m, 36H, 18 × C*H*$_{2b,}$, 1.72 (m, 4H, 2 × C*H*$_{2c}$), 3.39 (s, 6H, 2 × N$^+$-C*H*$_{3e}$), 3.63 (t, 4H, 2 × N$^+$-C*H*$_{2d}$), 3.81(t, 4H, 2 × N$^+$-C*H*$_{2h}$, spacer), 3.97 (t, 4H, 2 × N$^+$-C*H*$_{2f}$, head group), 4.10 (t, 4H, 2 × OC*H*$_{2i}$, spacer), 4.25 (t, 4H, 2 × OC*H*$_2$g, head group) and 4.95 (b s, 2H, 2 × O*H*) in its PMR spectrum.

1,4-Di[*n*-dodecyl(2-hydroxyethyl)methylammonium]butane dibromide (**7aIII**)
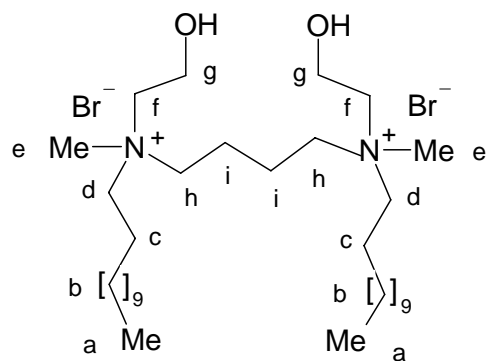
(**7aIII**)   (**7aIV**)
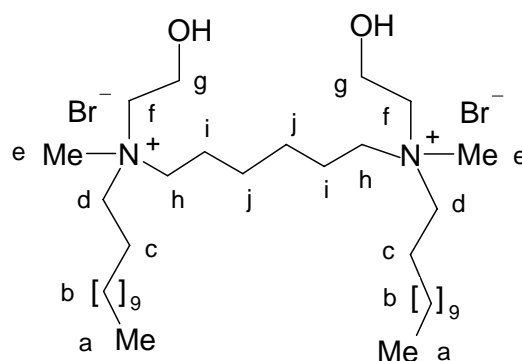
showed peaks at δ 0.85 (t, 6H, 2 × CH_{3a}), 1.25-1.34 (b m, 36H, 18 × CH_{2b}), 1.73-2.05 (m, 8H, 4 × CH_{2ci}), 3.26 (s, 6H, 2 × N$^+$-CH_{3e}), 3.40 (t, 4H, 2 × N$^+$-CH_{2d}), 3.62 (t, 4H, 2 × N$^+$-CH_{2h}), 3.78 (t, 4H, 2 × N$^+$-CH_{2f}), 4.09 (t, 4H, 2 × OCH_{2g}) and 5.08 (b s, 2H, 2 × OH, head group) in its PMR spectrum.

1,6-Di[*n*-dodecyl(2-hydroxyethyl)methylammonium]hexane   dibromide **(7aIV)** showed peaks at δ 0.85 (t, 6H, 2 × CH_{3a}), 1.25-1.34 (b m, 36H, 18 × CH_{2b}), 1.55-1.70 (m, 8H, 4 × CH_{2cj}), 1.93 (m, 4H, 2 × CH_{2i}), 3.29 (s, 6H, 2 × N$^+$-CH_{3e}), 3.47 (t, 4H, 2 × N$^+$-CH_{2d}), 3.62 (t, 4H, 2 × N$^+$-CH_{2h}), 3.70 (t, 4H, 2 × N$^+$-CH_{2f}), 4.09 (t, 4H, 2 × OCH_2g) and 5.06 (b s, 2H, 2 × OH) in its PMR spectrum.

1,4-Di{[(2-hydroxyethyl)methyl-*n*-tetradecylammonium]methyl}benzene di-bromide **(7bI)** exhibited similar PMR pattern as that obtained for **(7aI)** except that the number of protons at δ 1.25-1.35 were found to be 44 in its PMR spectrum.

(7bI)   **(7bII)**
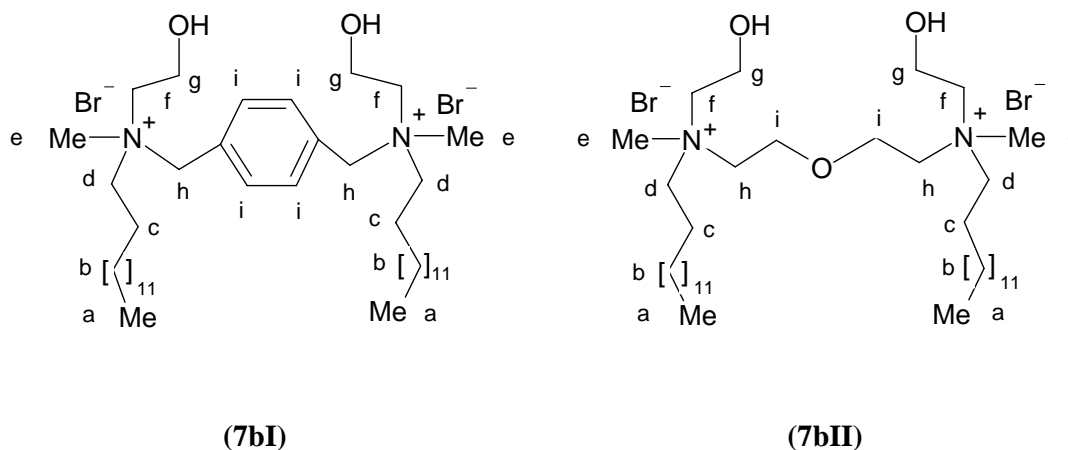
2,2'-Di{[(2-hydroxyethyl)methyl-*n*-tetradecylammonium]ethyl}ether dibrom-ide **(7bII)** exhibited similar PMR pattern as that obtained for **(7aII)** except that the number of protons at δ 1.25-1.35 were found to be 44 in its PMR spectrum.

1,4-Di[(2-hydroxyethyl)methyl-*n*-tetradecylammonium]butane   dibromide **(7bIII)** exhibited similar PMR pattern as that obtained for **(7aIII)** except that the number of protons at δ 1.25-1.35 were found to be 44 in its PMR spectrum.

1,6-Di[(2-hydroxyethyl)methyl-*n*-tetradecylammonium]hexane   dibromide **(7bIV)** exhibited similar PMR pattern as that obtained for **(7aIV)** except that the number of protons at δ 1.25-1.35 were found to be 44 in its PMR spectrum.
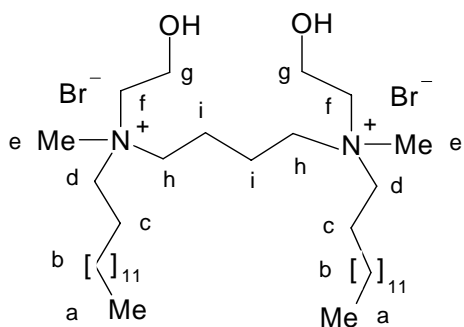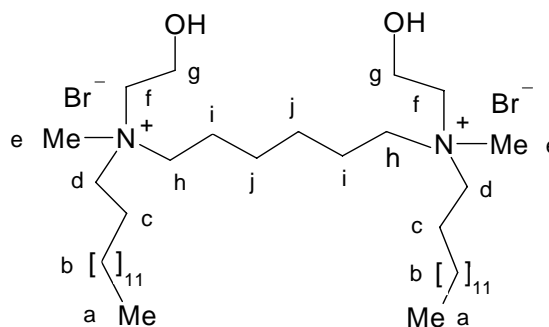
(7bIII)   **(7bIV)**

1,4-Di{[*n*-hexadecyl(2-hydroxyethyl)methylammonium]methyl}benzene dibromide **(7cI)** exhibited similar PMR pattern as that obtained for **(7aI)** except that the number of protons at δ 1.25-1.35 were found to be 52 in its PMR spectrum.
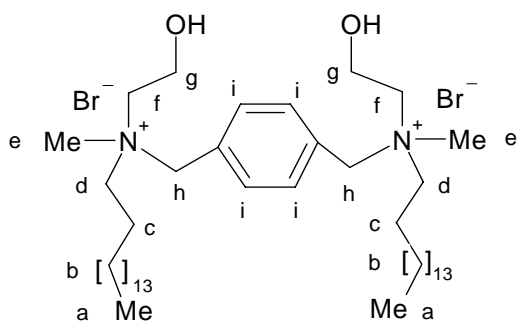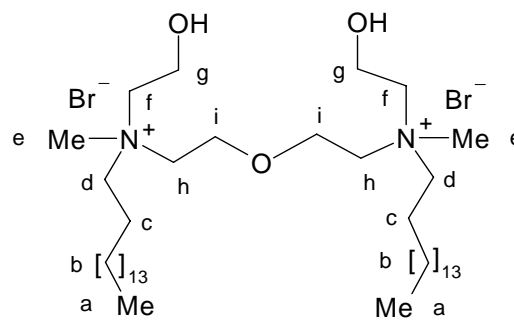
(7cI)   **(7cII)**

2,2'-Di{[(*n*-hexadecyl(2-hydroxyethyl)methylammonium]ethyl}ether   dibromide **(7cII)** exhibited similar PMR pattern as that obtained for **(7aII)** except that the number of protons at δ 1.25-1.35 were found to be 52 in its PMR spectrum.

1,4-Di[*n*-hexadecyl(2-hydroxyethyl)methylammonium]butane   dibromide **(7cIII)** exhibited similar PMR pattern as that obtained for **(7aIII)** except that the number of protons at δ 1.25-1.35 were found to be 52 in its PMR spectrum.

1,6-Di[(*n*-hexadecyl(2-hydroxyethyl)methylammonium]hexane   dibromide
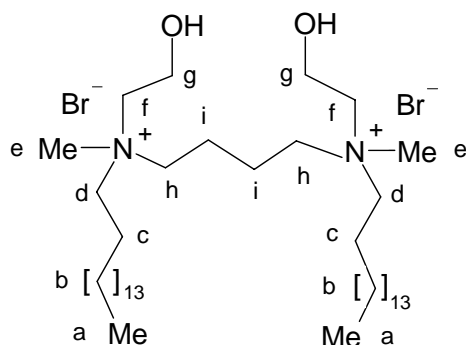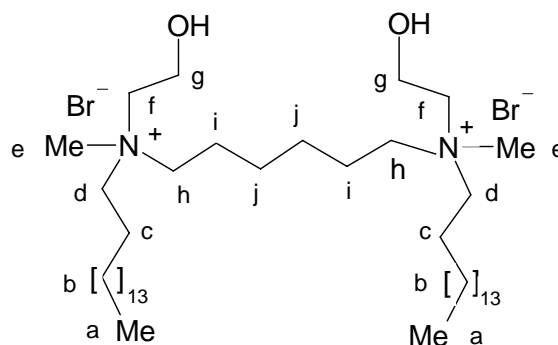
(7cIII)   **(7cIV)**

(7cIV) exhibited similar PMR pattern as that obtained for **(7aIV)** except that the number of protons at δ 1.25-1.35 were found to be 52 in its PMR spectrum.

1,4-Di{[(2-hydroxyethyl)methyl-*n*-octadecylammonium]methyl}benzene dibromide **(7dI)** exhibited similar PMR pattern as that obtained for **(7aI)** except that the number of protons at δ 1.25-1.35 were found to be 60 in its PMR spectrum.
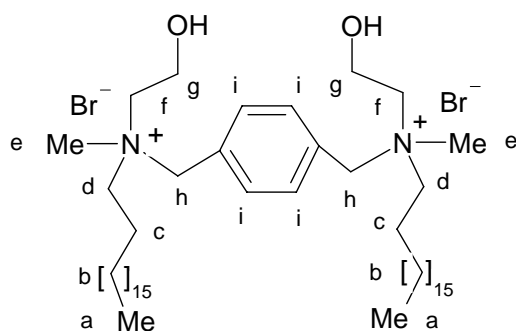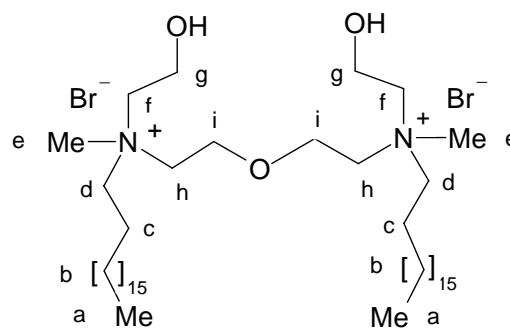
(7dI)   **(7dII)**

2,2'-Di{[(2-hydroxyethyl)methyl-*n*-octadecylammonium]ethyl}ether   dibromide **(7dII)** exhibited similar PMR pattern as that obtained for **(7aII)** except that the number of protons at δ 1.25-1.35 were found to be 60 in its PMR spectrum.

1,4-Di[(2-hydroxyethyl)methyl-*n*-octadecylammonium]butane dibromide **(7dIII)** exhibited similar PMR pattern as that obtained for **(7aIII)** except that the number of protons at δ 1.25-1.35 were found to be 60 in its PMR spectrum.

(7dIII)   **(7dIV)**
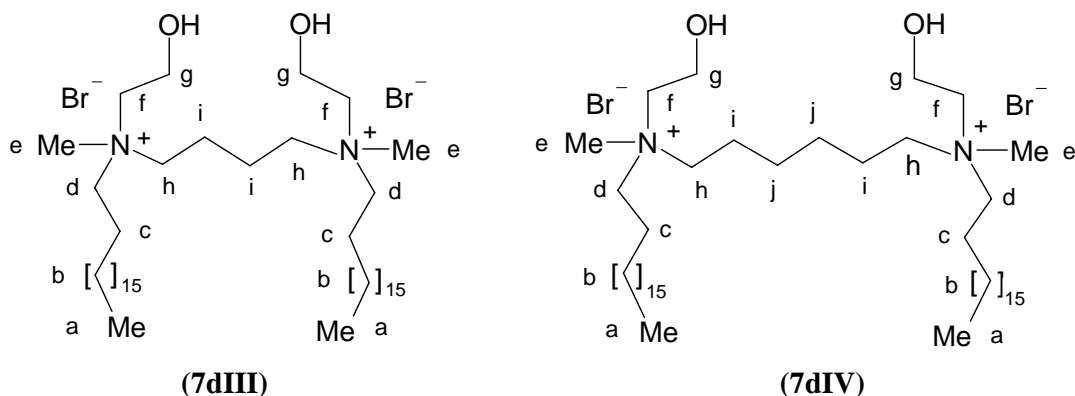
1,6-Di[(-2-hydroxyethyl)methyl-*n*-octadecylammonium)]hexane dibromide **(7dIV)** exhibited similar PMR pattern as that obtained for **(7aIV)** except that the number of protons at δ 1.25-1.35 were found to be 60 in its PMR spectrum.

3.1.3 Synthesis of DEA series of compounds

For the synthesis of GAs belonging to DEA series **Scheme 3** was adopted. Secondary amine **(8)** on reaction with the desired alkyl bromides **(5a-5d)** yielded the tertiary amines **(9a-9d)** as yellow colored viscous liquids. The tertiary amines on further reaction with the dibromo derivative of the desired spacers yielded the desired products **[10a (I-IV) - 10d (I-IV)]**.

1,4-Di{[*n*-dodecyldi(2-dihydroxyethyl)ammonium]methyl}benzene dibromide **(10aI** showed peaks at δ 0.924 (t, 6H, 2 × CH$_{3a}$), 1.319 (b m, 36H, 18 × CH$_{2b}$), 1.877 (m, 4H, 2 × CH$_{2c}$), 3.301 (t, 4H, 2 × N$^+$-CH$_{2d}$), 3.402-3.444 (b t, 8H, 4 × N$^+$-CH$_{2ef}$), 4.005 (b t, 8H, 4 × OCH$_{2gk}$), 4.813 (s, 4H, 4 × N$^+$-CH$_{2h}$), 5.466 (b s, 4H, 4 × OH) and 7.762 (s, 4H, Ar-H$_i$) in its PMR spectrum.
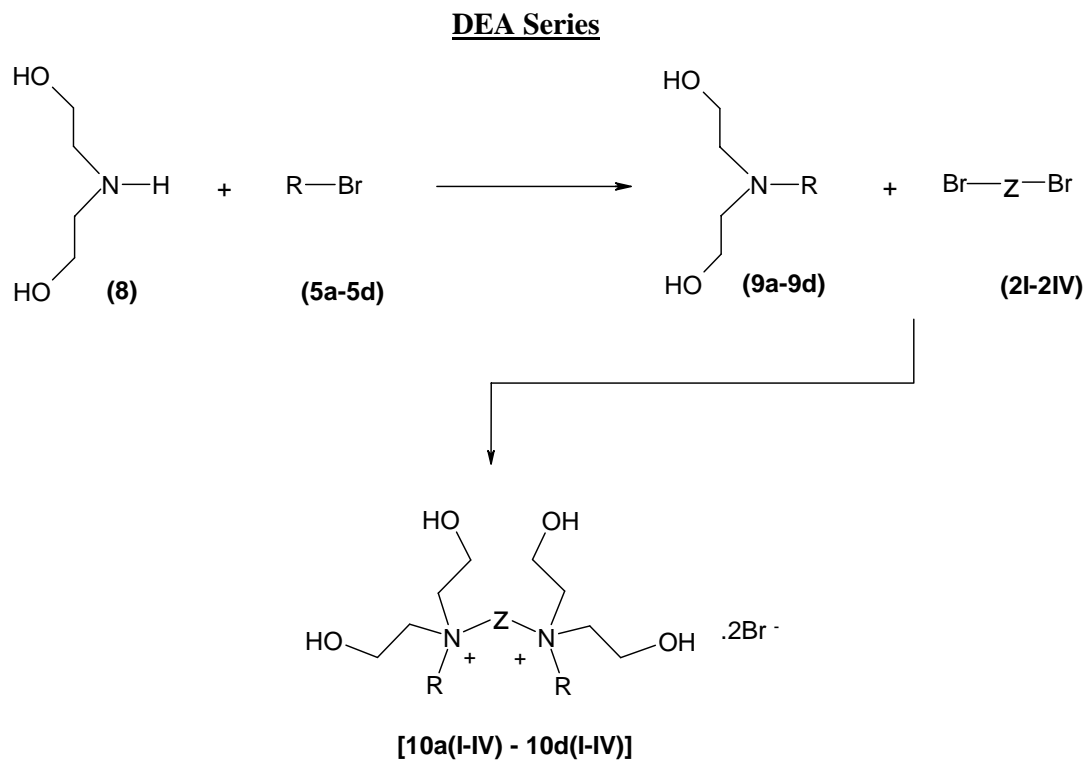
DEA Series

Scheme 3

R: a = $C_{12}H_{25}$; b = $C_{14}H_{29}$; c = $C_{16}H_{33}$; d = $C_{18}H_{37}$

Z: I = $-CH_2-C_6H_4-CH_2-$; II = $-CH_2-CH_2-O-CH_2-CH_2-$
III = $-(CH_2)_4-$; IV = $-(CH_2)_6-$

(10aI)   **(10aIII)**
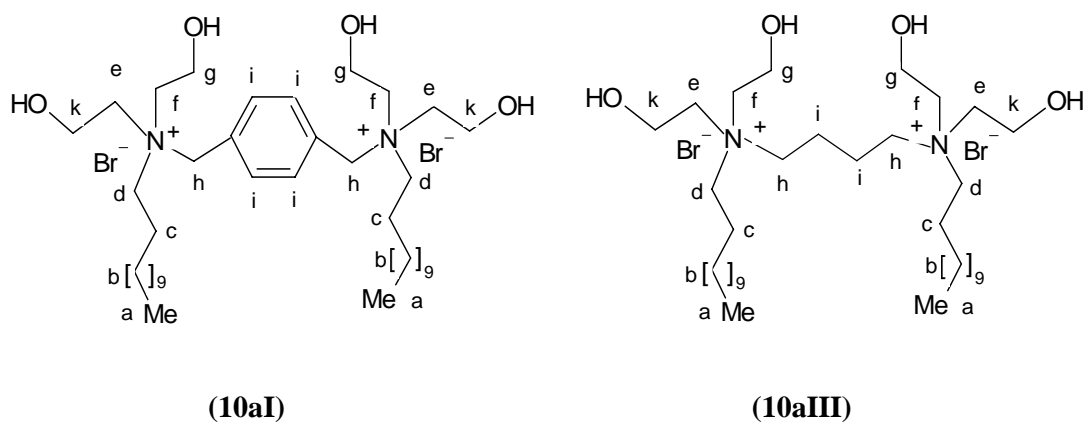
1,4-Di[*n*-dodecyldi(2-dihydroxyethyl)ammonium]butane dibromide (**10aIII**) showed peaks at δ 0.85 (t, 6H, 2 × CH$_{3a}$), 1.25 (b m, 36H, 18 × CH$_{2b}$), 1.67 (b m,

8H, 4 × CH_{2ci}, alkyl chain), 3.34 (b t, 8H, 4 × N^+-CH_{2dh}), 3.42 (b t, 8H, 4 × N^+-CH_{2ef}), 3.8 (b t, 8H, 4 × OCH_{2gk}) and 5.21 (b s, 4H, 4 × OH) in its PMR spectrum.

1,4-Di{[di(2-dihydroxyethyl)-*n*-tetradecyl-ammonium]methyl}benene dibromide **(10bI)** exhibited similar PMR pattern as that obtained for **(10aI)** except that the number of protons at δ 1.25-1.35 were found to be 44 in its PMR spectrum.

(10bI)   **(10bII)**
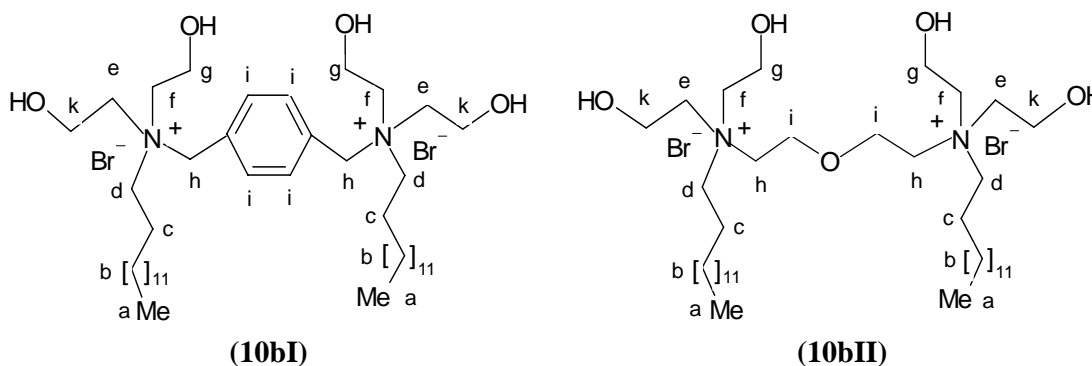
2,2'-Di{[di(2-dihydroxyethyl)-*n*-tetradecylammonium]ethyl}ether dibromide **(10bII)** showed peaks at δ 0.85 (t, 6H, 2 × CH_{3a}), 1.22 (b m, 44H, 22 × CH_{2b}), 1.71 (b t, 4H, 2 × CH_{2c}), 3.59 (t, 4H, 2 × N^+-CH_{2d}), 3.78-3.91 (b m, 12H, 4 × N^+-CH_{2efh}), 4.08-4.17 (b m, 12H, 6 × OCH_{2gik}) and 4.82 (b s, 4H, 4 × OH) in its PMR spectrum.

1,4-Di[di(2-hydroxyethyl)-*n*-tetradecylammonium]butane dibromide **(10bIII)** exhibited similar PMR pattern as that obtained for **(10aIII)** except that the number of protons at δ 1.25-1.35 were found to be 44 in its PMR spectrum.

1,6-Di[di(2-dihydroxyethyl)-*n*-tetradecylammonium]hexane dibromide **(10bIV)** showed peaks at δ 0.85 (t, 6H, 2 × CH_{3a}), 1.16-1.34 (b m, 44H, 22 × CH_{2b}), 1.53 (m, 4H, 4 × CH_{2c}), 1.66 (b m, 8H, 4 × CH_{2ij}),   3.37-3.70 (b m, 16H, 8 × N^+-CH_{2defh}), 4.07 (b t, 8H, 4 × OCH_{2gk}) and 4.97 (b s, 4H, 4 × OH) in its PMR spectrum.

1,4-Di{[*n*-hexadecyldi(2-dihydroxyethyl)ammonium]methyl}benzene dibromide **(10cI)** exhibited similar PMR pattern as that obtained for **(10aI)** except that the number of protons at δ 1.25-1.35 were found to be 52 in its PMR spectrum.
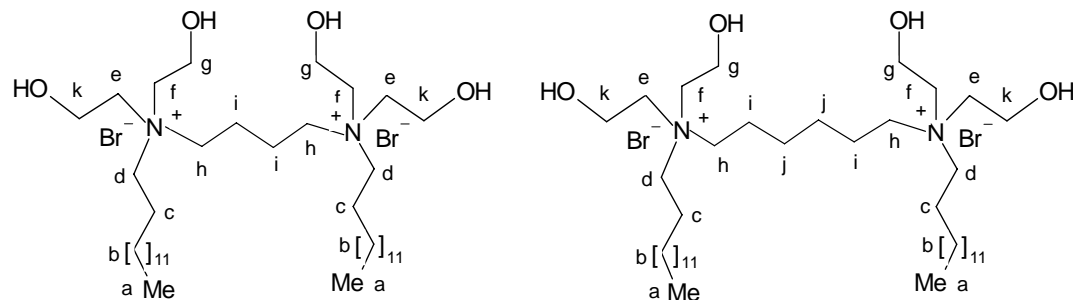
(10bIII)   **(10bIV)**
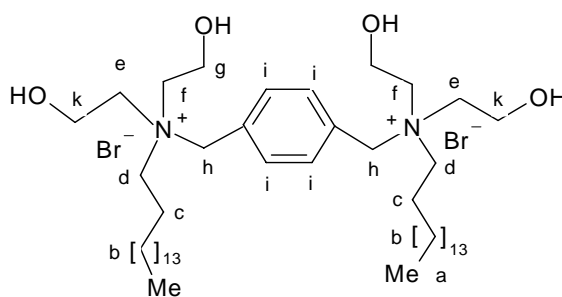
(10cI)

2,2'-Di{[*n*-hexadecyldi(2-hydroxyethyl)ammonium]butane dibromide (**10cIII)** exhibited similar PMR pattern as that obtained for **(10aIII)** except that the number of protons at δ 1.25-1.35 were found to be 52 in its PMR spectrum.

1,6-Dis[*n*-hexadecyldi(2-dihydroxyethyl)ammonium]hexane dibromide **(10cIV)** exhibited similar PMR pattern as that obtained for **(10bIV)** except that the number of protons at δ 1.25-1.35 were found to be 52 in its PMR spectrum.

1,4-Di{[di(2-hydroxyethyl)-*n*-octadecylammonium]methyl}benzene dibrom-ide **(10dI)** exhibited similar PMR pattern as that obtained for **(10aI)** except that the number of protons at δ 1.25-1.35 were found to be 60 in its PMR spectrum.
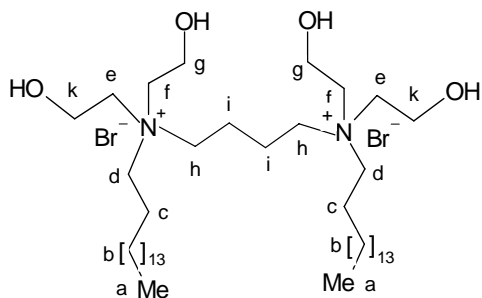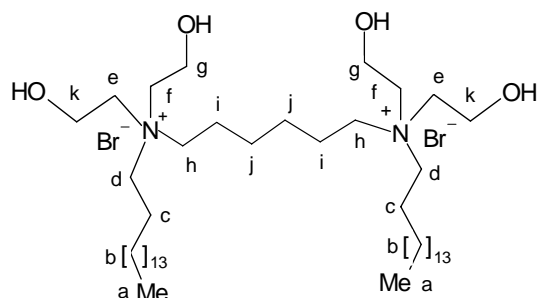
(10cIII)   **(10cIV)**
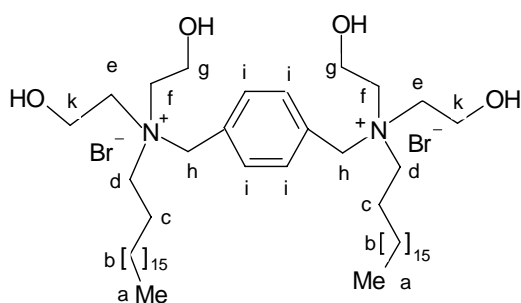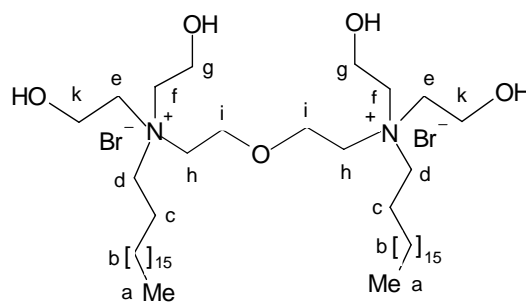
(10dI)   **(10dII)**

2,2'-Di{[di(2-dihydroxyethyl)-*n*-octadecylammonium]ethyl}ether dibromide **(10dII)** exhibited similar PMR pattern as that obtained for **(10bII)** except that the number of protons at δ 1.25-1.35 were found to be 60 in its PMR spectrum.

3.2 Studies related to reporter plasmid DNA

The synthesized GAs needed to be evaluated as vectors for their efficiency to transfect genetic material into the cells. For this purpose suitable genetic material was needed.The work carried out in this direction has been described here.

3.2.1 Bacterial transformation, isolation, and purification of plasmid DNA

A number of methods are available for transformation of nucleic acid construct into bacterial cells. Transform Aid™ bacterial transformation kit provides a rapid means of transformation of plasmid DNA into *E. coli* bacterial strain devoid of any other plasmid for future DNA multiplication and isolation for further

experiments. The kit was used to prepare the competent *E. coli* cells (cells ready to receive plasmid) for easy transformation with significantly higher efficiency than conventional calcium chloride heat shock method.

The transformation of *β*-galactgosidase (*pCMV-SPORT-β-gal*) plasmid into prepared competent cells was confirmed by the growth of the competent cells on agar plates with and without antibiotic, which acted as positive and negative controls. During the transformation process, observations of all of the three streaked agar plates have been shown below in **Table 4**.

Table 4. Observations during transformation of *pCMV-SPORT-β-gal* plasmid

Agar Plate	Observation	Inference
Positive Control: Prepared competent cells were grown on LB plate without the antibiotic	High cell growth observed throughout the plate	Competent cells were not damaged and were capable of growing on agar plate.
Negative Control: Prepared competent cells were grown on LB plate containing antibiotic (ampicillin)	No cell growth observed	Competent cells were sensitive to the antibiotic used.
Test Plate (Plasmid Transformation Plate): Prepared competent cells transform with *β-gal* plasmid and were grown on LB plate containing antibiotic (ampicillin).	Discrete colonies of cells were observed throughout the plate	Transformed cells acquiring plasmid DNA with antibiotic resistance were observed to be growing

The prepared competent cells were found to grow heavily on agar plate without ampicillin; however, on ampicillin containing plates, no cell growth was observed indicating complete suppression of cells by ampicillin. When transformed cells (i.e competent cells treated with plasmid containing antibiotic resistance marker base pairs) were allowed to grow on ampicillin containing plates, the actually transformed cells were found to grow because of the ampicillin resistance acquired by the cells. Transformed cells were selected and isolated by culturing the cells on appropriate antibiotic plate as the transformed bacterial cells were resistant to antibiotic. Pure culture of *E.coli* containing plasmid *β-gal* was stored as glycerol stock and working plates were used for the regular plasmid DNA isolation experiments.

The plasmid DNA was isolated from the working culture of transformed *E. coli* strains using the alkaline lysis method[193, 194]. Bacterial suspension when exposed to strong anionic detergent at high *p*H opens the cell wall denaturing the chromosomal DNA and protein and releasing the *p*DNA into the supernatant. Although the alkaline solution completely disrupts base paring, the strands of the closed circular *p*DNA are unable to separate from each other as they are topologically inter-wound. As long as the intensity and duration of exposure of alkali is not too harsh, the two strands of *p*DNA fall once again into register when the *p*H is returned to neutral. During lysis, bacterial proteins, broken cell walls and the denatured chromosomal DNA get enmeshed in large complexes that are coated with SLS. These complexes are efficiently precipitated from the solution when sodium ions are replaced with potassium ions. After the denatured material was removed by centrifugation, native *p*DNA can be recovered from the supernatant by addition of isopropyl alcohol and ethanol. The closed circular *p*DNA recovered from the lysate was further purified by using various techniques such as phenol–chloroform extraction or PEG-lithium chloride extraction.

The isolated plasmid DNA was purified by PEG-LiCl method. The purity of the plasmid was ascertained by agarose gel assay (two bands without smear indicating pure pDNA) and UV spectrophotometry for absorbance determination at 260 and 280 nm. The ratio of absorbance (A_{260}/A_{280}) was found to be in between 1.8-2.0 indicating pure plasmid DNA devoid of protein and RNA impurities. The concentration of plasmid is determined by absorbance at 260 nm by comparing it with the standard calibration curve or by the equation[195]:

$$1\ (OD_{260}) = 50\ \mu g \text{ of plasmid DNA/mL.}$$

The digestion study was used to confirm the *p*DNA transformation. The isolated purified plasmid DNA was digested with restriction endonuclease enzyme (Bam H1) for linearization of plasmid DNA. Linear *p*DNA was compared with molecular marker on 0.8 % agarose gel. The isolated *p*DNA after linearizing showed a single strong band corresponding to its theoretical molecular weight on the basis of the map provided by the supplier. *β-Gal* plasmid showed the linear band between 9.4 and 6.6

kb corresponding to its molecular weight of 7.8 kb (**Figure 26**), thereby confirming the plasmid DNA.
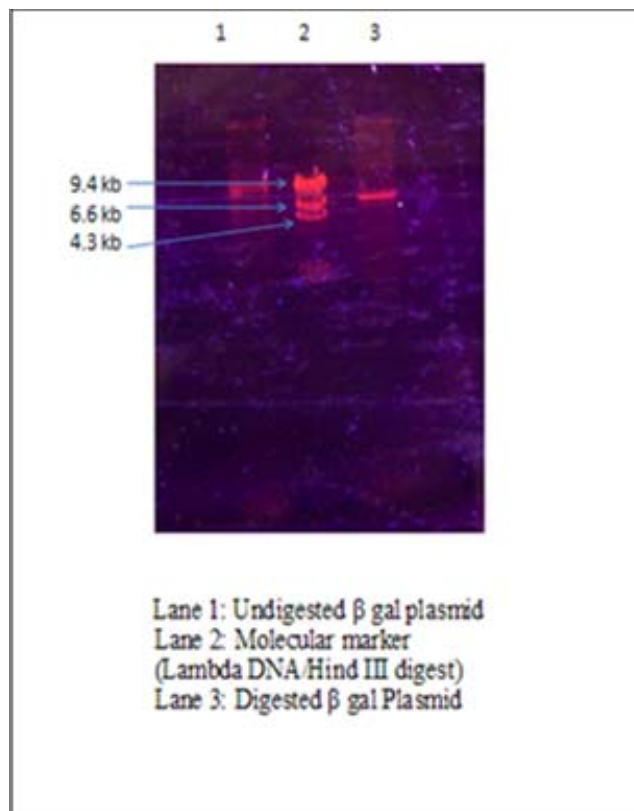
Figure 26. Digestion study of *β-gal* plasmid DNA using Bam H1

3.2.2 Analytical method development for the estimation of plasmid DNA and *β-galactosidase*

3.2.2.1 Estimation of plasmid DNA

The ratio of absorbance at 260 nm and 280 nm provides an estimate of the plasmid purity. The purified *p*DNA showed a ratio in between 1.8 to 2.0. The plasmid DNA was quantified spectrophometrically in Tris buffer of *p*H 8.0 at 260 nm. The calibration curve of the plasmid was constructed as shown in **Figure 27**.

. The DNA solution in Tris buffer showed absorption maxima at 260 nm and a correlation coefficient of 0.999, which indicated that the absorbance and

concentration of DNA are linearly related. The slope (0.02) of the regressed line indicated moderate sensitivity of the method. The method demonstrated linearity of the curve up to a range of 2-60 µg/ mL concentration.
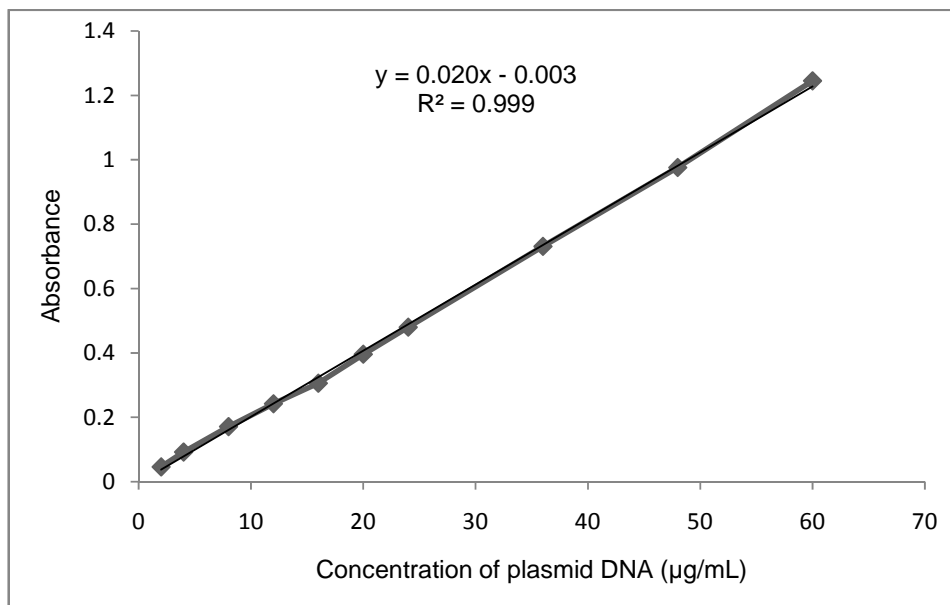
Figure 27. Calibration curve of plasmid DNA in Tris buffer (*p*H 8.0)

3.2.2.2 Estimation of *β*-galactosidase

β-Galactosidase protein estimation method representing a classical colorimetric assay was used for estimation of *β*-galactosidase gene expression[196]. It provides a simple, reliable and economical quantitative estimate of *β*-gal expression by measuring the enzyme activity directly. *o*-Nitrophenol galactopyranoside (ONPG) is colorless, while its hydrolyzed product *o*-nitrophenol (ONP) has a yellow color that absorbs light at 405 nm. The intensity of the developed color directly correlates with the quantity of *β*-galactosidase expressed in the cell.

The calibration curve showed **(Figure 28)** linear increment in absorbance with time at 405 nm. The curve after five minutes showed a correlation coefficient of 0.998 with Beer's Law limit of 5-50 mU and regression equation; y = 0.007 x + 0.009. However, calibration curve at 20 min **(Figure 29)** showed correlation coefficient of 0.997 with Beer's Law limit of 5-50 mU and regression equation; y = 0.029 x + 0.064.
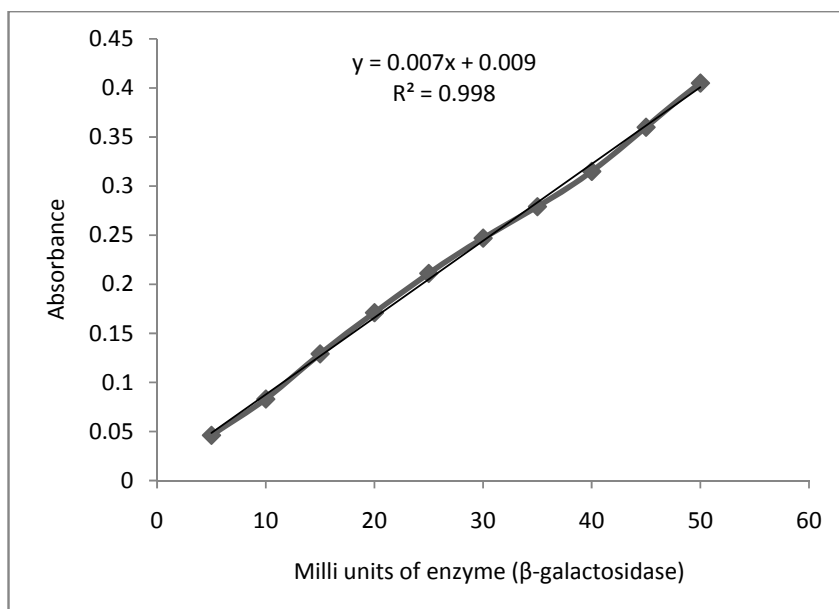
Figure 28. Calibration curve of *β*-galactosidase by reacting known quantity of β-galactosidase (mU) with ONPG after 5 minutes
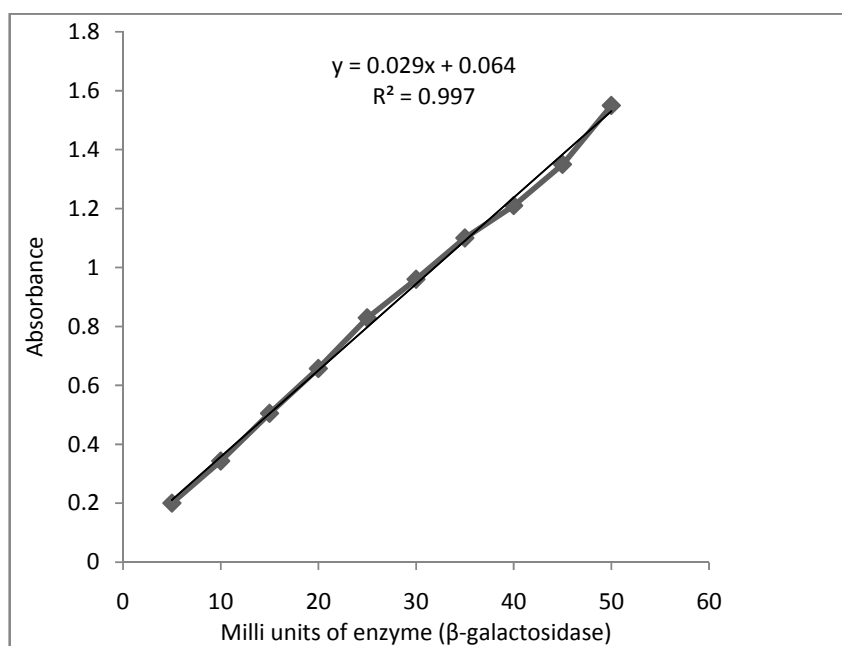
Figure 29. Calibration curve of *β*-galactosidase by reacting known quantity of *β*-galactosidase (mU) with ONPG after 20 minutes

The absorbance of ONP is converted into *β*-galactosidase activity and is used for the estimation of transfection efficiency of various transfecting agents under *in vitro* conditions following the protocol mentioned in the *in vitro* cell line studies.

3.3 Formulation development and characterization

3.3.1 Determination of critical miceller concentration

The determination of cmc using conductometry is based upon the principle that conductance of amphiphiles solution changes with concentration at different rates below and above critical miceller concentration. This difference in aggregation behavior is controlled by co-operativity of both inter-molecular and intra-molecular interactions of GAs, besides their interactions with solvents. The cmc values of all the synthesized GAs have been determined using conductance measurement[197].

The cmc values are obtained by using break point in concentration versus conductance plot. The representative graphs for GAs (**3I, 3II, 3III and 3IV**) have been shown in **Figure 30** and the cmc values of all the synthesized GAs are compiled in **Table 5**. All the measurements were carried out at 30 ^{o}C except for the GAs having *p*-xylene spacers which were dispersed in water at 50 ^{o}C.

All the GAs were observed to dissociate completely at very low concentration and their conductance increases linearly with increase in concentration up to cmc. Although, the conductance continues to increase beyond cmc also, but the rate of increase in conductance is slower compared to that below cmc. The nature and structure of a spacer between the two head groups of a GA are the key factors which distinguish GAs from conventional monomeric amphiphiles and are critical to the unique properties of GA. The spacer can be used to manipulate the hydrophobic interactions as well as to constrain the electrostatic repulsion between charged head groups. The cmc values obtained for DMA series indicate that as the nature of spacer changes from oxyethylene (**3II**, 22.2 X 10^{-3} M) to polymethylene (**3III**, 28.2 X 10^{-3} M; **3IV**, 44.8 X 10^{-3} M) to p-xylene (**3I**, 57.6 X 10^{-3} M), the cmc value increase. The result indicates that the nature of spacer has an important effect on the aggregation properties of GA. A hydrophilic, flexible spacer prompts micelle formation, which

leads to smaller cmc, larger aggregation number and a more negative Gibbs free energy change of micellization (ΔGmic)[198].
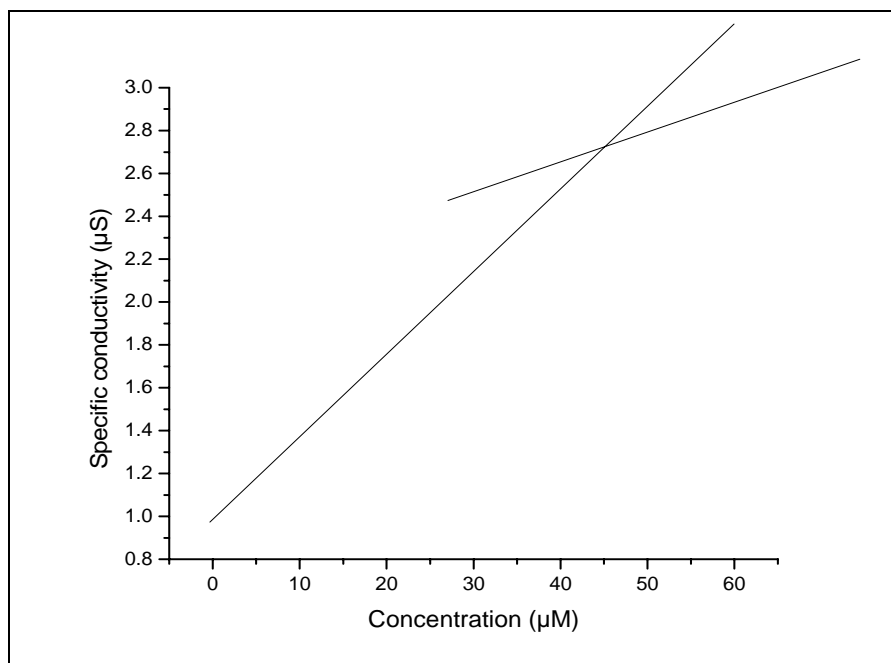
(A)
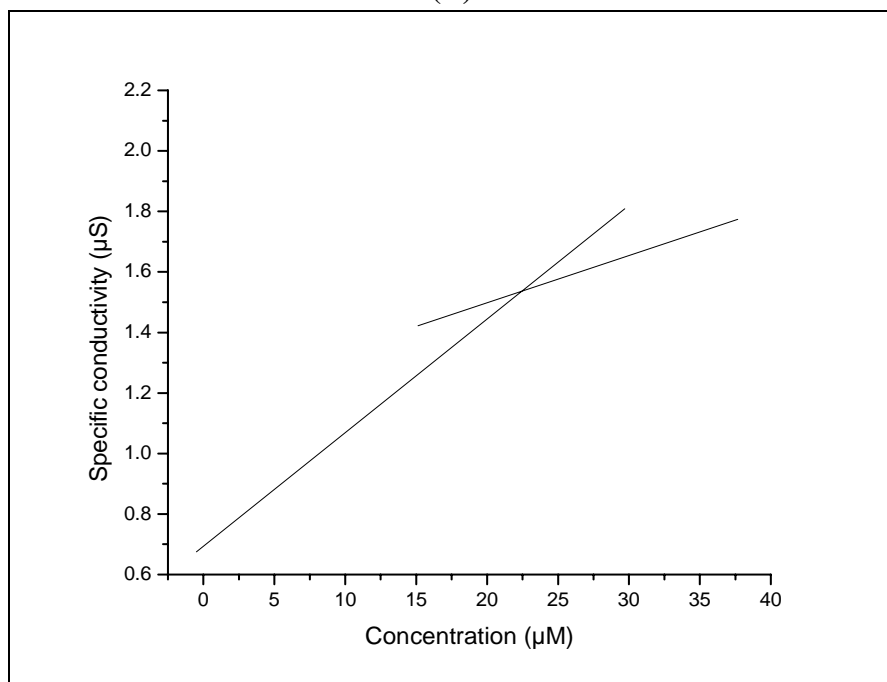
(B)
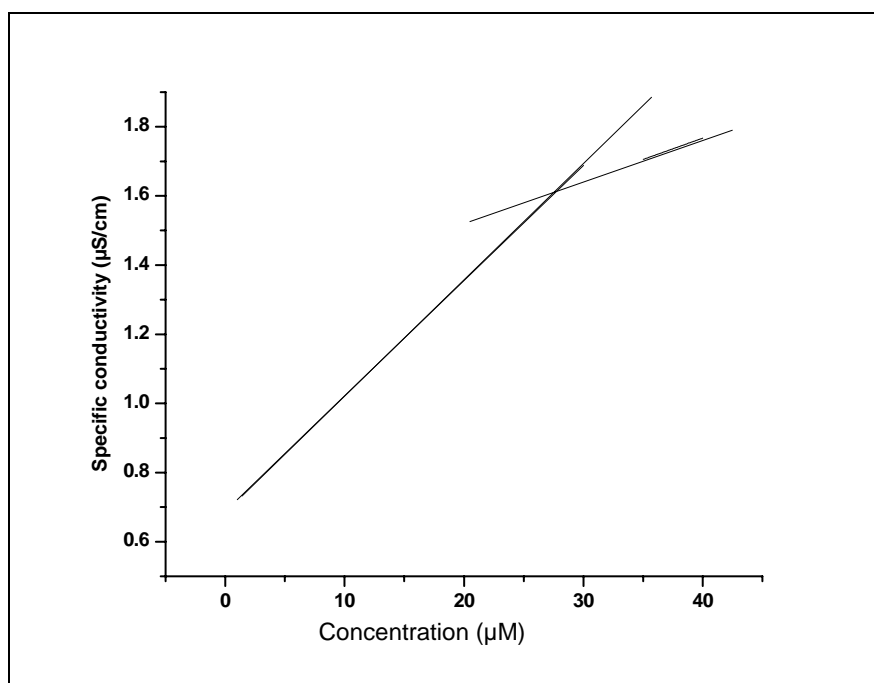
(C)
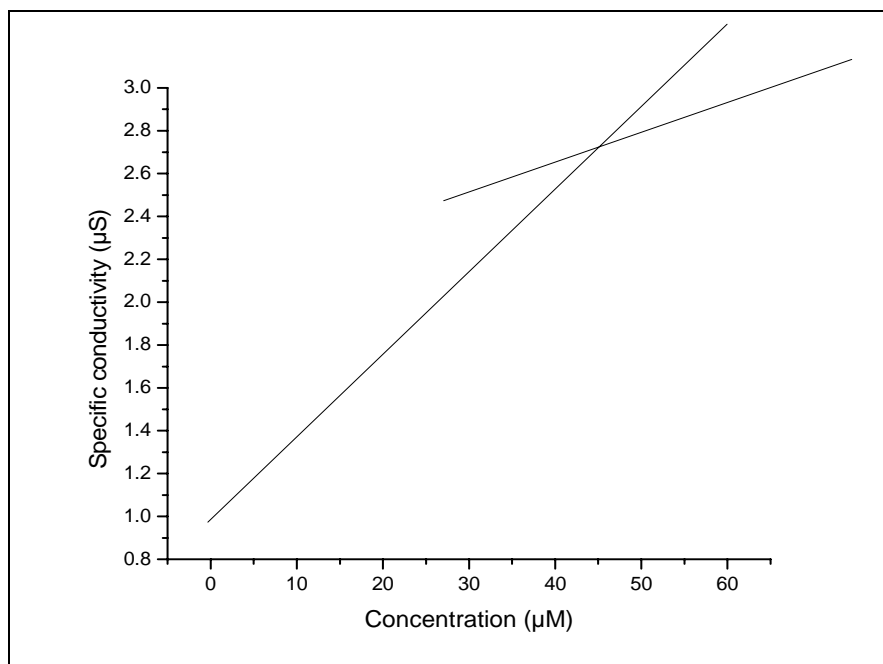
(D)

Figure 30. Representative plotes for cmc value determination using conductometry;
(A) **3I**, (B) **3II**, (C) **3III** and (D) **3IV**

The conformation of the GAs changes upon aggregation. In aggregation state the GA molecules must adopt the conformation where the two alkyl chains are as close to each other as possible, and the spacer is progressively incorporated into the aggregate hydrophobic core with the increasing hydrophobicity of the spacer. Among the compounds having different spacer groups, GAs with *p*-xylene spacers showed the highest cmc values followed by the GAs possessing hexamethylene spacers[199].

The variation in cmc values with the spacer chain length can be attributed to the conformational changes taking place at the polymethylene spacer. For the $(CH_2)_6$ spacer, the alkyl chain of the spacer remains in a fully extended conformation making it somewhat difficult to be located at micelle-water interface, whereas for longer spacers ($> (CH_2)_6$), the spacer tries to form a loop in the hydrophobic core of the

Table 5. List of synthesized GAs with their cmc values

S. No.	Compound Code	cmc (at 30 ^{0}C)	S. No.	Compound Code	cmc (at 30 ^{0}C)
DMA Series					
1	**3I**	57.6×10^{-6} M	3	**3III**	28.2×10^{-6} M
2	**3II**	22.2×10^{-6} M	4	**3IV**	44.8×10^{-6} M
MEA Series					
5	**7aI**	4.8×10^{-5} M	13	**7cI**	2.8×10^{-6} M
6	**7aII**	2.3×10^{-5} M	14	**7cII**	1.3×10^{-6} M
7	**7aIII**	2.9×10^{-5} M	15	**7cIII**	2.1×10^{-6} M
8	**7aIV**	3.6×10^{-5} M	16	**7cIV**	2.6×10^{-6} M
9	**7bI**	3.9×10^{-5} M	17	**7dI**	2.6×10^{-6} M
10	**7bII**	1.6×10^{-5} M	18	**7dII**	1.0×10^{-6} M
11	**7bIII**	2.3×10^{-5} M	19	**7dIII**	1.2×10^{-6} M
12	**7bIV**	2.4×10^{-5} M	20	**7dIV**	2.4×10^{-6} M
DEA Series					
21	**10aI**	6.4×10^{-6} M	27	**10cI**	4.1×10^{-6} M
22	**10aIII**	4.2×10^{-6} M	28	**10cIII**	1.1×10^{-6} M
23	**10bI**	4.4×10^{-6} M	29	**10cIV**	2.6×10^{-6} M
24	**10bII**	1.9×10^{-6} M	30	**10dI**	3.8×10^{-6} M
25	**10bIII**	2.3×10^{-6} M	31	**10dII**	1.3×10^{-6} M
26	**10bIV**	3.1×10^{-6} M			

micelle disrupting the micelle geometry. In brief, the spacer affects the aggregation of gemini surfactants mainly through its interaction with the alkyl chains as well as the

interaction between the spacers. Any structural variation in the spacer which promotes these interactions will promote the aggregation of gemini surfactants.

The surface active properties of GAs were found to be superior to their monomeric counterparts. For instance, **(3I)**, **(3II)**, **(3III)** and **(3IV)** of DMA series showed cmc values of 57.6×10^{-6}, 22.2×10^{-6}, 28.2×10^{-6} and 44.8×10^{-6} M respectively. These cmc values were found to be about 100 fold lower compared to monomeric surfactant, cetyl trimethyl ammonium bromide (1.3×10^{-3} M) [200].

Moreover, comparison of cmc value of GAs for a particular spacer showed that as the polarity of head group is increased by incorporation of hydroxyethyl group (**3III,** 28.2×10^{-5}; **7cIII**, 2.1×10^{-6}; **10cIII**, 1.1×10^{-6}), the cmc values of GAs decreased by 10 fold. Similar results (**Table 5**) were obtained for other spacers while maintaining the hydrophobic chain length. The results obtained are suggestive of superior surface active properties of polar GAs (MEA and DEA series) compared to the non-polar GAs (DMA series). This may be due to hydrogen bonding of $-C_2H_4OH$ groups with water through oxygen atom that is likely to provide additional hydration at the head group level resulting in screening of columbic forces of repulsion between charged heads and helping MEA and DEA series GAs to form aggregates at a lower concentration than those of DMA series [201, 202].

On comparing the cmc values for all the series, it was observed that cmc values showed dependency on hydrophobic chain length. For instance, the cmc values for **7aIII**, **7bIII**, **7cIII** and **7dIII** were found to be 2.9×10^{-5}, 2.3×10^{-5}, 2.1×10^{-6} and 1.2×10^{-6} respectively.

3.3.2 Preparation of GA formulations

All the synthesized GAs were formulated as liposomes either alone or with helper lipid DOPE above $\sim 70\ ^0$C in molar ratio of 1:1, 1:2 and 1:3. DOPE was selected as helper lipid due to its fusogenic property at endosomal stage[203]. Buffer system (HEPES, 20 mM) was selected to maintain the *p*H of the formulations to 7.4 as the non-ionic nature of HEPES does not provide any hindrance during lipoplex formation of the GAs with *p*DNA. A blend of solvents (chloroform:methanol, 1:1) was selected to completely dissolve the GAs with and without helper lipids. Cholesterol was also used as a helper lipid to improve the formulation characteristics.

3.3.3 Characterization of GA formulations

All the synthesized GAs were formulated either alone or with helper lipid DOPE at ~ 70 ^{0}C. Almost all GAs exhibited bimodular size distribution (two peaks in their size distribution report). The results reported here, are the average size (Z-average) for all the analysis. The results of plain formulations of **3III**, **7cIII**, **10cIII** and **7aIII** have been shown in **Table 6**. All the formulations showed positive zeta potentials (ZP) due to quaternary nitrogens in their molecule, which is a necessary requirement for complexation with anionic *p*DNA. Relatively higher values of Polydispersibilty Index (PDI) were obtained due to bimodular size distribution in the formulations. It may be due to free GA molecules along with their aggregates. The results showed that as the polarity of the head group increased in GAs from **3III** to **7cIII** to **10cIII**, Z-average (Z_{av}) increased from 325 to 369 to 400 nm, while the hydrophobic chain length was kept constant. This may be due to the increasing propensity of the head group to hydrate with increasing number of hydroxyethylated groups. Moreover, Z_{av} was found to vary with the hydrophobic chain length also i.e., 326 and 233 nm for **7cIII** and **7aIII** having similar head groups but with C_{16} and C_{12} chains in their structures respectively.

Table 6. Size and zeta potential of plain formulations

Formulation	Size, Z_{av} in nm (PDI)	Zeta Potential in mV
3III	326 (0.532)	30.1
7cIII	369 (0.698)	48.9
10cIII	400 (0.483)	46.4
7aIII	233 (0.349)	35.8

The method of preparation also had significant role on Z_{av} of the same formulations. For instance, formulation of **7cIII** showed Z_{av}, PDI and ZP of 725 nm, 0.802 and 52.9 respectively before sonication. Moreover, the incorporation of DOPE into the formulation resulted into increase in Z_{av}. **7cIII** showed Z_{av} of 129, 177, 339 and 417 nm when formulated as alone and in the ratios of 1:1, 1:2 and 1:3 respectively with DOPE at double dilution.

The lipoplexes of GA formulations were prepared with plasmid DNA at different N/P ratio (0.25-6). The N/P ratio is defined as molar ratio of number of positively charged nitrogens in cationic GA to the number of negatively charged phosphate of the anionic *p*DNA. All the complexes were prepared keeping the quantity of *p*DNA constant and varying the quantity of GA in the formulations.

Table 7. Size and zeta potential of 7bIII1 lipoplex

Formulation	N/P ratio	Size, Z_{av} in nm (PDI)	Zeta Potential in mV
7bIII1 blank		272 (0.327)	43.51
Lipoplex of **7bIII1** with *p*DNA	0.25	483 (0.614)	-20.90
	0.5	448 (0.372)	-12.90
	1.0	423 (0.328)	-4.80
	1.5	382 (0.318)	0.69
	2.0	329 (0.357)	1.26
	2.5	360 (0.225)	1.61
	3.0	422 (0.401)	2.82
	3.5	439 (0.280)	6.97
	4.0	481 (0.201)	6.66

However, the volumes of the cationic formulations and *p*DNA dilutions were kept constant during lipoplex preparation. The sizes of the prepared lipoplex were found to depend on the incubation time after mixing of the GA formulation and *p*DNA.

Table 8. Size and zeta potential of 7bII1 lipoplex

Formulation	N/P ratio	Size, Z_{av} in nm (PDI)	Zeta Potential in mV
7bII1 blank		214 (0.461)	29.6
Lipoplex of **7bII1** with *p*DNA	0.25	486 (0.725)	-14.9
	0.5	477 (0.313)	-9.08
	1.0	318 (0.348)	-2.98
	1.5	241 (0.266)	1.16
	2.0	222 (0.287)	2.91
	2.5	278 (0.315)	3.36
	3.0	290 (0.385)	6.83
	3.5	293 (0.291)	15.0
	4.0	345 (0.387)	16.9

The **7aIII** lipoplex have showed size of 166, 198 and 220 nm for incubation time of 15, 30 and 60 minutes, at N/P ratio of 1:1. The Z_{av} and ZP were also determined for

the lipoplex of formulations that showed best results under transfection studies (**7bIII1** and **7bII1** are compiled in **Tables 7** and **8** as representatives).

The blank formulation of **7bIII1** showed $Z_{av,}$ and ZP of 272 and 43.5 respectively. However, its lipoplex with *p*DNA showed different values for Z_{av} and ZP depending upon the N/P ratio. At lowest N/P ratio (0.25), the poyplex showed Z_{av} and ZP of 483 and -20.9. With the increasing N/P, the size of lipoplexes first decreased and then increased; however, ZP increased with the increased N/P ratio (-20.9 to 6.66).
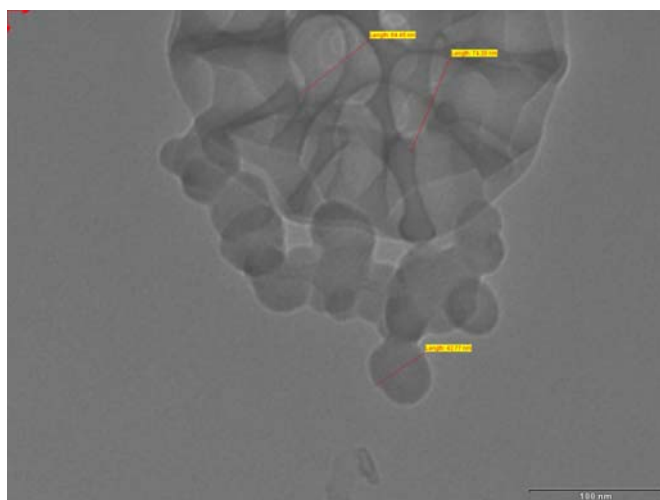
Figure 31. TEM image of **7bIII1** lipoplex at its optimized N/P ratio
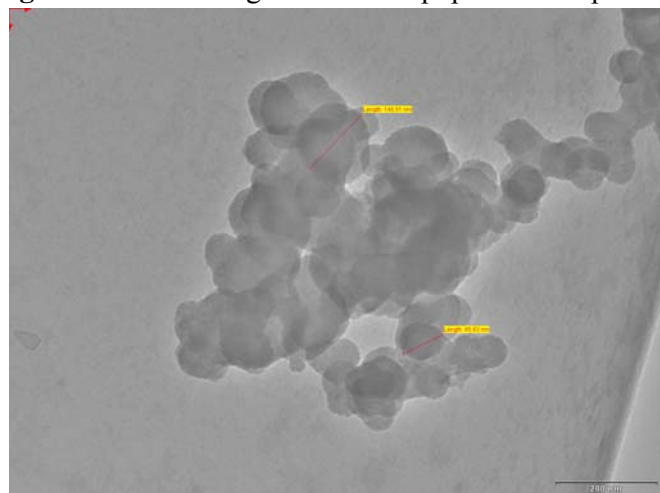
Figure 32. TEM image of **7bII1** lipoplex at its optimized N/P ratio

The formulation of **7bII1** showed Z_{av} and ZP of 214 nm and 29.6 mV. The results obtained for **7bII1** were similar in trend to that of **7bIII1** in the variation of Z_{av} and ZP with different N/P ratios.

Tranmission electron microscopy (TEM) photographs of the lipoplex of **7bIII1** and **7bII1** at their optimized N/P ratios have been shown in **Figures 31** and **32** respectively. The results obtained in TEM study were in consonance to those obtained with DLS.

3.3.4 Agarose gel retardation assay for *p*DNA complexation

Electrostatic interactions between the negatively charged *p*DNA and cationic liposomes as a function of N/P ratios were characterized by electrophoretic gel retardation assay. All the complexes were prepared keeping the quantity of *p*DNA constant and varying the quantity of the formulation. However, the volumes of cationic formulation and *p*DNA dilutions were kept constant during lipoplex preparation. In this study, the un-complexed *p*DNA would move out of the well; while the complexed *p*DNA would remain inside the well[204].

Gel electrophoretic patterns for GAs (**3cIII, 7cIII** and **10cIII**) have been shown in **Figure 33**. Lane 1 shows plain *p*DNA that moved out of the well under the influence of electrostatic force. However, other lanes exhibited retardation of *p*DNA as the N/P ratio increasing from 0.25 to 3.0. All GAs showed ~ 60 % retardation at N/P ratio of 0.5. About 100 % DNA retardation has been observed for all the GAs at N/P of 1.0. However, for N/P ratios higher than 1.0 complete retardation was observed. It should be noted that every GA molecule possessed two hard charges, which indicated that the whole plasmid DNA gets retarded at lipid/DNA mole ratio of 0.5. Significant retardation of DNA was also observed at N/P ratio of 0.5 (or GA/DNA mole ratio of 0.25) as well. No effect of head group polarity of GAs has been found in gel retardation study as all the GAs in the given figure have shown almost similar retardation pattern at similar N/P ratios.
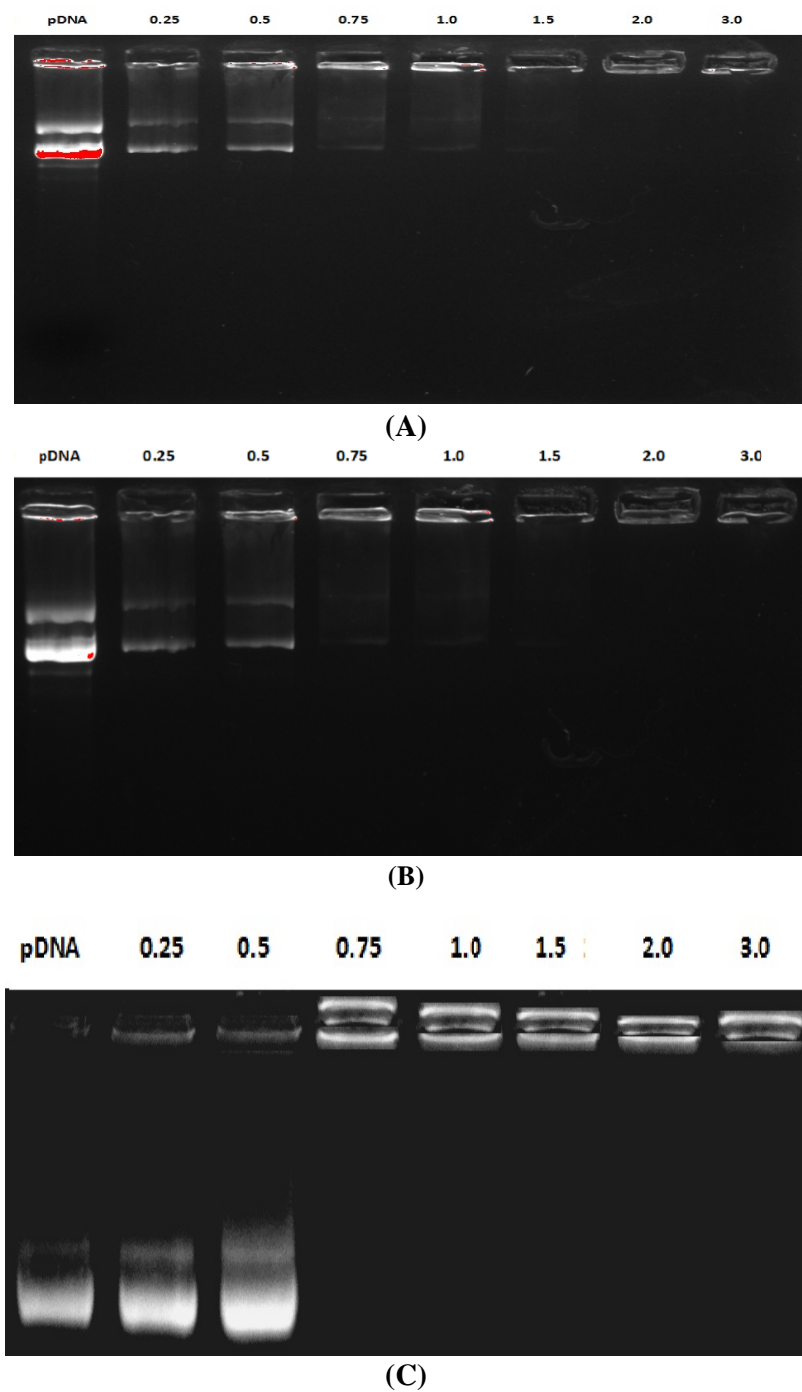
Figure 33. N/P complexation behavior of the synthesized GAs under gel electrophoresis; (A) **3cIII**, (B) **7cIII** and (C) **10cIII**. Lane 1 (plasmid DNA), lane 2 to 8 (N/P 0.25 to 3.0)

3.3.5. DNase I digestion study

A gene delivery carrier system should have the ability to protect *p*DNA from DNase enzyme. DNase I digestion study was performed to evaluate the *p*DNA protection capability of the synthesised GA formulations. The results obtained in the

(A)

(B)

(C)
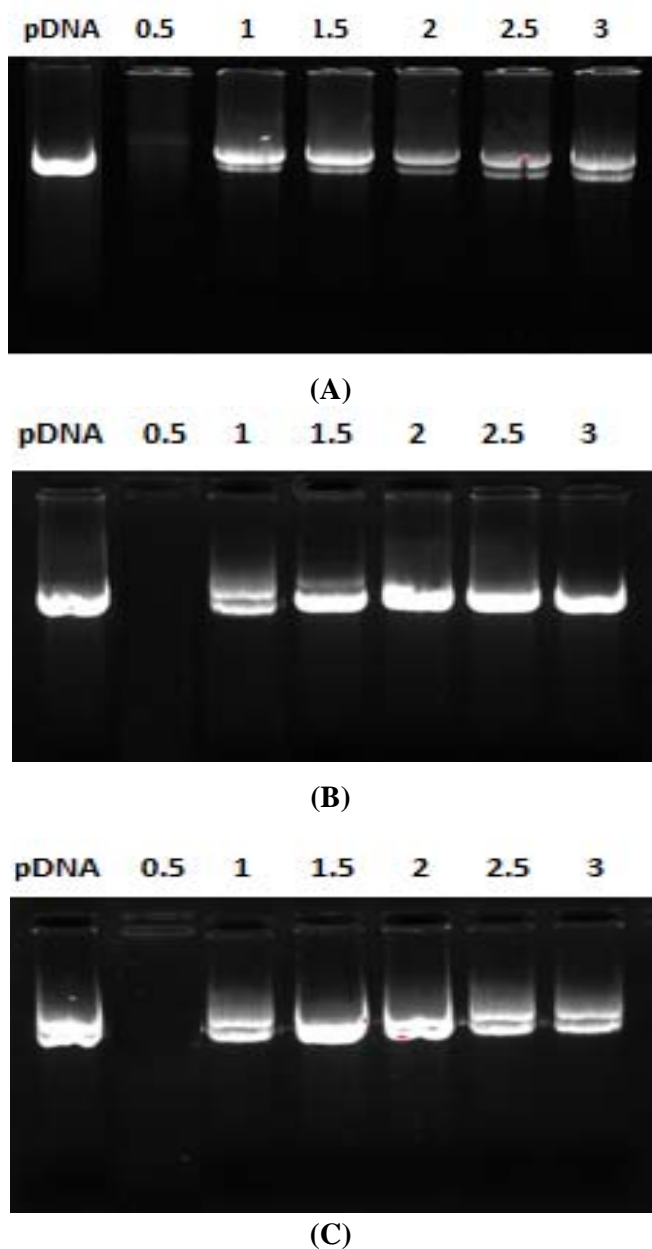
Figure 34. DNase digestion study to *p*DNA protection. (A) **3III,** (B) **7cIII** and (C) **10cIII**

study have been shown in **Figure 34** (A, B and C). Lane 1 shows naked *p*DNA without DNase treatment. At N/P 0.5 with all the GAs (**3III, 7cIII** and **10cIII**) under consideration, complete degradation of *p*DNA was observed. However, at N/P of 1 about 90 % of *p*DNA could be protected by GA formulations. Complete protection of the *p*DNA against DNase was observed at N/P ratios of more than 1. The naked DNA on treatment with DNase I showed complete degradation. No effect of head group polarity of GAs was observed in this study, while the hydrophobic tails were kept constant.

3.3.6 Circular Dichroism (CD) study for *p*DNA condensation

Circular dichroism provides information on the helical conformation of the double-stranded DNA. Cationic amphiphiles bind to the native B-form of the DNA and induce secondary structure formation, which reduces the number of basepairs/turn from 10 to 9.33[205]. The CD spectrum of plasmid DNA in HEPES buffer exhibits a positive band near 277 nm and a negative band near 245. The condensation of DNA into a chiral ψ-phase is instead indicated by an overall shift of the spectrum to higher values of wavelengths, an enhanced negative band and an almost complete flattening of the positive CD signal[206].

With the addition of GA, change in the B-form to ψ-form can be visualized in **Figure 35**. Moreover, increase in the N/P (+/- charge) ratio causes condensation of the DNA into ψ-DNA, a left handed highly organized tertiary structure, characterized by an increase of the negative signal of the CD spectra. An effective complexation between DNA and liposomes should yield compaction of the nucleic acid; this will promote the penetration of the nucleic acid into the target cell because of the reduced size of the polymer and will protect the genetic exogenous material from nuclease degradation. A crucial point for obtaining high transfection efficiency is, in fact, to maintain the therapeutic genes undamaged[207, 208]. Simberg et al. demonstrated that formation of the compact ψ-DNA is necessary for efficient gene delivery[209]
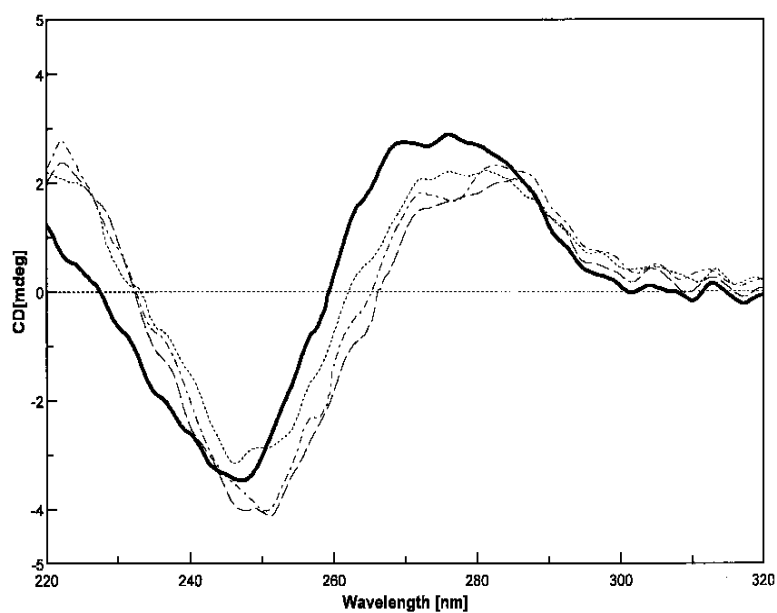
(A)
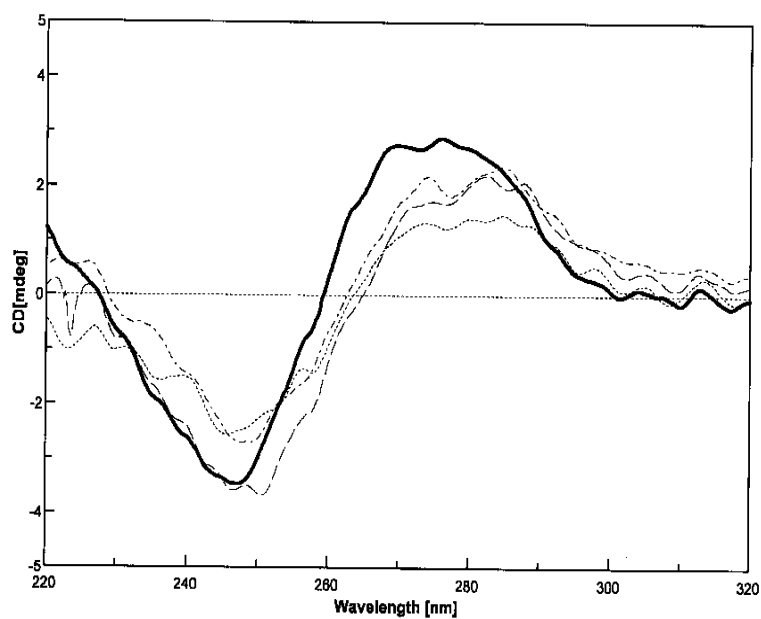
(B)
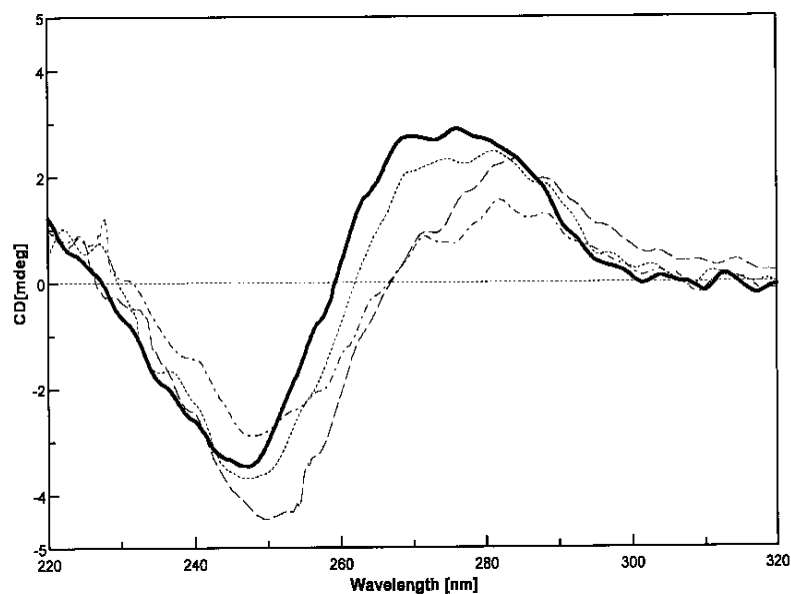
(C)

Figure 35. Circular dichroism spactra of (A) **3III**, (B) **7cIII** and (C) **10cIII**. Black
solid line (uncondensed plsmid), dot-dot-dot (N/P 0.5), dash-dot-dash
(N/P 1) and dash-dash-dash (N/P 2)

.

A comparison of the results obtained in the CD experiments **(Figure 35)** for
3III, **7cIII** and **10cIII** demonstrated that all the GAs are effective in condensing
*p*DNA into ψ-phase. The condensation properties of the cationic formulations depend
on the molecular structure of the cationic amphiphile as well as on the nature of DNA.
Under the same experimental conditions and equivalent amounts of GAs, **7cIII**
showed more effective condensation of plasmid DNA when compared to **3III** and
10cIII. This result can be connected with the work reported by Sakai's group who
used the Cryo-TEM to determine the aggregated form of DNA with
cetyltrimethylammonium bromide (CTAB) and concluded that the DNA morphology
changed from loosely packed spherical to rod like via toroidal structure by the
addition of CTAB[210]. DNA molecules take on a spaciously expanded random coil
form in good solvents or at high temperatures because of the strong electrostatic
repulsion between the negatively charged phosphate groups, whereas they can be in a
spherical, toroidal, rod-like, and highly folded solid-like form in poor solvents or at

low temperatures because of the suppressed electrostatic repulsion. Upon adding GA, the GA-*p*DNA complexes are formed due to the electrostatic interaction, thereby reducing the surface charge, so that the DNA molecules will take a tight conformation as deduced by the CD spectrum.

3.4 *In vitro* cell line studies

3.4.1 Transfection studies using *β*-Gal reporter plasmid in absence of Fetal bovine serum (FBS)

The transfection efficiency of each GA was evaluated in two cell lines (A549 and HeLa) using *β*-Gal reporter plasmid either all alone or with DOPE as helper lipid at N/P ratios of 0.5, 1, 2, 3, 4 and 6. The amount of *β*-galactosidase protein expressed in cells is directly proportional to the transfection efficiency of the used gene delivery carrier. The transfection results so obtained showed that all the GAs exhibited higher *β*-Gal expression when formulated along with DOPE. This may be due to an early release of lipoplex at endosomal stage inside the cells[180].

In A549 cell line, **3I (Figure 36A)** showed the highest β-Gal expression (0.76 mU) at N/P ratio of 2. However, in combination with DOPE (**3I1,** 1:1 molar ratio) the highest expression (1.19 mU) was obtained at N/P 4.

(A)

(B)
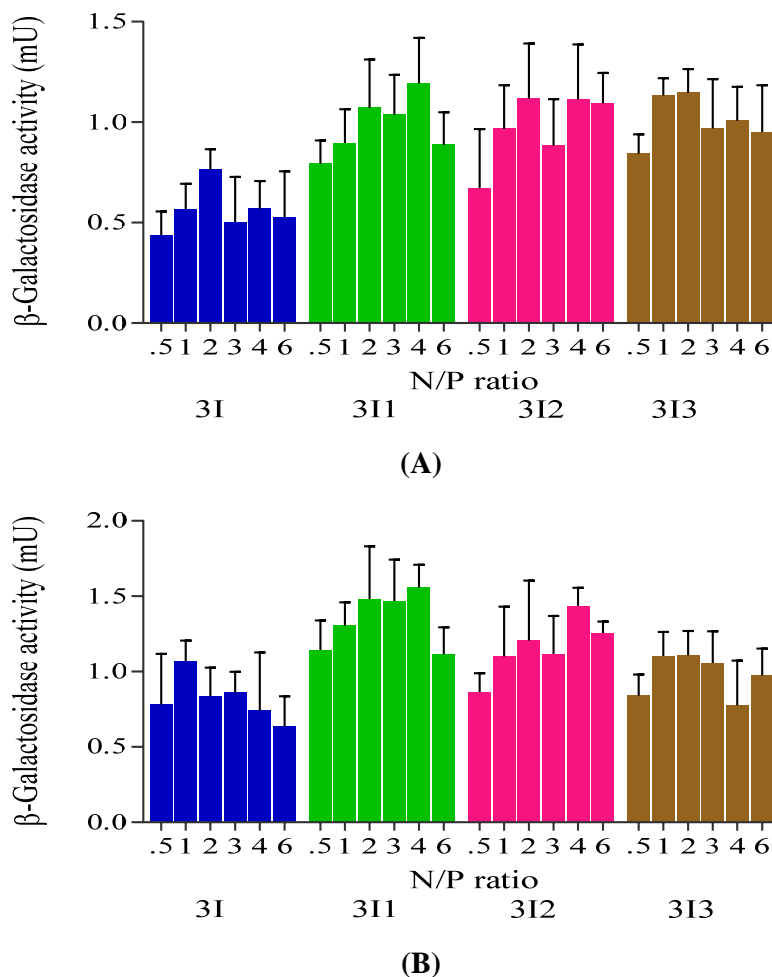
Figure 36. Transfection efficacies of **3I** alone and in combination with DOPE, 1:1 **(3I1)**, 1:2 **(3I2)** and 1:3 **(3I3)** in (A) A549 and (B) HeLa cell lines

In HeLa cell line, **3I** showed the highest **(Figure 36B)** β-Gal expression (1.06 mU) at N/P ratio of 1. However, in combination with DOPE (**3I1,** 1:1 molar ratio) the highest expression (1.55 mU) was obtained at N/P 4.

In A549 cell line, **3II (Figure 37A)** showed the highest β-Gal expression (1.02 mU) at N/P ratio of 1. However, in combination with DOPE (**3II1,** 1:1 molar ratio) the highest expression (1.67 mU) was obtained at N/P 3.

(A)

(B)
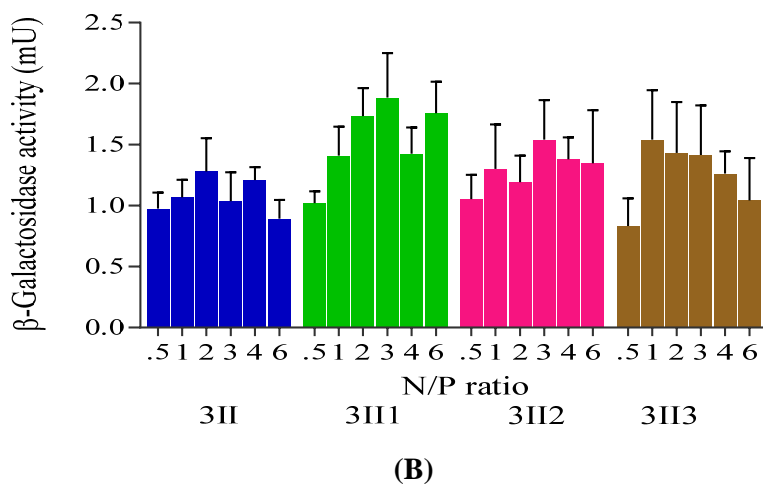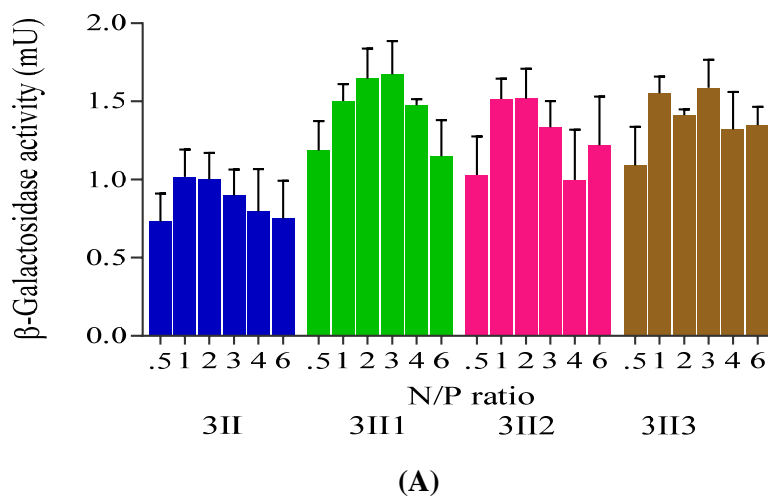
Figure 37. Transfection efficacies of **3II** alone and in combination with DOPE; 1:1 **(3II1)**, 1:2 **(3II2)** and 1:3 **(3II3)** in (A) A549 and (B) HeLa cell lines

In HeLa cell line, **3II (Figure 37B)** showed the highest β-Gal expression (1.28 mU) at N/P ratio of 2. However, in combination with DOPE (**3II1,** 1:1 molar ratio) the highest expression (1.88 mU) was obtained at N/P 3.

In A549 cell line, **3III (Figure 38A)** showed the highest β-Gal expression (0.94 mU) at N/P ratio of 1. However, in combination with DOPE (**3III1,** 1:1 molar ratio) the highest expression (1.60 mU) was obtained at N/P 4.
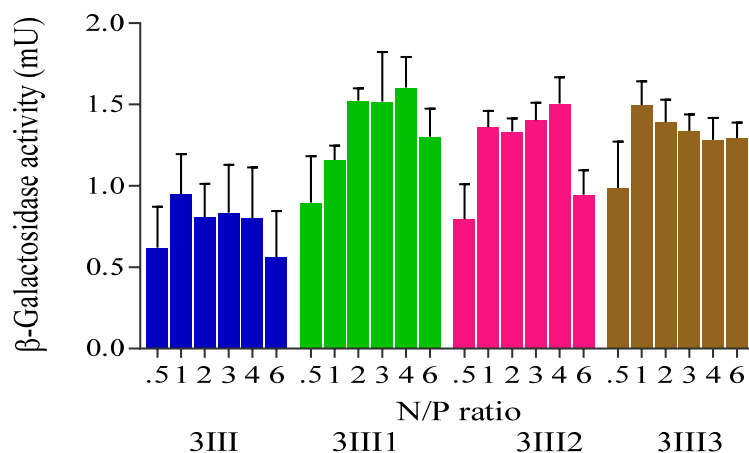
(A)
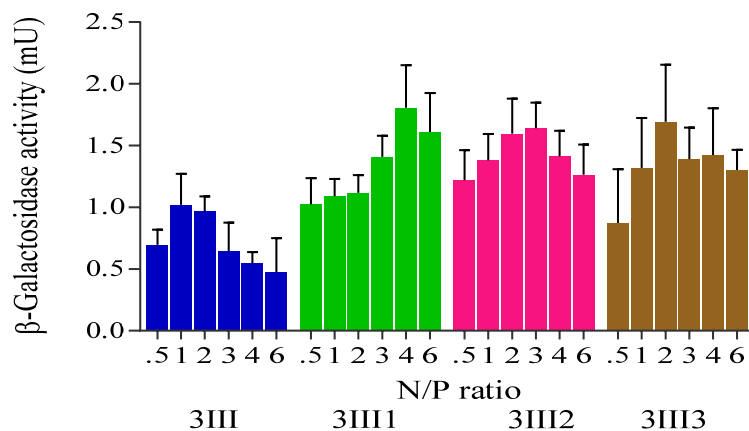
(B)

Figure 38. Transfection efficacies of **3III** alone and in combination with DOPE; 1:1 (**3III1**), 1:2 (**3III2**) and 1:3 (**3III3**) in (A) A549 and (B) HeLa cell lines

In HeLa cell line, **3III (Figure 38B)** showed the highest β-Gal expression (1.02 mU) at N/P ratio of 1. However, in combination with DOPE (**3III1,** 1:1 molar ratio) the highest expression (1.80 mU) was obtained at N/P 4.

In A549 cell line, **3IV (Figure 39A)** showed the highest β-Gal expression (0.88 mU) at N/P ratio of 2. However, in combination with DOPE (**3IV2**, 1:2 molar ratio) the highest expression (1.26 mU) was obtained at N/P 2.
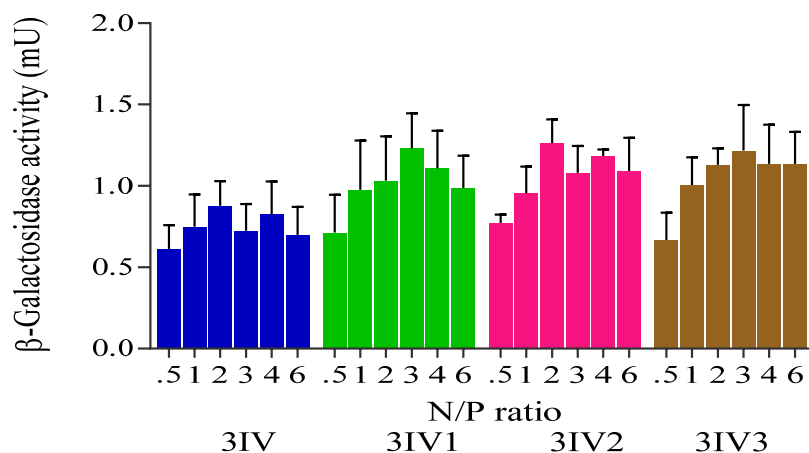
(A)
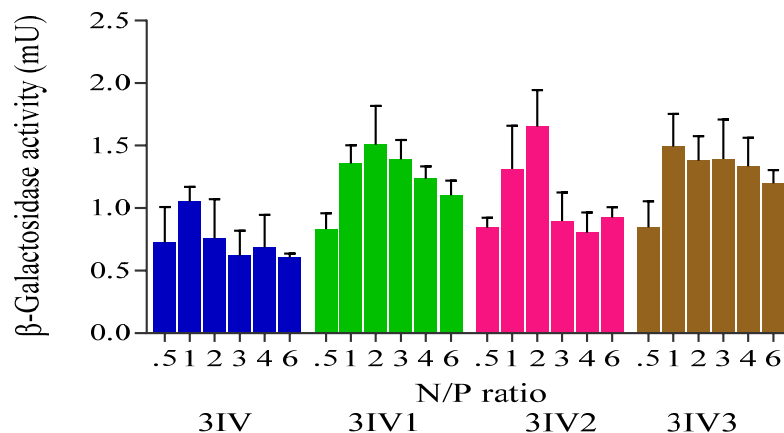
(B)

Figure 39. Transfection efficacies of **3IV** alone and in combination with DOPE; 1:1 (**3IV1**), 1:2 (**3IV2**) and 1:3 (**3IV3**) in (A) A549 and (B) HeLa cell lines

In HeLa cell line, **3IV (Figure 39B)** showed the highest β-Gal expression (1.05 mU) at N/P ratio of 1. However, in combination with DOPE (**3IV2,** 1:2 molar ratio) the highest expression (1.65 mU) was obtained at N/P 2.

In A549 cell line, **7aI (Figure 40A)** all alone and in combination with DOPE (**7aI1**, 1:1 molar ratio) showed the highest *β*-Gal expression of 0.17 and 0.62 mU at N/P ratio of 2.
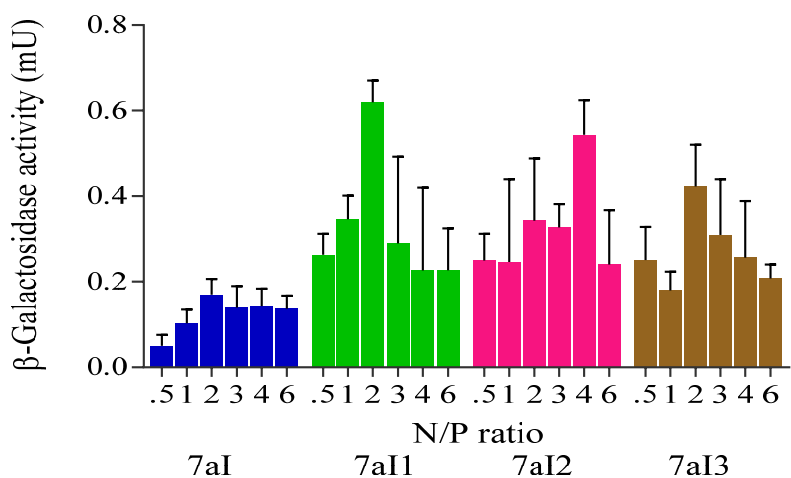
(A)
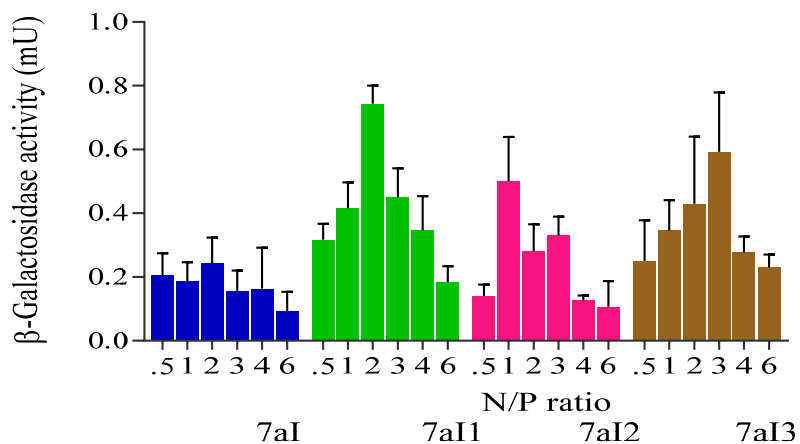
(B)

Figure 40. Transfection efficacies of **7aI** alone and in combination with DOPE; 1:1 (**7aI1**), 1:2 (**7aI2**) and 1:3 (**7aI3**) in (A) A549 and (B) HeLa cell lines

In HeLa cell line, **7aI (Figure 40B)** all alone and in combination with DOPE (**7aI1,** 1:1 molar ratio) showed the highest *β*-Gal expression of 0.24 and 0.74 mU at N/P ratio of 2.

In A549 cell line, **7aII (Figure 41A)** showed the highest β-Gal expression (0.32 mU) at N/P ratio of 2. In combination with DOPE (**7aII2**, 1:2 molar ratio) also the highest expression (0.96 mU) was obtained at N/P 2.
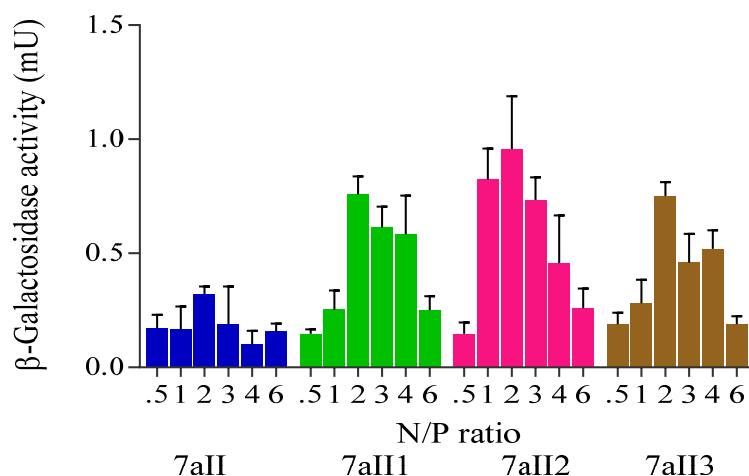
(A)
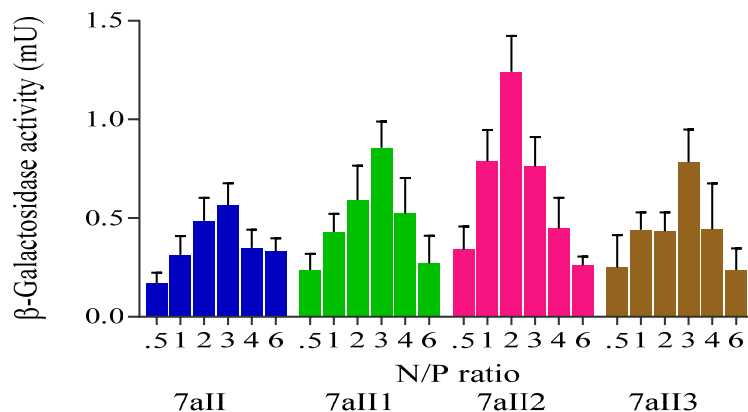
(B)

Figure 41. Transfection efficacies of **7aII** alone and in combination with DOPE; 1:1 (**7aII1**), 1:2 (**7aII2**) and 1:3 (**7aII3**) in (A) A549 and (B) HeLa cell lines

In HeLa cell line, **7aII (Figure 41B)** showed the highest β-Gal expression (0.56 mU) at N/P ratio of 3. However, with DOPE (**7aII2,** 1:2 molar ratio) the highest expression (1.24 mU) was obtained at N/P 2.

In A549 cell line, **7aIII (Figure 42A)** showed the highest *β*-Gal expression (0.29 mU) at N/P ratio of 1. In combination with DOPE (**7aIII2,** 1:2 molar ratio) the highest expression (0.95 mU) was obtained at the same N/P ratio of 1.

(A)

(B)
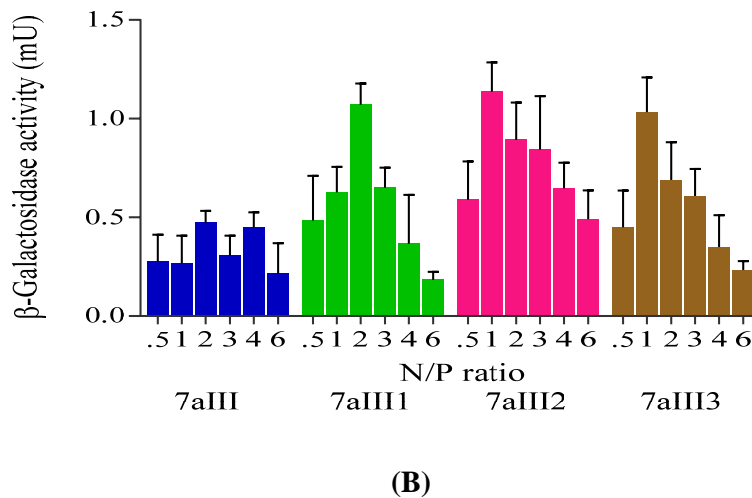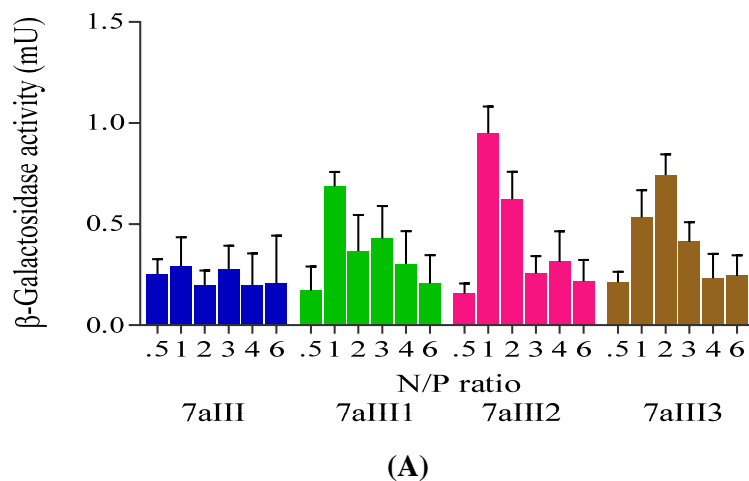
Figure 42. Transfection efficacies of **7aIII** alone and in combination with DOPE; 1:1 **(7aIII1)**, 1:2 **(7aIII2)** and 1:3 **(7aIII3)** in (A) A549 and (B) HeLa cell lines

In HeLa cell line, **7aIII (Figure 42B)** showed the highest *β*-Gal expression (0.48 mU) at N/P ratio of 2. However, in combination with DOPE (**7aIII2,** 1:2 molar ratio) the highest expression (1.13 mU) was obtained at N/P 1.

In A549 cell line, **7aIV (Figure 43A)** showed the highest β-Gal expression (0.22 mU) at N/P ratio of 2. However, in combination with DOPE (**7aIV1,** 1:1 molar ratio) the highest expression (0.44 mU) was obtained at N/P 3.

(A)

(B)
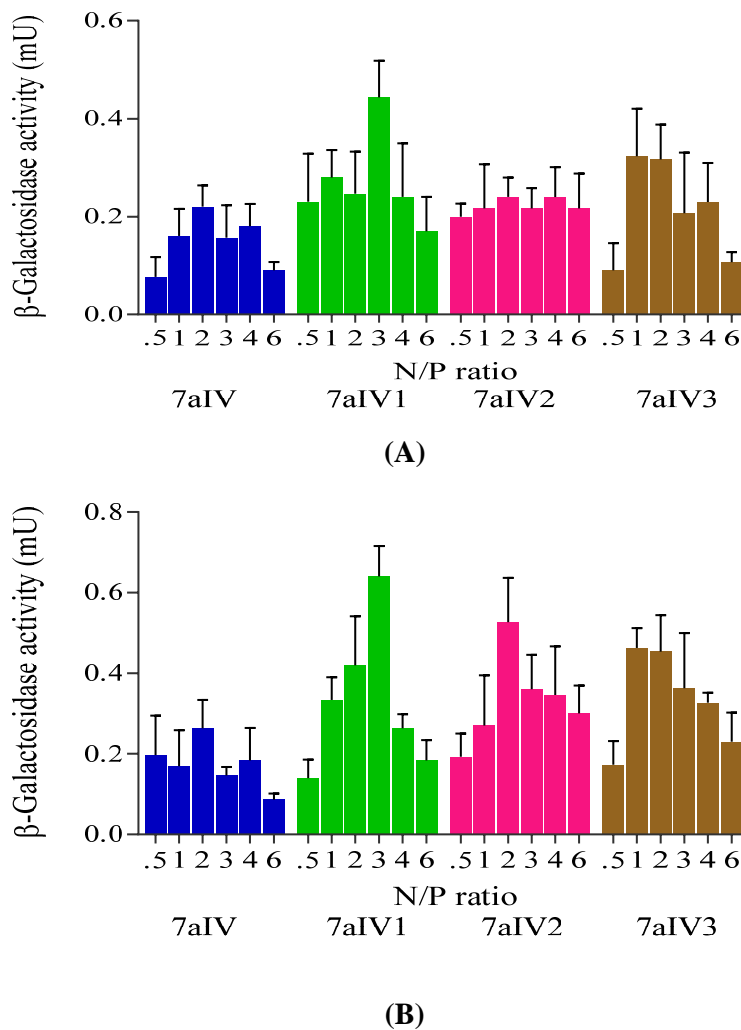
Figure 43. Transfection efficacies of **7aIV** alone and in combination with DOPE; 1:1 (**7aIV1**), 1:2 (**7aIV2**) and 1:3 (**7aIV3**) in (A) A549 and (B) HeLa cell lines

In HeLa cell line, **7aIV (Figure 43B)** showed the highest β-Gal expression (0.26 mU) at N/P ratio of 2. However, in combination with DOPE (**7aIV1,** 1:1 molar ratio) the highest expression (0.64 mU) was obtained at N/P 3.

In A549 cell line, **7bI (Figure 44A)** showed the highest β-Gal expression (0.84 mU) at N/P ratio of 1. In combination with DOPE (**7bI1**, 1:1 molar ratio) the highest expression (1.06 mU) was obtained at N/P 2.

(A)

(B)
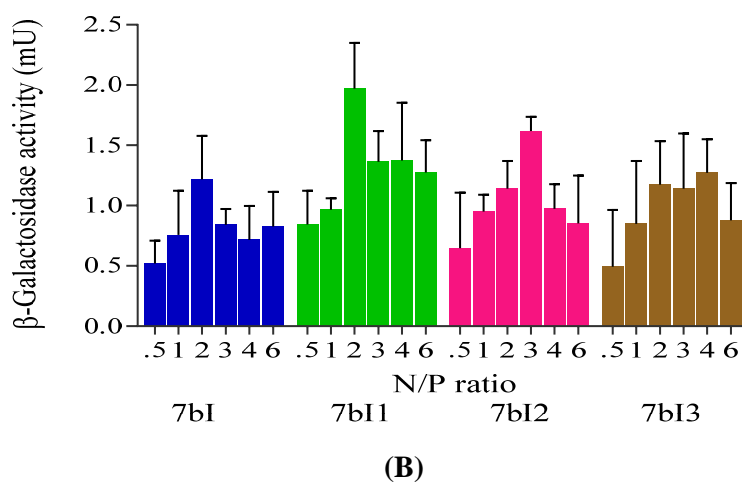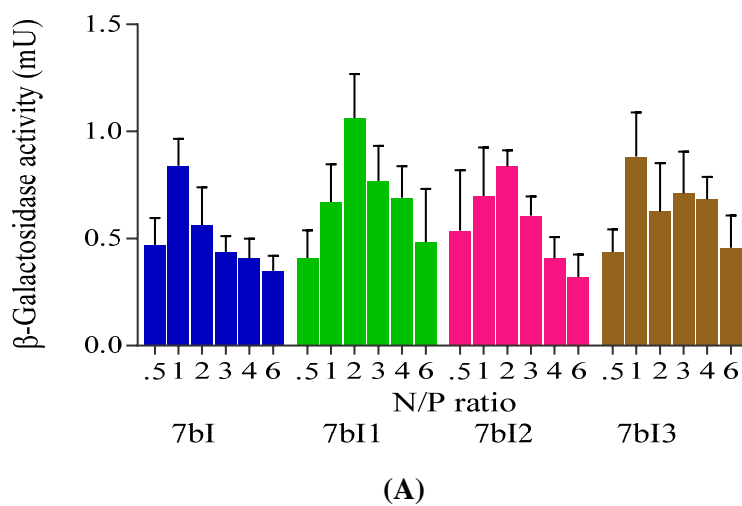
Figure 44. Transfection efficacies of **7bI** alone and in combination with DOPE; 1:1 (**7bI1**), 1:2 (**7bI2**) and 1:3 (**7bI3**) in (A) A549 and (B) HeLa cell lines

In HeLa cell line, **7bI (Figure 44B)** all alone and in combination with DOPE (**7bI1;** 1:1 molar ratio) showed highest β-Gal expression of 1.21 and 1.97 mU respectively at N/P ratio of 2.

In A549 cell line, **7bII (Figure 45A)** showed the highest β-Gal expression (1.42 mU) at N/P ratio of 1. In combination with DOPE (**7bII1**, 1:1 molar ratio) the highest expression (2.11 mU) was obtained at N/P 3.

(A)

(B)
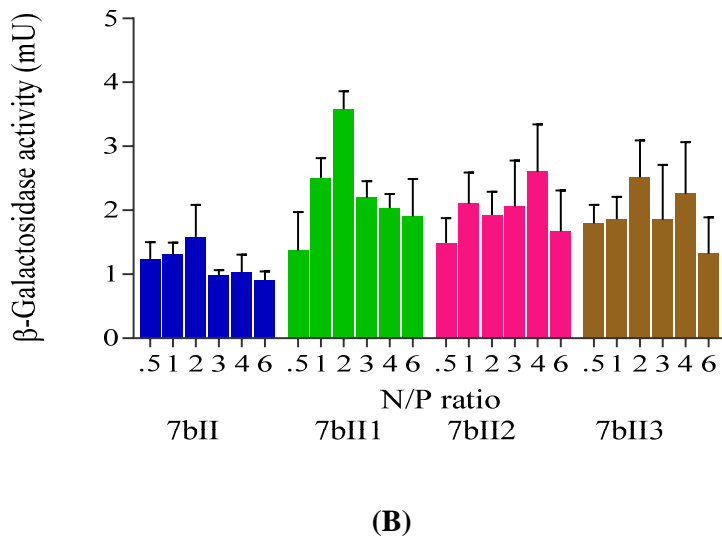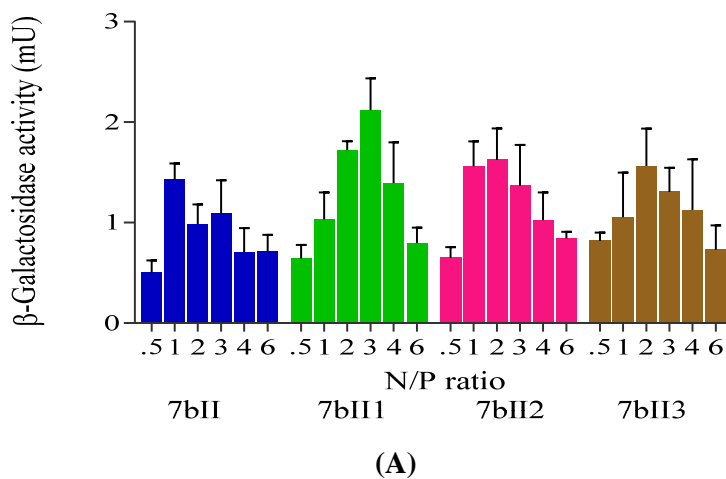
Figure 45. Transfection efficacies of **7bII** alone and in combination with DOPE; 1:1 (**7bII1**), 1:2 (**7bII2**) and 1:3 (**7bII3**) in (A) A549 and (B) HeLa cell lines

In HeLa cell line, **7bII (Figure 45B)** all alone and in combination with DOPE (**7bIII1;** 1:1 molar ratio) showed the highest β-Gal expression of 1.58 and 3.57 mU respectively at N/P ratio of 2.

In A549 cell line, **7bIII (Figure 46A)** showed the highest β-Gal expression (1.32 mU) at N/P ratio of 1. In combination with DOPE (**7bIII1,** 1:1 molar ratio) the highest expression (1.84 mU) was obtained at N/P 2.

(A)

(B)
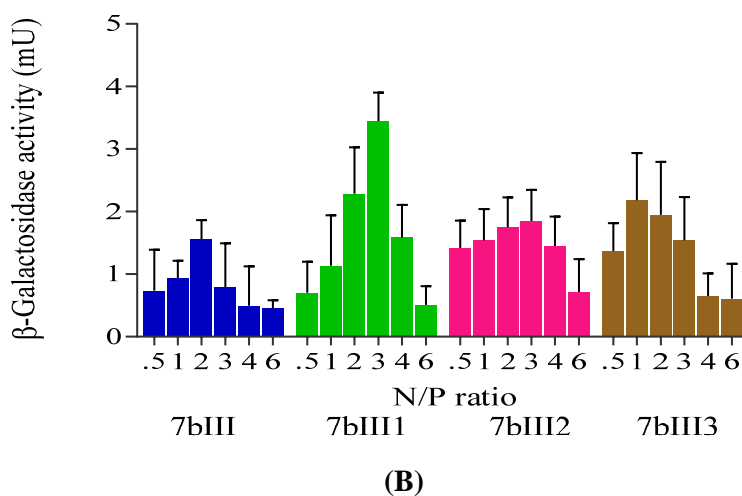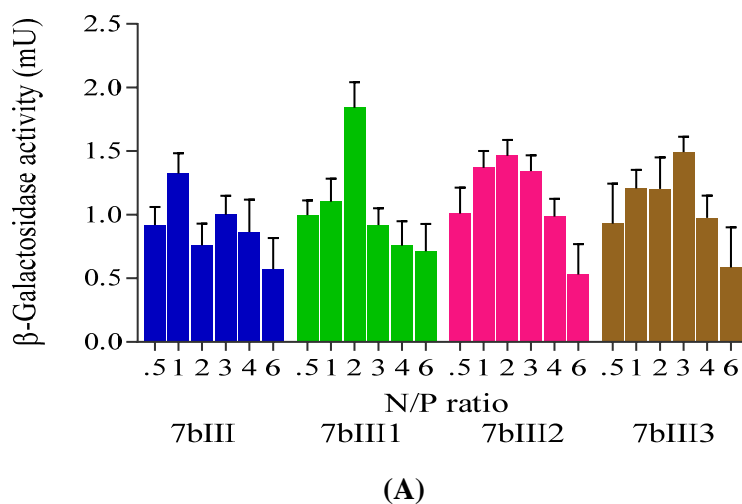
Figure 46. Transfection efficacies of **7bIII** alone and in combination with DOPE; 1:1 (**7bIII1**), 1:2 (**7bIII2**) and 1:3 (**7bIII3**) in (A) A549 and (B) HeLa cell lines

In HeLa cell line, **7bIII (Figure 46B)** showed the highest β-Gal expression (1.56 mU) at N/P ratio of 2. However, with DOPE (**7bIII1**, 1:1 molar ratio) the highest expression (3.44 mU) was obtained at N/P 3.

In A549 cell line, **7bIV (Figure 47A)** all alone and in combination with DOPE(**7bIV2**; 1:2 molar ratio) showed the highest β-Gal expression of 0.79 and 1.74 mU at N/P ratio of 1.
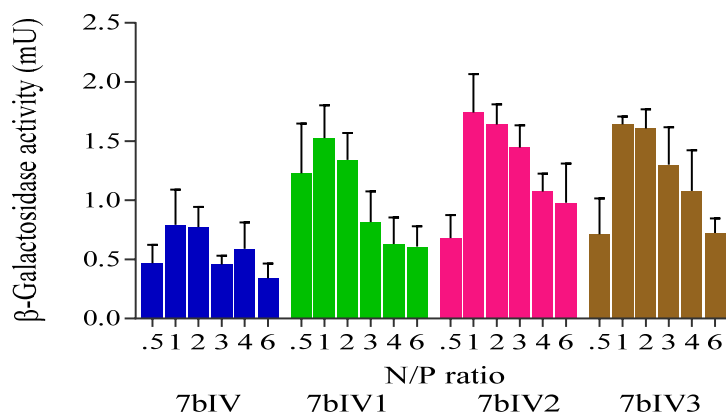
(A)
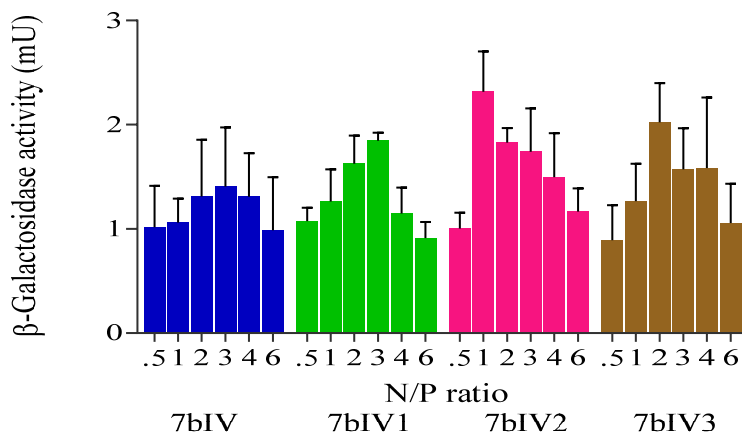
(B)

Figure 47. Transfection efficacies of **7bIV** alone and in combination with DOPE; 1:1 **(7bIV1)**, 1:2 **(7bIV2)** and 1:3 **(7bIV3)** in (A) A549 and (B) HeLa cell lines

In HeLa cell line, **7bIV (Figure 47B)** showed the highest β-Gal expression (1.4 mU) at N/P ratio of 3. However, with DOPE (**7bIV2**, 1:2 molar ratio) the highest expression (2.31 mU) was obtained at N/P 1.

In A549 cell line, **7cI (Figure 48A)** showed the highest β-Gal expression (0.79 mU) at N/P ratio of 3. However, in combination with DOPE (**7cI2**, 1:2 molar ratio) the highest expression (1.13 mU) was obtained at N/P 1.
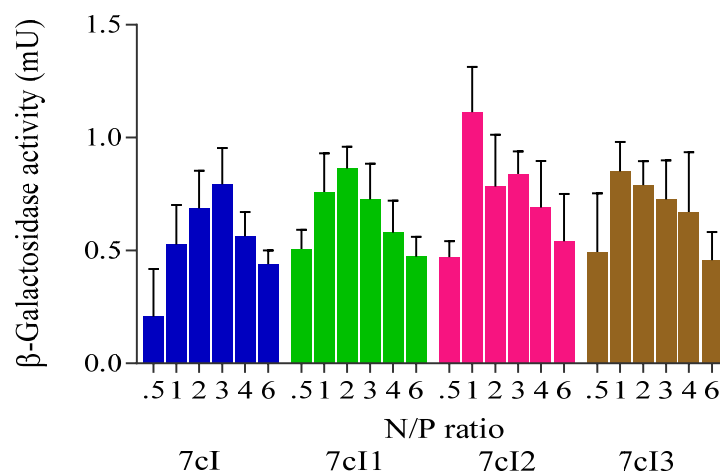
(A)
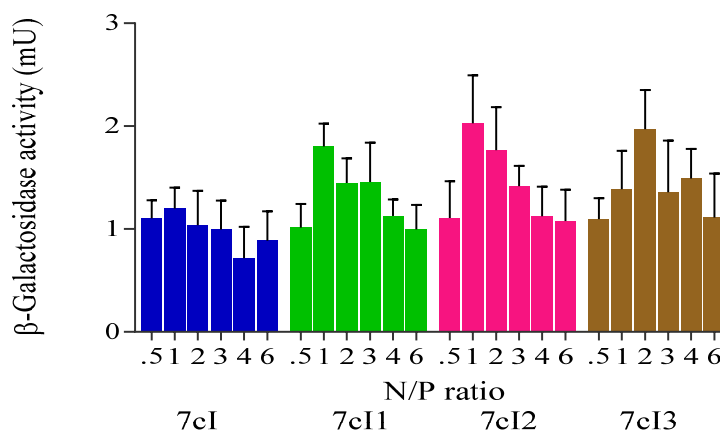
(B)

Figure 48. Transfection efficacies of **7cI** alone and in combination with DOPE; 1:1 **(7cI1)**, 1:2 **(7cI2)** and 1:3 **(7cI3)** in (A) A549 and (B) HeLa cell lines

In HeLa cell line, **7cI (Figure 48B)** all alone and in combination with DOPE **(7cI2,** 1:2 molar ratio) showed the highest β-Gal expression of 1.2 and 2.02 mU at N/P ratio of 1.

In A549 cell line, **7cII (Figure 49A)** showed the highest *β*-Gal expression (1.05 mU) at N/P ratio of 4. However, with DOPE (**7cII1,** 1:1 molar ratio) the highest expression (1.89 mU) was obtained at N/P 2.
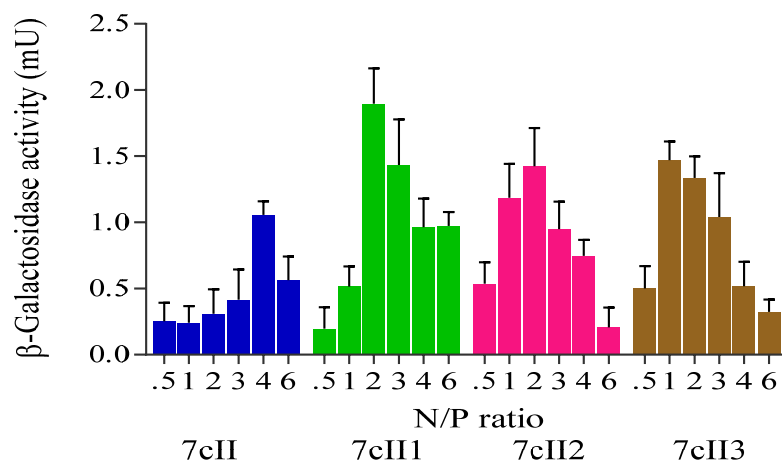
(A)
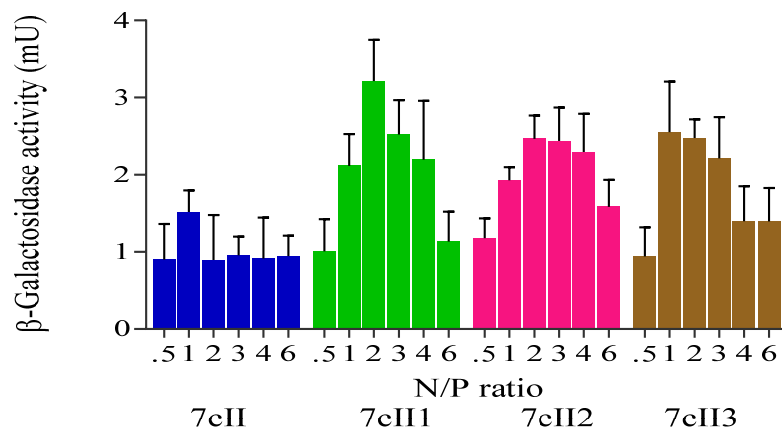
(B)

Figure 49. Transfection efficacies of **7cII** alone and in combination with DOPE; 1:1 (**7cII1**), 1:2 (**7cII2**) and 1:3 (**7cII3**) in (A) A549 and (B) HeLa cell lines

In HeLa cell line, **7cII (Figure 49B)** showed the highest *β*-Gal expression (1.52 mU) at N/P ratio of 1. However, with DOPE (**7cII1,** 1:1 molar ratio) the highest expression (3.21 mU) was obtained at N/P 2.

In A549 cell line, **7cIII (Figure 50A)** showed the highest β-Gal expression (1.11 mU) at N/P ratio of 4. However, with DOPE (**7cIII1**, 1:1 molar ratio) the highest expression (1.79 mU) was obtained at N/P 1.

(A)

(B)
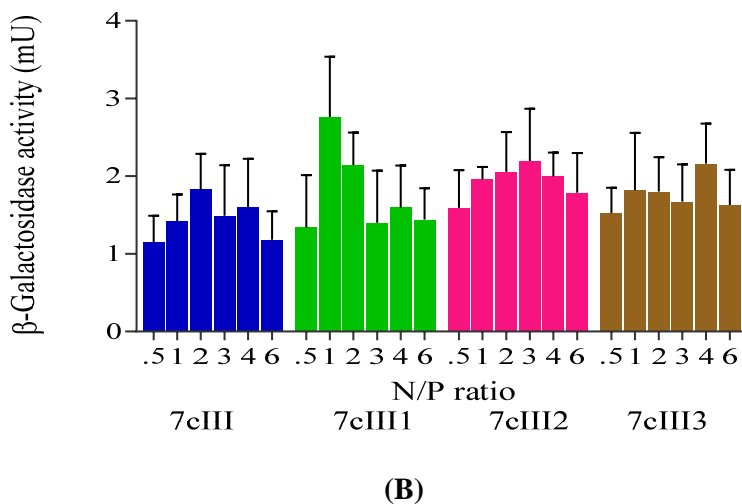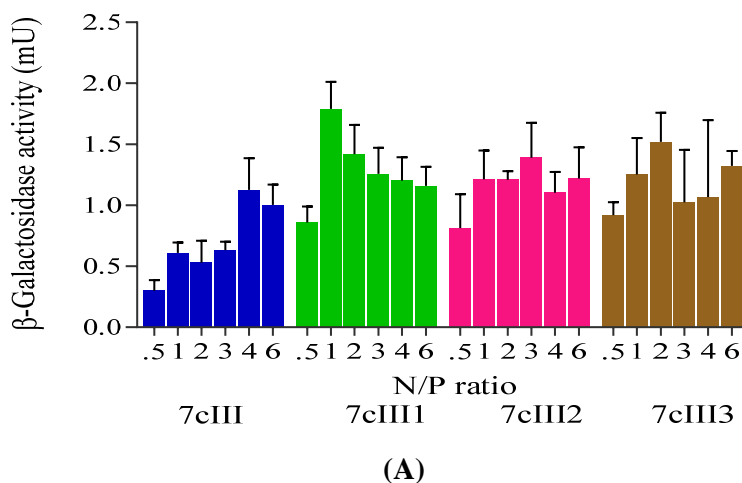
Figure 50. Transfection efficacies of **7cIII** alone and in combination with DOPE; 1:1 **(7cIII1)**, 1:2 **(7cIII2)** and 1:3 **(7cIII3)** in (A) A549 and (B) HeLa cell lines

In HeLa cell line, **7cIII (Figure 50B)** showed the highest β-Gal expression (1.83 mU) at N/P ratio of 2. However, with DOPE (**7cIII1,** 1:1 molar ratio) the highest expression (2.76 mU) was obtained at N/P 1.

In A549 cell line, **7cIV (Figure 51A)** all alone and in combination with DOPE (**7cIV2**, 1:2 molar ratio) showed the highest *β*-Gal expression of 1.01 and 1.45 mU at N/P ratio of 2.

(A)

(B)
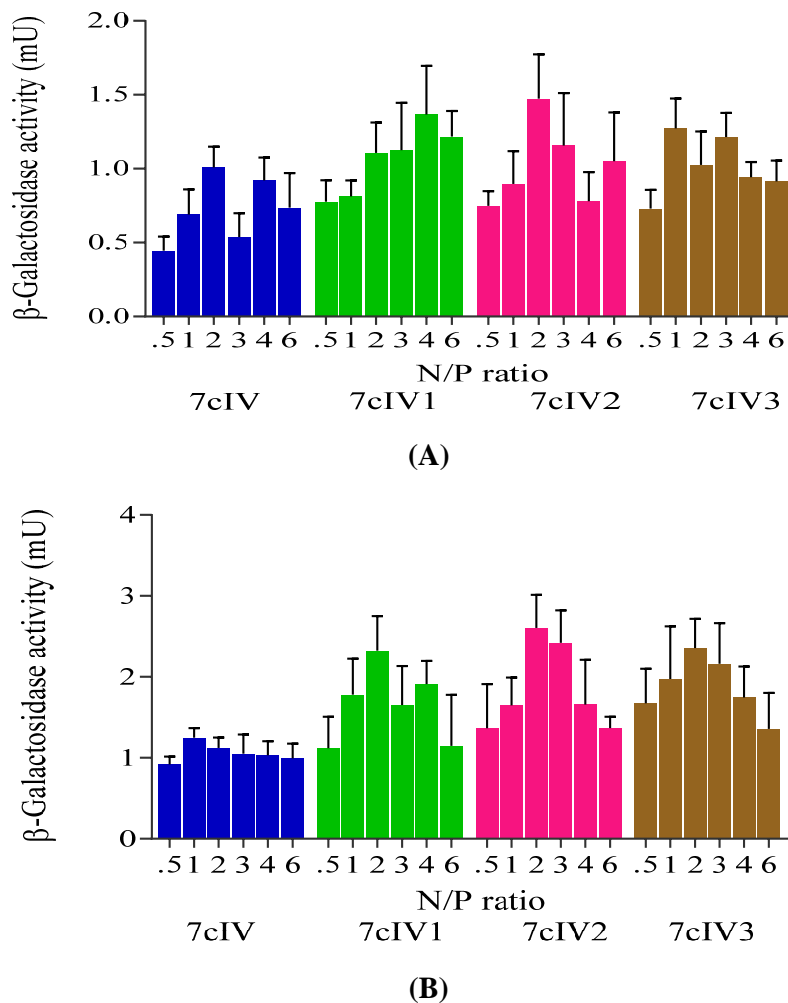
Figure 51. Transfection efficacies of **7cIV** alone and in combination with DOPE; 1:1 **(7cIV1)**, 1:2 **(7cIV2)** and 1:3 **(7cIV3)** in (A) A549 and (B) HeLa cell lines

In HeLa cell line, **7cIV (Figure 51B)** showed the highest *β*-Gal expression (1.24 mU) at N/P ratio of 1. However, with DOPE (**7cIV2,** 1:2 molar ratio) the highest expression (2.60 mU) was obtained at N/P 2.

In A549 cell line, **7dI (Figure 52A)** showed the highest β-Gal expression (0.30 mU) at N/P ratio of 2. However, with DOPE (**7dI1**, 1:1 molar ratio) the highest expression (1.0 mU) was obtained at N/P 3.
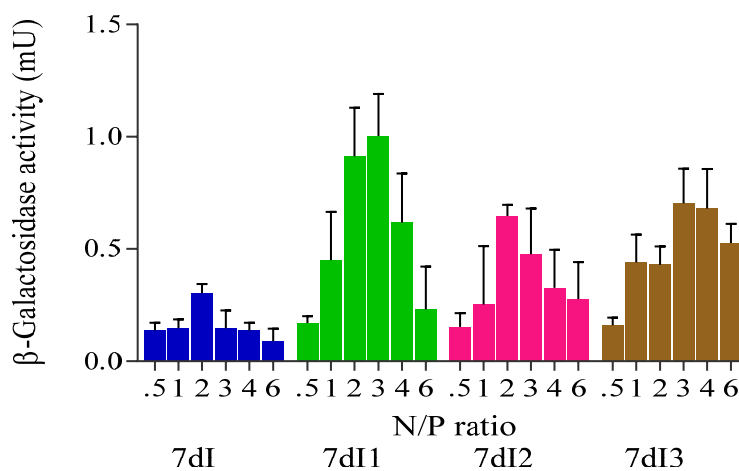
(A)
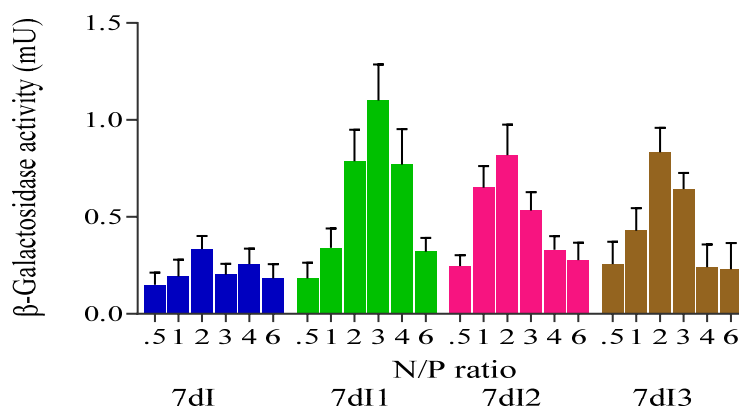
(B)

Figure 52. Transfection efficacies of **7dI** alone and in combination with DOPE; 1:1 **(7dI1)**, 1:2 **(7dI2)** and 1:3 **(7dI3)** in (A) A549 and (B) HeLa cell lines

The results for **7dI (Figure 52B)** were same in HeLa cell lne as obtained in A549 cell line.

In A549 cell line, **7dII (Figure 53A)** all alone and in combination with DOPE (**7dII1**, 1:1 molar ratio) showed the highest *β*-Gal expression of 0.31 and 1.04 mU at N/P ratio of 2.
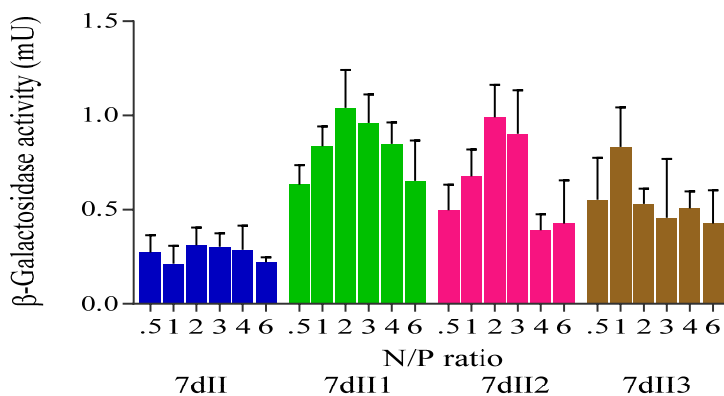
(A)
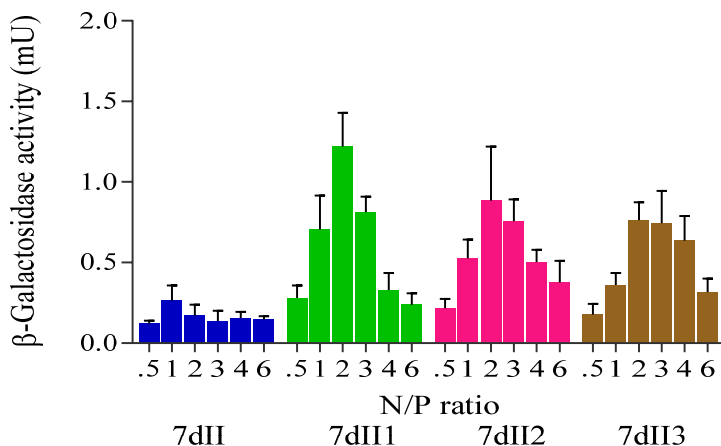
(B)

Figure 53. Transfection efficacies of **7dII** alone and in combination with DOPE; 1:1 (**7dII1**), 1:2 (**7dII2**) and 1:3 (**7dII3**) in (A) A549 and (B) HeLa cell lines

In HeLa cell line, **7dII (Figure 53B)** showed the highest *β*-Gal expression (0.26 mU) at N/P ratio of 1. However, with DOPE (**7dII1,** 1:1 molar ratio) the highest expression (1.21 mU) was obtained at N/P 2.

In A549 cell line, **7dIII (Figure 54A)** all alone and in combination with DOPE (**7dIII1**, 1:1 molar ratio) showed the highest *β*-Gal expression of 0.16 and 0.78 mU at N/P ratio of 1.

(A)

(B)
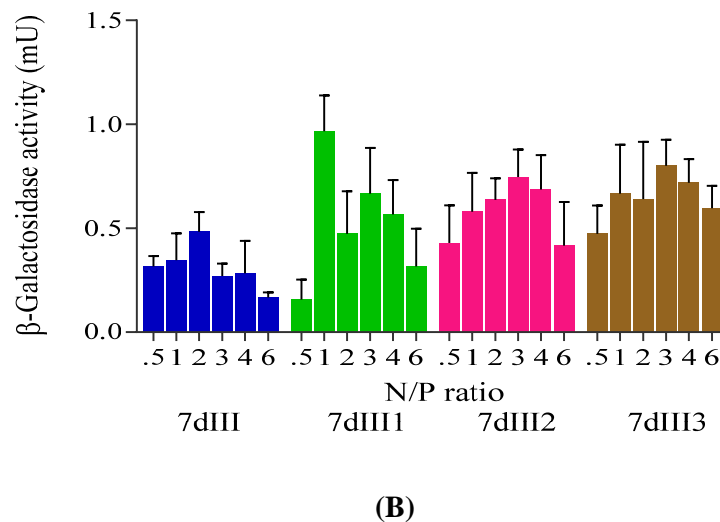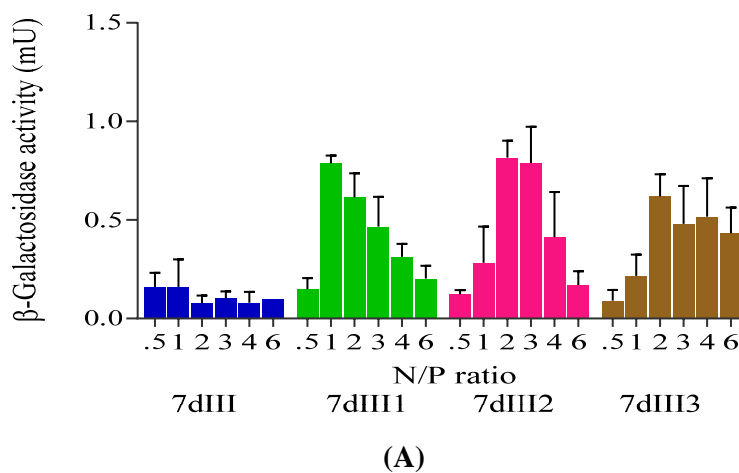
Figure 54. Transfection efficacies of **7dIII** alone and in combination with DOPE; 1:1 (**7dIII1**), 1:2 **(7dIII2)** and 1:3 **(7dIII3)** in (A) A549 and (B) HeLa cell lines

In HeLa cell line, **7dIII (Figure 54B)** showed the highest *β*-Gal expression (0.48 mU) at N/P ratio of 2. However, with DOPE (**7dIII1,** 1:1 molar ratio) the highest expression (0.96 mU) was obtained at N/P 1.

In A549 cell line, **7dIV (Figure 55A)** showed the highest *β*-Gal expression (0.27 mU) at N/P ratio of 1. However, with DOPE (**7dIV2**, 1:2 molar ratio) the highest expression (0.75 mU) was obtained at N/P 2.

(A)

(B)
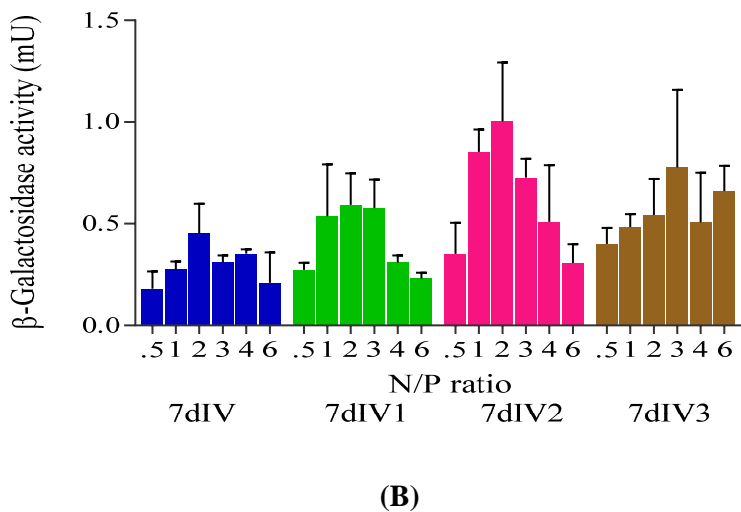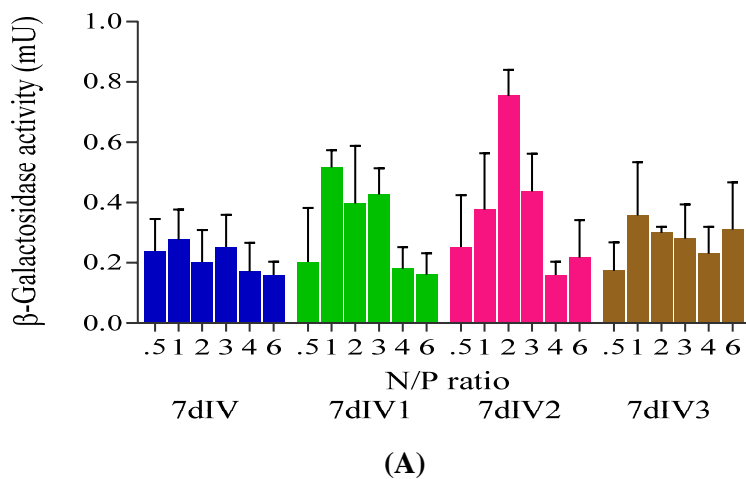
Figure 55. Transfection efficacies of **7dIV** alone and in combination with DOPE; 1:1 (**7dIV1**), 1:2 (**7dIV2**) and 1:3 (**7dIV3**) in (A) A549 and (B) HeLa cell lines

In HeLa cell line, **7dIV (Figure 55B)** all alone and in combination with DOPE (**7dIV2,** 1:2 molar ratio) showed the highest *β*-Gal expression of 0.45 and 1.0 mU at N/P of 2.

In A549 cell line, **10aI (Figure 56A)** showed the highest β-Gal expression (0.38 mU) at N/P ratio of 2. However, with DOPE (**10aI2**, 1:2 molar ratio) the highest expression (0.95 mU) was obtained at N/P 3.

(A)

(B)
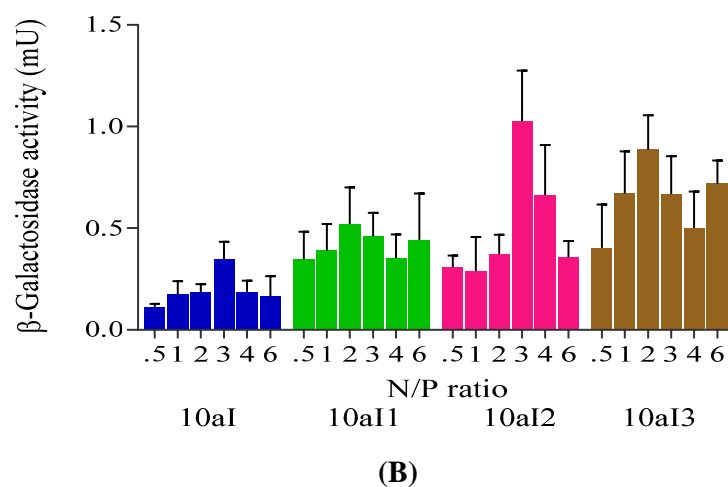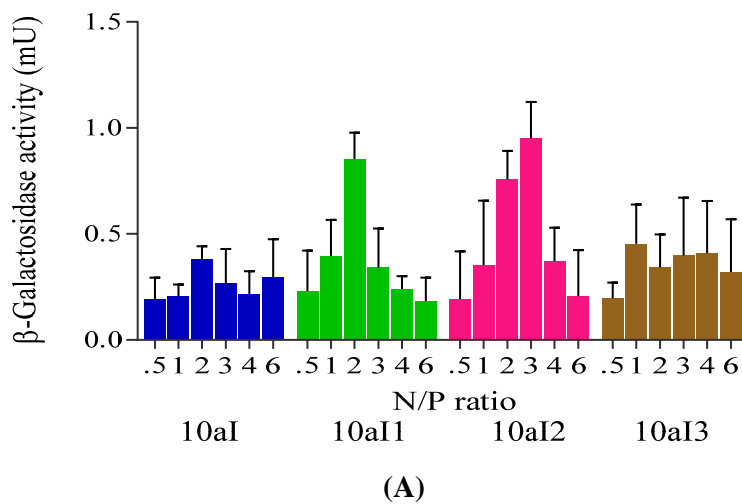
Figure 56. Transfection efficacies of **10aI** alone and in combination with DOPE; 1:1 (**10aI 1**), 1:2 (**10aI 2**) and 1:3 (**10aI 3**) in (A) A549 and (B) HeLa cell lines

In HeLa cell line, **10aI (Figure 56B)** all alone and in combination with DOPE (**10aI2,** 1:2 molar ratio) showed the highest β-Gal expression of 0.34 and 1.02 mU N/P ratio of 3.

In A549 cell line, **10aIII (Figure 57A)** all alone and in combination with DOPE (**10aIII2,** 1:2 molar ratio) showed the highest β-Gal expression of 0.33 and 0.99 mU at N/P ratio of 2.

(A)

(B)
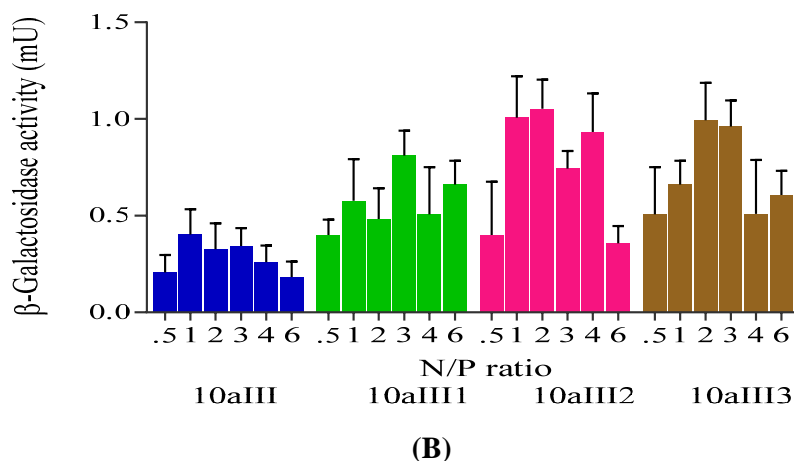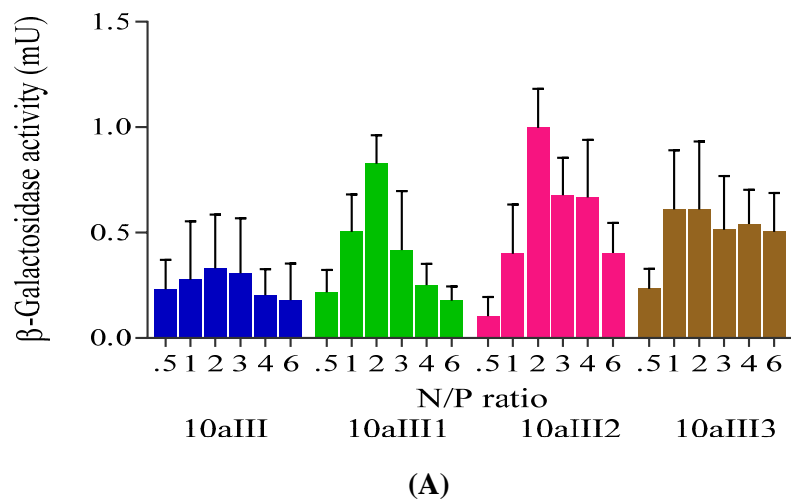
Figure 57. Transfection efficacies of **10aIII** alone and in combination with DOPE; 1:1 (**10aIII1**), 1:2 (**10aIII2)** and 1:3 (**10aIII3**) in (A) A549 and (B) HeLa cell lines

In HeLa cell line, **10aIII (Figure 57B)** showed the highest β-Gal expression (0.40 mU) at N/P ratio of 1. However, with DOPE (**10aIII2,** 1:2 molar ratio) the highest expression (1.05 mU) was obtained at N/P 2.

In A549 cell line, **10bI (Figure 58A)** all alone and in combination with DOPE (**10bI1**, 1:1 molar ratio) showed the highest β-Gal expression of 0.81 and 1.33 mU at N/P ratio of 1.

(A)

(B)
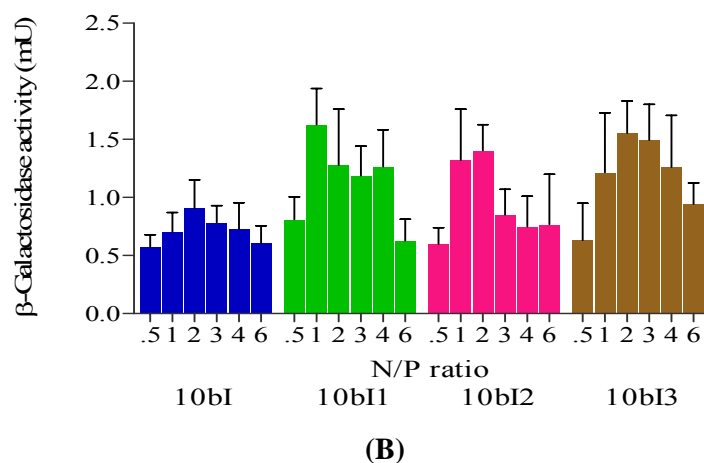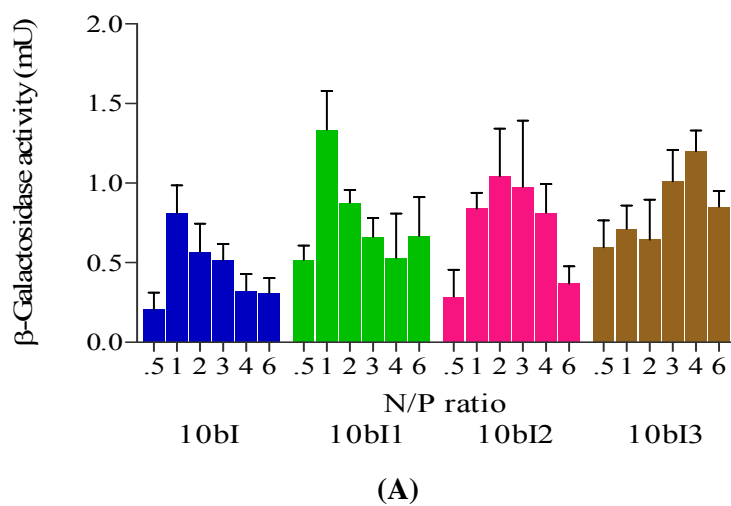
Figure 58. Transfection efficacies of **10bI** alone and in combination with DOPE; 1:1 **(10bI1)**, 1:2 **(10bI2)** and 1:3 **(10bI3)** in (A) A549 and (B) HeLa cell lines

In HeLa cell line, **10bI (Figure 58B)** showed the highest β-Gal expression (0.90 mU) at N/P ratio of 2. However, with DOPE (**10bI1,** 1:1 molar ratio) the highest expression (1.62 mU) was obtained at N/P 1.

In A549 cell line, **10bII (Figure 59A)** all alone and in combination with DOPE (**10bII2**, 1:2 molar ratio) showed the highest β-Gal expression of 0.52 and 2.05 mU at N/P ratio of 1.

(A)

(B)
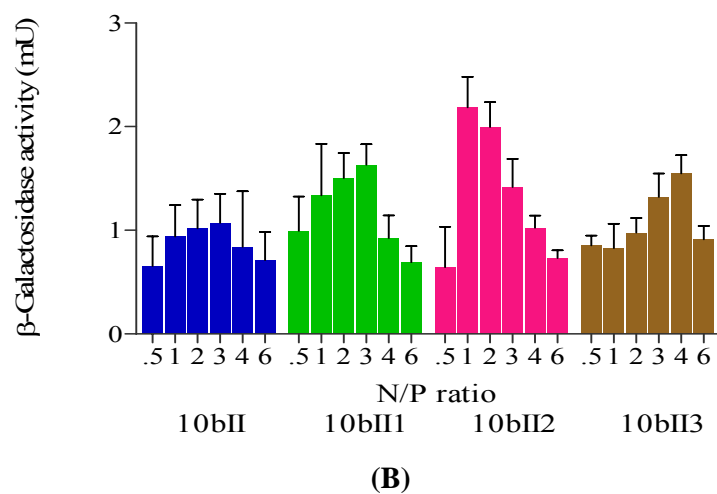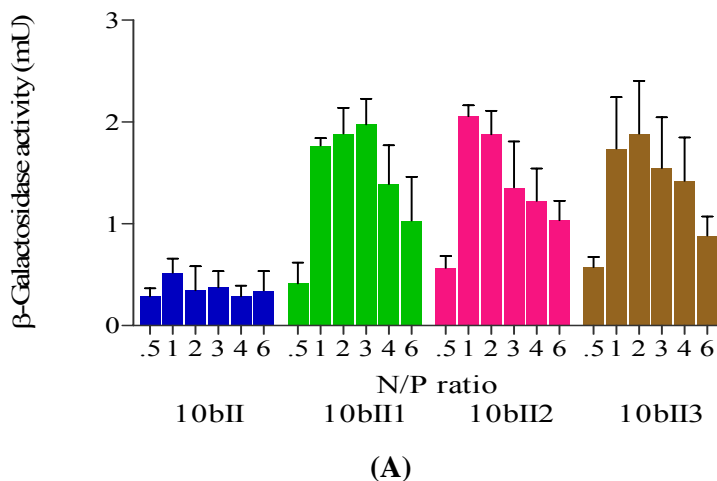
Figure 59. Transfection efficacies of **10bII** alone and in combination with DOPE; 1:1 (**10bII1**), 1:2 (**10bII2**) and 1:3 (**10bII3**) in (A) A549 and (B) HeLa cell lines

In HeLa cell line, **10bII (Figure 59B)** showed the highest β-Gal expression (1.07 mU) at N/P ratio of 3. However, with DOPE (**10bII2,** 1:2 molar ratio) the highest expression (2.18 mU) was obtained at N/P 1.

In A549 cell line, **10bIII (Figure 60A)** showed the highest β-Gal expression (0.60 mU) at N/P ratio of 3. However, with DOPE (**10bIII1**, 1:1 molar ratio) the highest expression (1.81 mU) was obtained at N/P 2.

(A)

(B)
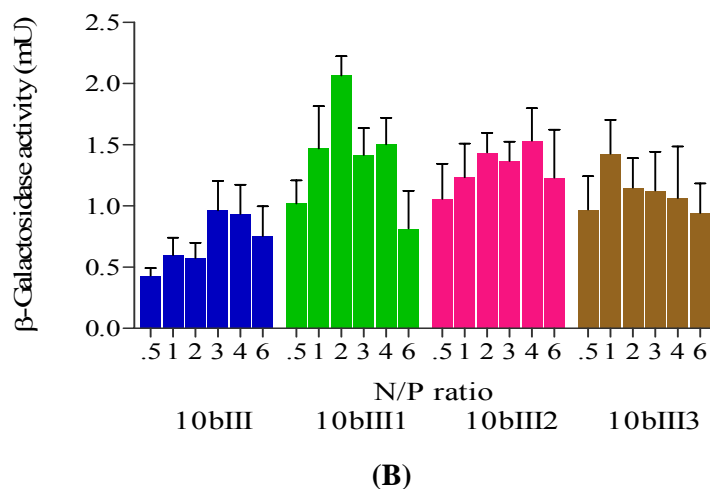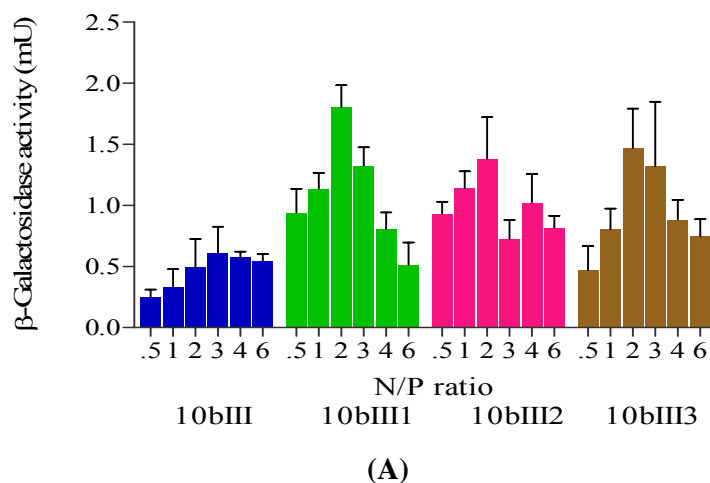
Figure 60. Transfection efficacies of **10bIII** alone and in combination with DOPE; 1:1 (**10bIII1**), 1:2 (**10bIII2**) and 1:3 (**10bIII3**) in (A) A549 and (B) HeLa cell lines

In HeLa cell line, **10bIII (Figure 60B)** showed the highest β-Gal expression (0.96 mU) at N/P ratio of 4. However, with DOPE (**10bIII1,** 1:1 molar ratio) the highest expression (2.06 mU) was obtained at N/P 2.

In A549 cell line, **10bIV (Figure 61A)** showed the highest β-Gal expression (0.59 mU) at N/P ratio of 2. However, with DOPE (**10bIV1**, 1:1 molar ratio) the highest expression (1.64 mU) was obtained at N/P 1.

(A)

(B)
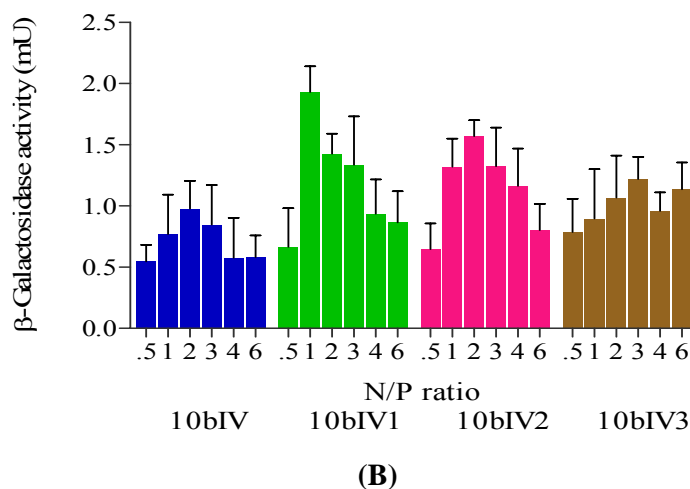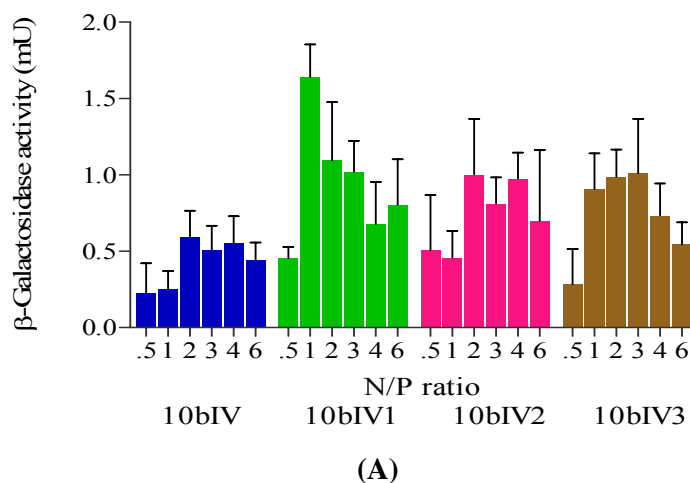
Figure 61. Transfection efficacies of **10bIV** alone and in combination with DOPE; 1:1 (**10bIV1**), 1:2 (**10bIV2**) and 1:3 (**10bIV3**) in (A) A549 and (B) HeLa cell lines

In HeLa cell line, **10bIV (Figure 61B)** showed the highest β-Gal expression (0.98 mU) at N/P ratio of 2. However, with DOPE (**10bIV1,** 1:1 molar ratio) the highest expression (1.93 mU) was obtained at N/P 1.

In A549 cell line, **10cI (Figure 62A)** showed the highest β-Gal expression (0.80 mU) at N/P ratio of 4. However, with DOPE (**10cI1**, 1:1 molar ratio) the highest expression (1.14 mU) was obtained at N/P 2.
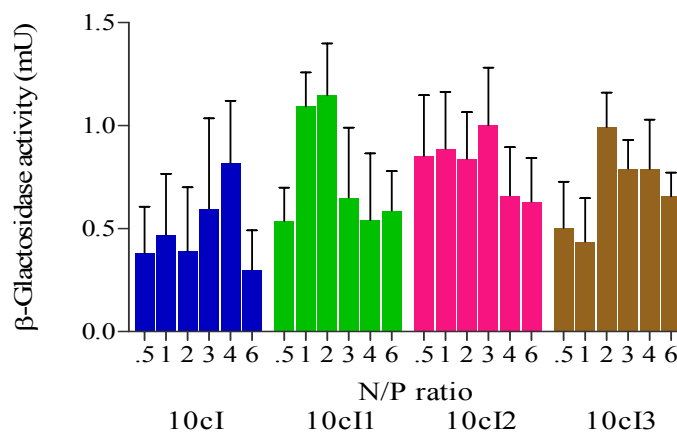
(A)
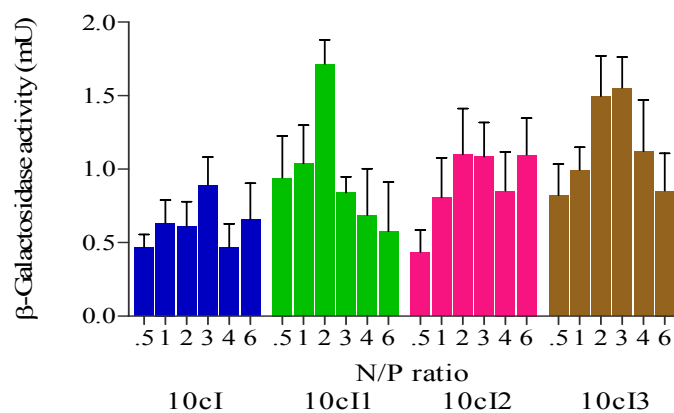
(B)

Figure 62. Transfection efficacies of **10cI** alone and in combination with DOPE; 1:1(**10cI1**), 1:2 **(10cI2)** and 1:3 **(10cI3)** in (A) A549 and (B) HeLa cell lines

In HeLa cell line, **10cI (Figure 62B)** showed the highest β-Gal expression (0.89 mU) at N/P ratio of 3. However, with DOPE (**10cI1,** 1:1 molar ratio) the highest expression (1.71 mU) was obtained at N/P 2.

In A549 cell line, **10cIII (Figure 63A)** all alone and in combination with DOPE (**10cIII1,** 1:1 molar ratio) showed the highest β-Gal expression of 1.02 and 1.98 mU at N/P ratio of 2.
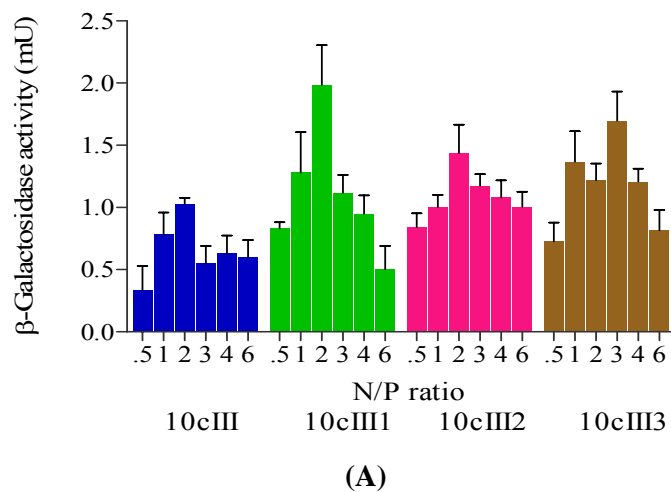
(A)
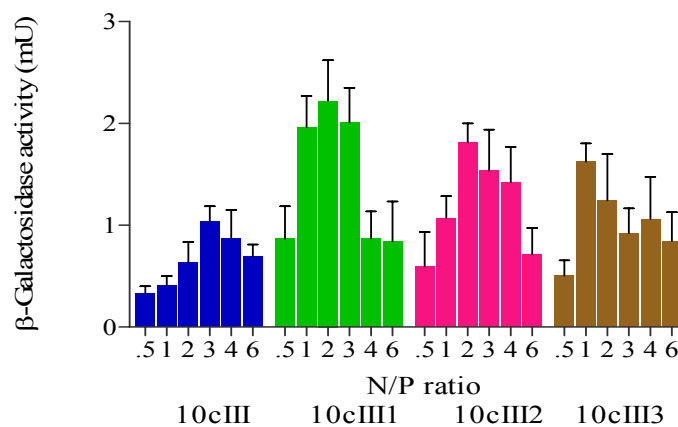
(B)

Figure 63. Transfection efficacies of **10cIII** alone and in combination with DOPE; 1:1 (**10cIII 1**), 1:2 (**10cIII 2**) and 1:3 (**10cIII 3**) in (A) A549 and (B) HeLa cell lines

In HeLa cell line, **10cIII (Figure 63B)** showed the highest β-Gal expression (1.04 mU) at N/P ratio of 3. However, with DOPE (**10cIII1,** 1:1 molar ratio) the highest expression (2.22 mU) was obtained at N/P 2.

In A549 cell line, **10cIV (Figure 64A)** all alone and in combination with DOPE (**10cIV1**, 1:1 molar ratio) showed the highest β-Gal expression of 0.93 and 1.70 mU at N/P ratio of 2.

(A)

(B)
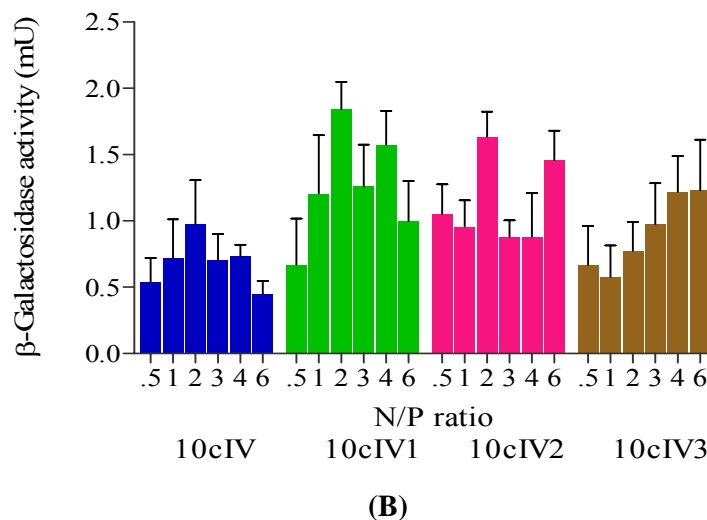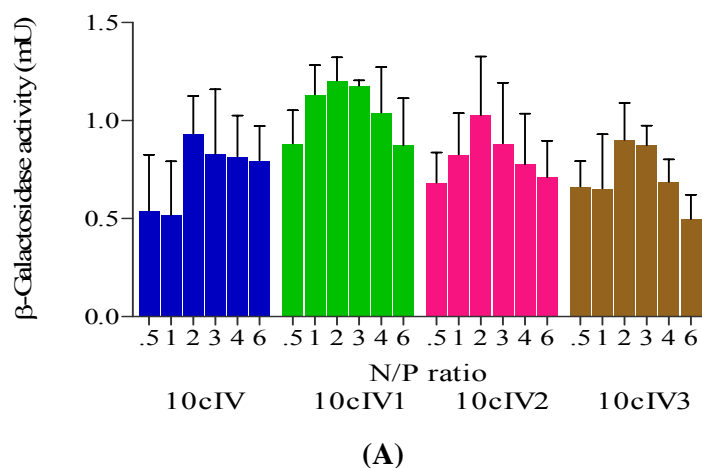
Figure 64. Transfection efficacies of **10cIV** alone and in combination with DOPE; 1:1(**10cIV1**), 1:2 (**10cIV2**) and 1:3 (**10cIV3**) in (A) A549 and (B) HeLa cell lines

In HeLa cell line, **10cIV (Figure 64B)** all alone and in combination with DOPE (**10cIV1**, 1:1 molar ratio) showed the highest β-Gal expression of 0.97 and 1.84 mU at N/P ratio of 2.

In A549 cell line, **10dI (Figure 65A)** showed the highest β-Gal expression (0.19 mU) at N/P ratio of 2. However, with DOPE (**10dI1**, 1:1 molar ratio) the highest expression (0.84 mU) was obtained at N/P 3.
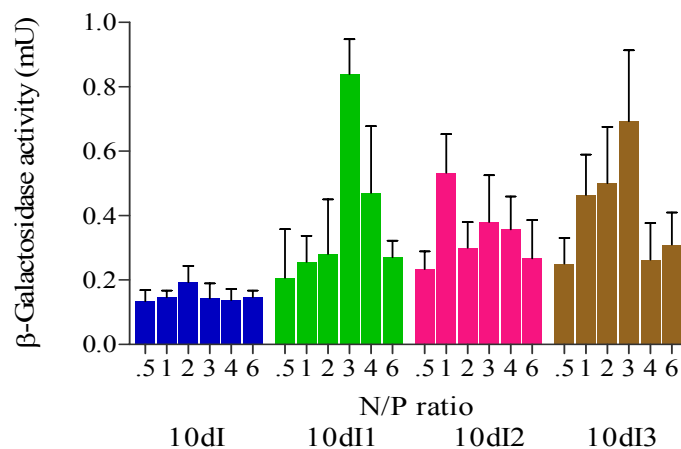
(A)
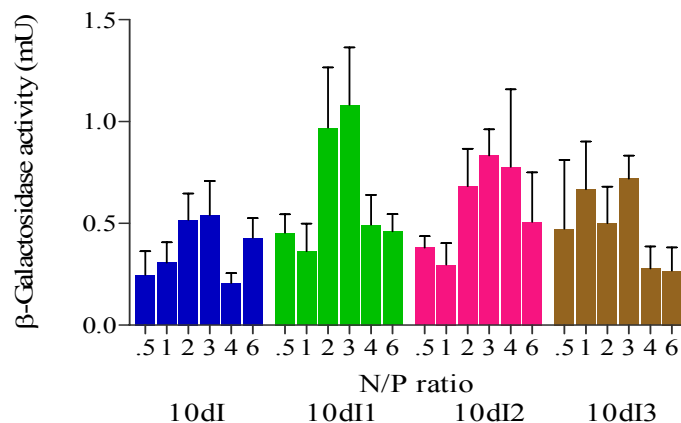
(B)

Figure 65. Transfection efficacies of **10dI** alone and in combination with DOPE; 1:1 (**10dI1**), 1:2 (**10dI2**) and 1:3 (**10dI3**) in (A) A549 and (B) HeLa cell lines

In HeLa cell line, **10dI (Figure 65B)** all alone and in combination with DOPE (**10dI1,** 1:1 molar ratio) showed the highest β-Gal expression of 0.54 and 1.08 mU at N/P ratio of 3.

In A549 cell line, **10dII (Figure 66A)** showed the highest β-Gal expression (0.48 mU) at N/P ratio of 1. However, with DOPE (**10dII1**, 1:1 molar ratio) the highest expression (0.99 mU) was obtained at N/P 4.
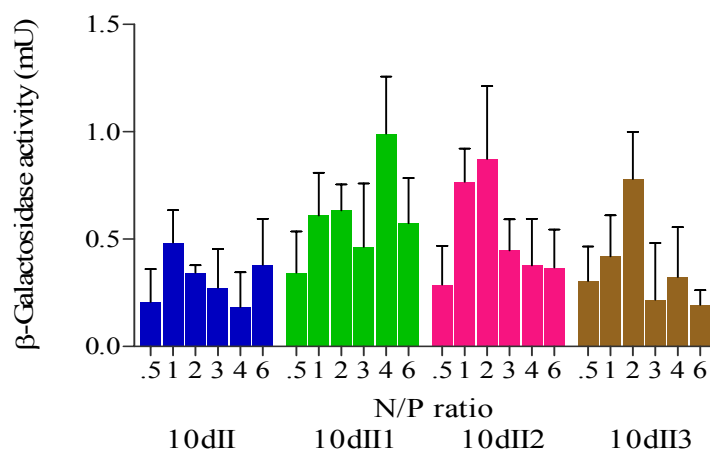
(A)
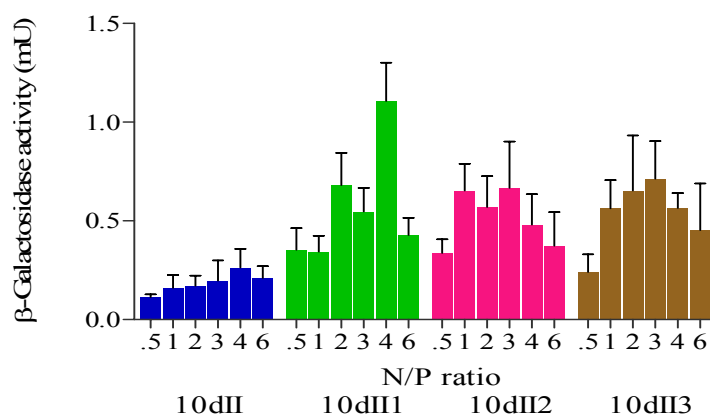
(B)

Figure 66. Transfection efficacies of **10dII** alone and in combination with DOPE; 1:1 **(10dII1)**, 1:2 **(10dII2)** and 1:3 **(10dII3)** in (A) A549 and (B) HeLa cell lines

In HeLa cell line, **10dII (Figure 66B)** all alone and in combination with DOPE (**10dII1,** 1:1 molar ratio) showed the highest β-Gal expression of 0.26 and 1.1 mU at N/P ratio of 4.

3.4.2 Effect of GA structures on transfection efficacy

● **Effect of variations in Head group**

Modulation in head group polarity significantly affects the transfection efficacy of GAs. For instance, incorporation of hydroxyethyl group in the head group region of GAs having C4 spacer and C16 hydrophobic chains increases the transfection efficacy e.g., **3III** (no hydroxyethyl group attached to quaternary nitrogens), **7cIII** (one hydroxyethyl group attached to each quaternary nitrogen) and **10cIII** (two hydroxyethyl groups attached to each quaternary nitrogen) showed the highest β-Gal expression of 0.94 (N/P 1) and 1.02 (N/P 1), 1.11 (N/P 4) and 1.83 (N/P 2), 1.02 (N/P 2) and 1.04 mU (N/P 3) in A549 and HeLa cell lines respectively. Thus, incorporation of hydroxyethyl group in head group region resulted into increased transfection efficacies of GAs. However, there was a little decrease in transfection activity on moving from one hydroxyethyl to two hydroxyethyl groups per quaternary nitrogen, while maintaining the hydrophobic chain length constant. The formulation of **3III**, **7cIII** and **10cIII** with DOPE at different molar ratios showed significant rise in transfection activity. **3III1**, **7cIII1** and **10cIII1** showed 1.6 (N/P 4) and 1.8 (N/P 4), 1.79 (N/P 1) and 2.76 (N/P 1), 1.98 (N/P 2) and 2.22 mU (N/P 2) activity in A549 and HeLa cell lines respectively. These results indicated a crucial role played by DOPE as helper lipid in gene delivery and the importance of hydroxyethylation in the head group region of GAs. Moreover, decrease in N/P ratio from 4 to 1 or 2 to achieve highest transfection indicated that smaller molar concentration of hydroethylated GAs (**7cIII1** and **10cIII1**) is required to exhibit the best transfection results compared to the non-hydroxyethylated GAs (**3III1**).

● **Effect of variations in Spacer**

The second variable substructure in the GAs i.e. the nature and length of spacers in GAs showed a significant effect on the transfection efficacy of GAs. For instance, when spacer changed from hydrophobic rigid ($CH_2C_6H_4CH_2$) to hydrophilic flexible ($CH_2CH_2OCH_2CH_2$) to hydrophobic flexible (polymethylene, $(CH_2)_6$ and $(CH_2)_4$) skeleton in **7bI** to **7bII** to **7bIII** to **7bIV** of MEA series, the transfection expression of 0.84 (N/P 1) and 1.21 (N/P 2), 1.42 (N/P 1) and 1.58 (N/P 2), 1.32 (N/P 1) and 1.56 (N/P 2), 0.79 (N/P 1) and 1.40 mU (N/P 3) were obtained in A549 and

HeLa cell lines respectively. However, the optimized formulations of **7bI1, 7bII1, 7bIII1, 7bIV2** with DOPE showed 1.06 (N/P 2) and 1.97 (N/P 2), 2.11 (N/P 3) and 3.57 (N/P 3), 1.84 (N/P 2) and 3.44 (N/P 2), 1.74 (N/P 1) and 2.31 mU (N/P 1) in A549 and HeLa cell lines respectively. Similarily **10bI**, **10bII**, **10bIII**, **10bIV** of DEA series possessing same spacer and hydrophobic chains showed 0.81 (N/P 1) and 0.90 (N/P 2), 0.52 (N/P 1) and 1.07 (N/P 3), 0.60 (N/P 3) and 0.96 (N/P 4), 0.59 (N/P 2) and 0.98 mU (N/P 2) of β-Gal expression in A549 and HeLa cell lines respectively. With DOPE, these GAs (**10bI1**, **10bII2**, **10bIII1**, **10bIV1**) showed β-Gal expression of 1.33 (N/P 1) and 1.62 (N/P 1), 2.05 (N/P 1) and 2.18 (N/P 1), 1.81 (N/P 2) and 2.06 (N/P 2), 1.64 (N/P 1) and 1.93 mU (N/P 1) in A549 and HeLa cell lines respectively. The results obtained in β-Gal expression for both the series showed that transfection efficacy follows the order; $(CH_2CH_2OCH_2CH_2) > (CH_2)_6 > (CH_2)_4 > CH_2C_6H_4CH_2$ for the spacer moiety, while keeping the hydrocarbon chain length and the head groups constant.

- **Effect of variations in hydrocarbon Chain length**

Hydrocarbon chain length the third variable structure also exhibited significant effect upon the transfection efficacy of the synthesized GAs. For instance, GAs of MEA series (**7aI**, **7bI**, **7cI**, **7dI**) having similar head groups and $CH_2C_6H_4CH_2$ as spacer but having C12 - C18 long hydrocarbon chains showed β-Gal expression of 0.17(N/P 2) and 0.24 (N/P 2), 0.84 (N/P 1) and 1.21 (N/P 2), 0.79 (N/P 3) and 1.20 (N/P 1), 0.30 (N/P 2) and 0.32 mU (N/P 2) in A549 and HeLa cell lines respectively. However, in combination with DOPE these GAs (**7aI1**, **7bI1**, **7cI2**, **7dI1**) showed β-Gal expression of 0.62 (N/P 2) and 0.74 (N/P 2), 1.06 (N/P 2) and 1.97 (N/P 2), 1.13 (N/P 1) and 2.02 (N/P 1), 1.0 (N/P 3) and 1.11 mU (N/P 3) in A549 and HeLa cell lines respectively. For GAs of DEA series (**10aI**, **10bI**, **10cI**, **10dI**) having similar head groups and $CH_2C_6H_4CH_2$ spacer but C12 - C18 long hydrocarbon chains, the results obtained were 0.38 (N/P 2) and 0.34 (N/P 3), 0.81(N/P 1) and 0.90 (N/P 2), 0.80 (N/P 4) and 0.89 (N/P 3), 0.19 (N/P 2) and 0.54 mU (N/P 3) in A549 and HeLa cell lines respectively. However, combined with DOPE these GAs (**10aI2**, **10bI1**, **10cI1**, **10dI1**) showed β-Gal expression of 0.95 (N/P 3) and 1.02 (N/P 3), 1.33 (N/P 1) and 1.62 (N/P 1), 1.14 (N/P 2) and 1.71 (N/P 2), 0.84 (N/P 3) and 1.08 mU (N/P 3)

in A549 and HeLa cell line respectively. These findings suggested that transfection efficacy of GAs and their formulations with DOPE were dependent upon hydrocarbon chain lengths and follows the order; C14 > C16 > C18 > C12, while keeping the head group and the spacer constant.

Various formulations of synthesized GAs that showed good *β*-Gal expression in A549 and HeLa cell lines have been compiled in **Figures 67** and **68** and compared with the expression of naked *β*-Gal plasmid (*p*DNA) as negative control and commercially available transfection reagents (Lipofectamine 2000, DCC:DOPE and DOTAP:DOPE liposomes) as positive control. Naked *p*DNA showed negligible *β*-Gal expression of 0.04 and 0.077 mU in A549 and HeLa cell lines respectively.
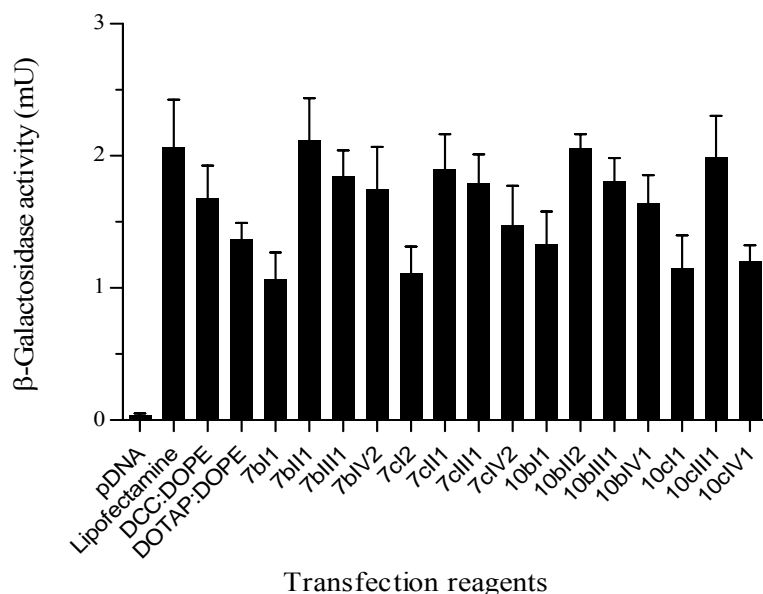
Figure 67. Comparative transfection efficacies of best GA formulations in A549 cell line at their optimized N/P ratios

All the GA formulations [**7bI1** (N/P 2), **7bII1** (N/P 3), **7bIII1** (N/P 2), **7bIV2** (N/P 1), **7cI2** (N/P 1), **7cII2** (N/P 2), **7cIII1** (N/P 1), **7cIV2** (N/P 2) of MEA series, **10bI1** (N/P 1), **10bII2** (N/P 1), **10bIII1** (N/P 2), **10bIV1** (N/P 1), **10cI1** (N/P 2), **10cIII1** (N/P 2) and **10cIV1** (N/P 2) of DEA series] showed their highest *β*-Gal expression of 1.06, 2.12, 1.84, 1.74, 1.11, 1.90, 1.79, 1.47, 1.33, 2.06, 1.80, 1.64, 1.15,

1.99, 1.20 mU and 1.97, 3.58, 3.45, 2.32, 2.03, 3.21, 2.76, 2.60, 1.63, 2.19, 2.07, 1.93, 1.72, 2.22, 1.84 mU in A549 and HeLa cell lines respectively. All the GA formulations exhibited the expression levels higher or comparable to DOTAP:DOPE liposomes (1.37 and 1.94 mU in A549 and HeLa cell lines respectively) and DC-Chol:DOPE liposomes (1.68 and 2.47 mU in A549 and HeLa cell lines respectively). However, some formulations (**7bII1**, **7bIII1**, **7cII2**, **7cIII1 and 10cIII1**) exhibited higher or comparable β-Gal expression to Lipofectamine 2000 (2.07 and 3.12 mU in A549 and HeLa cell lines respectively).

Figure 68. Comparative transfection efficacies of best GA formulations in HeLa cell line at their optimized N/P ratios

Moreover, the transfection efficacies of all the formulations including the standard ones were found to be higher in HeLa cells compared to A549 cell line at similar N/P ratios. This may be due to higher propensity of HeLa cells for transfection compared to A549 cells.

3.4.3. Effect of Serum on the transfection efficacy of GAs

Serum is known to decrease the transfection efficacies of gene delivery carriers. The transfection efficacies of optimized GA formulations showing the best results in A459 and HeLa cells in absence of serum were also determined in presence of Fetal Bovine Serum (FBS, 10 %). The decreases in transfection efficacy were noted in both A459 and HeLa cell lines for all the formulations tested (**Figures 69** and **70**). The standards (DCC:DOPE and DOTAP:DOPE) used in the study also showed significant reduction in their transfection efficacy. The GA formulations, **7bII1**, **7bIII1**, **7cII2**, **7cIII1** showed highest β-Gal expression of 1.63, 1.40, 1.58, 1.37 mU and 2.62, 2.37, 2.49, 2.18 mU in A549 and HeLa cell lines respectively at their optimized N/P ratios. The β-Gal expression of these formulations were significantly higher compared to the standards (DCC:DOPE and DOTAP:DOPE).
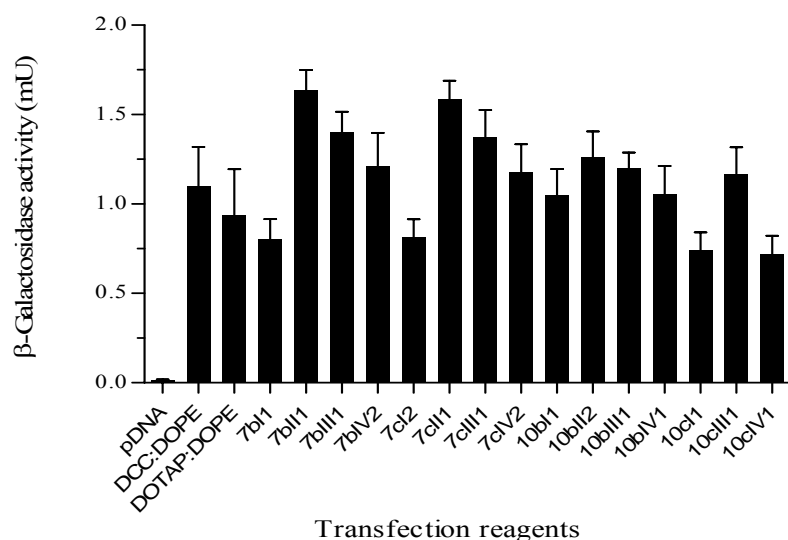
Figure 69. Comparative transfection efficacies of best GA formulations in A549 cell line in presence of FBS 10 %
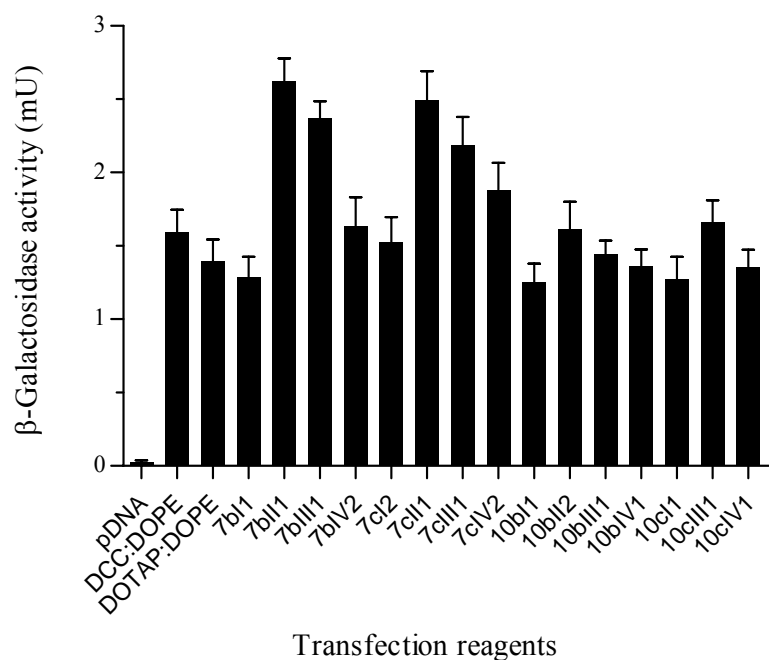
Figure 70. Comparative transfection efficacies of best GA formulations in HeLa cell line in presence of FBS 10 %

3.4.4. Effect of Cholesterol on the transfection efficacy of GAs

Cholesterol is known to impart serum compatibility to gene delivery carriers[211]. Cholesterol was incorporated in the GA formulations (**7bII1**, **7bIII1**, **7cII2**, **7cIII1**) in an attempt to improve their transfectiion efficacies in presence of serum. Cholesterol was added to all the formulations in two different molar concentrations such that GA:DOPE:cholesterol were in the ratios of 1:1:1 and 1:1:0.5. The transfection efficacies of the resulting formulations were checked in absence and presence of serum 10 % both in A549 and HeLa cell lines.

In A549 cell line, **7bII1A** (**7bII**:DOPE:cholesterol; 1:1:1) and **7bII1B** (**7bII**:DOPE:cholesterol; 1:1:0.5) **(Figure 71A)** showed highest *β*-Gal expression of 2.43 and 2.20 mU at N/P ratio of 3 in absence of serum. However, in presence of serum 10 %, these formulations showed 2.14 and 2.04 mU *β*-Gal expression respectively at N/P of 3.
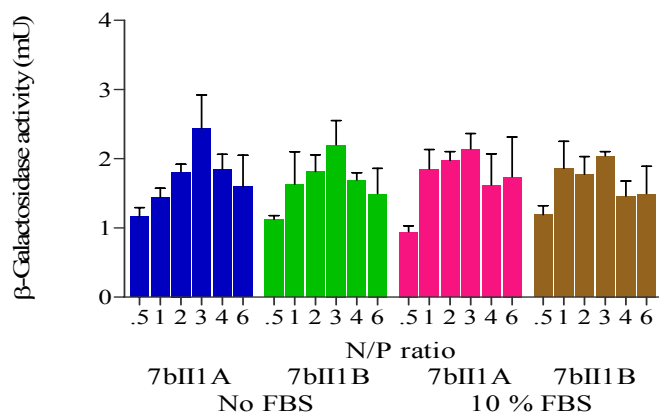
(A)
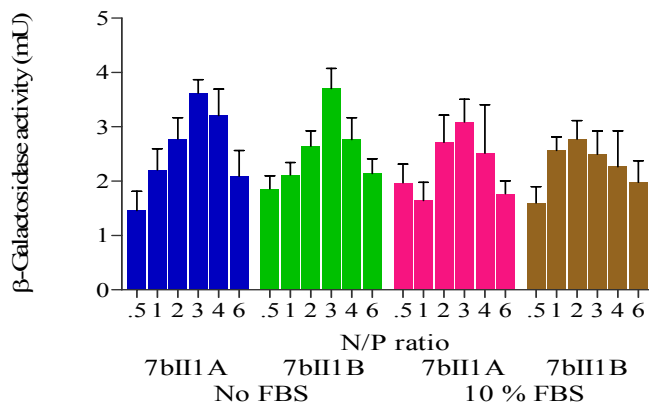
(B)

Figure 71. Transfection efficacies of **7bII1A** (**7bII**:DOPE:cholesterol; 1:1:1) and **7bII1B** (**7bII**:DOPE:cholesterol; 1:1:0.5) in (A) A549 and (B) HeLa cell lines in absence and presence of serum 10 %

In HeLa cell line, **7bII1A** (**7bII**:DOPE:cholesterol; 1:1:1) and **7bII1B** (**7bII**:DOPE:cholesterol; 1:1:0.5) **(Figure 71B)** showed the highest β-Gal expression of 3.61 and 3.70 at N/P ratio of 3 in absence of serum. However, in presence of serum 10 %, these formulations showed 3.09 and 2.77 mU β-Gal expression respectively at N/P of 3.

In A549 cell line, **7bIII1A** (**7bIII**:DOPE:cholesterol; 1:1:1) and **7bIII1B** (**7bIII**:DOPE:cholesterol; 1:1:0.5) **(Figure 72A)** showed the highest β-Gal expression of 1.94 and 1.73 respectively at N/P ratio of 2 in absence of serum. However, in presence of serum 10 %, these formulations showed 1.72 and 1.68 mU β-Gal expression at N/P of 2.
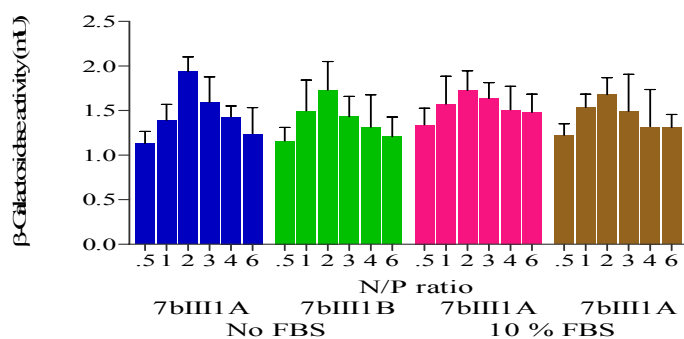
(A)
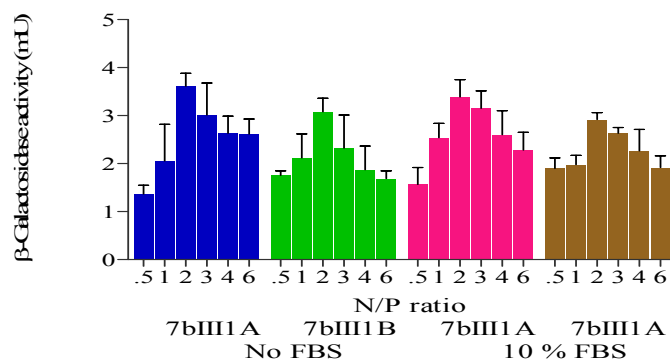
(B)

Figure 72. Transfection efficacies of **7bIII1A** (**7bIII**:DOPE:cholesterol; 1:1:1) and
7bIII1B (**7bIII**:DOPE:cholesterol; 1:1:0.5) in (A) A549 and (B) HeLa cell
lines in absence and presence of serum (10 %)

In HeLa cell line, **7bIII1A** (**7bIII**:DOPE:cholesterol; 1:1:1) and **7bIII1B** (**7bIII**:DOPE:cholesterol; 1:1:0.5) **(Figure 72B)** showed the highest β-Gal expression of 3.61 and 3.07 mU respectively at N/P ratio of 2 in absence of serum. However, in presence of serum 10 %, these formulations showed 3.39 and 2.92 mU β-Gal expression at N/P of 2.

In A549 cell line, **7cII1A** (**7cII**:DOPE:cholesterol; 1:1:1) and **7cII1B** (**7cII**:DOPE:cholesterol; 1:1:0.5) **(Figure 73A)** showed the highest β-Gal expression of 2.06 and 1.90 mU respectively at N/P ratio of 2 in absence of serum. However, in presence of serum 10 %, these formulations showed 1.57 and 1.47 mU β-Gal expression at N/P of 2.
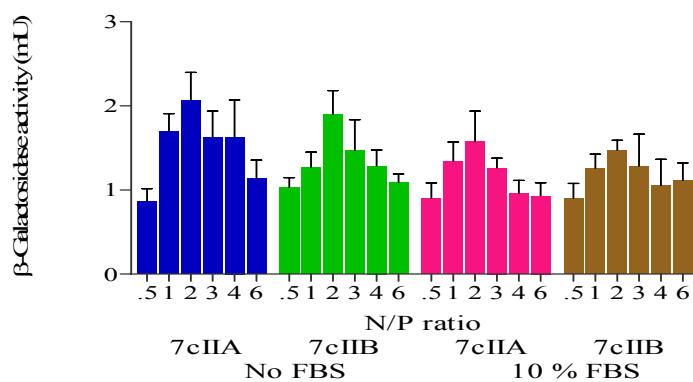
(A)
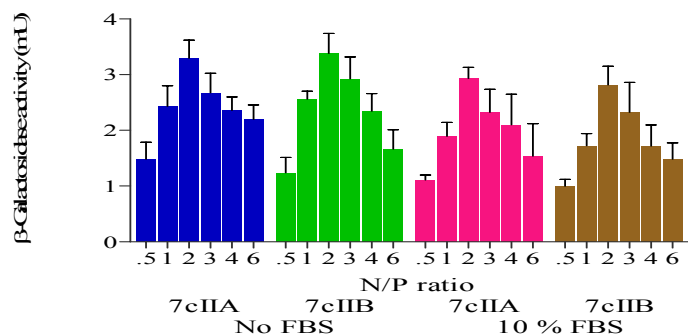
(B)

Figure 73. Transfection efficacies of **7cII1A** (**7cII**:DOPE:cholesterol; 1:1:1) and
7cII1B (**7cII**:DOPE:cholesterol; 1:1:0.5) in (A) A549 and (B) HeLa cell
lines in absence and presence of serum (10 %)

In HeLa cell line, **7cII1A** (**7cII**:DOPE:cholesterol; 1:1:1) and **7cII1B** (**7cII**:DOPE:cholesterol; 1:1:0.5) **(Figure 73B)** showed the highest β-Gal expression of 3.29 and 3.38 mU respecttively at N/P ratio of 2 in absence of serum. However, in presence of serum 10 %, these formulations showed 2.93 and 2.81 mU β-Gal expression at N/P of 2.

In A459 cell line, **7cIII1A** (**7cIII**:DOPE:cholesterol; 1:1:1) and **7cIII1B** (**7cIII**:DOPE:cholesterol; 1:1:0.5) **(Figure 74A)** showed the highest *β*-Gal expression of 1.96 and 1.81 mU respectively at N/P ratio of 1 in absence of serum. However, in presence of serum 10 %, these formulations showed 1.44 and 1.36 mU *β*-Gal expression at N/P of 1.
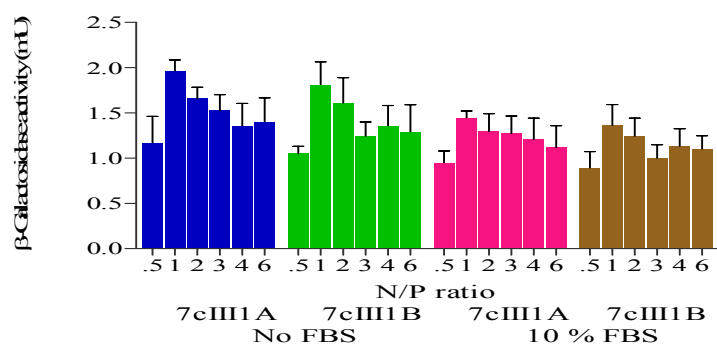
(A)
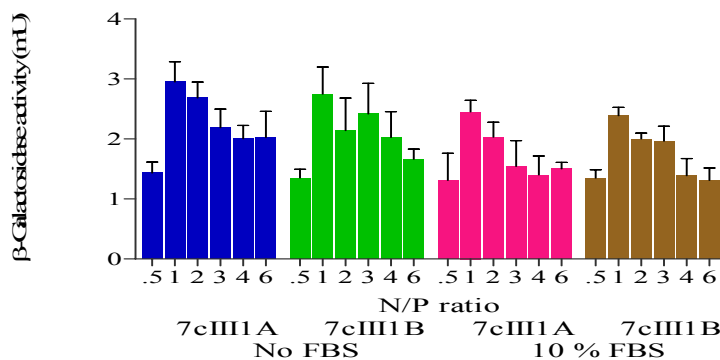
(B)

Figure 74. Transfection efficacies of **7cIII1A** (**7bIII**:DOPE:cholesterol; 1:1:1) and **7cIII1B** (**7bIII**:DOPE:cholesterol; 1:1:0.5) in (A) A549 and (B) HeLa cell lines in absence and presence of serum (10 %)

In HeLa cell line, **7cIII1A** (**7cIII**:DOPE:cholesterol; 1:1:1) and **7cIII1B** (**7cIII**:DOPE:cholesterol; 1:1:0.5) **(Figure 74B)** showed the highest *β*-Gal expression of 2.95 and 2.74 mU respectively at N/P ratio of 1 in absence of serum. However, in presence of serum 10 %, these formulations showed 2.45 and 2.38 mU *β*-Gal expression at N/P of 1.

3.4.5 MTT assay for cytotoxicity evaluation of GA formulations

Cytotoxicity is an important criterion in selecting a suitable GA for gene delivery. A good GA should exhibit not only a high transfection efficacy but a minimal level of toxicity too. The GA formulations showing good results in the transfection studies were evaluated for cell viability. Formulations of GAs [**3(I-IV)**, **7b(I-IV)**, **7b(I-IV)**, **10b(I-IV) and 10b(I-IV)**] with DOPE were evaluated for cell viability using MTT assay for cell toxicity under identical conditions as maintained in their transfection studies. The results are shown in **Figures 75-93.**

(A)

(B)
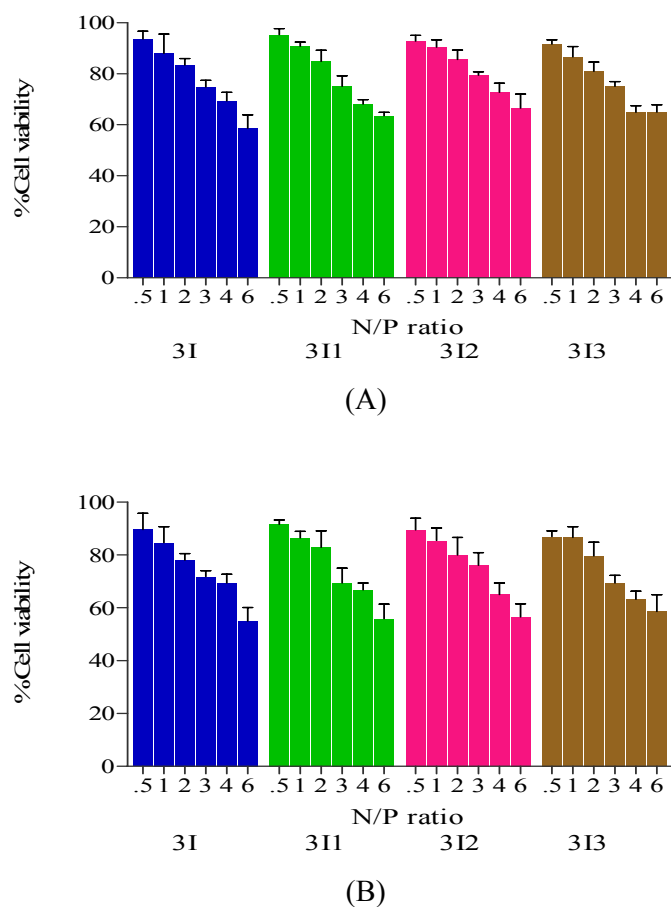
Figure 75. Percent cell viability of **3I** alone and in combination with DOPE; 1:1 **(3I1)**, 1:2 **(3I2)** and 1:3 **(3I3)** in (A) A549 and (B) HeLa cell lines
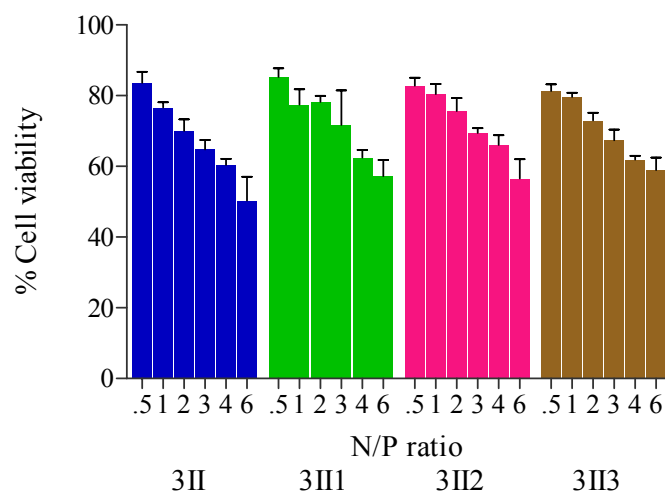
(A)
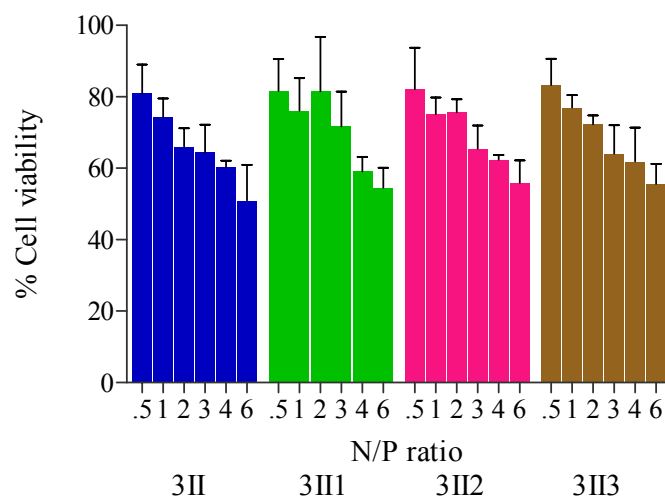
(B)

Figure 76. Percent cell viability of **3II** alone and in combination with DOPE; 1:1 **(3II1)**, 1:2 **(3II2)** and 1:3 **(3II3)** in (A) A549 and (B) HeLa cell lines
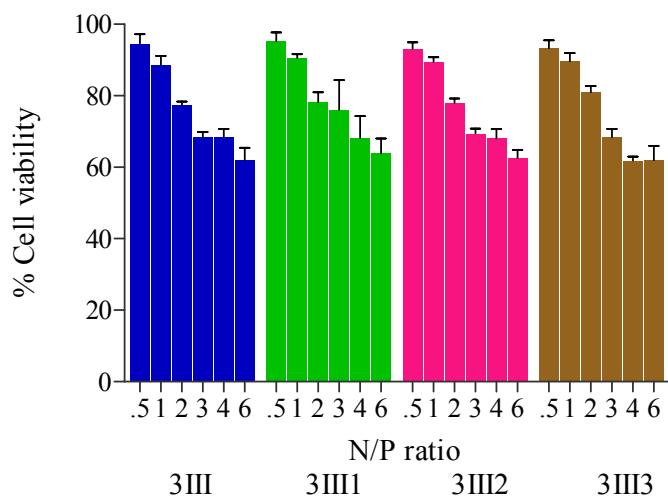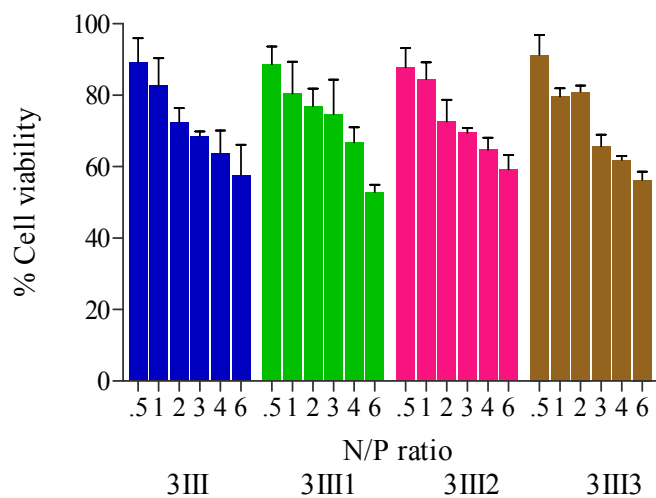
Figure 77. Percent cell viability of **3III** alone and in combination with DOPE; 1:1 **(3III1)**, 1:2 **(3III2)** and 1:3 **(3III3)** in (A) A549 and (B) HeLa cell lines
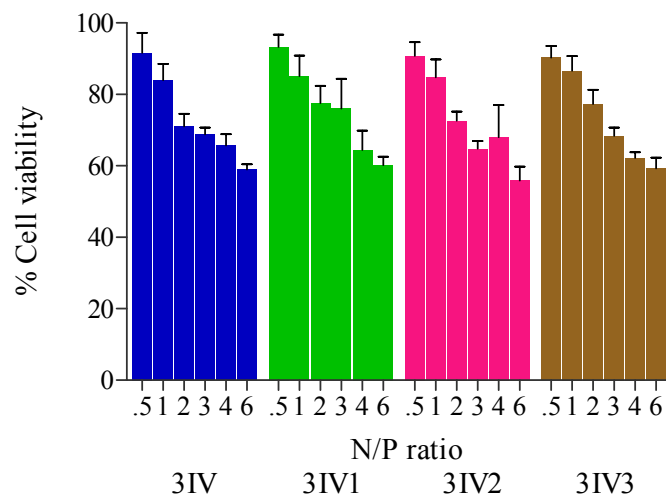
(A)
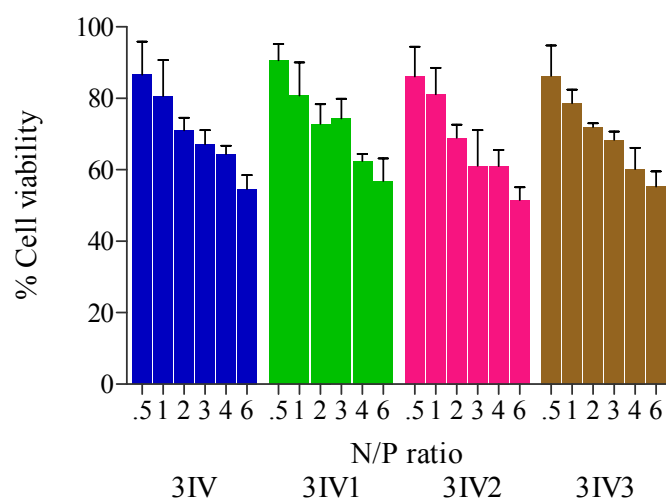
(B)

Figure 78. Percent cell viability of **3IV** alone and in combination with DOPE; 1:1 **(3IV1)**, 1:2 **(3IV2)** and 1:3 **(3IV3)** in (A) A549 and (B) HeLa cell lines
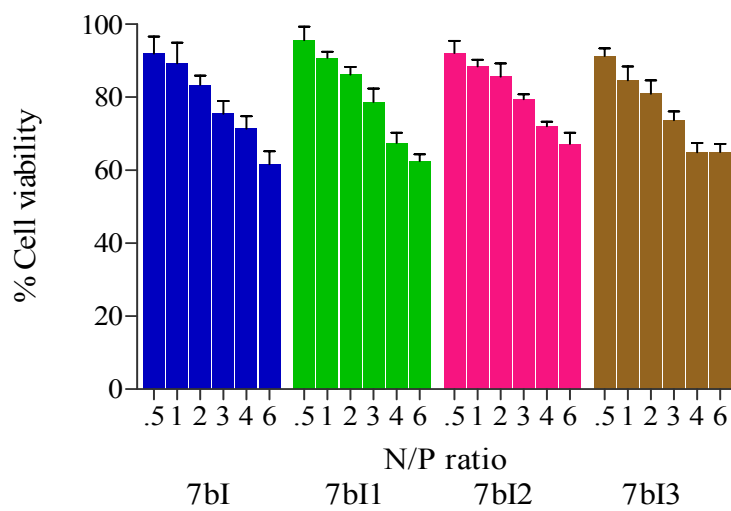
(A)
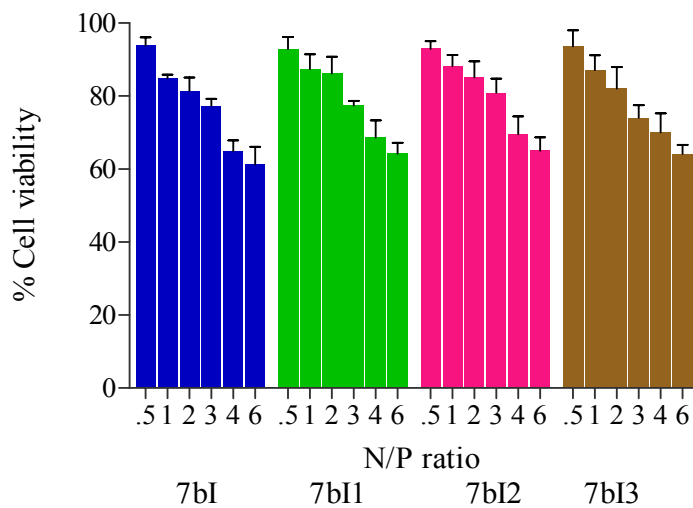
(B)

Figure 79. Percent cell viability of **7bI** alone and in combination with DOPE; 1:1 **(7bI1)**, 1:2 **(7bI2)** and 1:3 **(7bI3)** in (A) A549 and (B) HeLa cell lines
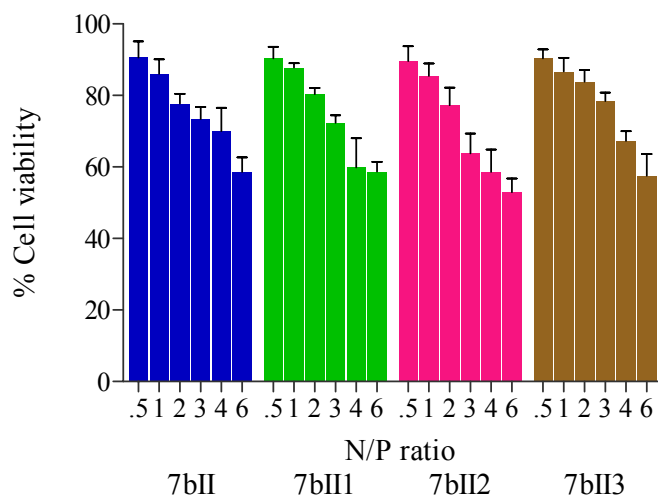
(A)
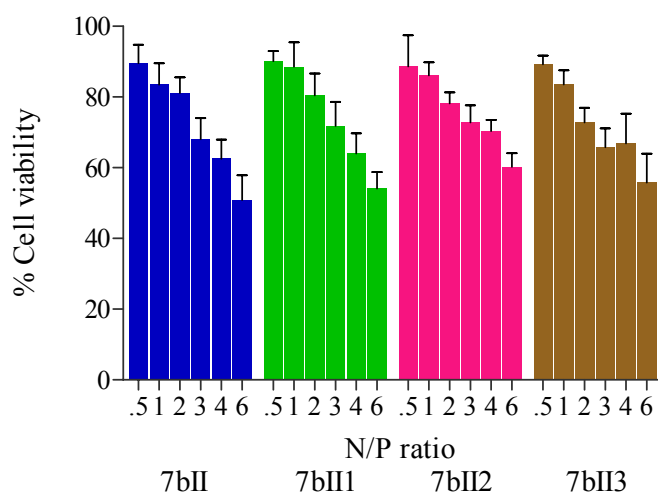
(B)

Figure 80. Percent cell viability of **7bII** alone and in combination with DOPE; 1:1 **(7bII1)**, 1:2 **(7bII2)** and 1:3 **(7bII3)** in (A) A549 and (B) HeLa cell lines
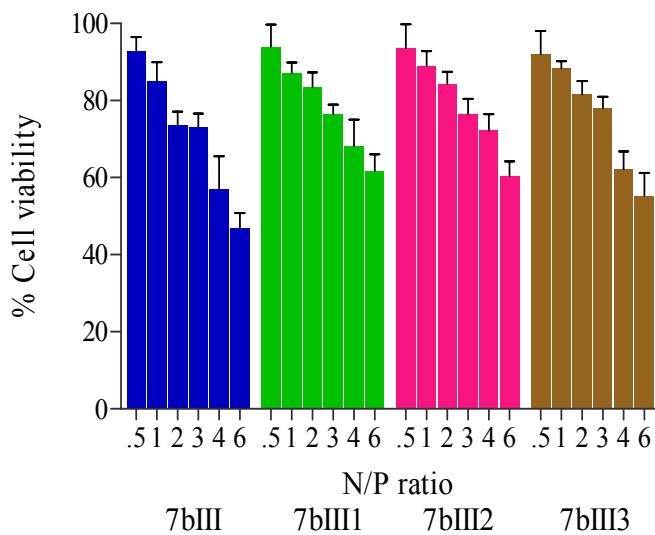
(A)
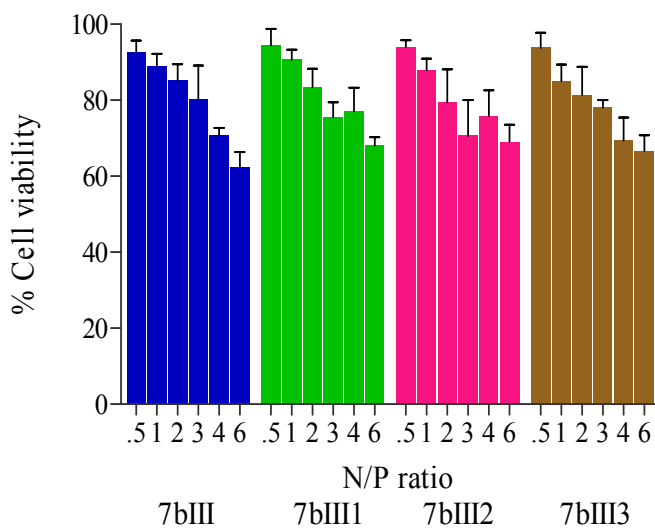
(B)

Figure 81. Percent cell viability of **7bIII** alone and in combination with DOPE;

1:1 **(7bIII1)**, 1:2 **(7bIII2)** and 1:3 **(7bIII3)** in (A) A549 and (B) HeLa
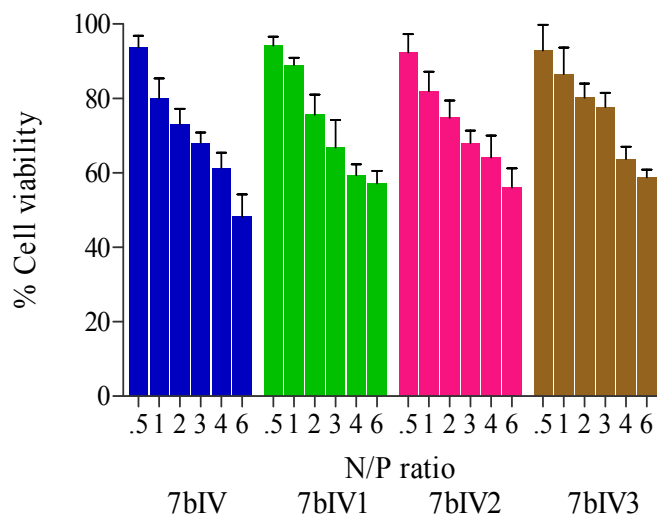
cell lines

(A)
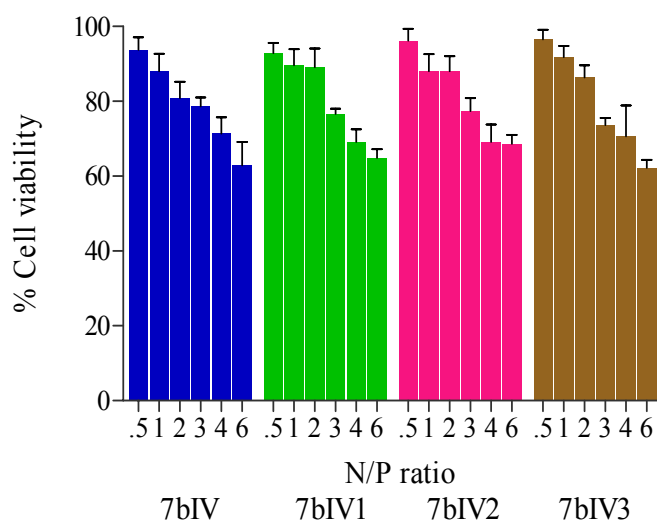
(B)

Figure 82. Percent cell viability of **7bIV** alone and in combination with
DOPE; 1:1**(7bIV1)**, 1:2 **(7bVI2)** and 1:3 **(7bIV3)** in (A) A549 and
(B) HeLa cell lines
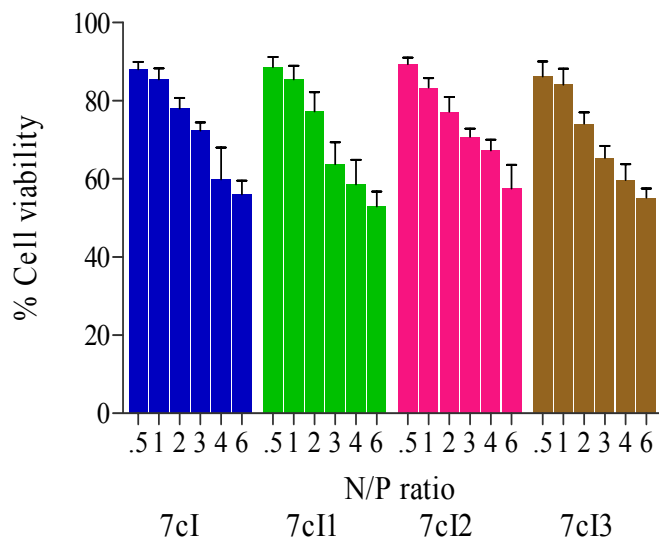
(A)
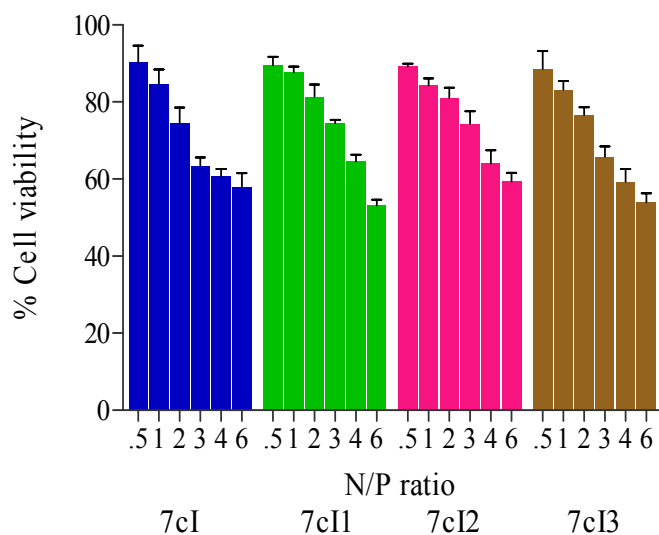
(B)

Figure 83. Percent cell viability of **7cI** alone and in combination with DOPE; 1:1 **(7cI1)**, 1:2 **(7cI2)** and 1:3 **(7cI3)** in (A) A549 and (B) HeLa cell lines
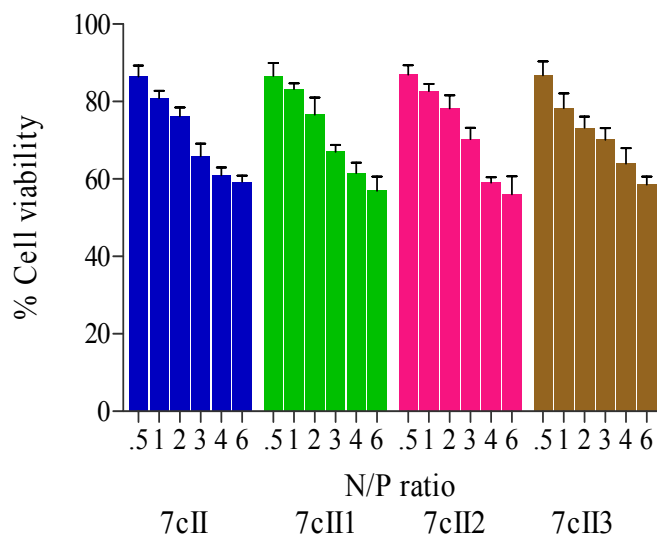
(A)
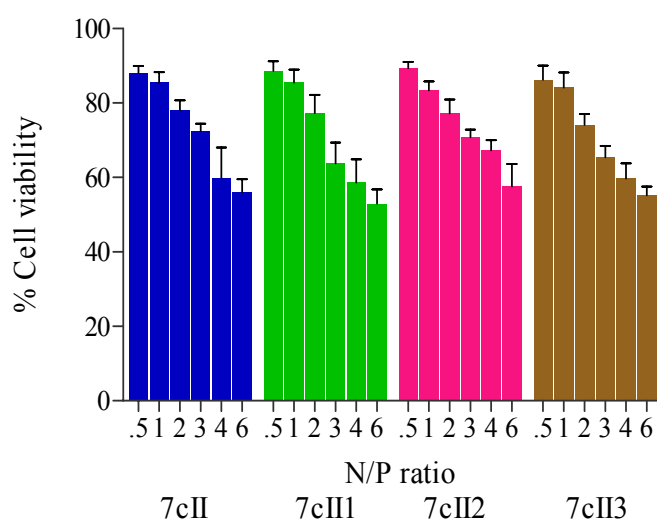
(B)

Figure 84. Percent cell viability of **7cII** alone and in combination with DOPE; 1:1 **(7cII1)**, 1:2 **(7cII2)** and 1:3 **(7cII3)** in (A) A549 and (B) HeLa cell lines

(A)

(B)
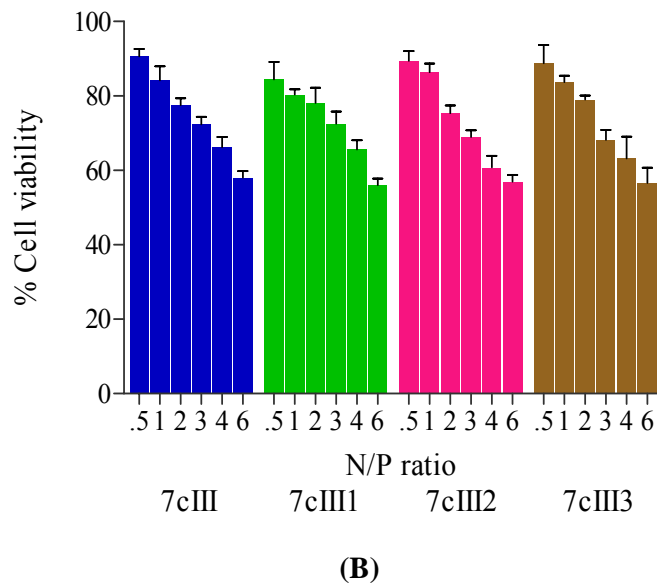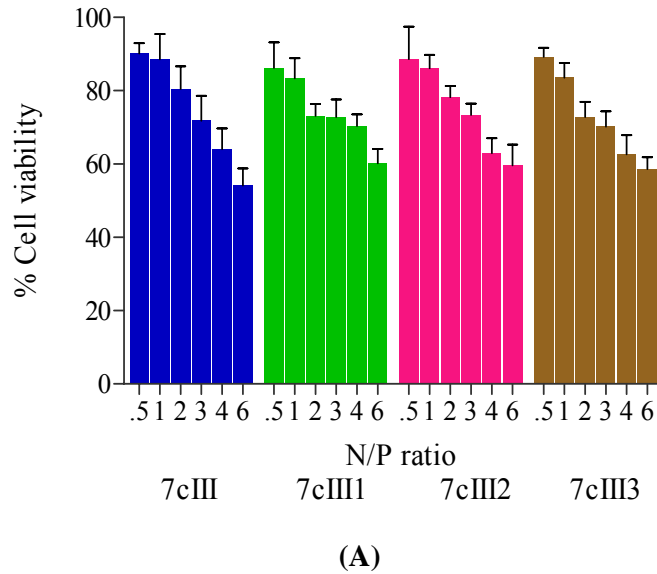
Figure 85. Percent cell viability of **7cIII** alone and in combination with
DOPE; 1:1 **(7cIII1)**, 1:2 **(7cIII2)** and 1:3 **(7cIII3)** in (A) A549 and
(B) HeLa cell lines

(A)

(B)
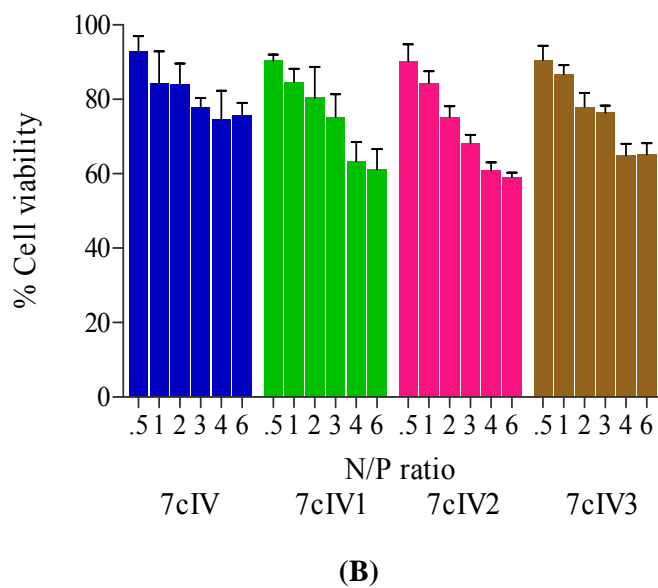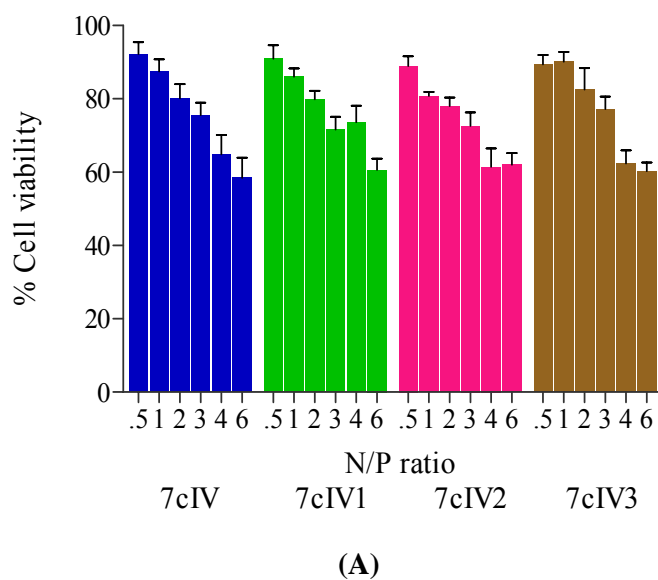
Figure 86. Percent cell viability of **7cIV** alone and in combination with
DOPE; 1:1 **(7cIV1)**, 1:2 **(7cIV2)** and 1:3 **(7cIV3)** in (A) A549 and
(B) HeLa cell lines
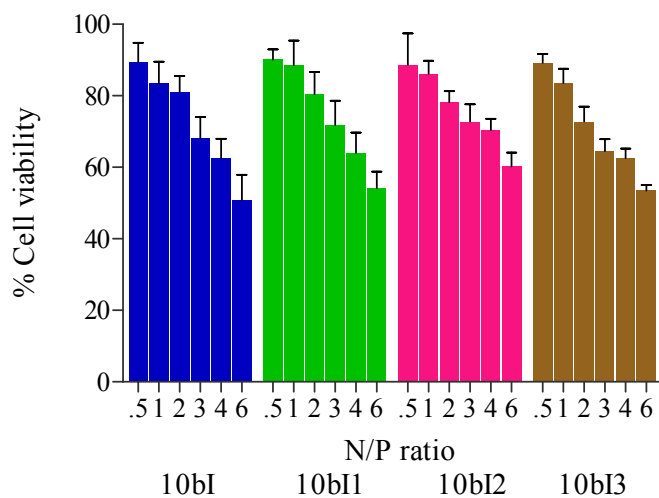
(A)
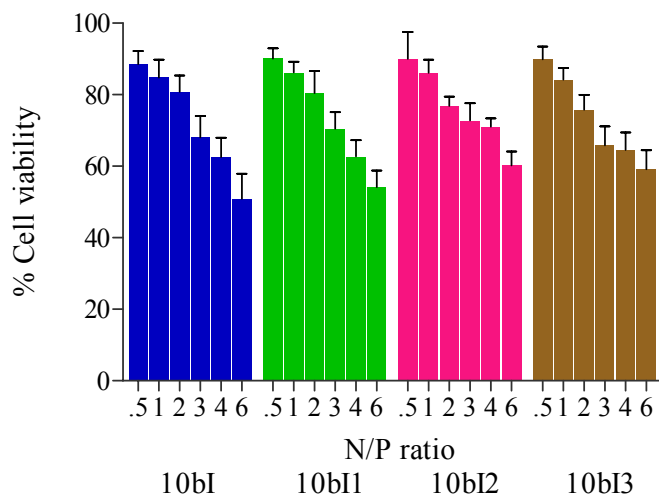
(B)

Figure 87. Percent cell viability of **10bI** alone and in combination with
DOPE; 1:1 **(10bI1)**, 1:2 **(10bI2)** and 1:3 **(10bI3)** in (A) A549 and
(B) HeLa cell lines

(A)

(B)
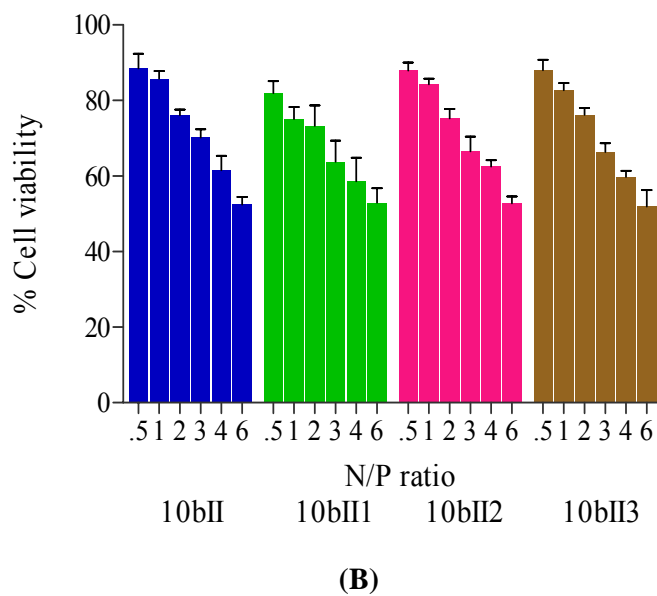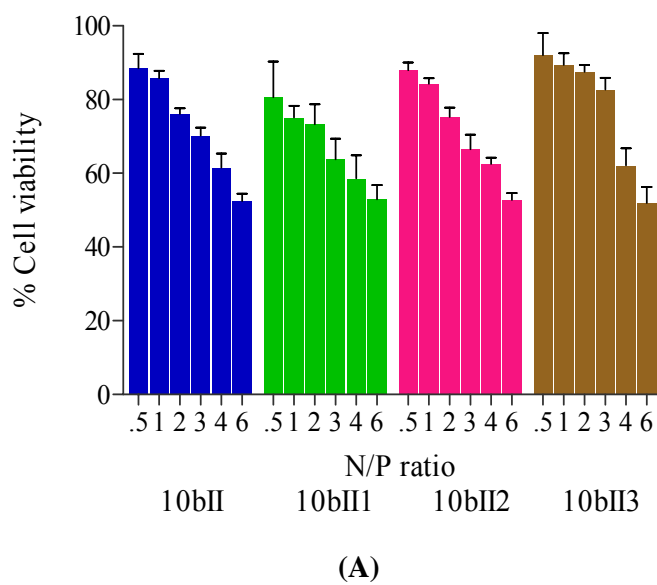
Figure 88. Percent cell viability of **10bII** alone and in combination with
DOPE; 1:1 **(10bII1)**, 1:2 **(10bII2)** and 1:3 **(10bII3)** in (A) A549
and (B) HeLa cell lines
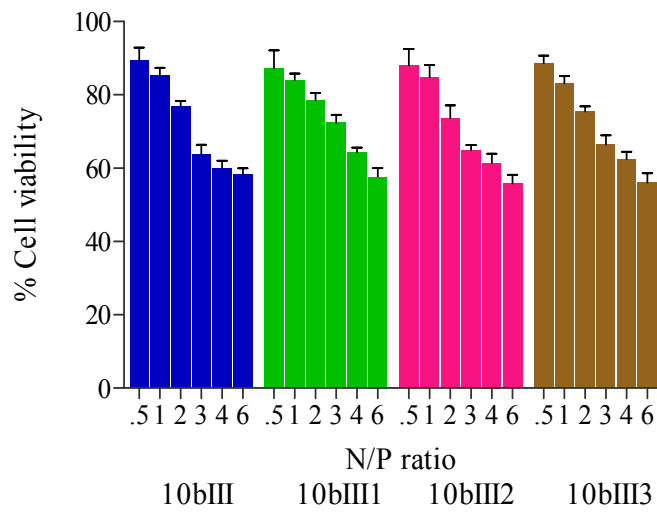
(A)
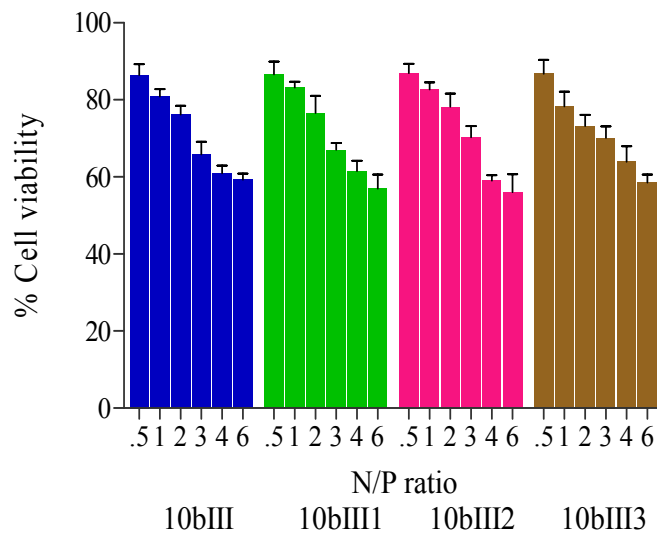
(B)

Figure 89. Percent cell viability of **10bIII** alone and in combination with
DOPE; 1:1 **(10bIII1)**, 1:2 **(10bIII2)** and 1:3 **(10bIII3)** in (A)
A549 and (B) HeLa cell lines
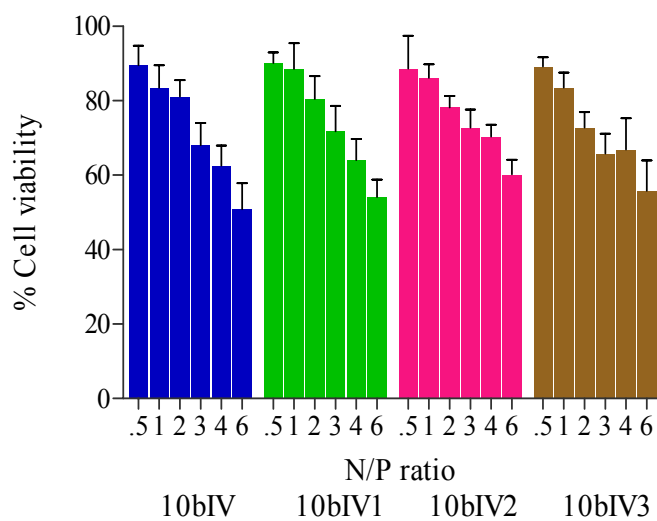
(A)
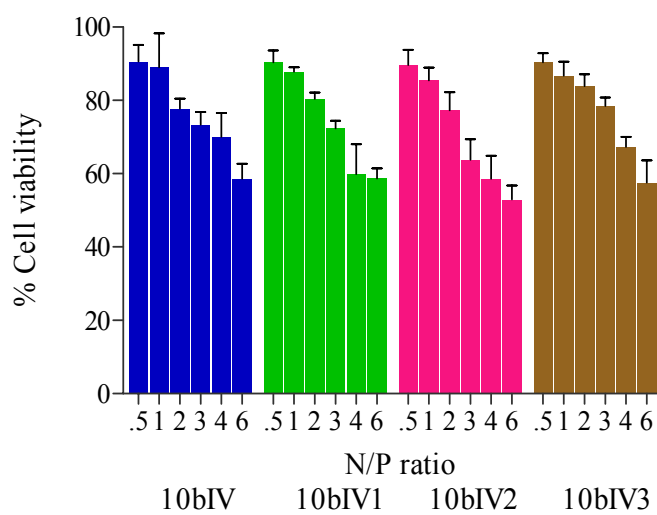
(B)

Figure 90. Percent cell viability of **10bIV** alone and in combination with DOPE; 1:1 (**10bIV1**), 1:2 (**10bIV2**) and 1:3 (**10bIV3)** in (A) A549 and (B) HeLa cell lines
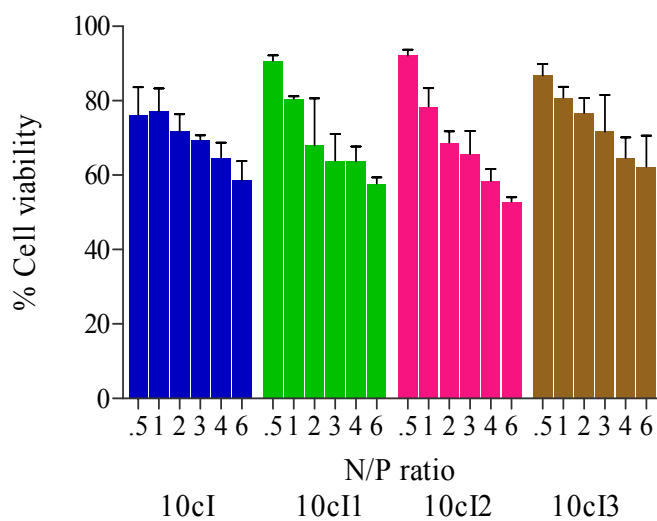
(A)
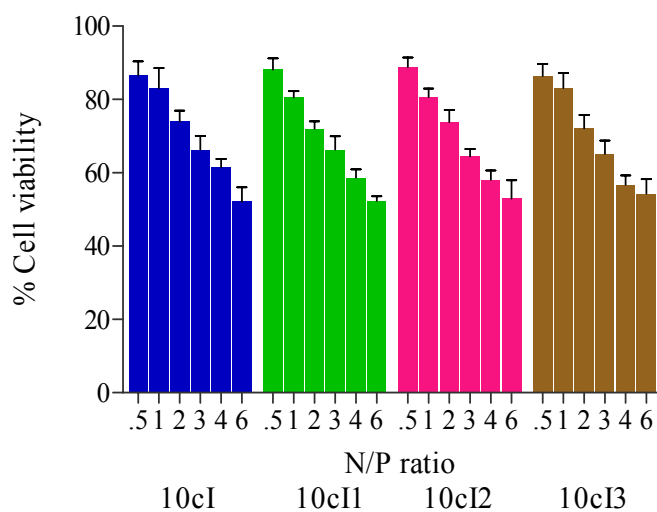
(B)

Figure 91. Percent cell viability of **10cI** alone and in combination with DOPE; 1:1 **(10cI1)**, 1:2 **(10cI2)** and 1:3 **(10cI3)** in (A) A549 and (B) HeLa cell lines
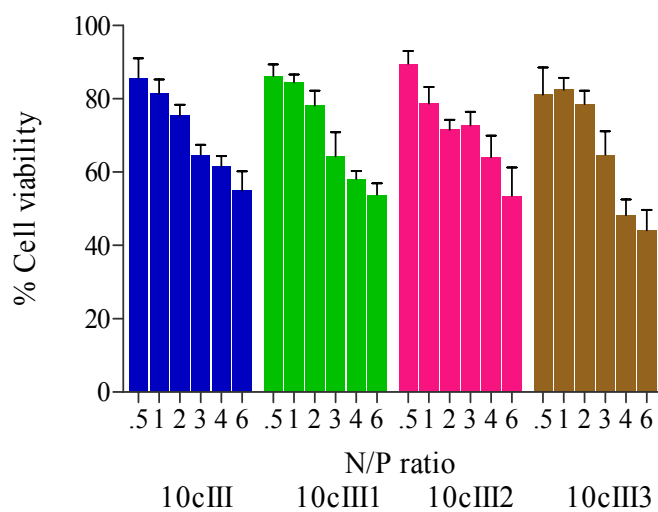
(A)
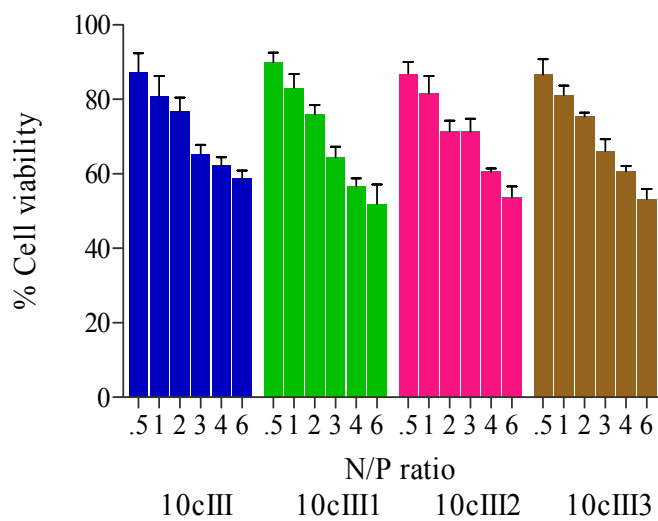
(B)

Figure 92. Percent cell viability of **10cIII** alone and in combination with
DOPE; 1:1 **(10cIII1)**, 1:2 **(10cIII2)** and 1:3 **(10cIII3)** in (A) A549
and (B) HeLa cell lines

(A)

(B)
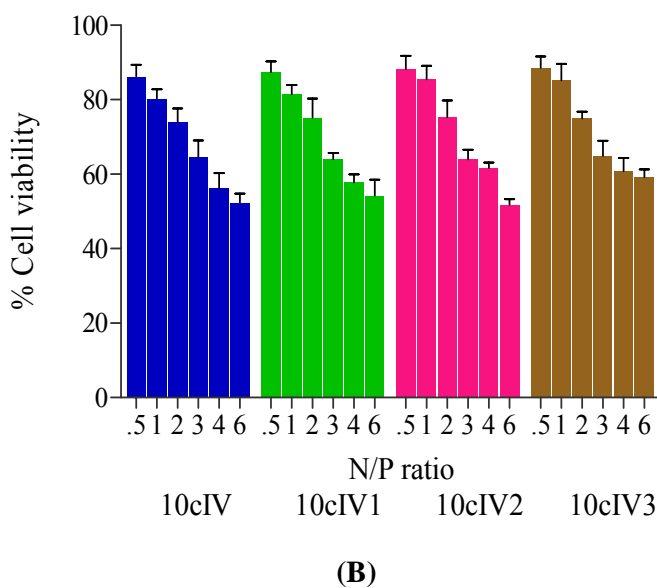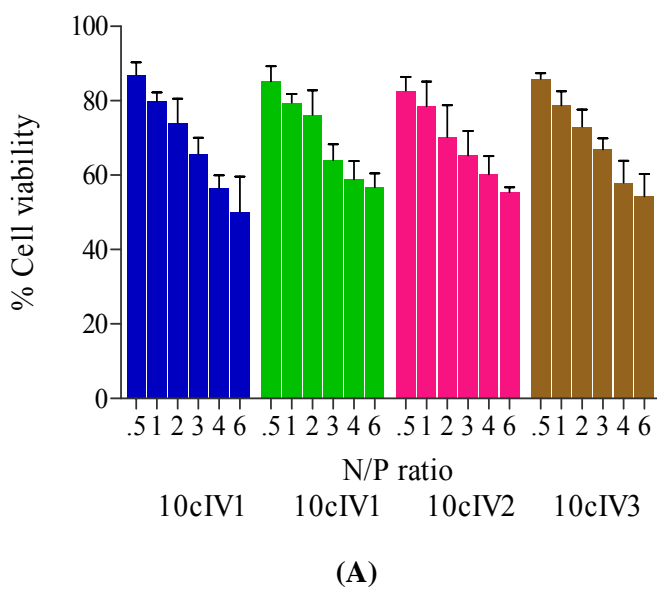
Figure 93. Percent cell viability of **10cIV** alone and in combination with
DOPE; 1:1 **(10cIV1)**, 1:2 **(10cIV2)** and 1:3 **(10cIV3)** in (A) A549
and (B) HeLa cell lines

Cell viability of the contol cells without treatment was considered as 100 %. All the GA formulations evaluated for MTT assay showed N/P ratio dependent cell viability. As the N/P ratio of the lipoplexes increased from 0.5 to 6, cell viability decreased in both of the cell lines for all the formulations. Cell viabilities of all the
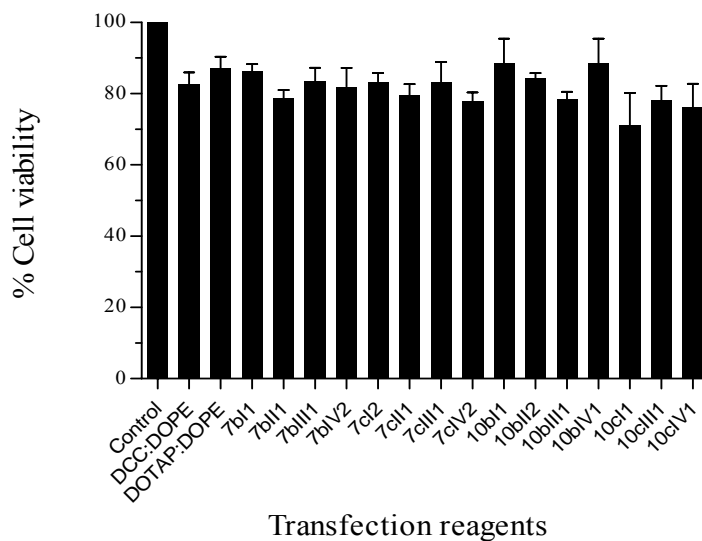
Figure 94. Compiled results of percent cell viability of GA formulations (showing best N/P results in transfection studies) in A549 cells
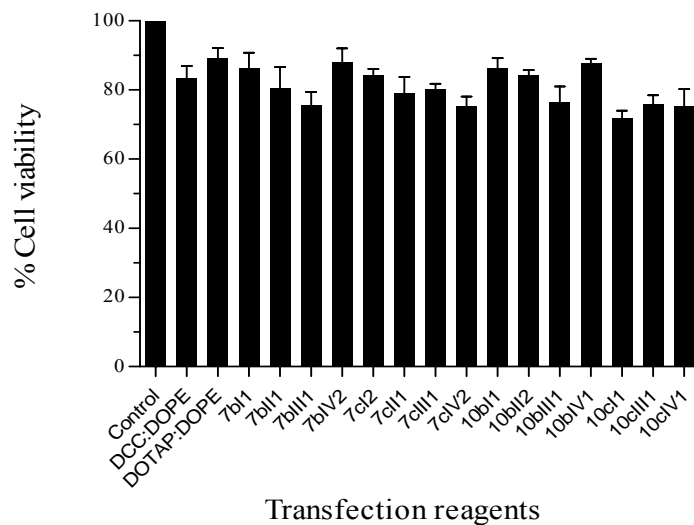
Figure 95. Compiled results of percent cell viability of GA formulations (showing best N/P results in transfection studies) in HeLa cells

GA formulations having the highest transfection efficacy have been evaluated and compared with standards (DCC:DOPE and DOTAP:DOPE liposomes) in A549 and HeLa cell lines respectively in **Figures 94** and **95**. The cell viabilities of almost all the formulations were comparable to that of standards (DCC:DOPE and DOTAP:DOPE liposomes). DCC:DOPE and DOTAP:DOPE liposomes showed cell viabilities of 82.6, 87.2 % and 83.38, 89.2 % in A549 and HeLa cell lines respectively. The cell viabilities were not found to dependent upon the hydrocarbon tails of GAs. However, GAs having oxyethylene spacers were found to be more toxic compared to the polymethylene and *p*-xylene spacers, while keeping the hydrocarbon chain length and head group constant. For instance, the cell viabilities of **7bI** (*p*-xylene spacer) and **7bII** (oxyethylene spacer) having similar hydrocarbon chains and head droups were found to be 91.9, 89.2, 83.3, 75.48, 71.4, 61.6 % and 90.64, 86.01, 77.74, 73.35, 70.07, 58.63 % respectively in A549 cell line at N/P ratios of 0.5, 1, 2, 3, 4, 6. In HeLa cell line, **7bI** (*p*-xylene spacer) and **7bII** (oxyethylene spacer) showed cell viabilities of 93.89, 84.89, 81.33, 77.36, 64.89, 61.33 % and 89.55, 83.44, 81.11, 68.0, 62.5, 50.89 % respectively at N/P ratios of 0.5, 1, 2, 3, 4, 6. It is clearly evident from the data that oxyethylene spacer yielded GAs with higher cytotoxicities than the GAs having *p*-xylene spacer at all the N/P ratios in both the cell lines.

3.4.6 Florescence-assisted cells sorting (FACS) studies

The amount of *β*-galactosidase protein expressed in cells is a measure of the efficacy of the gene delivery carriers. However, the number of cells transfected by transfection reagents is also important. The percentage of cells transfected during transfection experiments by the GA formulations showing promising results in *β*-Gal expression have been evaluated using FACS studies in 24-well format. The fluorescence of Green fluorescent protein (GFP) plasmid was observed and captured under fluoresence microscope.

The fluorescent images of GFP plasmid for the formulations; **7bII1**, **7bII1A**, **7bIII1**, **7bIII1A**, **7cII1**, **7cII1A**, **7cIII1** and **7cIII1A** have been shown in **Figures 96** and **97** in A549 and HeLa cells respectively. **Figures 98** and **99** showed percent of cells transfected with GFP plamid using these formulations compared with the plain GFP plasmid (negative control) and standards (Lipofectamine 2000, DCC:DOPE and

DOTAP:DOPE liposomes) in A549 cells in absence of serum. It was observed that formulations containing cholesterol (**7bII1A**, **7bIII1A**, **7cII1A** and **7cIII1A**) showed higher number of transfected cells compared to the respective formulations without cholesterol (**7bII1**, **7bIII1**, **7cII1** and **7cIII1**). This common observation was noted for both A549 and HeLa cell lines in absence of serum. For instance, formulation **7bII1** (**7bII**:DOPE, 1:1 molar ratio) showed the highest percent of transfected cells (14.41 and 18.78 % in A549 and HeLa cells respectively). Its efficiency further improved with the incorporation of cholesterol, **7bII1A** (**7bII**:DOPE:cholesterol,1:1:1 molar ratio) resulting into 16.18 and 21 % .transfected cells in A549 and HeLa cell line respectively in absence of serum. All of the formulatons showed significant increase in percent of transfected cells compared to the plain GFP plasmid. The percent transfected cells by various transfection reagents followed the order, **7bII1A** > Lipofectamine > **7bIII1A** > **7cII1A** > **7bII1** > **7bIII1** > **7cII1** > **7cIII1A** > **7cIII1** > DCC:DOPE > DOTAP:DOPE > control in A459 cells and **7bII1A** > Lipofectamine > **7bII1** > **7bIII1A** > **7cII1A** > **7bIII1** > **7cII1** > **7cIII1A** > **7cIII1** > DCC:DOPE > DOTAP:DOPE > control in HeLa cells in absence of serum at their optimized N/P ratios. All the formulstions showed significantly higher percent of transfected cells compared to DCC:DOPE and DOTAP:DOPE liposomes in both of the cell lines used. The formulation **7bII1A** showed higher percentage of transfected cells (16.18 and 21 % transfected cells in A549 and HeLa cell lines respectively) compared to Lipofectamine 2000 (15.94 and 19.32 % transfected cells in A549 and HeLa cell lines respectively) in absence of serum at its optimized N/P ratio. The formulations (**7bIII1A**, **7cII1A** and **7bII1**) showed comparable percent of transfected cells (14.99, 14.43 and 14.41 % respectively) to that of Lipofectamine 2000 (16.18 %) in A549 cell line at their optimized N/P ratios without FBS. The formulations (**7bII1**, **7bIII1A** and **7cII1A**) showed comparable percentage of transfected cells (18.78, 18.2 and 17.95 % respectively) to that of Lipofectamine 2000 (19.32 %) in HeLa cell line at their optimized N/P ratios without FBS.

Figure 96. Fluorescence images of GFP expression in A549 cells; (A) **7bII1**, (B) **7bII1A**, (C) **7bIII1**, (D) **7bIII1A**, (E) **7cII1**, (F) **7cII1A**, (G) **7cIII1** and (H) **7cIII1A** at their optimized N/P ratios in absence of serum
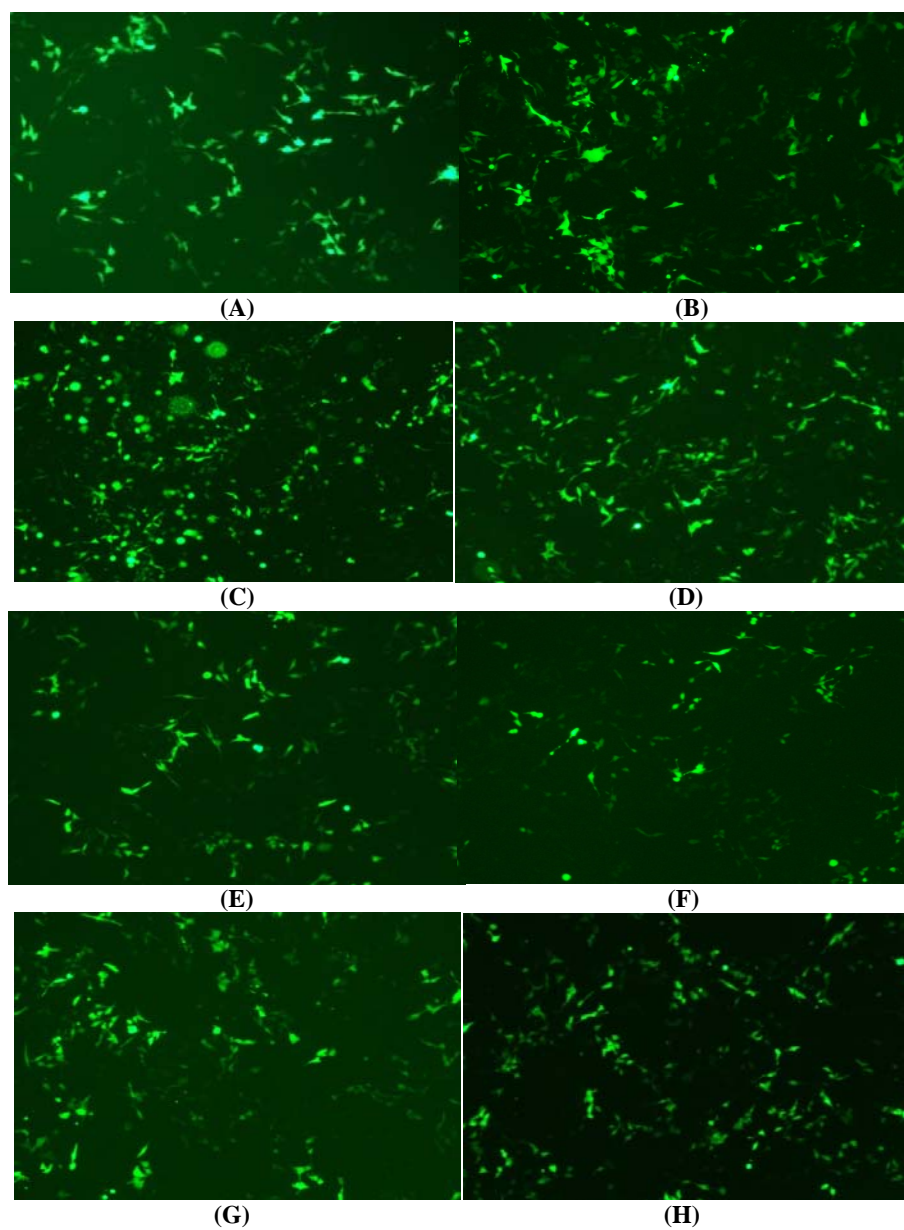
Figure 97. Fluorescence images of GFP expression in HeLa cells; (A) **7bII1**, (B) **7bII1A**, (C) **7bIII1**, (D) **7bIII1A**, (E) **7cII1**, (F) **7cII1A**, (G) **7cIII1** and (H) **7cIII1A** at their optimized N/P ratios in absence of serum
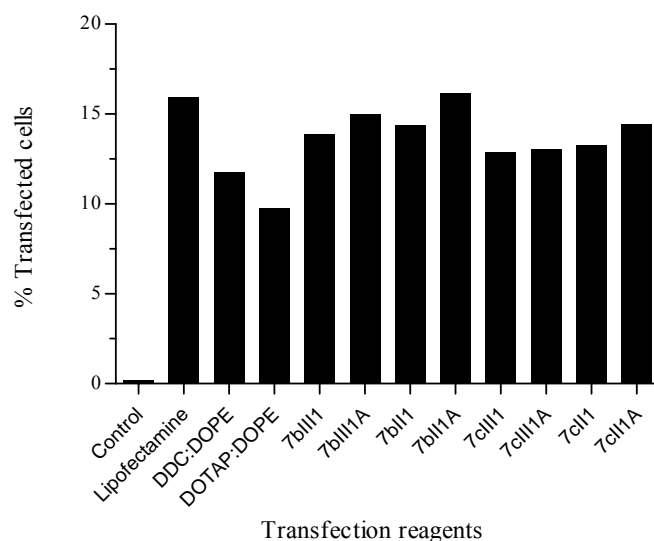
Figure 98. FACS studies of optimized formulations at optimized N/P ratios using GFP plasmid in A549 cells without FBS
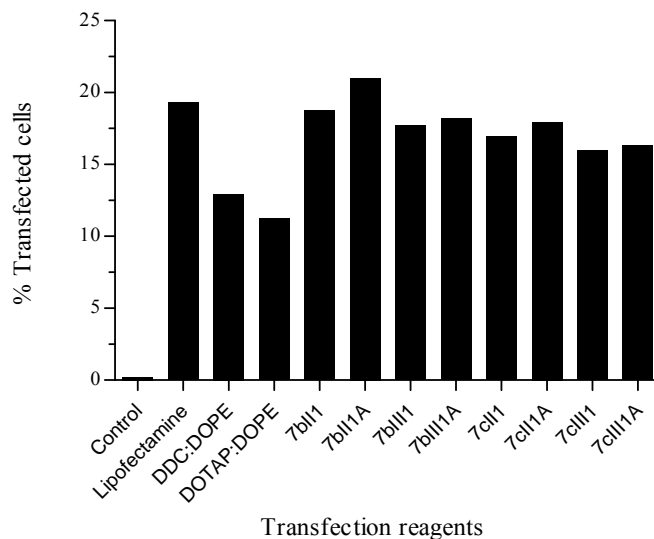
Figure 99. FACS studies of optimized formulations at optimized N/P ratios using GFP plasmid in HeLa cells without FBS

Figures 100 and **101** showed percentage of transfected cells by optimized GA formulations at their optimized N/P ratios in A549 and HeLa cells respectively in presence of FBS 10 %. The percentage of transfected cells by various formulations

followed the order: **7bII1A** > **7bIII1A** > **7cII1A** > **7cIII1A** > **7bII1** > **7cIII1** > **7bIII1** > DCC:DOPE > DOTAP:DOPE > **7cII1** > control in A459 cells and 7**bII1A** > **7bIII1A** > **7cII1A** > **7cIII1A** > **7bII1** > **7bIII1** > **7cIII1** > **7cII1** > DCC:DOPE > DOTAP:DOPE > control in HeLa cells in presence of serum 10 % at their optimized N/P ratios. Almost all the formulstions showed significantly higher percent of transfected cells compared to DCC:DOPE and DOTAP:DOPE liposomes in both of the cell lines used.
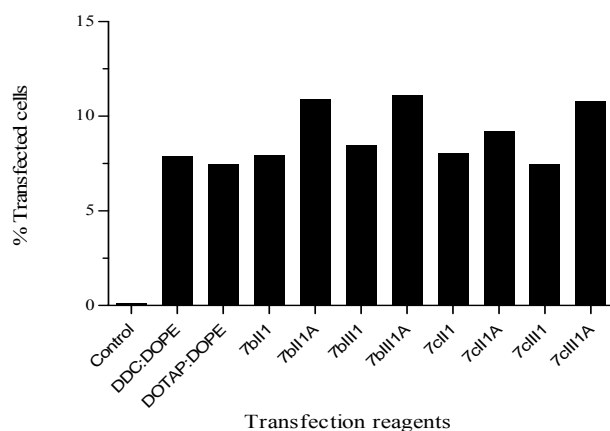
Figure 100. FACS studies of optimized formulations at optimized N/P ratios using GFP plasmid in A549 cells with FBS 10 %
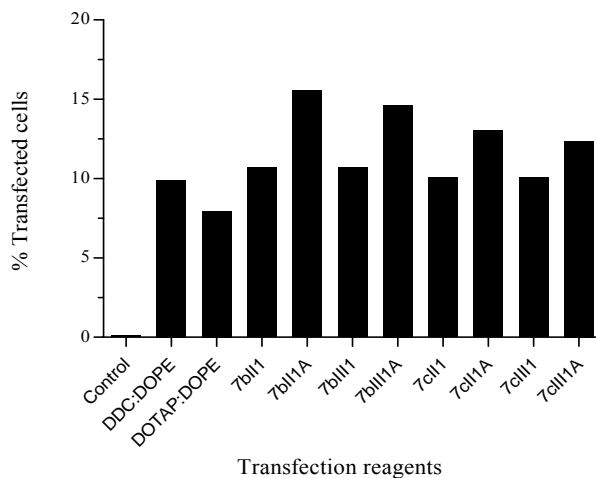
Figure 101. FACS studies of optimized formulations at optimized N/P ratios using GFP plasmid in HeLa cells with FBS 10 %

Cholesterol containing GA formulations (**7bII1A**, **7bIII1A**, **7cII1A** and **7cIII1A**) showed higher percentage of ransfected cells compared to their respective formulations without cholesterol (**7bII1**, **7bIII1**, **7cII1** and **7cIII1**) in both of the cell lines with FBS 10 %. For instance, formulation **7bII1** (**7bII**:DOPE, 1:1 molar ratio) showed the highest percent of transfected cells (8.49 and 10.71 % in A549 and HeLa cells respectively). Its efficiency further improved with the incorporation of cholesterol, **7bII1A** (**7bII**:DOPE:cholesterol,1:1:1 molar ratio) resulting into 11.13 and 15.57 % transfected cells in A549 and HeLa cell line respectively in presence of serum 10 %. These results indicated that incorporation of cholesterol improved the serum compatibility of lipoplex.

3.4.7 Intra-cellular trafficking study using confocal microscopy

Confocal microscopy was performed to track the intra-cellular trafficking of lipoplex of GA formulation (**7bIII1A**) showing the best results in the *in-vitro* transfection and FACS studies. The lipoplex was tagged with the green coloured dye by incubation with it overnight. The cells (A549 and HeLA) were treated with tagged formulation in 6-well format. The cells were harvested and fixed at 10, 20 and 30 minute. First row of **Figures 102** and **103** shows control groups of cells without any lipolplex treatment. First two images of each row represent phase contrast images of cells, while the third one is a merged image showing blue stained nucleus and morphology of cells. Second row (**Figures 102** and **103**) shows lipoplex (green colouerd dots) entering into the cytoplasm of the cells after 10 minutes of incubation. Third row (**Figures 102** and **103**) shows the accumulation of lipoplex (green colouerd dots) inside the nuclei of the cells after 20 minutes of incubation. Fourth row (**Figures 102** and **103**) shows further accumulation of of lipoplex (green colouerd dots) inside the nuclei of the cells after 30 minutes of incubation.
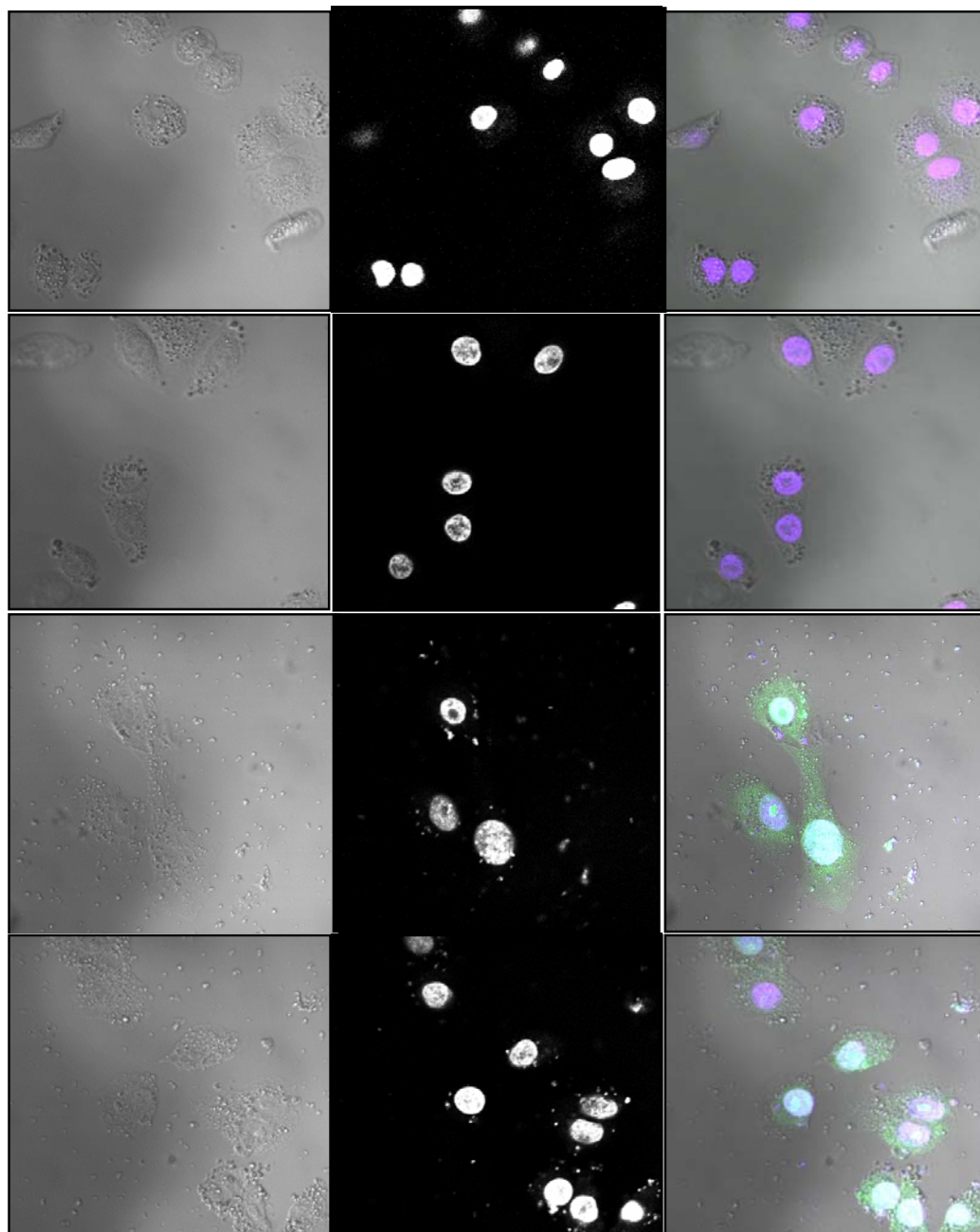
Figure 102. Confocal images for the uptake study in A549 cells; first row control group, second row after 10 minutes, third row after 20 minutes and fourth row after 30 minutes
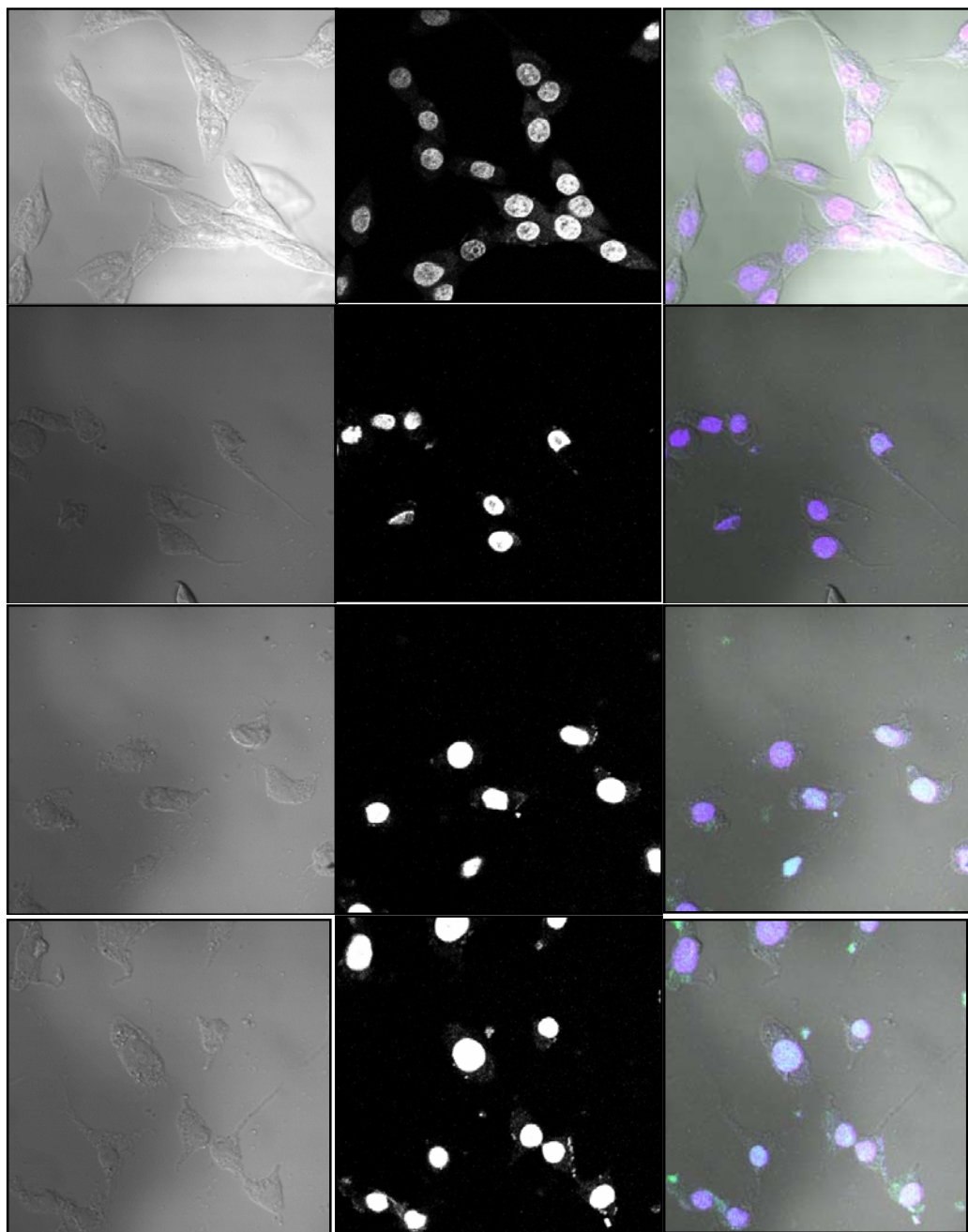
Figure 103. Confocal images for uptake study in HeLa cells; first row control group, second row after 10 minutes, third row after 20 minutes and fourth row after 30 minutes

3.5 *In-vivo* studies

3.5.1 Biodistribution and gamma scintigraphic studies

The lipoplex of the GA formulations showing the best results in the *in vitro* cell line studies were used for biodistribution studies in rats. The radiolabeling of the lipoplex at the optimized N/P ratios were carried out using direct labeling procedure with ^{99m}Tc by simple reduction method of the radioactive pertechnetate using stannous chloride. ^{99m}Tc labelled lipoplexes of **7bII1A** and **7bIII1A** with *p*DNA (15 µg) were injected in the tail vein of rats. The radioactivity in various organs was detected quantitatively at pre-determined time points (1, 6 and 24 hrs) and percent of radioactivity per gram of the tissues was plotted in **Figures 104 and 105.** At initial time point (1 hr) maximum of the lipoplex accumulated in vital organs like liver, spleen, lungs, kidneys etc. With the passage of time (6 hr), the accumulation of lipoplex increased in liver and speen, however it decreased in other organs. After 24 hrs, spleen was found to contain the maximum concentration of lipoplex followed by liver for both of the formulations.

Gamma-scintigraphic studies were performed on rabbits for qualitative assessment of optimized ^{99m}Tc-lebelled lipoplex. The scintigraphic images of ^{99m}Tc labelled lipoplex of **7bII1A** and **7bIII1A** have been shown in **Figure 106** after 1 hr of administration. The images showed the accumulation of ^{99m}Tc-lebelled lipoplex in liver, spleen, lungs and kidneys.
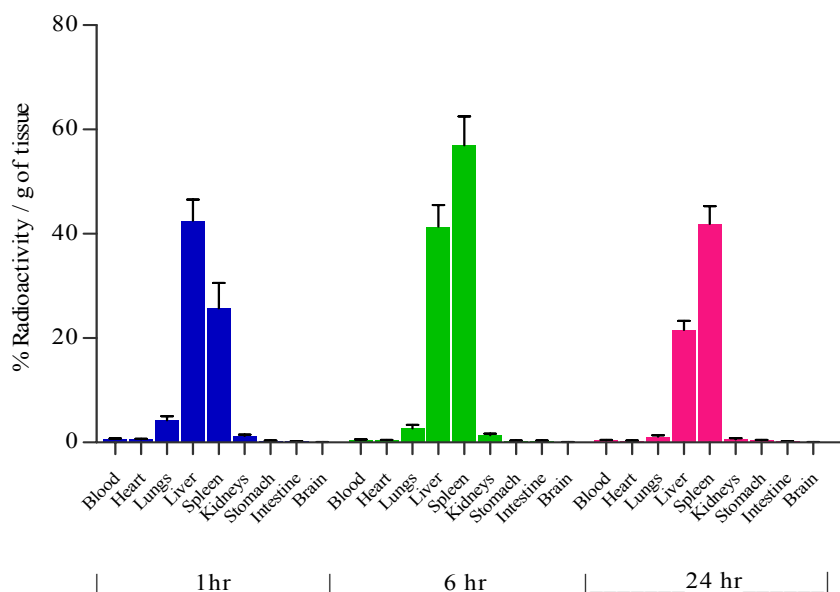
Figure 104. Quantitative biodistribution of ^{99m}Tc labelled **7bII1A** lipolex in

rats

Figure 105. Quantitative biodistribution of ^{99m}Tc labelled **7bIII1A** lipolex in

rats
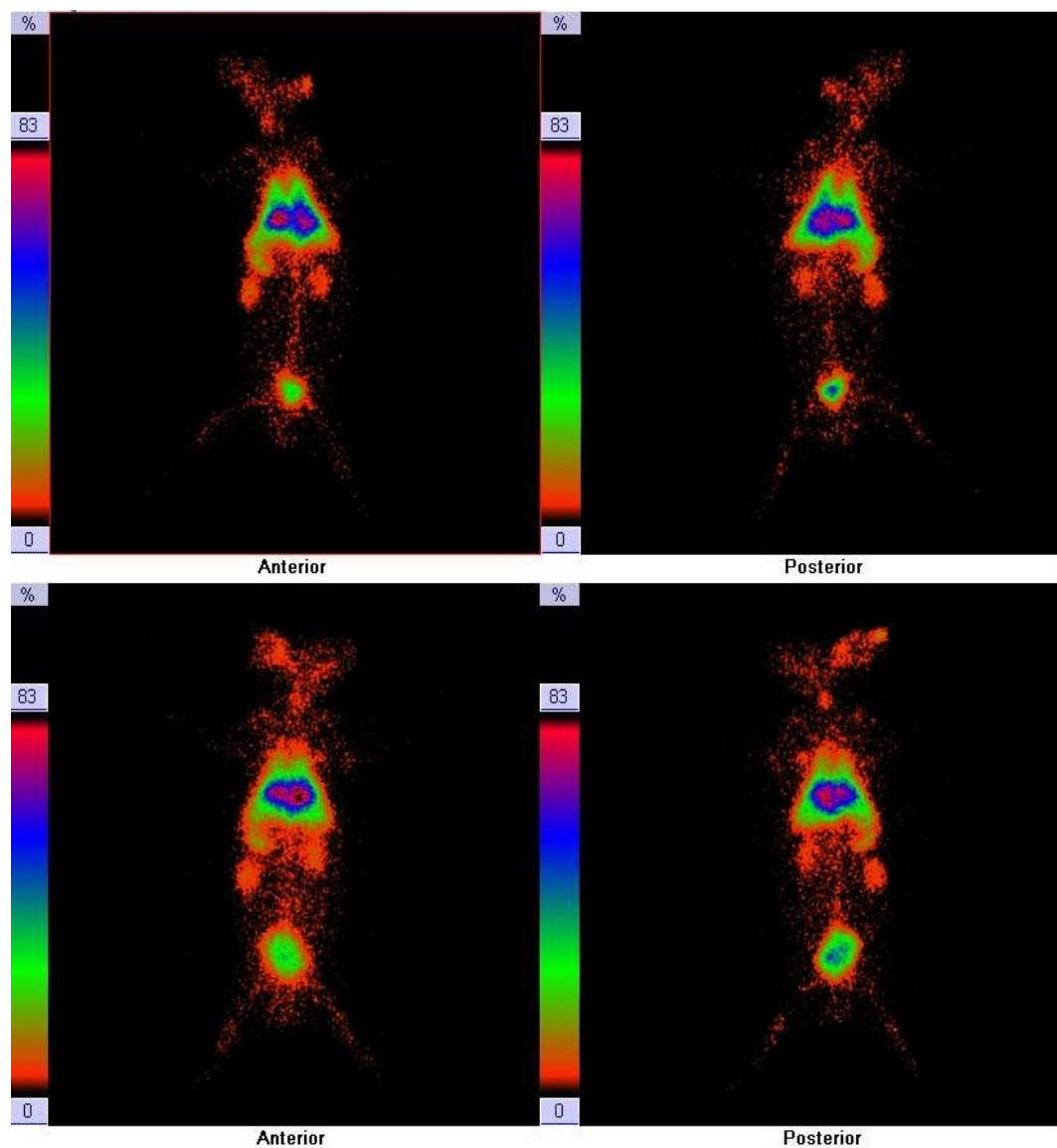
Figure 106. Gamma scintigraphy images of ^{99m}Tc labelled lipoplex administered rabbits; **7bII1A** lipolex (First row – anterior and posterior view), **7bIII1A** lipolex (Second row – anterior and posterior view)

4. EXPERIMENTAL

The experimental work carried out to achieve the aims and objectives of this thesis has been divided into the following heads:

- Synthesis and characterization of gemini amphiphiles
- Formulation development and characterization
- *In vitro* cell line studies
- *In vivo* studies

4.1 Synthesis and characterization of gemini amphiphiles

All the reagents and solvents required for synthesis were purified by general laboratory techniques before use. Melting points were determined using Veego make silicon oil bath-type melting point apparatus and are uncorrected. Purity of the compounds and completion of reactions were monitored by thin layer chromatography (TLC) on silica gel plates (60 F_{254}; Merck), visualizing with iodine vapors. The yields reported here are un-optimized. The IR spectra were recorded using ATR and KBr disc method for liquid and solid samples respectively on a Bruker FT-IR, model alpha. The PMR spectra were recoreded using Bruker 300 MHz spectrometer in dueterated solvents (CDCl$_3$ and DMSO-d$_6$, chemical shifts in δ ppm). Mass spectral data were obtained on a Scientific mass spectrometer (Thermo, DSQ II).

The synthesis of GAs following **Scheme 2** (MEA series) and **3** (DEA series) could be divided into two steps namely; synthesis of tertiary amines and quaternization of tertiary amines; however, **Scheme 1** (DMA series) involved direct quaternization of commercially available tertiary amines.

4.1.1 Synthesis of DMA series of GAs

4.1.1.1   1,4-Di[(*n*-hexadecyldimethylammonium)methyl]benzene dibromide (3I)

The title compound was prepared from *N*-hexadecyl-*N,N*-dimethylamine **(1)** (2.96 mL, 8.8 mmole) and dibromo-*p*-xylene **(2I)** (1.04 g, 4.0 mmole) in dry acetone. The reaction mixture was taken in a sealed tube and heated at ~80 °C for 2-3 days resulting in a white precipitate. The solvent was recovered under vacuum and the precipitate was washed with a mixture of hexane and ethyl acetate or diethyl ether.

The crude so obtained was re-crystallized 3-4 times using a mixture of methanol and ethyl acetate to afford the title product **(3I)** as a white solid (2.2 g, 70 %) (m.p. 237-39 ^{o}C).

Anal.:

> TLC   : 0.5 (10 % MeOH in CHCl$_3$).
>
> IR   : 3126, 1097 cm^{-1}.
>
> PMR   : δ 0.87 (t, 6H), 1.25-1.36 (b m, 52H), 1.67-1.85 (b m, 4H), 3.22 (s, 12H), 3.55 (t, 4H), 5.36 (s, 4H), 7.80 (s, 4H).

4.1.1.2   2,2'-Di(*n*-hexadecyldimethylammonium)ethyl]ether dibromide (3II)

The title compound was prepared from *N*-hexadecyl-*N,N*-dimethylamine **(1)** (2.96 mL, 8.8 mmole) and 2,2'-dibromodiethyl ether **(2II)** (0.51 mL, 4.0 mmole) following the method described for synthesis of compound **(3I)** to afford a white solid of compound **(3II)** (2.0 g, 67 %), (m.p. 243-45 ^{o}C).

Anal.:

> TLC   : 0.4 (10 % MeOH in CHCl$_3$).
>
> IR   : 1139, 1082, 973 cm^{-1}.
>
> PMR   : δ 0.88 (t, 6H), 1.25-1.35 (b m, 52H), 1.72 (b m, 4H), 3.44 (s, 12H), 3.58-3.63 (t, 4H), 4.07 (s, 4H), 4.33 (t, 4H).

4.1.1.3   1,4-Di(*n*-hexadecyldimethylammonium)butane dibromide (3III)

The title compound was prepared from *N*-hexadecyl-*N,N*-dimethylamine **(1)** (2.96 mL, 8.8 mmole) and 1,4-dibromobutane **(2III)** (0.49 mL, 4.0 mmole) following the method described for synthesis of compound **(3I)** to afford compound **(3III)** as white solid (2.2 g, 71 %) (m.p. 232-34 ^{o}C).

Anal.:

> TLC   : 0.4 (10 % MeOH in CHCl$_3$).
>
> IR   : 3353, 1099 cm^{-1}.
>
> PMR   : δ 0.88 (t, 6H), 1.25-1.36 (b m, 52H), 1.77-1.77 (b m, 4H), 2.18 (t, 4H), 3.26 (s, 12H), 3.37-3.42 (t, 4H), 4.00 (t, 4H).

4.1.1.4   1,6-Di(*n*-hexadecyldimethylammonium)hexane dibromide (3IV)

The title compound was prepared from *N*-hexadecyl-*N,N*-dimethylamine **(1)** (2.96 mL, 8.8 mmole) and 1,6-dibromohexane **(2IV)** (0.61 mL, 4.0 mmole) following the method described for synthesis of compound **(3I)** to afford compound **(3IV)** as a white solid (2.1 g, 68 %) (m.p. 238-40 $^{\circ}$C).

Anal.:

TLC   : 0.5 (10 % MeOH in CHCl$_3$).

IR   : 3423, 1099 cm^{-1}.

PMR   : δ 0.88 (t, 6H), 1.25-1.35 (b m, 52H), 1.61-1.72 (b m, 10H), 2.06 (t, 4H), 3.46 (s, 12H), 3.76 (t, 4H).

4.1.2 Synthesis of MEA series of GAs

4.1.2.1 *N*-Dodecyl-*N*-methylethanolamine (6a)

A mixture of *N*-methylethanolamine **(4)** (3.55 mL, 44 mmole), 1-bromododecane **(5a)** (9.67 mL, 40 mmole) and anhydrous sodium carbonate (2.32 g, 22 mmole) in dry ethanol was refluxed under anhydrous conditions for 12-14 hrs. The reaction mixture was cooled to room temperature, filtered, and ethanol was recovered under vacuum resulting in a white crude product. The white crude product so obtained was dissolved in dichloromethane/diethyl ether and washed with brine for 4-5 times. The organic layer was separated, dried over anhydrous sodium sulphate and recovered to obtain the desired product **(6a)** as a yellowish colored liquid (8.9 g, 95 %).

Anal.:

TLC   : R$_f$ 0.65 (10 % MeOH in CHCl$_3$).

IR   : 3393, 1038 cm^{-1}.

4.1.2.2 *N*-Methyl-*N*-tetradecylethanolamine (6b)

The title compound was prepared from *N*-methylethanolamine **(4)** (3.55 mL, 44 mmole), 1-bromotetradecane **(5b)** (10.97 mL, 40 mmole) and anhydrous sodium carbonate (2.32 g, 22 mmole) following the method described for synthesis of compound **(6a)** to afford the tertiary amine **(6b)** as a yellowish colored liquid (10 g, 94 %).

Anal.:

      TLC   : R_f 0.7 (10 % MeOH in CHCl$_3$).

      IR   : 3337, 1038 cm^{-1}.

4.1.2.3 *N*-Hexadecyl-*N*-methylethanolamine (6c)

The title compound was prepared from *N*-methylethanolamine **(4)** (3.55 mL, 44 mmole), 1-bromohexadecane **(5c)** (12.26 mL, 40 mmole) and anhydrous sodium carbonate (2.32 g, 22 mmole) following the method described for synthesis of compound **(6a)** to afford compound **(6c)** as a yellowish colored liquid (11.4 g, 95 %). Anal.:

      TLC   : R_f 0.7 (10 % MeOH in CHCl$_3$).

      IR   : 3386, 1040 cm^{-1}.

4.1.2.4 *N*-Methyl-*N*-octadecylethanolamine (6d)

The title compound was prepared from *N*-methylethanolamine **(4)** (3.55 mL, 44 mmole), 1-bromooctadecane **(5d)** (13.65 mL, 40 mmole) and anhydrous sodium carbonate (2.32 g, 22 mmole) following the method described for synthesis of compound **(6a)** to afford compound **(6d)** as yellowish colored waxy solid (12.3 g, 92 %) (m.p. 58-60 ^{o}C). Anal.:

      TLC   : R_f 0.75 (10 % MeOH in CHCl$_3$).

      IR   : 3337, 1038 cm^{-1}.

4.1.2.5 1,4-Di{[*n*-dodecyl(2-hydroxyethyl)methylammonium]methyl}benzene dibromide (7aI)

The title compound was prepared from *N*-dodecyl-*N*-methylethanolamine **(6a)** (2.16 g, 8.8 mmole) and dibromo-*p*-xylene **(2I)** (1.04 g, 4.0 mmole) in dry acetone. The reaction mixture was taken in a sealed tube and heated at ~80 ^{o}C for 2-3 days resulting in white precipitate. The solvent was recovered under vacuum and the precipitate was washed with mixture of hexane and ethyl acetate or diethyl ether. The crude so obtained was re-crystallized 3-4 times using a mixture of methanol and ethyl acetate to afford the title product **(7aI)** as a white solid (1.8 g, 64 %) (m.p. 216-18 ^{o}C).

Anal.:

TLC : R$_f$ 0.3 (10 % MeOH in CHCl$_3$).

IR : 3311, 1472, 1099, 1038 cm^{-1}.

PMR : δ 0.59 (t, 6H), 0.99 (b m, 36H), 1.53 (m, 4H), 2.72 (s, 6H), 3.076 (t, 4H), 3.173-3.214 (t, 4H), 3.649 (t, 4H), 4.404 (t, 4H), 5.121 (b s, 2H), 7.431 (s, 4H).

4.1.2.6 2,2'-Di{[*n*-dodecyl(2-hydroxyethyl)methylammonium]ethyl}ether dibromide (7aII)

The title compound was prepared from *N*-dodecyl-*N*-methylethanolamine **(6a)** (2.16 g, 8.8 mmole) and 2,2'-dibromodiethyl ether **(2II)** (0.51 mL, 4.0 mM) following the method described for synthesis of compound **(7aI)** to afford the desired product **(7aII)** as a white solid (1.6 g, 58 %) (m.p. 215-18 $^{\circ}$C).

Anal.:

TLC : R$_f$ 0.3 (10 % MeOH in CHCl$_3$).

IR : 3334, 1129, 1082, 1049 cm^{-1}.

PMR : δ 0.85 (t, 6H), 1.25-1.34 (b m, 36H), 1.72 (m, 4H), 3.39 (s, 6H), 3.63(t, 4H), 3.81(t, 4H,), 3.97 (t, 4H), 4.10 (t, 4H), 4.25 (t, 4H), 4.95 (b s, 2H).

4.1.2.7 1,4-Di[*n*-dodecyl(2-hydroxyethyl)methylammonium]butane dibromide (7aIII)

The title compound was prepared from *N*-dodecyl-*N*-methylethanolamine **(6a)** (2.16 g, 8.8 mmole) and 1,4-dibromobutane **(2III)** (0.49 mL, 4.0 mM) following the method described for synthesis of compound **(7aI)** to afford compound **(7aIII)** as a white solid (2.0 g, 70 %) (m.p. 217-19 $^{\circ}$C).

Anal.:

TLC : R$_f$ 0.35 (10 % MeOH in CHCl$_3$).

IR : 3316, 1132, 1045 cm^{-1}.

PMR : δ 0.85 (t, 6H), 1.25-1.34 (b m, 36H), 1.73-2.05 (m, 8H), 3.26 (s, 6H), 3.40 (t, 4H,), 3.62 (t, 4H), 3.78 (t, 4H), 4.09 (t, 4H), 5.08 (b s, 2H).

MS : m/z 621.8, (M$^+$).

4.1.2.8 1,6-Di[*n*-dodecyl(2-hydroxyethyl)methylammonium]hexane dibromide (7aIV)

The title compound was prepared from *N*-dodecyl-*N*-methylethanolamine **(6a)** (2.16 g, 8.8 mmole) and 1,6-dibromohexane **(2IV)** (0.61 mL, 4.0 mM) following the method described for synthesis of compound **(7aI)** to afford the desired product **(7aIV)** as a white solid (1.7 g, 60 %) (m.p. 195-98 $^{\circ}$C).

Anal.:

        TLC   : R$_f$ 0.35 (10 % MeOH in CHCl$_3$).

        IR   : 3299, 1090, 1048 cm^{-1}.

        PMR   : δ 0.85 (t, 6H), 1.25-1.34 (b m, 36H), 1.55-1.70 (m, 8H), 1.93 (m, 4H), 3.29 (s, 6H), 3.47 (t, 4H), 3.62 (t, 4H), 3.70 (t, 4H), 4.09 (t, 4H), 5.06 (b s, 2H).

4.1.2.9 1,4-Di{[(2-hydroxyethyl)methyl-*n*-tetradecylammonium]methyl}benzene dibromide (7bI)

The title compound was prepared from *N*-tetradecyl-*N*-methyl-2-hydroxyethylamine **(6b)** (2.40 g, 8.8 mmole) and dibromo-*p*-xylene **(2I)** (1.04 g, 4.0 mmole) following the method described for synthesis of compound **(7aI)** to afford the product **(7bI)** as a white solid (2.1 g, 67 %) (m.p. 217-19 $^{\circ}$C).

Anal.:

        TLC   : R$_f$ 0.3 (10 % MeOH in CHCl$_3$).

        IR   : 3312, 2994, 1102, 1050 cm^{-1}.

        PMR   : δ 0.88 (t, 6H), 1.25-1.35 (b m, 44H), 1.81(m, 4H), 3.20 (s, 6H), 3.42 (t, 4H), 3.58 (b m, 8H), 4.14 (t, 4H), 5.08 (b s, 2H), 7.77 (s, 4H).

4.1.2.10 2,2'-Di{[(2-hydroxyethyl)methyl-*n*-tetradecylammonium]ethyl}ether dibromide (7bII)

The title compound was prepared from *N*-methyl-*N*-tetradecylethanolamine **(6b)** (2.40 g, 8.8 mmole) and 2,2'-dibromodiethyl ether **(2II)** (0.51 mL, 4.0 mM) following the method described for synthesis of compound **(7aI)** to afford the quaternary product **(7bII)** as a white solid (1.8 g, 60 %) (m.p. 234-36 $^{\circ}$C).

Anal.:

> TLC : R_f 0.3 (10 % MeOH in CHCl$_3$).
>
> IR : 3290, 1132, 1082, 1049 cm^{-1}.
>
> PMR : δ 0.85 (t, 6H), 1.25-1.34 (b m, 44H), 1.71-2.07 (m, 4H), 3.39 (s, 6H), 3.63 (t, 4H), 3.81(t, 4H), 3.98 (t, 4H), 4.10 (t, 4H), 4.25 (t, 4H), 4.97 (b s, 2H).

4.1.2.11   1,4-Di[(2-hydroxyethyl)methyl-*n*-tetradecylammonium]butane dibromide (7bIII)

The title compound was prepared from *N*-methyl-*N*-tetradecylethanolamine **(6b)** (2.40 g, 8.8 mmole) and 1,4-dibromobutane **(2III)** (0.49 mL, 4.0 mmole) following the method described for synthesis of compound **(7aI)** to afford the product **(7bII)** as a white solid (2.2 g, 72 %) (m.p. 231-33 °C).

Anal.:

> TLC : R_f 0.35 (10 % MeOH in CHCl$_3$).
>
> IR : 3352, 1132, 1045 cm^{-1}.
>
> PMR : δ 0.86 (t, 6H), 1.25-1.35 (b m, 44H), 1.75-2.07 (m, 8H), 3.27 (s, 6H), 3.44 (t, 4H), 3.63 (t, 4H), 3.79 (t, 4H), 4.10 (t, 4H), 5.07 (b s, 2H).

4.1.2.12   1,6-Di[(2-hydroxyethyl)methyl-*n*-tetradecylammonium]hexane dibromide (7bIV)

The title compound was prepared from *N*-methyl-*N*-tetradecylethanolamine **(6b)** (2.40 g, 8.8 mmole) and 1,4-dibromohexane **(2IV)** (0.61 mL, 4.0 mmole) following the method described for synthesis of compound **(7aI)** to afford the compound **(7bIV)** as a white solid (2.0 g, 65 %) (m.p. 231-33°C).

Anal.:

> TLC : R_f 0.35 (10 % MeOH in CHCl$_3$).
>
> IR : 3286, 1090, 1056 cm^{-1}.
>
> PMR : δ 0.88 (t, 6H), 1.25-1.34 (b m, 44H), 1.56 (m, 4H), 1.71 (m, 4H), 1.98 (t, 4H) 3.29 (s, 6H), 3.48 (t, 4H), 3.67-3.76 (t, 4H), 4.09 (t, 4H), 5.06 (b s, 2H).

4.1.2.13 1,4-Di{[(*n*-hexadecyl(2-hydroxyethyl)methylammonium]methyl}benz-ene dibromide (7cI)

The title compound was prepared from *N*-hexadecyl-*N*-methylethanolamine **(6c)** (2.64 g, 8.8 mmole) and dibromo-*p*-xylene **(2I)** (1.04 g, 4.0 mmole) following the method described for synthesis of compound **(7aI)** to afford the product **(7cI)** as a white solid (2.0 g, 60 %) (m.p. 217-19 ^{o}C).

Anal.:

    TLC   : R$_f$ 0.35 (10 % MeOH in CHCl$_3$).
    IR   : 3310, 2997, 1099, 1048 cm^{-1}.
    PMR   : δ 0.85 (t, 6H), 1.22 (b m, 52H), 1.77-2.08 (m, 4H), 2.96 (s, 6H), 3.30
            (b t, 8H), 3.88 (t, 4H), 4.63 (t, 4H), 5.35 (b s, 2H), 7.67 (s, 4H).

4.1.2.14 2,2'-Di{[(*n*-hexadecyl(2-hydroxyethyl)methylammonium]ethyl}ether di-bromide (7cII)

The title compound was prepared from *N*-hexadecyl-*N*-methylethanolamine **(6c)** (2.64 g, 8.8 mmole) and 2,2'-dibromodiethyl ether **(2II)** (0.51 mL, 4.0 mM) following the method described for synthesis of compound **(7aI)** to afford the product **(7cII)** as a white solid (2.2 g, 66 %) (m.p. 227-29°C).

Anal.:

    TLC   : R$_f$ 0.35 (10 % MeOH in CHCl$_3$).
    IR   : 3322, 1132, 1082, 1049 cm^{-1}.
    PMR   : δ 0.88 (t, 6H), 1.25-1.34 (b m, 52H), 1.71 (m, 4H), 2.08 (t, 4H), 3.39
            (s, 6H), 3.62 (t, 4H), 3.81(t, 4H), 4.09 (t, 4H), 4.25 (t, 4H), 4.98 (b s,
            2H).

4.1.2.15 1,4-Di[*n*-hexadecyl(2-hydroxyethyl)methylammonium]butane dibromide (7cIII)

The title compound was prepared from *N*-hexadecyl-*N*-methylethanolamine **(6c)** (2.64 g, 8.8 mmole) and 1,4-dibromobutane **(2III)** (0.49 mL, 4.0 mmole) following the method described for synthesis of compound **(7aI)** to afford the product **(7cIII)** as a white solid (2.1 g, 65 %) (m.p. 223-25 ^{o}C).

Anal.:

      TLC   : R_f 0.4 (10 % MeOH in CHCl$_3$)

      IR   : 3318, 1087, 1046 cm^{-1}

      PMR : δ 0.85 (t, 6H), 1.25-1.35 (b m, 52H), 1.74-2.05 (m, 8H), 3.26 (s, 6H),

               3.40 (t, 4H), 3.61(t, 4H), 3.82 (t, 4H), 4.10 (t, 4H), 5.08 (b s, 2H).

      MS   : m/z, 735.9 (M$^+$).

4.1.2.16 1,6-Di[(*n*-hexadecyl(2-hydroxyethyl)methylammonium]hexane dibromide (7cIV)

The title compound was prepared from *N*-hexadecyl-*N*-methylethanolamine **(6c)** (2.64 g, 8.8 mmole) and 1,4-dibromohexane **(2IV)** (0.61 mL, 4.0 mmole) following the method described for synthesis of compound **(7aI)** to afford the product **(7cIV)** as a white solid (2.0 g, 62 %) (m.p. 228-30 $^{\circ}$C).

Anal.:

      TLC   : R_f 0.4 (10 % MeOH in CHCl$_3$).

      IR   : 3290, 1090, 1048 cm^{-1}.

      PMR : δ 0.85 (t, 6H), 1.25-1.34 (b m, 52H), 1.56-1.71 (m, 8H), 1.97 (m, 4H),

               3.29 (s, 6H), 3.49 (t, 4H), 3.71 (b t, 8H), 4.10 (t, 4H), 5.07 (b s, 2H).

4.1.2.17 1,4-Di{[(2-hydroxyethyl)methyl-*n*-octadecylammonium]methyl}benzene dibromide (7dI)

The title compound was prepared from *N*-methyl-*N*-octadecylethanolamine **(6d)** (2.88 g, 8.8 mmole) and dibromo-*p*-xylene **(2I)** (1.04 g, 4.0 mmole) following the method described for synthesis of compound **(7aI)** to afford the product **(7dI)** as a white solid (2.3 g, 66 %) (m.p. 218-20 $^{\circ}$C).

Anal.:

      TLC   : R_f 0.4 (10 % MeOH in CHCl$_3$).

      IR   : 3312, 2997, 1099, 1049 cm^{-1}.

      PMR : δ 0.85 (t, 6H), 1.25-1.37 (b m, 60H), 1.67 (m, 4H), 3.20 (s, 6H), 3.58-

               3.60 (b t, 8H), 4.09 (t, 4H), 4.90 (t, 4H), 5.30 (b s, 2H), 7.8 (s, 4H).

4.1.2.18 2,2'-Di{[(2-hydroxyethyl)methyl-*n*-octadecylammonium]ethyl}ether di-bromide (7dII)

The title compound was prepared from *N*-methyl-*N*-octadecylethanolamine **(6d)** (2.88 g, 8.8 mmole) and 2,2'-dibromodiethyl ether **(2II)** (0.51 mL, 4.0 mM) following the method described for synthesis of compound **(7aI)** to afford **(7dII)** as a white solid (2.0 g, 56 %) (m.p. 224-26 $^{\circ}$C).

Anal.:

      TLC   : R_f 0.4 (10 % MeOH in CHCl$_3$).

      IR   : 3323, 1132, 1082, 1049 cm^{-1}.

      PMR : δ 0.85 (t, 6H), 1.25-1.35 (b m, 60H), 1.71 (m, 4H), 1.99 (t, 4H), 3.39 (s, 6H), 3.63(t, 4H), 3.81(t, 4H), 4.10 (t, 4H), 4.26 (t, 4H), 4.95 (b s, 2H).

4.1.2.19 1,4-Di[(2-hydroxyethyl)methyl-*n*-octadecylammonium]butane dibromide (7dIII)

The title compound was prepared from *N*-methyl-*N*-octadecylethanolamine **(6d)** (2.88 g, 8.8 mmole) and 1,4-dibromobutane **(2III)** (0.49 mL, 4.0 mmole) following the method described for synthesis of compound **(7aI)** to afford **(7dIII)** as a white solid (2.3 g, 65 %) (m.p. 230-32°C).

Anal.:

      TLC   : R_f 0.4 (10 % MeOH in CHCl$_3$).

      IR   : 3223, 1092, 1048 cm^{-1}.

      PMR : δ 0.85 (t, 6H), 1.25-1.35 (b m, 60H), 1.75-2.11 (m, 8H), 3.24 (s, 6H), 3.42 (t, 4H), 3.58 (t, 4H), 3.89 (t, 4H), 4.10 (t, 4H), 5.05 (b s, 2H).

4.1.2.20 1,6-Di[(-2-hydroxyethyl)methyl-*n*-octadecylammonium)]hexane dibro-mide (7dIV)

The title compound was prepared from *N*-methyl-*N*-octadecylethanolamine **(6d)** (2.88 g, 8.8 mmole) and 1,4-dibromohexane **(2IV)** (0.61 mL, 4.0 mmole) following the method described for synthesis of compound **(7aI)** to afford **(7dIV)** as a white solid (2.2 g, 61 %) (m.p. 230-32 $^{\circ}$C).

Anal.:

> TLC : R$_f$ 0.45 (10 % MeOH in CHCl$_3$).

> IR : 3289, 1090, 1048 cm^{-1}.

> PMR : δ 0.85 (t, 6H), 1.25-1.35 (b m, 60H), 1.56-1.73 (m, 8H), 1.98 (t, 4H), 3.28 (s, 6H), 3.46 (t, 4H,), 3.71(b t, 8H), 4.10 (t, 4H), 5.04 (b s, 2H).

4.1.3 Synthesis of DEA series of GAs

4.1.3.1 *N*-Dodecyl-*N*,*N*-di(2-hydroxyethyl)amine (9a)

A mixture of diethanolamine **(8)** (4.23 mL, 44 mmole), 1-bromododecane **(5a)** (9.7 mL, 40 mM) and anhydrous sodium carbonate (2.32 g, 22 mmole) in dry ethanol was refluxed under anhydrous conditions for 16-18 hrs. The reaction mixture was cooled to room temperature, filtered and the solvent removed under vacuum resulting in a white crude product. The white crude product was then dissolved in dichloromethane/diethyl ether and washed with brine for 4-5 times. The organic layer was dried over anhydrous sodium sulphate and recovered to obtain the desired product **(9a)** as a yellowish colored liquid (9.9 g, 94 %).

Anal.:

> TLC : 0.55 (10 % MeOH in CHCl$_3$).

> IR : 3337, 1150, 1041cm^{-1}.

4.1.3.2 *N*,*N*-Di(2-hydroxyethyl)-*N*-tetradecylamine (9b)

The title compound was prepared from diethanolamine **(8)** (4.23 mL, 44 mmole), 1-bromotetradecane **(5b)** (10.97 mL, 40 mmole) and anhydrous sodium carbonate (2.32 g, 22 mmole) following the method described for synthesis of compound **(9a)** to afford the tertiary amine **(9b)** as a yellowish colored liquid (10.6 g, 90 %).

Anal.:

> TLC : R$_f$ 0.60 (10 % MeOH in CHCl$_3$).

> IR : 3346, 1150, 1043 cm^{-1}.

4.1.3.3 *N,N*-Di(2-hydroxyethyl)-*N*-hexadecylamine (9c)

The title compound was prepared from diethanolamine **(8)** (4.23 mL, 44 mmole), 1-bromohexadecane **(5c)** (12.26 mL, 40 mmole) and anhydrous sodium carbonate (2.32 g, 22 mmole) following the method described for synthesis of compound **(9a)** to afford the desired tertiary amine **(9c)** as a yellowish colored waxy solid (11.8 g, 90 %) (m.p. 54-56 $^{\circ}$C).

Anal.:

      TLC   : R_f 0.65 (10 % MeOH in CHCl$_3$).

      IR   : 3342, 1150, 1044 cm^{-1}.

4.1.3.4 *N,N*-Di(2-hydroxyethyl)-*N*-octadecylamine (9d)

The title compound was prepared from diethanolamine **(8)** (4.23 mL, 44 mmole), 1-bromooctadecane **(5d)** (13.65 mL, 40 mmole) and anhydrous sodium carbonate (2.32 g, 22 mmole) following the method described for synthesis of compound **(9a)** to afford the desired tertiary amine **(9d)** as a yellowish colored waxy solid (13 g, 90 %) (m.p. 60-62 $^{\circ}$C).

Anal.:

      TLC   : R_f 0.7 (10 % MeOH in CHCl$_3$).

      IR   : 3377, 1150, 1043 cm^{-1}.

4.1.3.5 1,4-Di{[(*n*-dodecyl di(2-dihydroxyethyl)ammonium]methyl}benzene dib-romide (10aI)

The title compound was prepared from *N*-dodecyl-*N,N*-di(2-hydroxyethyl)amine **(9a)** (2.4 g, 8.8 mmole) and dibromo-*p*-xylene **(2I)** (1.04 g, 4.0 mmole) in acetone. The reaction mixture was taken in a sealed tube and heated at ~100 $^{\circ}$C for 2-3 days resulted in white precipitate. The solvent was removed under vacuum and the precipitate so obtained was washed with a mixture of hexane and ethyl acetate or diethyl ether. The crude so obtained was re-crystallized 3-4 times using a mixture of methanol and ethyl acetate to afford the product **(10aI)** as a white solid (1.9 g, 65 %) (208-10 $^{\circ}$C).

Anal.:

      TLC   : 0.25 (10 % MeOH in CHCl$_3$)

IR : 3409, 3114, 1099, 1046 cm^{-1}.

PMR : δ 0.924 (t, 6H), 1.319 (b m, 36H), 1.877 (m, 4H), 3.301 (t, 4H), 3.402-3.444 (b t, 8H), 4.005 (b t, 8H), 4.813 (s, 4H), 5.466 (b s, 4H), 7.762 (s, 4H).

4.1.3.6   1,4-Di[*n*-dodecyldi(2-dihydroxyethyl)ammonium]butane dibromide (10aIII)

The title compound was prepared from *N*-dodecyl-*N,N*-di(2-hydroxyethyl)amine **(9a)** (2.4 g, 8.8 mmole) and 1,4-dibromobutane **(2III)** (0.49 mL, 4.0 mmole) following the method described for synthesis of compound **(10aI)** to afford the desired product **(10aIII)** as a white solid (1.8 g, 62 %) (m.p. 160-62 $^{\mathrm{o}}$C).
Anal.:

TLC : 0.25 (10% MeOH in CHCl$_3$)

IR : 3338, 1071, 1037 cm^{-1}.

PMR : δ 0.85 (t, 6H), 1.25 (b m, 36H), 1.67 (b m, 8H), 3.34 (b t, 8H), 3.42 (b t, 8H), 3.8 (b t, 8H), 5.21 (b s, 4H).

4.1.3.7   1,4-Di{[di(2-dihydroxyethyl)-*n*-tetradecyl-ammonium]methyl}benene dibromide (10bI)

The title compound was prepared from *N,N*-di(2-hydroxyethyl)-*N*-tetradecylamine **(9b)** (2.64 g, 8.8 mmole) and dibromo-*p*-xylene **(2I)** (1.04 g, 4.0 mmole) following the method described for synthesis of compound **(10aI)** to afford the desired product **(10bI)** as a white solid (2.2 g, 66 %) (m.p. 207-09 $^{\mathrm{o}}$C).
Anal.:

TLC : R$_f$ 0.3 (10 % MeOH in CHCl$_3$).

IR : 3388, 3109, 1099, 1047 cm^{-1}.

PMR : δ 0.85 (t, 6H), 1.25 (b m, 44H), 1.80 (m, 4H), 3.39 (t, 8H), 3.92 (b t, 8H), 4.74 (b t, 8H), 5.36 (b s, 4H), 7.69 (s, 4H).

4.1.3.8   2,2'-Di{[di(2-dihydroxyethyl)-*n*-tetradecylammonium]ethyl}ether dibromide (10bII)

The title compound was prepared from *N,N*-di(2-hydroxyethyl)-*N*-tetradecylamine **(9b)** (2.64 g, 8.8 mmole) and 2,2'-dibromodiethyl ether **(2II)** (0.51

mL, 4.0 mmole) following the method described for synthesis of compound **(10aI)** to afford the desired product**(10bII)** as a white solid (2.1 g, 62 %) (m.p. 218-20). Anal.:

      TLC   : 0.3 (10 % MeOH in CHCl$_3$).

      IR   : 3300, 1103, 1076, 978 cm^{-1}.

      PMR : δ 0.85 (t, 6H), 1.22 (b m, 44H), 1.71 (b t, 4H), 3.59 (t, 4H), 3.78-3.91 (b m, 12H), 4.08-4.17 (b m, 12H), 4.82 (b s, 4H).

4.1.3.9   1,4-Di[di(2-hydroxyethyl)-*n*-tetradecylammonium]butane dibromide (10bIII)

The title compound was prepared from *N,N*-di(2-hydroxyethyl)-*N*-tetradecylamine **(9b)** (2.64 g, 8.8 mmole) and 1,4-dibromobutane **(2III)** (0.49 mL, 4.0 mmole) following the method described for synthesis of compound **(10aI)** to afford the desired product **(10bIII)** as a white solid (1.9 g, 58 %) (m.p 223-25 $^{\circ}$C). Anal.:

      TLC   : 0.3 (10 % MeOH in CHCl$_3$).

      IR   : 3337, 1071, 1036 cm^{-1}.

      PMR : δ 0.85 (t, 6H), 1.25 (b m, 44H), 1.67 (b m, 8H), 3.28 (b t, 8H), 3.42 (b t, 8H), 3.8 (b t, 8H), 5.23 (b s, 4H).

4.1.3.10 1,6-Di[di(2-dihydroxyethyl)-*n*-tetradecylammonium]hexane dibromide (10bIV)

The title compound was prepared from *N,N*-di(2-hydroxyethyl)-*N*-tetradecylamine **(9b)** (2.64 g, 8.8 mmole) and 1,4-dibromohexane **(2IV)** (0.61 mL, 4.0 mmole) following the method described for synthesis of compound **(10aI)** to afford the desired compound **(10bIV)** as a white solid (1.9 g, 60 %) (m.p 229-31 $^{\circ}$C). Anal.:

      TLC   : 0.3 (10 % MeOH in CHCl$_3$).

      IR   : 3224, 1071, 1049 cm^{-1}.

      PMR : δ 0.85 (t, 6H), 1.16-1.34 (b m, 44H), 1.53 (m, 4H), 1.66 (b m, 8H), 3.37-3.70 (b m, 16H), 4.07 (b t, 8H), 4.97 (b s, 4H).

4.1.3.11   1,4-Di{[*n*-hexadecyldi(2-dihydroxyethyl)ammonium]methyl}benzene

dibromide (10cI)

The title compound was prepared from *N,N*-di(2-hydroxyethyl)-*N*-hexadecylamine **(9c)** (2.92 g, 8.8 mmole) and dibromo-*p*-xylene **(2I)** (1.04 g, 4.0 mmole) following the method described for synthesis of compound **(10aI)** to afford the desired compound **(10cI)** as a white solid (2.5 g, 62 %) (m.p. 210-12 $^{\circ}$C).

Anal.:

   TLC   : R$_f$ 0.3 (10 % MeOH in CHCl$_3$).

   IR   : 3384, 3108, 1096, 1049 cm^{-1}.

   PMR   : δ 0.83 (t, 6H), 1.22 (b m, 52H), 1.81 (m, 4H), 3.20 (t, 4H), 3.31 (b t, 8H, 3.92 (b t, 8H,) 4.72 (s, 4H), 5.38 (b s, 4H), 7.67 (s, 4H).

4.1.3.12   2,2'-Di{[*n*-hexadecyldi(2-hydroxyethyl)ammonium]ethyl}ether dibrom-

ide (10cIII)

The title compound was prepared from *N,N*-di(2-hydroxyethyl)-*N*-hexadecylamine **(9c)** (2.92 g, 8.8 mmole) and 1,4-dibromobutane **(2III)** (0.49 mL, 4.0 mmole) following the method described for synthesis of compound **(10aI)** to afford the desired compound **(10cIII)** as a white solid (2.3 g, 67 %) (m.p. 228-30 $^{\circ}$C).

Anal.:

   TLC   : 0.3 (10 % MeOH in CHCl$_3$).

   IR   : 3335, 1098, 1068 cm^{-1}.

   PMR   : δ 0.88 (t, 6H), 1.07-1.26 (b m, 52H), 1.70-1.84 (b m, 8H), 3.35 (b t, 8H), 3.52 (b t, 8H), 3.91(b t, 8H), 5.26 (b s, 4H).

4.1.3.13   1,6-Dis[*n*-hexadecyldi(2-dihydroxyethyl)ammonium]hexane dibromide

(10cIV)

The title compound was prepared from *N,N*-di(2-hydroxyethyl)-*N*-hexadecylamine **(9c)** (2.92 g, 8.8 mmole) and 1,4-dibromohexane **(2IV)** (0.61, 4.0 mmole) following the method described for synthesis of compound **(10aI)** to afford the desired compound **(10cIV)** as a white solid (2.0 g, 57 %) (m.p 229-31 $^{\circ}$C).

Anal.:

   TLC   : 0.3 (10 % MeOH in CHCl$_3$).

IR   : 3308, 1071, 1044 cm^{-1}.

PMR   : δ 0.85 (t, 6H), 1.24 (b m, 56H), 1.66 (m, 8H), 3.33 (b m, 8H), 3.42 (b m, 8H), 3.8 (b t, 8H), 5.10 (b s, 4H).

4.1.3.14   1,4-Di{[di(2-hydroxyethyl)-*n*-octadecylammonium]methyl}benzene dibromide (10dI)

The title compound was prepared from *N,N*-di(2-hydroxyethyl)-*N*-octadecylamine **(9d)** (3.16 g, 8.8 mmole) and dibromo-*p*-xylene **(2I)** (1.04 g, 4.0 mmole) following the method described for synthesis of compound **(10aI)** to afford the desired compound **(10dI)** as a white solid (2.6 g, 69 %) (m.p. 224-26 °C).

Anal.:

TLC   : R$_f$ 0.5 (10 % MeOH in CHCl$_3$).

IR   : 3313, 1096, 1049 cm^{-1}.

PMR   : δ 0.85 (t, 6H), 1.23 (b m, 60H), 1.78 (m, 4H), 3.12-3.33 (b m, 16H), 3.91-4.64 (b t, 8H), 7.67 (b s, 4H).

4.1.3.15   2,2'-Di{[di(2-dihydroxyethyl)-*n*-octadecylammonium]ethyl}ether dibromide (10dII)

The title compound was prepared from *N,N*-di(2-hydroxyethyl)-*N*-octadecylamine **(9d)** (3.16 g, 8.8 mmole) and 2,2'-dibromodiethyl ether **(2II)** (0.51 mL, 4.0 mmole) following the method described for synthesis of compound **(10aI)** to afford the desired compound **(10dII)** as a white solid (2.1 g, 56 %) (m.p. 226-28 °C).

Anal.:

TLC   : 0.5 (10 % MeOH in CHCl$_3$).

IR   : 3300, 1105, 1074, 978 cm^{-1}.

PMR   : δ 0.85 (t, 6H), 1.23-1.65 (b m, 60H), 3.27-3.37 (b t, 8H), 3.49 (t, 8H), 3.64 (b m, 4H), 3.80 (b m, 12H), 5.28 (b s, 4H).

4.2 Studies related to reporter plasmid DNA

4.2.1 Bacterial transformation; isolation and purification of plasmid DNA

4.2.1.1 Transformation of plasmid DNA using Transform Aid™ bacterial transformation kit (Fermentas)

(A) Materials

Bacterial Strain: *Escherichia coli* strain (*E.coli* DH5α)

Solutions: TransformAid™ Bacterial Transformation Kit containing C medium, T
     solution-A and T solution-B.

Media: Sterile Luria broth (LB) for initial growth of culture (LB 2 % w/v in water)
     Sterile Luria broth (2 % w/v in water) with antibiotic (ampicillin, 100 μg/mL)
     Sterile Luria broth agar plates (LB 2 % w/v and agar 1.5 % w/v in water)
     Sterile Luria broth agar plates (LB 2 % w/v and Agar 1.5 % w/v in water)
     with antibiotic (ampicillin, 100 μg/mL)

Nucleic Acid: Recombinant Plasmid DNA (pDNA) constructs, *pCMV-SPORT-β-gal*
     (7.8 kb)

(B) Method

1. To the lyophilized powder containing bacterial strain, autoclaved sterile LB (0.5 mL) was added aseptically in laminar air flow, mixed the contents thoroughly and spread the loopful of solution on LB agar plate.

2. An LB plate was seeded with a single bacterial colony using the streak plate method and incubated it overnight at 37 °C.

3. Culture tubes containing C medium (1.5 mL) were pre-warmed at 37 °C for at least 20 min before the transformation.

4. LB antibiotic agar plates were pre-warmed at 37 °C in incubator for 20 min before plating.

5. T-Solution (A) and T-solution (B) were thawed and the contents were mixed thoroughly. T-solution (A) (250 μL) and T-solution (B) (250 μL) were withdrawn in separate tubes and kept on ice.

6. A portion of freshly streaked bacterial culture (4 x 4 mm size) was transferred to pre-warmed C-medium (1.5 mL) using an inoculating loop. Cells were suspended by mixing gently and the tubes were incubated at 37 °C for 2 hrs in a shaker.

7. Bacterial cells were pelletized by centrifugation at 10000 rpm, 4 °C for 1 min (Sigma Centrifuge) and the supernatant was discarded.

8. Pelletized cells were resuspended in T-solution (300 μL) and incubated on ice for 5 min.

9. The suspension was centrifuged at 10,000 rpm, 4 °C for 1 min and the supernatant was discarded.

10. Pelleted cells were resuspended in T-solution (120 µL) and incubated on ice for 5 min. (**Note: After addition of T solution, in step 10, the cells become competent)**

11. Supercoiled DNA (1 µL) (10-100 pg) was added up into new micro-centrifuge tubes and chilled on ice for 2 min.

12. The prepared competent cells (50 µL) were added to each tube containing DNA, mixed the contents and incubated the tubes on ice for 5 min.

13. The prepared competent cells (10 µL) (from step 10) were added to an LB agar plate as a positive and negative control.

14. The above solutions were immediately plated on pre-warmed LB antibiotic agar plates and incubated overnight at 37 °C.

15. The plates used were of the following types:

     Positive Control: Prepared competent cells grown on LB plate without addition of antibiotic.

     Negative Control: Prepared competent cells grown on LB plate containing antibiotic.

     Plasmid Transformation Plate: Plasmid incorporated competent cells grown on LB plate containing antibiotic.

(C) Maintenance of bacterial cells containing plasmids

1. Transformed cell colonies were selected and cultured on LB agar plate with appropriate antibiotic (ampicillin).

2. Glycerol stock solution of the bacterial cells were prepared by pelletization of the bacteria cells and stored in sterile Water: Glycerol (1:1) at -70 °C.

3. Working cell culture plates containing transformed bacterial cells were further used for plasmid isolation with every 15 days sub-culturing.

Transformed cells were selected and isolated by culturing the cells on appropriate antibiotic plate as the transformed bacterial cells were resistant to antibiotic. Pure culture of *E.coli* containing plasmid *β*-gal was stored as glycerol stock and working plates were used for the regular plasmid isolation experiments.

4.2.1.2 Plasmid isolation and purification (*Alkaline lysis method*) [193, 194]

(A) Materials

(a) Buffers and solutions

- **Tris-HCl (1 M):** Tris base (121.1 g) was dissolved in distilled water (800 mL) and its *p*H was adjusted to 8.0 by adding concentrated HCl (42 mL). Final *p*H was adjusted and the volume was made up with water to 1.0 L and sterilized by autoclaving.

- **EDTA (0.5 M; *p*H 8.0):** Disodium EDTA. $2H_2O$ (186.1 g) was dissolved in distilled water (800 mL) with vigorous stirring on a magnetic stirrer, its *p*H was adjusted to 8.0 with sodium hydroxide solution (10 %) and the final volume was made upto 1.0 L with distilled water. Finally, the solution was sterilized by autoclaving.

- **NaCl (1 M):** Sodium chloride (58.4 g) was dissolved in distilled water (900 mL) with vigorous shaking, the final volume was made up with water to 1.0 L and the solution was sterilized by autoclaving.

- **10X Tris-EDTA (TE):** Tris-HCl (100 mM) (*p*H 8.0) and EDTA (10 mM) (*p*H 8.0) were prepared in distilled water, sterilized by autoclaving and stored at room temperature.

- **10X Sodium chloride–Tris–EDTA (STE) buffer (*p*H 7.4):** Tris-HCl (100 mM) (*p*H 8.0), EDTA (10 mM) (*p*H 8.0) and NaCl (1 M) in distilled water was prepared and sterilized by autoclaving and stored at room temperature.

- **Alkaline lysis I:** Tris-Cl (25 mM) (*p*H 8.0), EDTA (10 mM) (*p*H 8.0) and glucose (50 mM) in distilled water was prepared and sterilized by autoclaving and stored at 4 °C.

- **Alkaline lysis II:** NaOH (0.2 M) and sodium lauryl sulphate (1 % w/v) in freshly autoclaved water was prepared and the remaining solution was discarded after use.

- **Potassium acetate (5 M):** Potassium acetate (490.5 g) was dissolved in autoclaved water (500 mL) and the volume was made to 1 L and stored at 4 °C.

- **Alkaline lysis III:** Potassium acetate (60 mL, 5 M) and glacial acetic acid (11.5 mL) were mixed and the volume was made to 100 mL with autoclaved water and stored at 4 ^{o}C.

- **50X Tris-Acetate-EDTA buffer (TAE):** Tris base (242 g) was dissolved in autoclaved water (500 mL) and mixed with EDTA (100 mL, 0.5 M) (*p*H 8.0) and glacial acetic acid (37.1 mL) and the volume was made to 1.0 L with autoclaved water and stored at 4 ^{o}C.

- **Tris saturated phenol (*p*H 8):** Crystalline phenol (500 g) was melted, mixed with hydroxyquonoline (0.1 %) and vacuum distilled. This distilled phenol (200 g) was stored in dark container with tight closure. The phenol for DNA purification was prepared by equilibrating the distilled pure phenol with Tris Buffer (200 mL, *p*H 10.0) for 2 times followed by equilibration with Tris buffer (*p*H 8.0), until *p*H of phenol reached to 8.0. The liquid phenol was kept under the layer of Tris buffer till further used.

- **Phenol-Chloroform-Isoamyl alcohol:** The solution was freshly prepared by mixing phenol: chloroform: isoamyl alcohol in the ratio of 25:24:1 (v/v) to purify the pDNA from soluble proteins and chromosomal DNA.

- **Ethidium bromide:** Ethidium bromide (10 mg) was dissolved in sterile distilled water (1.0 mL). The solution was stored in eppendorf tube covered by aluminum foil in cool and dark place.

- **Gel loading dye (Bromophenol blue):** The gel loading dye was prepared by dissolving bromophenol blue (0.25 % w/v) in glycerol (30 % v/v) in water.

- **Tris (10 mM, *p*H 8.0):** Tris buffer (1 M, 1 mL) was diluted to 100 mL with sterile water with *p*H maintained to 8.0.

- **Ethanol (70 %):** Absolute ethanol diluted to 70 % v/v using distilled water.

- **Lithium chloride (5 M):** LiCl (21.2 g) was dissolved in water (100 mL), sterilized by passing it through a 0.22 μm filter and stored at 4 °C.

- **Polyethylene glycol 8000 (PEG 8000) (% w/v):** Appropriate concentration of PEG 8000 was dissolved in sterile water with warming if necessary. Sterilized by passing it through a 0.22 μm filter and the solution was stored at room temperature.

- **Sodium acetate (3 M):** Sodium acetate.trihydrate (408.3 g) was dissolved in water (800 mL) and *p*H was adjusted to 5.2 with glacial acetic acid or to *p*H 7.0 with dilute acetic acid. Final volume of the solution was adjusted to 1 L by distilled water and sterilized by autoclaving.

- **Lysozyme (10 mg/mL):** Lysozyme solution (10 mg/mL) was prepared in Tris-HCl buffer (10 mM, *p*H 8.0). The solution was freshly prepared before use.

- **DNase-free RNase-A (1 mg/mL)**: DNase-freeRNase-A solution (1 mg/mL) was prepared in Tris-HCl buffer (10 mM, *p*H 8.0). The solution was freshly prepared before every use, heated to 60 ^{0}C for 1 hr to destroy DNase.

(b) Medium: LB Media with ampicillin antibiotic (100 µg/mL of culture).

(c) Culture: *E. coli* culture containing *pCMV-SPORT-β-gal.*

(B) Plasmid amplification and isolation by maxi-precipitation

1. Rich medium (LB) (30 mL) was inoculated containing the ampicillin antibiotic with a single colony of transformed bacteria.

2. The culture was incubated at 37 °C with shaking (200 rpm) until the bacteria reach late log phase (OD$_{600}$ = approx. 0.6).

3. LB medium (500 mL) containing the ampicillin antibiotic in a 2.0 L flask was inoculated with the late-log-phase culture (25 mL). The culture was incubated for approximately 12-16 hrs at 37 °C with vigorous shaking on a rotary shaker.

4. Bacterial cells from the 500 mL culture were harvested by centrifugation at 5000 rpm, 4 °C for 10 min. Supernatant was discarded and the centrifuge tubes were inverted on paper towel to remove the last traces of the media.

5. Bacterial cell pellet was re-suspended in ice-cold STE buffer (200 mL) and bacterial cells were collected by centrifugation as described in step 4.

6. The pellet was re-suspended in Alkaline Lysis-I (18 mL) with gentle vortexing and to that freshly prepared lysozyme (2 mL) and RNase-A (50 µL) were added.

7. Freshly prepared Alkaline Lysis-II (40 mL) was added, mixed thoroughly by gently inverting the centrifuge tubes several times and incubated at room temperature for 5 min.

8. Ice-cold Alkaline Lysis-III (20 mL) was added; contents were mixed gently by swirling the centrifuge tubes several times until two liquid phases were indistinguishable and incubated on ice for 10 min.

9. Centrifugation of the bacterial lysate was carried out at 15,000 rpm, 4 °C for 30 min. After the completion of centrifugation, clear supernatant was decanted into a centrifuge tube and the pellet was discarded.

10. To the supernatant, equal amount of phenol-chloroform-isoamyl alcohol was added. The tubes were vortexed and centrifuged at 10,000 rpm, 4 ^{0}C for 15 min. The supernatant was removed and similarly treated again with chloroform alone to remove residual traces of phenol. Finally, the clear supernatant was separated into a measuring cylinder.

11. To the clear supernatant, isopropanol (0.6 volume) was added, mixed well and stored for 10 min at room temperature.

12. The precipitated nucleic acids were recovered by centrifugation at 15,000 rpm, room temperature for 15 min.

13. The supernatant was carefully decanted and the centrifuge tubes were inverted on a paper towel to allow the last traces of the supernatant to be removed. The pellet was rinsed with ethanol (70 %) and air dried at room temperature.

14. The pellet was dissolved in sufficient volume of TE buffer.

15. The purity of plasmid preparations was determined by 1.0 % agarose gel electrophoresis.

16. Plamid DNA concentration of TE buffer obtained in step 14 was measured by UV absorption at 260 nm. The purity of pDNA was estimated by measuring the optical density at 260 nm and 280 nm and calculating the ratio of A_{260}/A_{280} which was generally 1.8 to 2.0.

(C) Plasmid purification by polyethylene glycol 8000 – Lithium chloride Precipitation[212]

1. Crude large-scale plasmid preparation (3.0 mL) was transferred to a centrifuge tube and chilled to 0 °C on an ice bath.

2. Ice-cold lithium chloride solution (3 mL, 5 M) was added to the crude plasmid preparation, mixed well and centrifuged at 14,000 rpm, at 4 °C for 15 min.

3. Supernatant was transferred to a fresh centrifuge tube and an equal volume of isopropanol was added with proper mixing. Precipitate of nucleic acids was recovered by centrifugation at 14,000 rpm, room temperature for 20 min.

4. Supernatant was decanted carefully and the tubes were inverted to decant the last drops of supernatant. Pellet was rinsed with ethanol (70 %) and discarded completely by inverting the tubes on paper towels.

5. Pellet of nucleic acid was dissolved in 1X TE (1.0 mL, *p*H 8.0). RNase-A (40 µL, 20 µg/mL) was added to it and the suspension was stored at room temperature for 30 min.

6. Sodium chloride (500 µL, 1.6 M) and PEG-8000 (13 % w/v) were added and mixed properly and kept on ice for 30 min.

7. Centrifuged at 20,000 rpm, 4 °C for 15 min. Supernatant was decanted carefully and the pellet was dissolved in 1X TE (600 µL, *p*H 8.0). Sodium acetate (80 µL, 3.0 M) and cold ethanol (1.6 mL) was added, mixed thoroughly and kept at -20 °C for 10 min and 0 °C for 30 min.

8. Centrifuged at 14,000 rpm, 4 °C for 15 min. Supernatant was discarded and the pellet was rinsed with ethanol (70 %) and air dried.

9. Pellet was dissolved in 1X TE (600 µL, *p*H 8.0) and stored overnight at room temperature. Absorbance at 260 and 280 nm (A_{260}, A_{280}) and their ratio (A_{260}/A_{280}) were measured in TE (*p*H 8.0) and concentration of the plasmid DNA was calculated assuming that, **1 OD_{260} = 50 µg of plasmid DNA/mL**

10. Agarose gel (1.0 %) electrophoresis was carried out to check the purity of the plasmid.

11. Purified *p*DNA was stored in aliquots at -20 °C until further use.

(D) Plasmid digestion study[213]

(a) Materials

1. Purified *β-gal* plasmid

2. Molecular Markers (Fermentas)

3. Restriction enzyme (Bam H1 for *β-gal* and EcoRI or p53 plasmid) (Fermentas)

4. Bovine Serum Albumin (10 X solution)

5. Restriction Endonuclease Buffer (*p*H 8.0) [A typical restriction endonuclease buffer contains magnesium chloride, sodium or potassium chloride, Tris-HCl, 2-mercaptoethanol (2-ME) or dithiothreitol (DTT), and bovine serum albumin (BSA)] (Fermentas).

(b) Method

1. To the plasmid DNA (2.0 µL), autoclaved distilled water (5.5 µL), 10X BSA solution (1.0 µL), restriction enonuclease buffer (1.0 µL) and 1.0 unit (0.5 µL) of restriction endonuclease enzyme (Bam H1) were added.

2. The mixture was allowed to incubate overnight at 37 ^{0}C.

3. The above cocktail was loaded along with molecular marker and supercoiled pDNA in three different wells into agarose gel (0.7 %) containing ethidium bromide and visualized under UV light and captured as photograph.

4.2.2 Analytical method development for the estimation of plasmid DNA and *β*-galactosidase

4.2.2.1 Estimation of plasmid DNA

The plasmid DNA was quantified spectrophometrically in Tris buffer (*p*H 8.0) at 260 nm. The initial concentration of isolated plasmid was determined by estimation at 260 nm i.e. absorbance of 1 ≈ 50 µg/mL pDNA concentration[195]. Briefly, serial dilutions of pDNA were made in Tris buffer *p*H 8.0 to give final concentration range of 2-60 µg/mL. The solutions were shaken well and the absorbance was measured at 260 nm using Tris buffer as blank by UV visible spectrophotometer (Schimadzu 1700).

4.2.2.2 Estimation of *β*-galactosidase

β-Galactosidase estimation was performed in 96 well plate. Fresh stock solution of *β*-galactosidase (140 unit/mg stock, Sigma Aldrich) was prepared by diluting 10 µL of 1 unit/µL (7.14 µg/µL) to 990 µL of lysis buffer (0.25 M Tris-HCl, *p*H 8.0, 0.5 % Nonidet–P40) and vortexed to make 1:1000 stock solution. Using this stock solution, 50 µL of each *β*-galactosidase standards per well were prepared as given below[196]:

Table 9: Preparation of working standard solutions of *β*-galactosidase

from stock   solution

β-Galactosidase working standard (milli units)	Volume of 1:1000 stock solution (µL)	Volume of lysis buffer (µL)
0	0	50
5	5	45
10	10	40
15	15	35
20	20	30
25	25	25
30	30	20
35	35	15
40	40	10
45	45	5
50	50	0

To this 50 µL of standard solution in lysis buffer, substrate solution (50 µL) [(1.33 mg/mL *o*-nitrophenolgalactopyranoside (ONPG, Sigma-Aldrich)], sodium phosphate (0.2 mole, *p*H 7.3) and magnesium chloride (2 mmole) were added in well plate. All samples were mixed by pipetting the well contents and were incubated at 37 ^{0}C. Absorbance was taken after 5 min and 20 min at 405 nm using ELISA (BioRed) plate reader. The experiments were performed in triplicate and the values were reported as mean $\pm$ SD.

4.3 Formulation development and characterization

The synthesized GAs were formulated either alone or with a helper lipid (DOPE) and characterized for formulation parameters as discussed follow:

4.3.1 Determination of critical miceller concentration (cmc)

Conductance as a function of GA concentration was measured using Digital Conductivity Meter 306 (Equiptronic, Mumbai, INDIA) with cell constant of 1.01 cm^{-1}S at 30 ± 0.2 °C. Serial dilutions of GAs covering the range of 10^{-3} to 10^{-6} mmole

were prepared in double distilled water and conductance of the solutions so prepared were measured. Specific conductance of the solutions was plotted against the concentration. Inflexion point in the graph afforded the cmc values for the GAs under study[200].

4.3.2 Preparation of GA formulations

The formulations were prepared using each GA alone and in combination with helper lipid DOPE. Each GA alone and its mixture with DOPE in molar ratios of 1:1, 1:2 and 1:3 were dissolved in a mixture of solvent (chloroform: methanol, 1:1) in glass vials such that the total lipid quantity remained constant. The solvent was removed by evaporation under a stream of nitrogen. For removal of residual amounts of solvent the samples were further maintained overnight under high vacuum. The resulting dry films were hydrated using 20 mM HEPES buffer, *p*H 7.4 and incubated for 30 min at ~70 $^{\circ}$C followed by vigorous vortexing and repeated freeze thawing (ice cold water to ~70 °C) with intermittent vortexing to ensure hydration. The resulting suspensions were sonicated for 3 min and passed through polycarbonate filters (0.22 µm) 2-3 times. Cholesterol was also included as helper lipid in optimum GA:DOPE formulations such that the final formulations contained GA:DOPE:cholesterol in molar ratios of 1:1:1 and 1:1:0.5[126].

The lipoplex was prepared by mixing the freshly prepared formulations of cationic GA and plasmid DNA under gentle vortexing in DMEM at different N/P ratios (0.5, 1, 1.5, 2.0, 2.5, 3.0, 4.0 and 6.0) and incubated at 37 °C for 15 min. All the complexes were prepared keeping the quantity of *p*DNA constant and varying the quantity of formulation. However, the volumes of cationic formulation and *p*DNA dilutions were kept constant during lipoplex preparation. All the complexes were used immediately for characterization and transfection after the incubation[109].

4.3.3 Characterization of GA formulations

The particle size (z-average) and poly-dispersibilty index (PDI) of GA formulations and lipoplex were determined by photon correlation spectroscopy (PCS) using a Malvern Zetasizer Nano (Malvern Instruments, UK)[214]. The Zetasizer Nano is operating with a 4 mW, 18 mm Helium–neon gas laser at 633 nm and non-invasive

back-scatter technique (NIBS) at a constant temperature of 25 °C. The measurements were conducted in manual mode using 20 sub-runs of 10 seconds. The size distribution by intensity and volume was calculated from the correlation function using multiple narrow mode of Dispersion Technology Software version 4.0 (Malvern, Herrenberg, Germany). The resulting size distribution shows the hydrodynamic diameter.

Electrophoretic mobility (μm/s) was measured using small volume disposable zeta cell and converted to zeta potential by in-built software using Helmholtz–Smoluchowski equation. The liposomes and lipoplexes (0.2 mL) of GAs were diluted to 1.0 mL with DMEM for the measurement of size and zeta potential.

For TEM, briefly a drop of lipoplex prepared at optimized N/P ratios was applied to the copper grid and allowed to dry. After excess removal with a filter paper, uranyl acetate (2 % in water) was then dropped on the complexes and allowed to dry for 2 min. Excess was removed by a filter paper, then the grid was observed on electronic microscope[214].

4.3.4 Agarose gel retardation assay for pDNA complexation

The DNA-binding ability of the cationic GA was assessed by a gel retardation assay on agarose gel (1 %) (pre-stained with ethidium bromide, 0.1 %) across the varying N/P ratios of 0.25 to 8. *pCMV-SPORT-β-gal* (300 ng) was complexed with the varying amount of cationic GA in a total volume of 20 µL in HEPES buffer, *p*H 7.4, and incubated at room temperature for 20-25 min. Loading buffer (4 µL) (0.25% bromophenol blue in 40 % w/v sucrose in H_2O) was added to it, and the resulting solution (24 µL) was loaded on each well. The samples were electrophoresed with Tris-acetate (TAE) buffer at 80 V for 40 min and the DNA bands were visualized in the gel documentation unit[204].

4.3.5 DNase I digestion study

In a typical assay, *p*DNA (1000 ng) was complexed with varying amounts of cationic GA formulations to obtain N/P ratios in a total volume of 30 µL in HEPES buffer, *p*H 7.4, and incubated at room temperature for 30 min on a rotary shaker. Subsequently, the complexes were treated with DNase I (10 µL) (at a final

concentration of 1µg/mL) in presence of MgCl$_2$ (20 mmole) and incubated for 20 min at 37 °C. The reactions were then halted by adding EDTA (to a final concentration of 50 mM) and incubated at 60 °C for 10 min in a water bath. The aqueous layer was washed with 50 µL of phenol/chloroform/isoamyl alcohol mixture (25:24:1 v/v) and centrifuged at 10000 rpm for 5 min. The aqueous supernatants were separated, loaded (25 µL) on a 1% agarose gel (pre-stained with ethidium bromide), and electrophoresed at 100 V for 1 hr[204].

4.3.6 Circular Dichroism (CD) study for *p*DNA condensation

To determine the conformational change of DNA upon binding with cationic GAs, CD experiments were performed using Circular Dichroism spectrometer (JASCO-J815), at measurement range of 320-200 nm; scanning speed of 50 nm/min; band width of 1 nm, response of 1 sec and quartz cuvette of cell length 0.2 cm[205].

Serial dilution of *p*DNA and GAs were prepared in HEPES buffer *p*H 7.4 and mixed to achieve different N/P ratios. The CD spectra were registered at T = 303 K immediately after addition of pDNA to liposomal suspension (t = 0) and after 30 min. In the absence of GA surfactant, CD spectrum exhibits a positive band near 277 nm and a negative band near 245 nm indicating a typical B-form of DNA[206].

4.4 *In vitro* cell line studies

- **Materials**

Dubelcous Modified Eagle Media (DMEM), *β*-galactosidase (140 U/mg) enzyme and o-Nitro Phenol β-Galactopyranoside (ONPG) and DAPI were purchased from Sigma Aldrich St. Louis, M.O. Fetal bovine serum (FBS), Trypsin-EDTA, MTT [3-(4,5-dimethylthiazol-2yl)-2,5-diphenyltetrazolium bromide], Phosphate buffer saline (PBS), Nonidet P-40 (NP-40) and antibiotic cocktail (penicillin–streptomycin-amphotericin b) were purchased from Himedia, Mumbai. HeLa and A549 cell lines were procured from the National Centre for Cell Sciences (NCCS), Pune, India. Cells were cultured at 37 °C in Dulbecco's modified Eagle's medium (DMEM) with fetal bovine serum (10 %) and penicillin-streptomycin-amphotericin B (1 %) solution in a humidified atmosphere containing 5 % CO$_2$.

4.4.1 Transfection studies using reporter gene assay

4.4.1.1 Transfection studies in absence of serum

To evaluate the transfection efficiency of the cationic GAs alone and their formulations to induce gene expression in HeLa and A549 cells, *pCMV*.SPORT-*β-gal* (300 ng) was used to form the lipoplex at various N/P ratios (1 to 8)[170-172]. The cells were seeded in 96 well plates at a density of 5000 cells/well in DMEM (200 µL) growth medium supplemented with FBS (10 %) and penicillin–streptomycin-amphotericin B (1 %) solution. After 18-24 hrs, the cells were treated with diluted lipoplex in 200 µL plain DMEM per well. After 4 hrs of incubation of formulation treatment the culture media was removed, cells were washed with PBS, *p*H 7.4 and 200 µL of complete growth medium added to each well. After 48 hrs, the culture media was removed, cells were washed with PBS *p*H 7.4 and lysed using 50 µL lysis buffer (0.5 % Nonidet P-40 in Tris buffer *p*H 8.0) and were treated with 50 µL of 2X ONPG solution, a substrate for *β*-galactosidase enzyme. After 15 min of incubation at 37 °C, the intensity of yellow color was measured in ELISA micro well plate reader (Biorad, Model 680 XR, Mumbai, India) at 405 nm as a function of quantity of *β*-galactosidase protein expressed in the cells which converts the ONPG into *o*-nitrophenol yielding yellow color. In all of the experiments, naked DNA transfected cells were used as negative control.

4.4.1.2 Transfection studies in presence of serum

To evaluate the serum compatibility of lipoplexes containing optimized GA:DOPE ratio, transfection studies were performed in presence of serum (10 %), while other variables were kept constant as in the case of transfection in absence of serum.

4.4.2 MTT assay for cytotoxicity evaluation

Cytotoxicities of all formulations were assessed by the 3-(4,5-dimethylthiazol-2-yl)-2,5-diphenyltetrazolium bromide (MTT) reduction assay. The cytotoxicity assay was performed in 96-well plates by maintaining the same ratio of number of cells to the amount of cationic formulation, as used in the transfection experiments. After 4 hrs of incubation of formulation treatment the culture media was removed, cells were

washed with PBS, *p*H 7.4 and 200 µL complete growth medium added to each well. After 48 hrs, the culture media was removed; cells were washed with PBS *p*H 7.4; MTT solution (50 µL, 1 mg/mL in plain DMEM) was added to each well and incubated at 37 °C for 4 hrs. After incubation, DMEM was removed and DMSO (100 µL) was added to each well. The plate was mechanically shaken for few minutes to dissolve purple colored formazan crystals. The optical density was measured at 570 nm keeping the reference at 650 nm using plate reader. The percent viability was calculated using the formula given below[215, 216].

$$\text{Cell Viability (\%)} = \frac{\text{Sample absorbance at 570 nm}}{\text{Control absorbance at 570 nm}} \times 100$$

4.4.3 Florescence-assisted cells sorting (FACS) studies

The cells were seeded in 24 well plates at a density of 50000 cells/well in DMEM growth medium (1 mL) supplemented with FBS (10 %) and penicillin–streptomycin- amphotericin B (1 %) solution. After 18-24 hrs, the cells were treated with diluted lipoplex in plain DMEM (500 µL) per well. After 4 hrs of incubation of formulation treatment the culture media was removed, cells were washed with PBS (*p*H 7.4) and complete growth medium (1 mL) was added to each well. The cells were processed for FACS analysis using the following protocol in absence of light to prevent quenching of fluorescence[217]:

1) Transfection was analyzed in wells after 48 hrs using fluorescence microscope (Nikon).

2) Media was aspirated from all the wells into micro-centrifuge tubes.

3) Each well was washed with 100 µL of 1X PBS and aspirated into respective micro-centrifuge tubes.

4) Trypsin-EDTA (250 µL) was added to each well and incubated for 5-10 min at 37 °C.

5) Detachment of cells in each well was observed under microscope and complete media (100 µL) was added to each well. The media in all wells was aspirated to respective micro-centrifuge tubes.

6) Micro-centrifuge tubes were centrifuged at 4 °C and 8000 rpm for 10 min.

7) Filtrates were discarded and pellets were re-suspended in 1X PBS (500 µL), given a washing with PBS; then centrifuged again at afore-mentioned conditions.

8) Filtrates were discarded and added 1X PBS (500 µL) to each micro-centrifuge tube.

9) Added paraformaldehyde (500 µL, 8 %) to each micro-centrifuge and left for 5-10 min to fix the cells and centrifuged at afore-mentioned conditions.

10) Supernatants were discarded and tubes were given a wash with 1X PBS (500 µL); centrifuged at same conditions to remove paraformaldehyde completely.

11) Filtrates were discarded again and pellets finally re-suspened in 1X PBS (500 µL) to obtain the samples ready for FACS reading.

12) The presence of GFP was detected by emission at a wavelength of 508 nm using flow cytometer (Guava Easy cyte; Guava Technologies Inc.). For each cell sample, 5000 events were collected.

4.4.4 Intra-cellular trafficking study using confocal microscopy

Cells were cultured in complete growth media in 6 well plate containing a glass coverslip and seeded with 2×10^5 cells per well. After attaining the required confluency, cells were transfected with transfection medium (lipoplex of optimized formulation at optimized N/P ratio with tagged pDNA). After different time intervals (10, 20 and 30 minutes) cells were washed with 1X PBS (1 mL) (three times) and treated with paraformladehyde (1 mL, 4 %) for 10 min to fix the cells. Paraformaldehyde was removed and cells were washed with 1X PBS (1 mL) (three times). Cells were treated with nuclear staining dye DAPI (0.7 mL) for 1 hr and washed with 1X PBS (1 mL) (three times). Cover slips were mounted on glass slides and fluorescence was viewed and photographed on a confocal microscope (Zeiss, LSM-510 META, Germany) using argon laser at excitation wavelength of 488 nm and emission wavelength of 520 nm[218].

4.5 *In vivo* studies

▪ **Materials**

Diethylenetriaminepentaacetic acid (DTPA) and stannous chloride dihydrate (SnCl$_2$. H$_2$O) were purchased from sigma-aldrich, St. Louis, M.O. ^{99m}Tc in the form of Sodium pertechnetate, separated from molybdenum-99 (99m) by solvent extraction method, was provided by Regional Center for Radiopharmaceutical Division (Northern Region), Board of Radiation and Isotope Technology (BRIT, Delhi, India). Instant thin layer chromatography ITLC-SG plates were purchased from Gelman science. Inc., Ann Arbor, MI.

4.5.1 Optimization of radiolabeling lipoplexes by direct labeling procedure

The radiolabeling of lipoplexes at the optimized N/P ratios were carried out using direct labeling procedure with ^{99m}Tc by simple reduction method using stannous chloride. Lipoplex were prepared by mixing required amount of liposomal suspension in Milli-Q water (0.25 mL) and *p*DNA (15 μg) in Milli-Q water (0.25 mL). After 20 min, added to it ^{99m}Tc (in saline), bicarbonate buffer (0.1 mL, 0.5M, *p*H 9.0) to maintain the final *p*H to 6.0- 6.5, followed by the addition of stannous chloride solution (0.1 mL, 1mg/ mL), to achieve a final formulation concentration of 2.5 mCi/mL. The labeling was carried out by mixing the reagents at ambient temperature for 10 to 15 minutes. Radiolabeling efficiency and radiochemical purity of the labeled complex was estimated by ITLC chromatography technique. Labeling procedure was standardized with respect to reagent concentrations and reaction parameters to achieve stable labeling in higher yields.

4.5.2 Biodistribution studies

Biodistribution studies of ^{99m}Tc-lebelled lipolpexes were carried out according to method approved by local IAEC of Institute of Nuclear Medicine and Allied Science, Ministry of Defense, Government of India. India. Balb/C mice were injected ^{99m}Tc labeled lipoplexes (0.2 mL animal) by tail vein. Blood was withdrawn by cardiac puncture after different time interval and the mice were sacrificed by cervical dislocation. Subsequently, brain and other tissues (liver, lungs, spleen, stomach, intestine, kidney and tail) were dissected, washed twice using normal saline, made

free from adhering tissue/fluid, and weighed. Radioactivity present in each tissue/organ was measured using shielded well-type gamma scintillation counter. (Scintillation counter, Electronics Corporation of India Ltd., Mumbai). Three animals were used for each time point (1, 6 and 24 hrs) for every formulation. Radiopharmaceutical uptake per gram in each tissue/organ was calculated as a fraction of administered dose using the equation as given below[219]:

$$\% \text{ Radioactivity/gm of tissue} = (\text{counts in sample x100}) / (\text{weight of sample x total counts injected}).$$

4.5.3 Gamma scintigraphic studies in rabbit

For scintigraphic studies, rabbits were administered with 0.3 mL of optimized ^{99m}Tc-lebelled lipoplex of all the formulations intravenously through ear vein. The rabbits were anaesthetized using 0.5 mL of 10 mg/ml diazepam intramuscular injection and placed on the imaging board. Imaging was performed using Single Photon Emission Computerized Tomography (SPECT, LC 75-005, Diacam, Siemens AG, Erlanger, Germany) gamma camera at 30 minutes post injection[219].

5. SUMMARY AND CONCLUSION

Gene therapy has enormous potential for the treatment of diseases of the mankind. Although the fundamental principle underlining gene therapy is straightforward theoretically, but it is difficult to achieve satisfactorily in practice. Naked plasmid DNA is an attractive non-viral gene vector due to its inherent simplicity and because it is easily produced in bacteria and manipulated using standard recombinant DNA techniques. However, DNA is a long, slender, hydrophilic and poly-anionic molecule having micrometer dimensions, its systemic applications are limited when delivered alone.

The lack of safe and efficient gene-delivery system is a limiting obstacle to human gene therapy. Both viral and non-viral delivery systems have been tried to satisfy the needs of gene therapy, but so far no ideal vector system has been discovered for gene delivery. Synthetic gene delivery agents, although safer than viruses, generally do not possess the required efficacy. In recent years, a variety of effective polymers and amphiphiles have been specifically designed for gene delivery and much has been learnt about their structure–function relationships. With the growing understanding of gene delivery mechanisms and continued creative efforts of scientists in this direction, it is very likely that non-viral gene delivery systems will evolve and become important tools for human gene therapy in very near future.

The major problems associated with the gene delivery are the size and the negative charge of DNA. Therefore cationic carriers are of great interest in gene delivery to reduce the micron sized DNA into suitable nano-sized carriers utilizing the electrostatic charge interaction. The first report was published in 1989 stated that the double chain monovalent quaternary ammonium lipid, *N*-[1-(2,3-dioleyloxy)propyl]-*N,N,N*-trimethylammonium chloride, effectively bound and delivered DNA to cultured cells, paved the pathway to design and synthesize hundreds of synthetic amphiphilic gene delivery carriers. These amphiphiles differ by the number of charges in their hydrophilic head and the structure of their hydrophobic moiety. The polar 'head-groups' of cationic lipidic non-viral vectors generally consisted of monovalent quaternary ammonium salts such as CTAB and DOTAP. It appeared that introduction of a second quaternary ammonium group could increase the strength of its interaction with DNA and perhaps afforded an improved transfection agent. So, diquaternary

GAs are one of the most widely studied category of cationic surfactants used component in gene delivery carriers.

The superior amphiphilic properties of cationic GAs are applied to the complex problem of introducing genes into cells. GAs typically show enhanced surfactant properties relative to corresponding monovalent (single chain, single head group) compounds. This makes them special for biological (and especially biomedical) applications, where it is essential to optimize the safety profile of any foreign compound; the first and the simplest step is to minimize its concentration *in vivo*. Using less amount of the compound to achieve the same effect also has clear economic advantages. Moreover, diquaternary GAs, have the advantage of being easily prepared and offer a wide range of possibilities for structure modulations as they are composed of three basic parts namely, head, spacer and hydrocarbon chains allowing the design of GAs showing low toxicity, very low immunogenicity, high stability in biological fluids and biodegrability, which are essential requirements for a gene delivery system. The multivalent positive charge in the head group of GAs allowed efficient complexation and compactation of polyanionic DNA into particles (lipoplex) of small sizes that could be easily endocytosed by the cells. The double hydrocarbon chains provide a propensity of forming vesicular structure depending upon the packing parameter of the gemini molecule. Moreover, the nature, length and stereochemistry of spacer also have significant effects on the transfection efficacy of GAs.

It became evident from the literature that modifications in the head group region of lipidic carriers cause significant improvement in the transfection efficacy. For instance, examples are there in literature where improved transfetion efficacy was achieved following hydroxyethylation of the quaternary nitrogen.

Apart from modular design for the required structural features for efficient gene delivery carriers, formulation factors are equally important. DOPE and cholesterol have shown promising results when formulated with cationic carriers including gemini amphiphiles. These helper components favor the endosomal escape of lipoplexes by using different mechanisms which is one of the crucial steps in gene delivery.

Keeping the above discussed points in mind, it was planned to synthesize hydroxyethylated diquaternary gemini amphiphiles and determine their potential as non-viral gene delivery carriers. To verify the importance of hydroxylethyl group on the quaternary nitrogen atoms, it was planned to attach the hydroxyethyl group to nitrogen atom in a systematic way i.e. synthesis of GAs without hydroxylethyl group, synthesis of GAs with one hydroxylethyl group on each quaternary nitrogen and synthesis of GAs with two hydroxylethyl groups on each quaternary nitrogens. The idea of doing so was to evaluate the impact of hydroxylethyl group attached to the quaternary nitrogens of GAs on their transfection efficacy and cytotoxicity. While making such a change, other variables like length of hydrocarbon chain and nature of polymethylene spacer were kept constant.

It was also thought of making changes like varying the hydrophobic flexible (polymethylene) linkers to rigid (*p*-xylene) and to hydrophilic flexible (oxyethylene) linkers in the synthesized GAs. Length of hydrophobic tail was also planned to be varied to optimize structural features in the synthesized GAs for effective gene delivery. It was also planned to develop formulations containing synthesized GAs along with DOPE and cholesterol as helper lipids. It was envisaged to evaluate the formulations so developed for DNA complexation and to see the stability of the complexed DNA against DNase; and try to develop a relationship between the GA structures with transfection efficiency and cytotoxicity.

The synthesized GAs have been characterized by TLC, melting point, IR and PMR data. The critical miceller concentration of all the GAs was determined using conductometry. All the measurements were carried out at 30 ^{o}C except for the GAs having p-xylene spacers which were dispersed in water at 50 ^{o}C. All the GAs were observed to dissociate completely at very low concentrations and their conductance increases linearly with increase in concentration up to cmc. Although, the conductance continues to increase beyond cmc also, but the rate of increase in conductance is lower compared to that below cmc. The nature and structure of a spacer between the two head groups of a GA are the key factors which distinguish GAs from conventional monomeric amphiphiles and are critical to the unique properties of GA. The spacer can be used to manipulate the hydrophobic interactions as well as to constrain the electrostatic repulsion between charged head groups. The

cmc values obtained for DMA series indicate that as the nature of spacer changes from oxyethylene (**3II**, 22.2 X 10^{-3} M) to polymethylene (**3III**, 28.2 X 10^{-3} M; **3IV**, 44.8 X 10^{-3} M) to p-xylene (**3I**, 57.6 X 10^{-3} M), the cmc value increases.

The surface active properties of GAs were found to be better than their monomeric counterparts. For instance, **(3I), (3II), (3III)** and **(3IV)** of DMA series showed cmc values of 57.6 × 10^{-6}, 22.2 × $10^{-6,}$ 28.2 × 10^{-6} and 44.8 × 10^{-6} M respectively. These cmc values were found to be 100 fold higher compared to monomeric surfactant, cetyl trimethyl ammonium bromide (1.3 × 10^{-3} M). Moreover, comparison of cmc values of GAs for a particular spacer showed that as the polarity of head group is increased by incorporation of hydroxyethyl group (**3III,** 28.2 × 10^{-5}; **7cIII**, 2.1 × 10^{-6}; **10cIII**, 1.1 × 10^{-6}), the cmc values of GAs deceased by 10 fold. Similar results were obtained for other spacers while maintaining the hydrophobic chain length. The results obtained are suggestive of superior surface active properties of polar GAs (MEA and DEA series) compared to non-polar GAs (DMA series). This may be due to hydrogen bonding of -C_2H_4OH groups with water through oxygen atom that is likely to provide additional hydration at the head group level resulting in screening of columbic forces of repulsion between charged heads and helping MEA and DEA series GAs to form aggregates at a lower concentrations than those of DMA series. On comparing the cmc values for all the series, it was observed that cmc values showed dependency on hydrophobic chain length. For instance, the cmc values for **7aIII**, **7bIII**, **7cIII** and **7dIII** were found to be 2.9 × 10^{-5}, 2.3 × 10^{-5}, 2.1 × 10^{-6} and 1.2 × 10^{-6} respectively.

All the synthesized GAs were formulated as liposomes either alone or with helper lipid DOPE above ~ 70 ^{0}C in molar ratio of 1:1, 1:2 and 1:3. DOPE was selected as helper lipid due to its fusogenic property at endosomal stage. Cholesterol was also used as helper lipid to improve the formulation characteristics.

Plasmid DNA of interest (*pCMV-SPORT-β-gal,* 7.8 kb) was incorporated into bacterial cells (*E. coli*) using Transform Aid™ bacterial transformation kit. Transformed bacterial cells were selected and isolated by culturing the cells on appropriate antibiotic plate. Pure culture of *E.coli* containing plasmid *β-gal* was stored as glycerol stock and working plates were used for the regular plasmid DNA isolation experiments. The plasmid DNA was isolated from the working culture of transformed

E. coli strains using the alkaline lysis method. The isolated plasmid DNA was purified by PEG-LiCl method. The purity of the plasmid was ascertained by agarose gel assay (two bands without smear indicating pure pDNA) and UV spectrophotometry for absorbance determinations at 260 and 280 nm. The ratio of absorbance (A_{260}/A_{280}) was found to be in between 1.8-2.0 indicating pure pDNA devoid of protein and RNA impurities. The concentration of plasmid is determined by absorbance at 260 nm by comparing it with the standard calibration curve or by the equation:

$$1 \text{ (OD}_{260}) = 50 \text{ μg of plasmid DNA/mL.}$$

The digestion study (using restriction endonuclease enzyme, Bam H1) was used to confirm the *p*DNA transformation.

All the synthesized GAs formulations were characterized for zeta potential, particle size and size distribution. Almost all GAs exhibited bimodular size distribution (two peaks in their size distribution report). All the formulations showed positive zeta potentials (ZP) due to quaternary nitrogens in their structure, which is a necessary requirement for complexation with anionic *p*DNA. Relatively higher values of Polydispersibilty Index (PDI) were obtained due to bimodular size distribution in the formulations. It may be due to free GA molecules along with their aggregates. The results showed that as the polarity of the head group increased in GAs from **3III** to **7cIII** to **10cIII**, Z-average (Z_{av}) increased from 325 to 369 to 400 nm, while the hydrophobic chain length was kept constant. This may be due to the increasing propensity of the head group to hydrate with increasing number of hydroxyethylated groups. Moreover, Z_{av} was found to depend upon the hydrophobic chain length i.e., 326 and 233 nm for **7cIII** and **7aIII** having similar head groups but with C_{16} and C_{12} chains in their structures respectively. The method of preparation also had significant role on Z_{av} of the same formulations. For instance, formulation of **7cIII** showed Z_{av}, PDI and ZP of 725 nm, 0.802 and 52.9 respectively before sonication. Moreover, the incorporation of DOPE into the formulation resulted into increase in Z_{av}. **7cIII** showed Z_{av} of 129, 177, 339 and 417 nm when formulated all alone and in the ratios of 1:1, 1:2 and 1:3 respectively with DOPE at double dilution.

The lipoplex of GA formulations were prepared with *p*DNA at different N/P ratio (0.25-6). The N/P ratio is defined as molar ratio of number of positively charged

nitrogens in cationic GA to the number of negatively charged phosphate of the anionic *p*DNA. All the complexes were prepared keeping the quantity of *p*DNA constant and varying the quantity of GA in the formulations. However, the volumes of the cationic formulations and *p*DNA dilutions were kept constant during lipoplex preparation. The sizes of prepared lipoplex were found to depend on the incubation time after mixing of GA formulation and *p*DNA. The **7aIII** lipoplex have showed size of 166, 198 and 220 nm for incubation time of 15, 30 and 60 minutes, at N/P ratio of 1:1.

The Z_{av} and ZP were also determined for the lipoplex of formulations that showed best results in transfection studies (**7bIII1** and **7bII1**). The blank formulation of **7bIII1** showed $Z_{av,}$ and ZP of 272 and 43.5 respectively. However, its lipoplex with *p*DNA showed different values for Z_{av} and ZP depending upon the N/P ratio. At lowest N/P ratio (0.25), the poyplex showed Z_{av} and ZP of 483 and -20.9. With increasing N/P, the size of lipoplex decreased first and then increased; however, ZP increased with the increased N/P ratio (-20.9 to 6.66). The formulation of **7bII1** showed Z_{av} and ZP of 214 nm and 29.6 mV. The results obtained for 7bII1 were similar in trend to that of **7bIII1** in variation of Z_{av} and ZP with N/P ratio. Tranmission electron microscopy (TEM) photographs of the lipoplex of **7bIII1** and **7bII1** at their optimized N/P ratios were in consonance to those obtained with DLS.

Electrostatic interactions between the negatively charged *p*DNA and cationic liposomes as a function of N/P ratios were characterized by electrophoretic gel retardation assay. Gel electrophoretic patterns for GAs (**3cIII, 7cIII** and **10cIII**) have been shown in **Figure 33**. Lane 1 showed plain *p*DNA that moved out of the well under the influence of electrostatic force. However, other lanes exhibited retardation of *p*DNA as the N/P ratio increased from 0.25 to 3.0. All GAs showed about 60 % retardation at N/P ratio of 0.5. About 100 % DNA retardation have been observed for all the GAs at N/P of 1.0. However, for higher N/P than 1.0 complete retardation was observed. It should be noted that every GA molecule possessed two hard charges, which indicated that the whole plasmid DNA got retarded at lipid/DNA mole ratio of 0.5. Significant retardation of DNA was also observed at N/P ratio of 0.5 (or GA/DNA mole ratio of 0.25) as well. No effect of head group polarity of GAs has

been found in gel retardation study as all the GAs in the given figure have shown almost similar retardation pattern at similar N/P ratios.

DNase I digestion study was performed to evaluate the *p*DNA protection behaviour of the synthesised GA formulations. The results obtained in the study have been shown in **Figure 34** (A, B and C). Lane 1 showed naked *p*DNA without DNase treatment. At N/P 0.5 with all the GAs (**3III, 7cIII** and **10cIII**) under consideration, complete degradation of *p*DNA was observed. However, at N/P 1, ~ 90 % of *p*DNA could be protected by GA formulations. Complete protection of the *p*DNA against DNase was observed at N/P ratio of more than 1. The naked DNA on treatment with DNase I showed complete degradation. No effect of head group polarity of GAs was observed in this study, while the hydrophobic tails were kept constant.

Circular dichroism provides information on the helical conformation of the double-stranded DNA. Cationic amphiphiles bind to the native B-form of the DNA and induce secondary structure formation, which reduces the number of base pairs/turn from 10 to 9.33. The CD spectrum of plasmid DNA in HEPES buffer exhibits a positive band near 277 nm and a negative band near 245. With the addition of GA, change in the B-form to ψ-form can be visualized in **Figure 35**. Moreover, increase in the N/P (+/- charge) ratio causes condensation of the DNA into ψ-DNA, a left handed highly organized tertiary structure, characterized by an increase of the negative signal of the CD spectra. An effective complexation between DNA and liposomes should yield compaction of the nucleic acid; this will promote the penetration of the nucleic acid into the target cell and will protect the genetic exogenous material from nuclease degradation. A crucial point to obtain high transfection efficiency is, in fact, to maintain the therapeutic genes undamaged. The comparison of the results obtained in the CD experiments **(Figures 35)** for **3III**, **7cIII** and **10cIII** demonstrated that all the GAs are effective in condensing *p*DNA into ψ-phase. Moreover, the condensation properties of the cationic formulations depend on the molecular structure of the cationic amphiphile as well as on the nature of DNA. Under the same experimental conditions and equivalent amounts of GAs, **7cIII** showed more effective condensation of plasmid DNA compared to **3III** and **10cIII**.

The transfection efficiency of each GA was evaluated in two cell lines (A549 and HeLa) using β-Gal reporter plasmid either alone or with DOPE as helper lipid at

N/P ratios of 0.5, 1, 2, 3, 4 and 6. The amount of β-galactosidase protein expressed in cells is directly proportional to the transfection efficiency of the gene delivery carrier used. The transfection results so obtained showed that all of the GAs exhibited higher β-Gal expression when formulated along with DOPE. This may be due to early release of lipoplex at endosomal stage inside the cells. It was observed that modulation in head group polarity significantly affects the transfection efficacy of GAs. For instance, incorporation of hydroxyethyl group in the head group region of GAs having C4 spacer and C16 hydrophobic chains e.g., **3III** (no hydroxyethyl group attached to quaternary nitrogens), **7cIII** (one hydroxyethyl group attached to each quaternary nitrogen) and **10cIII** (two hydroxyethyl groups attached to each quaternary nitrogen) showed the highest β-Gal expression of 0.94 (N/P 1) and 1.02 (N/P 1), 1.11 (N/P 4) and 1.83 (N/P 2), 1.02 (N/P 2) and 1.04 mU (N/P 3) in A549 and HeLa cell lines respectively. Thus, incorporation of hydroxyethyl group in head group region resulted into increased transfection efficacies of GAs. However, there was a little decrease in transfection activity on moving from one hydroxyethyl to two hydroxyethyl groups per quaternary nitrogen, while maintaining the hydrophobic chain length constant.

The formulation of **3III**, **7cIII** and **10cIII** with DOPE at different molar ratios showed significant rise in transfection activity. **3III1**, **7cIII1** and **10cIII1** showed 1.6 (N/P 4) and 1.8 (N/P 4), 1.79 (N/P 1) and 2.76 (N/P 1), 1.98 (N/P 2) and 2.22 mU (N/P 2) activity in A549 and HeLa cell lines respectively. These results indicated a crucial role played by DOPE as helper lipid in gene delivery and the importance of hydroxyethylation in the head group region of GAs. Moreover, decrease in N/P ratio from 4 to 1 or 2 to achieve highest transfection indicated that smaller molar concentration of hydroxyethylated GAs (**7cIII1** and **10cIII1**) is required to exhibit the best transfection results compared to non-hydroxyethylated GAs (**3III1**).

The nature and length of spacers in GAs showed a significant effect on the transfection efficacy of GAs. For instance, when spacer was changed from hydrophobic rigid ($CH_2C_6H_4CH_2$) to hydrophilic flexible ($CH_2CH_2OCH_2CH_2$) to hydrophobic flexible (polymethylene, $(CH_2)_6$ and $(CH_2)_4$) groups in **7bI** to **7bII** to **7bIII** to **7bIV** of MEA series, the transfection expression of 0.84 (N/P 1) and 1.21 (N/P 2), 1.42 (N/P 1) and 1.58 (N/P 2), 1.32 (N/P 1) and 1.56 (N/P 2), 0.79 (N/P 1)

and 1.40 mU (N/P 3) were obtained in A549 and HeLa cell lines respectively. However, their optimized formulations with DOPE (**7bI1, 7bII1, 7bIII1, 7bIV2)** showed 1.06 (N/P 2) and 1.97 (N/P 2), 2.11 (N/P 3) and 3.57 (N/P 3), 1.84 (N/P 2) and 3.44 (N/P 2), 1.74 (N/P 1) and 2.31 mU (N/P 1) activity in A549 and HeLa cell lines respectively. Similarily **10bI**, **10bII**, **10bIII**, **10bIV** of DEA series possessing the same spacer and hydrophobic chains showed 0.81 (N/P 1) and 0.90 (N/P 2), 0.52 (N/P 1) and 1.07 (N/P 3), 0.60 (N/P 3) and 0.96 (N/P 4), 0.59 (N/P 2) and 0.98 mU (N/P 2) of β-Gal expression in A549 and HeLa cell lines respectively. With DOPE, these GAs (**10bI1**, **10bII2**, **10bIII1**, **10bIV1**) showed β-Gal expression of 1.33 (N/P 1) and 1.62 (N/P 1), 2.05 (N/P 1) and 2.18 (N/P 1), 1.81 (N/P 2) and 2.06 (N/P 2), 1.64 (N/P 1) and 1.93 mU (N/P 1) in A549 and HeLa cell lines respectively. The results obtained in β-Gal expression for both the series showed that transfection efficacy follows the order; $(CH_2CH_2OCH_2CH_2) > (CH_2)_6 > (CH_2)_4 > CH_2C_6H_4CH_2$ for the spacer moiety, while keeping the hydrocarbon chain length and the head groups constant.

Hydrocarbon chain length also exhibited significant effect upon the transfection efficacy of synthesized GAs. For instance, GAs of MEA series (**7aI**, **7bI**, **7cI**, **7dI**) having similar head groups and $CH_2C_6H_4CH_2$ as spacers but having C12 - C18 long hydrocarbon chains showed β-Gal expression of 0.17(N/P 2) and 0.24 (N/P 2), 0.84 (N/P 1) and 1.21 (N/P 2), 0.79 (N/P 3) and 1.20 (N/P 1), 0.30 (N/P 2) and 0.32 mU (N/P 2) in A549 and HeLa cell lines respectively. However, with DOPE these GAs (**7aI1**, **7bI1**, **7cI2**, **7dI1**) showed β-Gal expression of 0.62 (N/P 2) and 0.74 (N/P 2), 1.06 (N/P 2) and 1.97 (N/P 2), 1.13 (N/P 1) and 2.02 (N/P 1), 1.0 (N/P 3) and 1.11 mU (N/P 3) in A549 and HeLa cell lines respectively. For GAs of DEA series (**10aI**, **10bI**, **10cI**, **10dI**) having similar head groups and $CH_2C_6H_4CH_2$ spacers but C12 - C18 long hydrocarbon chains, the results obtained were 0.38 (N/P 2) and 0.34 (N/P 3), 0.81(N/P 1) and 0.90 (N/P 2), 0.80 (N/P 4) and 0.89 (N/P 3), 0.19 (N/P 2) and 0.54 mU (N/P 3) in A549 and HeLa cell lines respectively. However, with DOPE these GAs (**10aI2**, **10bI1**, **10cI1**, **10dI1**) showed β-Gal expression of 0.95 (N/P 3) and 1.02 (N/P 3), 1.33 (N/P 1) and 1.62 (N/P 1), 1.14 (N/P 2) and 1.71 (N/P 2), 0.84 (N/P 3) and 1.08 mU (N/P 3) in A549 and HeLa cell line respectively. These findings suggested that transfection efficacy of GAs and their formulations with DOPE were

dependent upon hydrocarbon chain lengths and follow the order; C14 > C16 > C18 > C12, while the head group and the spacer were kept constant.

Various formulations of synthesized GAs that showed good β-Gal expression in A549 and HeLa cell lines have been compared with the expression of naked β-Gal plasmid (*p*DNA) as negative control and commercially available transfection reagents (Lipofectamine 2000, DCC:DOPE and DOTAP:DOPE liposomes) as positive control. Naked *p*DNA showed negligible β-Gal expression of 0.04 and 0.077 mU in A549 and HeLa cell lines respectively. All the GA formulations [**7bI1** (N/P 2), **7bII1** (N/P 3), **7bIII1** (N/P 2), **7bIV2** (N/P 1), **7cI2** (N/P 1), **7cII2** (N/P 2), **7cIII1** (N/P 1), **7cIV2** (N/P 2) of MEA series, and **10bI1** (N/P 1), **10bII2** (N/P 1), **10bIII1** (N/P 2), **10bIV1** (N/P 1), **10cI1** (N/P 2), **10cIII1** (N/P 2) and **10cIV1** (N/P 2) of DEA series] showed their highest β-Gal expression of 1.06, 2.12, 1.84, 1.74, 1.11, 1.90, 1.79, 1.47, 1.33, 2.06, 1.80, 1.64, 1.15, 1.99, 1.20 mU and 1.97, 3.58, 3.45, 2.32, 2.03, 3.21, 2.76, 2.60, 1.63, 2.19, 2.07, 1.93, 1.72, 2.22, 1.84 mU in A549 and HeLa cell lines respectively. All the GA formulations exhibited the expression levels higher or comparable to DOTAP:DOPE liposomes (1.37 and 1.94 mU in A549 and HeLa cell lines respectively) and DC-Chol:DOPE liposomes (1.68 and 2.47 mU in A549 and HeLa cell lines respectively). However, some formulations (**7bII1**, **7bIII1**, **7cII2**, **7cIII1 and 10cIII1**) exhibited higher or comparable β-Gal expression to Lipofectamine 2000 (2.07 and 3.12 mU in A549 and HeLa cell lines respectively). Moreover, the transfection efficacies of all the formulations including the standards were found to be higher in HeLa cells compared to A549 cell line at similar N/P ratios. This may be due to higher propensity of HeLa cells for transfection compared to A549 cells.

Serum is known to decrease the transfection efficacies of gene delivery carriers. The transfection efficacies of optimized GA formulations showing the best results in A459 and HeLa cells in absence of serum were also determined in presence of FBS 10 %. The decreases in transfection efficacy were noted in both A459 and HeLa cell lines for all the formulations tested (**Figures 69** and **70**). The standards (DCC:DOPE and DOTAP:DOPE) used in the study also showed significant reduction in their transfection efficacy. The GA formulations, **7bII1**, **7bIII1**, **7cII2**, **7cIII1** showed highest β-Gal expression of 1.63, 1.40, 1.58, 1.37 mU and 2.62, 2.37, 2.49, 2.18 mU in A549 and HeLa cell lines respectively at their optimized N/P ratios. The

β-Gal expression of these formulations were significantly higher compared to the standards (DCC:DOPE and DOTAP:DOPE).

Cholesterol is known to impart serum compatibility to gene delivery carriers. Cholesterol was incorporated in the GA formulations (**7bII1**, **7bIII1**, **7cII2**, **7cIII1**) in an attempt to improve their transfectiion efficacies in presence of serum. Cholesterol was added to all the formulations in two different molar concentrations such that GA:DOPE:cholesterol were in the ratios of 1:1:1 and 1:1:0.5. The transfection efficacies of the resulting formulations were checked in absence and presence of serum 10 % both in A549 and HeLa cell lines. The results obtained showed that incorporation of cholesterol resulted into improved transfection efficacies of all the GA formulations tested both in presence and absence of FBS.

Cytotoxicity is an important criterion in selecting a suitable GA for gene delivery. A good GA should exhibit not only a high transfection efficacy but a minimal level of toxicity too. The GA formulations showing good results in the transfection studies were evaluated for cell viability. Formulations of GAs [**3(I-IV)**, **7b(I-IV)**, **7b(I-IV)**, **10b(I-IV)** and **10b(I-IV)**] with DOPE were evaluated for cell viability using MTT assay for cell toxicity under identical conditions as maintained in their transfection studies. The results are shown in **Figures 75-93.** Cell viability of the control cells without treatment was considered as 100 %. All the GA formulations evaluated for MTT assay showed N/P ratio dependent cell viability. As the N/P ratio of lipoplex increased from 0.5 to 6, cell viability decreased in both of the cell lines for all the formulations. Cell viabilities of all the GA formulations have been evaluated and compared with standards (DCC:DOPE and DOTAP:DOPE liposomes) in A549 and HeLa cell lines respectively in **Figures 94** and **95**. The cell viabilities of almost all the formulations were comparable to that of standards (DCC:DOPE and DOTAP:DOPE liposomes). DCC:DOPE and DOTAP:DOPE liposomes showed cell viabilities of 82.6, 87.2 % and 83.38, 89.2 % in A549 and HeLa cell lines respectively. The cell viabilities were not found to dependent upon the hydrocarbon tails of GAs. However, GAs having oxyethylene spacers were found to be more toxic compared to the polymethylene and *p*-xylene spacer, while keeping the hydrocarbon chain length and head group constant. For instance, the cell viabilities of **7bI** (*p*-xylene spacer) and **7bII** (oxyethylene spacer) having similar hydrocarbon chains and

head droups were found to be 91.9, 89.2, 83.3, 75.48, 71.4, 61.6 % and 90.64, 86.01, 77.74, 73.35, 70.07, 58.63 % respectively in A549 cell line at N/P ratios of 0.5, 1, 2, 3, 4, 6. In HeLa cell line, **7bI** (*p*-xylene spacer) and **7bII** (oxyethylene spacer) showed cell viabilities of 93.89, 84.89, 81.33, 77.36, 64.89, 61.33 % and 89.55, 83.44, 81.11, 68.0, 62.5, 50.89 % respectively at N/P ratios of 0.5, 1, 2, 3, 4, 6. It is clearly evident from the data that oxyethylene spacer yielded GAs with higher cytotoxicities than the GAs having *p*-xylene spacer at all the N/P ratios in both the cell lines.

The amount of *β*-galactosidase protein expressed in cells is a measure of the efficacy of the gene delivery carriers. However, the number of cells transfected by transfection reagents is also important. The percentage of cells transfected during transfection experiments by reagents showing promising results in *β*-Gal expression have been evaluated using FACS studies in 24-well format. The fluorescence of Green fluorescence plasmid (GFP) was observed and captured under fluoresence microscope. The fluorescent images of GFP plasmid for the formulations; **7bII1**, **7bII1A**, **7bIII1**, **7bIII1A**, **7cII1**, **7cII1A**, **7cIII1** and **7cIII1A** have been shown in **Figures 96** and **97** in A549 and HeLa cells respectively. **Figures 98** and **99** showed percent of cells transfected with GFP plamid using these formulations compared with the plain GFP plasmid (negative control) and standards (Lipofectamine 2000, DCC:DOPE and DOTAP:DOPE liposomes) in A549 cells in absence of serum. It was observed that formulations containing cholesterol (**7bII1A**, **7bIII1A**, **7cII1A** and **7cIII1A**) showed higher number of transfected cells compared to the respective formulations without cholesterol (**7bII1**, **7bIII1**, **7cII1** and **7cIII1**). This common observation was noted for both A549 and HeLa cell lines in absence of serum. For instance, formulation **7bII1** (**7bII**:DOPE, 1:1 molar ratio) showed the highest percent of transfected cells (14.41 and 18.78 % in A549 and HeLa cells respectively). Its efficiency further improved with the incorporation of cholesterol **7bII1A** (**7bII**:DOPE:cholesterol,1:1:1 molar ratio) resulting into 16.18 and 21 % transfected cells in A549 and HeLa cell line respectively in absence of serum. All of the formulatons showed significant increase in percent of transfected cells compared to the plain GFP plasmid. The percent transfected cells by various transfection reagents followed the order, **7bII1A** > Lipofectamine > **7bIII1A** > **7cII1A** > **7bII1** > **7bIII1** > **7cII1** > **7cIII1A** > **7cIII1** > DCC:DOPE > DOTAP:DOPE > control in A459 cells

and **7bII1A** > Lipofectamine > **7bII1** > **7bIII1A** > **7cII1A** > **7bIII1** > **7cII1** > **7cIII1A** > **7cIII1** > DCC:DOPE > DOTAP:DOPE > control in HeLa cells in absence of serum at their optimized N/P ratios. All the formulstions showed significantly higher percent of transfected cells compared to DCC:DOPE and DOTAP:DOPE liposomes in both of the cell lines used. The formulation **7bII1A** showed higher percentage of transfected cells (16.18 and 21% transfected cells in A549 and HeLa cell lines respectively) compared to Lipofectamine 2000 (15.94 and 19.32 % transfected cells in A549 and HeLa cell lines respectively) in absence of serum at its optimized N/P ratio. The formulations (**7bIII1A**, **7cII1A** and **7bII1**) showed comparable percent of transfected cells (14.99, 14.43 and 14.41 % respectively) to that of Lipofectamine 2000 (16.18 %) in A549 cell line at their optimized N/P ratios without FBS. The formulations (**7bII1**, **7bIII1A** and **7cII1A**) showed comparable percentage of transfected cells (18.78, 18.2 and 17.95 % respectively) to that of Lipofectamine 2000 (19.32 %) in HeLa cell line at their optimized N/P ratios without FBS.

   Figures 100 and **101** showed percentage of transfected cells by optimized transfetion reagents at their optimized N/P ratios in A549 and HeLa cells respectively with FBS 10 %. The percentage of transfected cells by various transfection reagents followed the order: **7bII1A** > **7bIII1A** > **7cII1A** > **7cIII1A** > **7bII1** > **7cIII1** > **7bIII1** > DCC:DOPE > DOTAP:DOPE > **7cII1** > control in A459 cells and **7bII1A** > **7bIII1A** > **7cII1A** > **7cIII1A** > **7bII1** > **7bIII1** > **7cIII1** > **7cII1** > DCC:DOPE > DOTAP:DOPE > control in HeLa cells in presence of 10 % serum at their optimized N/P ratios. Almost all the formulstions showed significantly higher percent of transfected cells compared to DCC:DOPE and DOTAP:DOPE liposomes in both of the cell lines used.

   Cholesterol containing GA formulations (**7bII1A**, **7bIII1A**, **7cII1A** and **7cIII1A**) showed higher percentage of transfection of the cells compared to their respective formulations without cholesterol (**7bII1**, **7bIII1**, **7cII1** and **7cIII1**) in both of the cell lines with FBS 10 %. For instance, formulation **7bII1** (**7bII**:DOPE, 1:1 molar ratio) showed highest percent of transfection of cells (8.49 and 10.71 % in A549 and HeLa cells respectively). Its efficiency further improved with the incorporation of cholesterol, **7bII1A** (**7bII**:DOPE:cholesterol,1:1:1 molar ratio)

resulting into 11.13 and 15.57 % transfected cells in A549 and HeLa cell line respectively in presence of serum 10 %. These results indicated that incorporation of cholesterol had improved the serum compatibility of lipoplex.

Confocal microscopy was performed to track the intra-cellular trafficking of lipoplex of GA formulation (**7bIII1A**) showing the best results in the *in-vitro* transfection and FACS studies. First row of **Figures 102** and **103** showed control groups of cells without any lipolplex treatment. First two images of each row represent phase contrast images of cells, while third one is merged image showing blue stained nucleus and morphology of cells. Second row (**Figures 102** and **103**) showed lipoplex (green colouerd dots) entering in the cytoplasm of the cells after 10 minutes of incubation. Third row (**Figures 102** and **103**) showed the accumulation of lipoplex (green colouerd dots) inside the nuclei of the cells after 20 minutes of incubation. Fourth row (F**igures 102** and **103**) showed further accumulation of of lipoplex (green colouerd dots) inside the nuclei of the cells after 30 minutes of incubation

The lipoplex of GA formulations showing the best results under the *in vitro* cell line studies were used for biodistribution studies in rats. The radioactivity of ^{99m}Tc labelled lipoplex of **7bII1A** and **7bIII1A** in various organs was detected quantitatively at pre-determined time points (1, 6 and 24 hrs) and percent of radioactivity per gram of tissue was plotted in **Figures 104 and 105.** At initial time point (1 hr) maximum of the lipoplex accumulated in vital organs like liver, spleen, lungs, kidneys etc. With the passage of time (6 hr), the accumulation of lipoplex increased in liver and speen, however decreased in other organs. After 24 hrs, spleen was found to contain the maximum lipoplex followed by liver for both of the formulations.

Gamma-scintigraphic studies were performed on rabbits for qualitative assessment of optimized ^{99m}Tc-lebelled lipoplex. The scintigraphic images of ^{99m}Tc labelled lipoplex of **7bII1A** and **7bIII1A** have been shown in **figure 106** after 1 hr of administration. The images showed the accumulation ^{99m}Tc-lebelled lipoplex in liver, spleen, lungs and kidneys.

6. REFERENCES

1. Ledley, F. D., *Pharm Res.,* **1996**, 13, 1595.

2. Vacik, J.; Dean, B. S.; Zimmer, W. E.; Dean, D. A., *Gene Ther.*, **1999**, 6, 1006.

3. Schaffer, D. V., Lauffenburger, D. A., *J. Biol. Chem.*, **1998**, 273, 28004.

4. Rao, G.; Yadava, P., Jeffrey, H., *The Open Drug Delivery Journal,* **2007**, 1, 7.

5. Gene Therapy Clinical Trials Worldwide Cited 2011 September, Available from: http://www.wiley.co.uk/genmed/clinical.

6. Han, S.; Mahato, R. I.; Sung, Y. K., Kim, S. W., *Mole. Ther.*, **2000**, 2, 302.

7. Rolland, A., Advanced Gene Delivery: From Concepts to Pharmaceutical Products, Harwood Academic Publisher, **1999**, p 59.

8. Frank, M.; Fries, L., *Today,* **1991**, 12, 322.

9. Ruponen, M.; Yla-Herttuala, S.; Urtti, A., *Biochim. Biophys. Acta,* **1999**, 1415, 331.

10. Gruenberg, J.; Maxfield, F. R., *Curr. Opin. Cell Biol.,* **1995**, 7, 552.

11. Robinson, M. S.; Watts, C.; Zerial, M., *Cell,* **1996**, 84, 13.

12. Colin, M.; Moritz, S.; Fontanges, P.; Kornprobst, M.; Delouis, C.; Keller, M.; Miller, A. D.; Capeau, J.; Coutelle, C.; Brahimi-Horn, M. C., *Gene Ther.,* **2001**, 8, 1643.

13. Cotton, M.; Wagner, E., *Curr. Opin. Biotechnol.*, **1993**, *4*, 705-10.

14. Gao, X.; Kim, S. K.; Liu, D., *The AAPS J.,* **2007**, 9, E92.

15. Jinturkar, K.; Rathi, M.; Misra, A., Gene delivery using physical methods, *in*, Challenges in delivery of therapeutic genomics and proteomics, **2011**, 1, p 83.

16. Young, L. S.; Searle, P. F.; Onion, D.; Mautner, V., *J. Pathol.* **2006**, 208, 299.

17. Yang, Y.; Nunes, F. A.; Berencsi, K.; Goenczoel, E.; Engelhardt, J. F.; Wilson, J. M., *Nat. Genet.*, **1994***, 7, 362.

18. Yang, Y.; Nunes, F. A.; Berencsi, K.; Furth, E. E.; Gonczol, E.; Wilson, J. M., *Proc. Nat. Acad. Sci. USA.*, **1994***, 91, 4407.

19. Knowles, M. R.; Hohneker, K. W.; Zhou, Z.; Olsen, J. C.; Noah, T. L.; Hu, P. C.; Leigh, M. W.; Engelhardt, J. F.; Edwards, L. J.; Jones, K. R., *New Engl. J. Med.*, **1995***, 333, 823.

20.   Crystal, R. G.; Mc Elvaney, N. G.; Rosenfeld, M. A.; Chu, C. S.; Mastrangeli, A.; Hay, J. G.; Brody, S. L.; Jaffe, H. A.; Eissa, N. T.; Danel, C., *Nat. Genet.*, **1994**, 8, 42.

21.   Yang, T. A.; Heiser, W. C.; Sedivy, J. M., *Nucleic Acids Res.*, **1995**, 23, 2803.

22.   Zhang, L.; Nolan, E.; Kreitschitz, S.; Rabussay, D. P., *Biochim. Biophys. Acta*, **2002**, 1572, 1.

23.   Chang, D. C.; Reese, T. S., *Biophys J.*, **1990**, 58, 1.

24.   Heiser, W. C., *Anal. Biochem.*, **1994**, 217, 185.

25.   Eisenbraum, M. D.; Fuller, D. H.; Haynes, J. R., *DNA Cell. Biol.*, **1993**, 12, 791.

26.   Barber, M. A., *Philipp J. Sci.*, **1914**, 9, 307.

27.   Graessmann, M.; Graessmann, A., *Methods Enzymol.*, **1983**, 101, 482.

28.   Liu, D. X.; Knapp, J. E., *Curr. Opin. Mol. Ther.*, **2001**, 3, 192.

29.   Zhang, G.; Gao, X.; Song, Y. K.; Vollmer, R.; Stolz, D. B; Gasiorowski, J. Z., *Gene Ther.*, **2004**, 11, 675.

30.   Kim, H. J.; Greenleaf, J. F.; Kinnick, R. R.; Bronk, J. T.; Bolander, M.E., *Hum. Gene Ther.*, **1996**, 7, 1339.

31.   Wyber, J. A.; Andrews, J.; D'Emanuele, A., *Pharm. Res.*, **1997**, 14, 750.

32.   Jinsong, H.; Kevin, L; Winston, W. Y.; Kao, S.; Chia-Yang, L., *Brain Res. Bull.*, **2010**, 81, 256.

33.   Asahara, T.; Shinomiya, K.; Naito, T.; Shiota, H., *Japanese J. Ophthalmol.*, **2001**, 45, 31.

34.   Cullander, C., *Adv. Drug Deliv. Rev.*, **1992**, 9, 119.

35.   Scherer, F.; Anton. M.; Schillinger, U.; Henke, J.; Bergemann, C.; Kruger, A., et al., *Gene Ther.*, **2002**, 9, 102.

36.   Huth, S.; Lausier, J.; Gersting, S.; Rudolph, C.; Welsch, U.; Rosenecker, J., *J. Gene Med.*, **2004**, 6, 923.

37.   Hashimoto, T.; Yamaoka, T., Polymeric gene carrier, in, Taira, K.; Kataoka, K.; Niidome, T.; Eds. Non-viral gene therapy - gene design and delivery. Tokyo: Springer Verlag, **2005**, p 35.

38.   Laemmli, U. K., *Proc. Natl. Acad. Sci. USA.*, **1975**, 72, 4288.

39.   Kwoh, D. Y.; Coffin, C. C.; Lollo, C. P.; Jovenal, J.; Banaszyk, M. G.; Mullen, P., et al. *Biochim. Biophys. Acta*, **1999**, 1444, 171.

40. Choi, Y. H.; Liu, F.; Kim, J. S.; Choi, Y. K.; Park, J. S.; Kim, S. W., *J. Control Rel.*, **1998**, 54, 39.

41. Liu, G.; Molas, M.; Grossmann, G. A.; Pasumarthy, M.; Perales, J. C.; Cooper, M. J.; et al. *J. Biol. Chem.*, **2001**, 276, 34379.

42. Pouton, C. W.; Lucas, P.; Thomas, B. J.; Uduehi, A. N.; Milroy, D. A.; Moss, S. H., *J. Control Rel.*, **1998**, 53, 289.

43. Katayose, S.; Kataoka, K., *J. Pharm. Sci.*, **1998**, 87, 160.

44. Trubetskoy, V. S.; Torchilin, V. P.; Kennel, S. L.; Huang, L., *Bioconjug Chem.*, **1999**, 3, 323.

45. Sonawane, N. D.; Szoka, F. C.; Verkman, A .S., *J. Biol. Chem.*, **2003**, 278, 44826.

46. Boussif, O.; Lezoualch, F.; Zanta, M. A.; Mergny, M. D.; Scherman, D.; Demeneix, B., et al. *Proc. Natl. Acad. Sci. USA*. **1995**, 92, 7297.

47. Godbey, W. T.; Wu, K. K.; Mikos, A. G. *J. Biomed. Mat. Res.*, **1999**, 45, 268.

48. Fischer, D.; Li, Y.; Ahlemeyer, B.; Krieglstein, J.; Kissel, T., *Biomaterials*, **2003**, 24, 1121.

49. Dash, P. R.; Read, M. L.; Barrett, L. B.; Wolfert, M. A.; Seymour, L. W., *Gene Ther.*, **1999**, 6, 643.

50. Petersen, H.; Fechner, P. M.; Martin, A. L.; Kunath, K.; Stolnik, S.; Roberts, C. J., et al. *Bioconjugate Chem.*, **2002**, 13, 845.

51. Benns, J. M.; Maheshwari, A.; Furgeson, D. Y.; Mahato, R. I.; Kim, S. W., *J. Drug Target*, **2001**, 9, 123.

52. Chiu, S. J.; Ueno, N. T.; Lee, R. J. *J Control Rel.*, **2004**, 97, 357.

53. Schipper, N. G. M.; Varum, K. M.; Artursson, P., *Pharm. Res.*, **1996**, 113, 1686.

54. Lehr, C. M.; Bouwstra, J. A.; Schacht, E. H.; Junginger, H. E., *Int. J. Pharm.*, **1992**, 78, 43.

55. Rolland, A. P., *Crit. Rev. Ther. Drug* Carrier *Syst.*, **1998**, 15, 143.

56. Liu,W. G.; Yao, K. D., *J. Control Rel.*, **2002**, 83, 1.

57. Lopata, M. A.; Cleveland, D. W.; Sollner-Webb, B., *Nucleic Acids Res.* **1984**, 12, 5707.

58. Reeves, R.; Gorman, C.; Howard, B., *Nucleic Acids Res.*, **1985**, 13, 3599.

59. Selden, R. F.; Burke-Howie, K.;, Rowe, M.E.; Goodman, H. M.; Moore, D. D., *Mol. Cell Biol.*, **1986**, 6, 3173.

60. Azzam, T.; Eliyahu, H.; Shapira, L.; Linial, M.; Barenholz, Y.; Domb, A. J., *J. Med. Chem.*, **2002**, 45, 1817.

61. Lynn, D. M.; Langer. R., *J. Am. Chem. Soc.* **2000**, 122, 10761.

62. Danusso, F.; Ferruti, P., *Polymer.* **1970**, 11, 88.

63. Ferruti, P.; Barbucci, R., *Adv. Polymer Sci.*, **1984**, 58, 55.

64. Van de Cherng, J. Y.; Wetering, P.; Talsma, H.; Crommelin, D. J.; Hennink, W. E., *Pharm. Res.*, **1996**, 13, 1038.

65. Van de Wetering, P.; Cherng, J. Y.; Talsma, H.; Crommelin, D. J.; Hennink, W. E., *J. Control Rel.*, **1998**, 53, 145.

66. Lim, Y. B; Choi, Y. H.; Park, J. S., *J. Am. Chem. Soc.*, **1999**, 121, 5633.

67. Putnam, D.; Langer, R., *Macromolecules,* **1999**, 32, 3658.

68. Lim, Y. B.; Kim, C. H.; Kim, K.; Kim, S. W.; Park, J. S., *J. Am. Chem. Soc.*, **2000**, 122, 6524.

69. Lim, Y. B.; Han, S. O.; Kong, H. U.; Lee, Y.; Park, J. S.; Jeong, B., et al. *Pharm. Res.*, **2000**, 17, 811.

70. Schmolka, I. R., *J. Am. Oil Chem. Soc.*, **1977**, 54, 110.

71. Nagarajan, R., *Colloids Surf. B.*, **1999**, 16, 55.

72. Astafieva, L.; Maksimova, I.; Lukanidin, E.; Alakhov, V.; Kabanov, A., *FEBS Lett.*, **1996**, 389, 278.

73. Cho, C. W.; Cho, Y. S.; Lee, H. K.; Yeom, Y. I.; Park, S. N.; Yoon, D. Y., *Biotechnol. Appl. Biochem.*, **2000**, 32, 21.

74. Hedley, M. L. *Expert Opin. Biol. Ther.*, **2003**, 3, 903.

75. Jones, D. H.; Corris, S.; McDonald, S.; Clegg, J. C.; Farrar, G. H., *Vaccine.* **1997**, 15, 814.

76. Oster, C. G.; Kissel, T., *J. Microencap.*, **2005**, 22, 235.

77. Bhattacharya, S.; Bajaj, A., *Curr. Opin. Chem. Biol.*, **2005**, 9, 647.

78. Felgner, P.L.; Gadek, T. R.; Holm, M.; Roman, R.; Chan, H. W.; Wenz, M., et al. *Proc. Natl. Acad. Sci. USA.*, **1987**, 84, 7413.

79. Felgner, P. L.; Eppstein, D. A., SYNTEX (USA) INC. EP0172007, **1986**.

80. Wheeler, C.J.; Felgner, P. L.; Tsai, J. T.; Marshall, J.; Sukhu, L.; Doh, S. G., et al., *Proc. Natl. Acad. Sci. USA.*, **1996**, 93, 11454.

81. San, H.; Yang, Z. Y.; Pompili, V. J.; Jaffe, M. L.; Plautz, G. E.; Xu, L., et al., *Hum. Gene Ther.*, **1993**, 4, 781.

82. Ren, T.; Liu, D., *Tetrahedron Lett.*, **1999**, 40, 209.

83. Ren, T.; Liu, D., *Bioorg. Med. Chem. Lett.*, **1999**, 9, 1247.

84. Haces, A.; Ciccarone, V., Gaithersburg, M. D., Life Technologies, WO/1995/017373, **1995**.

85. Nantz, M. H., Bennett, M. J.; Malone, R. W., The University Of California, USA. WO/1996/010555, **1996**.

86. Behr, J. P., *Tetrahedron Lett.*, **1986**, 27, 5861.

87. Behr, J. P.; Demeneix, B.; Loeffler, J. P.; Perez-Mutul, J., *Proc. Natl. Acad. Sci. USA.*, **1989**, 86, 6982.

88. Deshmukh, H. M.; Haung, L., *New J. Chem.*, **1997**, 21, 113.

89. Gao, X.; Huang, L., *Biochem. Biophys. Res. Commun.*, **1991**, 179, 280.

90. Caplen, N. J.; Alton, E.; Middleton, P. G.; Dorin, J. R.; Stevenson, B. J.; Gao, X., et al., *Nat. Med.*, **1995**, 1, 39.

91. Gill, D. R.; Southern, K. W.; Mofford, K. A.; Seddon, T.; Huang, L.; Sorgi, F., et al., *Gene Ther.*, **1997**, 4, 199.

92. Rainer, B.; Abdesslame, N.; Yves, C., Transgene SA, WO/1998/037916, **1998**.

93. Hawley-Nelson, P.; Ciccarone, V.; Gebeyehu, G.; Jesse, J.; Felgner, P. L., *Focus.* **1993**, 15, 73.

94. Jessee, J. A.; Hearl, W. G., Life Technologies, WO/1994/027435, **1994**.

95. Gullilat, G.; Joel, A. J., Life Technologies, US6075012, **2000**.

96. Carl, J. W., Vical Inc., WO/1998/014439, **1998**.

97. Carl, J. W., US6022874, **1998**.

98. Haces, A., WO/2000/012454, **2000**.

99. Ruysschaert, J. M.; Ouahabi, A.; Willeaume, V.; Huez, G.; Fuks, R.; Vandenbranden, M, et al., *Biochem. Biophys. Res. Comm.*, **1994**, 203, 1622.

100. Heath, T. D.; Solodin, I., Megabios Corp., **1995**, WO/1995/014381.

101. Byk, G.; Dubertret, C.; Schwartz, B.; Frederic, M.; Jaslin, G.; Rangara, R., et al., *Lett. Pept. Sci.*, **1997**, 4, 263.

102. Frederic, M.; Scherman, D.; Byk, G., *Tetrahedron Lett.*, **2000**, 41, 675.

103. Lin, K. Y.; Lewis, J. G.; Matteucci, M. D.; Wagner, R. W., Gilead Sci. Inc., **1996**, WO/1996/001840.

104. Chicco, A. J.; Sparagna, G. C. *Am. J. Physiol. Cell Physiol.,* **2007**,292, C33-44.

105. Matsumoto, K.; Kusaka, J.; Nishibori, A.; Hara, H., *Mol. Microbiol.*, **2006**, 61, 1110.

106. Kasireddy, K.; Ahmad, M.U.; Ali, S. M.; Ahmad, I., *Tetrahedron Lett.*, **2004**, 45, 2743.

107. Kasireddy, K.; Ali, S. M.; Ahmad, M. U.; Choudhury, S.; Chien, P. Y.; Sheikh, S.; Ahmad, I., *Bioorg Chem.* **2005**, 33, 345.

108. Chien, P. Y.; Wang, J.; Carbonaro, D.; Lei, S.; Milerr, B.; Sheikh, S.; Ali, S. M.; Ahmad, M. U.; Ahmad, I., *Cancer Gene Ther.*, **2005**, 12, 321.

109. Bajaj, A.; Paul, B.; Kondaiah, P.; Bhattacharya, S., *Bioconjugate Chem.*, **2008**, 19, 1283.

110. Chabaud, P.; Camplo, M.; Payet, D.; Serin, G.; Moreau, L.; Barthelemy, P.; Grinstaff, M. W., *Bioconjugate Chem.*, **2006**, 17, 466.

111. Li, S.; Tseng, W. C.; Stolz, D. B.; Wu, S. P.; Watkins, S. C.; Huang, L., *Gene Ther.*, **1999**, 6, 585.

112. Bajaj, A.; Paul, B.; Indi, S. S.; Kondaiah, P.; Bhattacharya, S., *Bioconjugate Chem.*, **2007**, 18, 2144.

113. Bajaj, A.; Kondaiah, P.; Bhattacharya, S., *Biomacromolecules*, **2008**, 9, 991.

114. Van der Woude, I.; Wagenaar, A.; Meekel, A. A.; Ter Beest, M. B.; Ruiters, M. H.; Engberts, J. B.; Hoekstra, D., *Proc. Natl. Acad. Sci. USA.*, **1997**, 94, 1160.

115. Meekel, A. A. P.; Wagenaar, A.; Smisterova, J.; Kroeze, J. E.; Haadsma, P.; Bosgraaf, B.; Stuart, M. C. A.; Brisson, A.; Ruiters, M. H. J.; Hoekstra, D.; Engberts, J. B. F. N., *Eur. J. Org. Chem.*, **2000**, 665.

116. Roosjen, A.; Smisterova, J.; Driessen, C.; Anders, J. T.; Wagenaar, A.; Hoekstra, D.; Hulst, R.; Engberts, J. B. F.N., *Eur. J. Org. Chem.*, **2002**, 1271.

117. Ilies, M. A.; Seitz, W. A.; Caproiu, M. T.; Wentz, M.; Garfield, R. E.; Balaban, A. T., *Eur. J. Org. Chem.*, **2003**, 2645.

118. Ilies, M. A.; Seitz, W. A.; Ghiviriga, I.; Johnson, B. H.; Miller, A.; Thompson, E. B.; Balaban, A. T., *J. Med. Chem.*, **2004**, 47, 3744.

119. Matsuo, H.; Chevallier, J.; Mayran, N.; Le Blanc, I.; Ferguson, C.; Faure, J.; Blanc, N. S.; Matile, S.; Dubochet, J.; Sadoul, R.; Parton, R.,G.; Vilbois, F.; Gruenberg, J., *Science*, **2004**, 303, 531.

120. Ilies, M. A.; Seitz, W. A.; Johnson, B. H.; Ezell, E. L.; Miller, A. L.; Thompson, E. B.; Balaban, A. T., *J. Med. Chem.*, **2006**, 49, 3872.

121. Rose, J. K.; Buonocore, L.; Whitt, M. A., *Biotechniques*, **1991**, 10, 520.

122. Rosenzweig, H. S.; Rakhmanova, V. A.; MacDonald, C., *Bioconj. Chem.*, **2001**, 12, 258.

123. Badea, I.; Wettig, S.; Verrall, R.; Foldvari, M., *Eur. J. Pharm. Biopharm.*, **2007**, 65, 414.

124. Badea, I.; Verrall, R.; Baca-Estrada, M.; Tikoo, S.; Rosenberg, A.; Kumar, P.; Foldvari, M., *J. Gene Med.*, **2005**, 7, 1200.

125. Luciani, P.; Bombelli, C.; Colone, M.; Giansanti, L.; Ryhanen, S. J.; Saily, V. M. J.; Mancini, G.; Kinnunen, P. K. J., *Biomacromolecules*, **2007**, 8, 1999.

126. Bombelli, C.; Faggioli, F.; Luciani, P.; Mancini, G.; Sacco, M. G., *J. Med. Chem.*, **2005**, 48, 5378.

127. Bombelli, C.; Borocci, S.; Diociaiuti, M.; Faggioli, F.; Galantini, L.; Luciani, P.; Mancini, G.; Sacco, M. G., *Langmuir.* **2005**, 21, 10271.

128. Bombelli, C.; Faggioli, F.; Luciani, P.; Mancini. G.; Sacco, M. G., *J. Med. Chem.*, **2007**, 50, 6274.

129. Ryhanen, S. J.; Saily, M. J.; Paukku, T.; Borocci, S.; Mancini, G.; Holopainen, J. M.; Kinnunen, P. K. J., *Biophys. J.*, **2003**, 84, 578.

130. Fisicaro, E.; Compari, C.; Duce, E.; Donofrio, G.; Rozycka-Roszak, B.; Wozniak, E., *Biochim. Biophys. Acta*, **2005**, 1722, 224.

131. Vijayanathan, V.; Thomas, T.; Antony, T., *Nucleic Acids Res.*, **2004**, 32, 127.

132. Vijayanathan, V.; Thomas, T.; Shirahata, A., *Biochemistry.* **2001**, 40, 13644.

133. Wettig, S. D.; Badea, I.; Donkuru, M. D.; Verrall, R. E.; Foldvari, M., *J. Gene Med.*, **2007**, 9, 649.

134. Gao, X.; Huang, L., *Biochem. Biophys. Res. Commun.*, **1991**, 179, 280.

135. Bajaj, A.; Kondiah, P.; Bhattacharya, S., *J. Med. Chem.*, **2007**, 50, 2432**.**

136. Ghosh, Y. K.; Visweswariah, S. S.; Bhattacharya, S., *FEBS Lett.*, **2000**, 473, 341.

137. Ghosh, Y. K.; Visweswariah, S. S.; Bhattacharya, S., *Bioconjugate Chem.*, **2002**, 13, 378.

138. Bajaj, A.; Kondaiah, P.; Bhattacharya, S., *Bioconjugate Chem.*, **2007**, 18, 1537.

139. Tang, F.; Hughes, J. A., *Biochem. Biophys. Res. Commun.*, **1998**, 242, 141.

140. Tang, F.; Hughes, J. A., *Bioconjugate Chem.*, **1999**, 10, 791.

141. Bajaj, A.; Kondiah, P.; Bhattacharya, S., *J. Med. Chem.*, **2008**, 51, 2533.

142. McGregor, C.; Perrin, C.; Monck, M.; Camilleri, P.; Kirby, A. J., *J. Am. Chem. Soc.*, **2001**, 123, 6215.

143. Camilleri, P.; Kremer, A.; Edwards, A.; Jennings, K.; Jenkins, O.; Marshall, I.; McGregor, C.; Neville, W.; Rice, S.; Smith, R.; Wilkinson, M.; Kirby A., *J. Chem. Soc. Chem. Commun.*, **2000**, 1253.

144. Jennings, K. H.; Marshall, I. C. B.; Wilkinson, M. J.; Kremer, A.; Kirby, A. J.; Camilleri, P., *Langmuir*, **2002**, 18, 2426.

145. Blessing, T.; Remy, J. S.; Behr, J. P., *Proc. Natl. Acad. Sci. USA.*, **1998**, 95, 1427.

146. Behr, J. P. *J. Chem. Soc. Chem. Commun.*, **1989**, 101.

147. Dauty, E.; Remy, J. S.; Blessing, T.; Behr, J. P., *J. Am. Chem. Soc.*, **2001**, 123, 9227.

148. Ronsin, G.; Perrin, C.; Guedat, P.; Kremer, A.; Camilleri, P.; Kirby, A. J., *J. Chem. Soc. Chem. Commun.*, **2001**, 2234.

149. Buijnsters, P. A.; Rodriguez, C. L. G.; Willighagen, E. L.; Sommerdijk, N. A. M.; Kremer, A.; Camilleri, P.; Feiters, M. C.; Nolte, R. J. M.; Zwanenburg, B., *Eur. J. Org. Chem.*, **2002**, 8, 1397.

150. Bergsma, M.; Fielden, M. L.; Engberts, J. B. F. N., *J. Colloid Interface Sci.*, **2001**, 243, 491.

151. Johnsson, M.; Wagenaar, A.; Engberts, J. B. F. N., *J. Am. Chem. Soc.* **2003**, 125, 757.

152. Bell, P. C.; Bergsma, M.; Dolbnya, I. P.; Bras, W.; Stuart, M. C. A.; Rowan, A. E.; Feiters, M. C.; Engberts, J. B. F. N., *J. Am. Chem. Soc.*, **2003**, 125, 1551.

153. Johnsson, M.; Wagenaar, A.; Stuart, M. C. A.; Engberts, J. B. F. N., *Langmuir.* **2003**, 19, 4609.

154. Klijn, J. E.; Stuart, M. C. A.; Scarzello, M.; Wagenaar, A.; Engberts, J. B. F. N., *J. Phys. Chem. B.*, **2007**, 111, 5204.

155. Scarzello, M.; Klijn, J. E.; Wagenaar, A.; Stuart, M. C. A.; Hulst, R.; Engberts J. B. F. N., *Langmuir.* **2006**, 22, 2558.

156. Wasungu, L.; Scarzello, M.; Dam, G. V.; Molema, G.; Wagenaar, A.; Engberts, J. B. F. N.; Hoekstra, D., *J. Mol. Med.*, **2006**, 84, 774.

157. Wasungu, L.; Stuart, M. C. A.; Scarzello, M.; Engberts, J. B. F. N.; Hoekstra, D., *Biochim. Biophys. Acta*, **2006**, 1758, 1677.

158. Asokan, A.; Cho, M. J., *Bioconjugate chem.*, **2004**, 15, 1166.

159. Camilleri, P.; Kirby, A. J.; Perrin, C.; McGregor, C., US 20030119188A1, **2003**.

160. Camilleri, P.; Kirby, A. J.; Perrin. C.; Rosin, G. A. B.; Guedat, P., US 20040138139A1, **2004**.

161. Camilleri, P.; Guedat, P.; Kirby, A. J.; Kremer, A., Smithline Becham pIc., Cambridge University Technical Service Ltd., US 20050089493A1, **2005**.

162. Castro, M. J.; Christopher, K.; Ladlow, M.; Patel, A., Glaxo group limited, US 7425645 B2, **2008**.

163. Castro, M. J.; Kitson, C.; Ladlow, M.; Patel, A., Glaxo group limited, US 7569720 B2, **2009**.

164. Wettig, S.; Verrall, R. E.; Foldvari, M., University of Saskatchewan, US 20090054368A1, **2009**.

165. Castro, M. J.; Kitson, C.; Ladlow, M.; Patel, A., US 20090149401A1, **2009**.

166. Wheeler, C., Vical Incorporated, San Diego, assignee. US 6696424B1, **2004**.

167. Camilleri, P.; Engberts, J. B. F. N.; Fieldon, M. L.; Kremer, A., Smithkline Beecham pIc, assignee, US 7005300B1, **2006**.

168. Bennett, M. J.; Aberle, A. M.; Balasubramaniam, R. P.; Malone, J. G; Malone, R. W.; Nantz, M. H., *J. Med. Chem.*, **1997**, 40, 4069.

169. Felgner, J. H.; Kumar, R.; Sridhar, C. N.; Wheeler, C. J.; Tsai, Y. J.; Border, R., *et al.*, *J. Biol. Chem.*, **1994**, 269, 2550.

170. Srilakshmi, G. V.; Sen, J.; Chaudhuri, A.; Ramadas, Y.; Rao, N. M., *Biochim. Biophys. Acta*, **2002**, 1559, 87.

171. Banerjee, R.; Das, P. K.; Srilakshmi, G. V.; Chaudhuri, A.; Rao, N. M., *J. Med. Chem.* **1999**, 42, 4292.

172. Laxmi, A. A.; Vijayalakshmi, P.; Balagopala Kaimal, T. N.; Chaudhuri, A.; Ramadas, Y.; Rao, N. M., *Biochem. Biophys. Res. Commun.*, **2001**, 289, 1057.

173. Banerjee, R.; Mahidhar, Y. V.; Chaudhuri, A.; Gopal, V.; Rao, N. M., *J. Med. Chem.*, **2001**, 44, 4176.

174. Ghosh, Y. K.; Visweswariah, S. S.; Bhattacharya, S., *FEBS Lett.*, **2000**, 473, 341.

175. Fichert, T.; Regelin, A.; Massing, U., *Bioorg. Med. Chem. Lett.*, **2000**, 10, 787.

176. Xu, Y.; Szoka, F. C. J., *Biochemistry*, **1996**, 35, 5616.

177. Zelphati, O.; Szoka, F. C. J., *Proc. Nat. Acad. Sci. USA*, **1996**, 93, 11493.

178. Bhattacharya, S.; Mandal, S. S., *Biochemistry*, **1998**, 37, 7764.

179. Zabner, J.; Fasbender, A. J.; Moninger, T.; Poellinger, K. A.; Welsh, M. J., *J. Biol. Chem.*, **1995**, 270, 18997.

180. Radler, J. O.; Koltover, I.; Salditt, T.; Safinya, C. R., *Science*, **1997**, 275, 810.

181. Koltover, I.; Salditt, T.; Radler, J. O.; Safinya, C. R., *Science,* **1998**, 281, 78.

182. Escriou, V.; Carriere, M.; Wils, P.; Scherman, D., *J. Gene Med.*, **2001**, 3, 179.

183. Brunner, S.; Sauer, T.; Carotta, S.; Cotton, M.; Saltik, M.; Wagner, E., *Gene Ther.*, **2000**, 7, 401.

184. Middaugh, C. R.; Evans, R. K.; Montgomery, D. L.; Casimiro, D. R., *J. Pharm. Sci.*, **1998**, 87, 130.

185. Miller, J., Experiments in molecular genetics. Cold Spring Harbor Laboratory: Cold Spring Harbor, New York. **1977**, p 352.

186. Kirby, A.; Camilleri, P.; Engberts, J. B. F. N.; Feiters, M. C.; Nolte, R. J. M.; Soderman, O.; Bergsma, M.; Bell, P. C.; Fielden, M. L.; Rodriguez, C. L. G; Guedat, P.; Kremer, A.; McGregor, C.; Perrin, C.; Ronsin, G.; Eijk, M. C P., *Angew Chem. Int. Ed.*, **2003,** 42, 1448.

187. Kumar, M.; Jinturkar, K.; Yadav, M. R.; Misra, A. N., *Crit. Rev. Ther. Drug Carr. Systems*, **2010**, 27, 237.

188. Bombelli, C.; Giansanti, L.; Luciani, P.; Mancini, G., *Curr. Med. Chem.*, **2009**, 16,171.

189. Hasegawa, S.; Hirashima, N.; Nakanishi, M., *Bioorg. Med. Chem. Lett.* **2002**, 12, 1299.

190. Hui, S. W.; Langner, M.; Zhao, Y.; Ross, P.; Hurley. E.; Chan, E., *Biophys. J.*, **1996**, 71, 590.

191. Siegel, D. P.; Epand, R. M., *Biophys. J.*, **1997**, 73, 3089.

192. Almeida, P. F. F.; Vaz, W. L. C.; Thompson, T. E., *Biochemistry*, **1992,** 31, 6739.

193. Sambrook, J.; Fritsch, E. F.; Maniatis, T., Molecular cloning. A laboratory manual, Cold Spring Harbour Laboratory Press, **1989**, p 1.23.

194. Bimboim, H. C.; Doly, J., *Nucleic Acids Res.,* **1979,** 7, 1513.

195. Manchester, K. L. *Bio Techniques*, **1995**, 19, 208.

196. Miller, J. H., Experiments in Molecular Genetics, Cold Spring Harbor Laboratories, **1972,** p 352.

197. Zana, R., Gemini surfactants: synthesis, interfacial and solution-phase behavior, and applications, Marcel Dekker Inc, New York, **2004**, p 109.

198. Wang, X.; Wang, J.; Wang, Y.; Yan, H.; Li, P.; Thomas, R. K., *Langmuir*, 2004, 20, 53.

199. Zana, R.; Benrroau, M.; Rueff, R., *Langmuir,* **1991**, 7, 1072.

200. Ralston, A. W.; Eggenberger, D. N.; Harwood, H. J.; Dubrow, P. J., *J. Am. Chem. Soc.*, **1947**, 69, 2095.

201. Wettig, S. D.; Verrall, R. E., *J. Colloid Interface Sci.*, **2001**, 235, 310.

202. Borse, M.; Sharma, V.; Aswal, V. K.; Pokhriyal, N. K.; Joshi, J. V.; Goyal, P. C.; Devi, S., *Phys. Chem. Chem. Phys.*, **2004**, 6, 3508.

203. Choi, J. S.; Lee, E. J.; Jang, H. S.; Park, J. S., *Bioconjugate Chem.*, **2001,** 12, 108.

204. Wuand, W.; Cseke, L. J., DNA footprinting and gel retardation assay, in, Cseke, L. J.; Peter, B.; Kaufman, P. B.; Podila, G. K.; Tsai, C. J., Eds, Handbook of molecular and cellular methods in biology and medicine, Second Edition, CRC Press **2003**, p 156.

205. Zhang, Z.; Huang, W.; Tang, J.; Wang, E.; Dong, S., *Biophys. Chem.*, **2002**, 97, 7.

206. Keller, D.; Bustamante, C., *J. Chem. Phys.*, **1986**, 84, 2972.

207. Zuidam, N. J.; Barenholz, Y.; Minsky, A., *FEBS Lett.*, **1999**, 457, 419.

208. Zuidam, N. J.; Barenholz, Y. *Biochim. Biophys. Acta*, **1998**, 1368, 115.

209. Simberg, D.; Danino, D.; Talmon, Y.; Minsky, A.; Ferrari, M. E.; Wheeler, C. J.; Barenholz, Y., *J. Biol. Chem.*, **2001**, 276, 47453.

210. Nakanishi, H.; Tsuchiya, K.; Okubo, T.; Sakai, H.; Abe, M., *Langmuir*, **2007**, 23, 345.

211. Lenssen, K.; Jantscheff, P.; Kiedrowski, G.; Massing, U., *Chem. Bio. Chem.*, **2002**, 3, 852.

212. Nicoletti, V. G.; Condorelli, D. F., *Bio. Techniques*, **1993**, 14, 532.

213. Davis, R. W.; Botstein, D.; Roth, J. R., A manual for genetic engineering: Advanced bacterial genetics. Cold spring Harbor Laboratory, **1980**, p 253.

214. Baichao, M.; Zhang, S.; Jiang, H.; Zhao, B.; Hongtao, L., *J. Controlled Rel.*, **2007**, 123, 184.

215. Van Meerloo, J.; Kaspers, G. J.; Cloos, J., *Methods Mol. Biol.*, **2011**, 731, 237-45.

216. Sylvester, P. W., *Methods Mol. Biol.*, **2011**, 716, 157.

217. Soboleski, M. R.; Oaks, J.; Halford, W. P., *The FASEB J*. **2005**, 19, 440.

218. Davda, J.; Labhasetwar, V., *Int. J. Pharm*., **2002**, 233, 51.

219. Pathak, A.; Kumar, P.; Chuttani, K.; Jain, S.; Mishra, A. K.; Vyas, S. P.; Gupta, K. C., *ACS Nano.*, **2008**, 2854.